

AD-A023 602

INVESTIGATION OF THE EFFECTIVENESS OF POLYMERS IN THE
TREATMENT OF NITROCELLULOSE-MANUFACTURING WASTEWATER

Rensselaer Polytechnic Institute

Prepared for:

Army Mobility Equipment Research
and Development Center

March 1976

DISTRIBUTED BY:

NTIS

National Technical Information Service
U. S. DEPARTMENT OF COMMERCE

SECURITY CLASSIFICATION OF THIS PAGE (When Data Entered)

REPORT DOCUMENTATION PAGE		READ INSTRUCTIONS BEFORE COMPLETING FORM
1. REPORT NUMBER	2. GOVT ACCESSION NO.	3. RECIPIENT'S CATALOG NUMBER
4. TITLE (and Subtitle) "Investigation of the Effectiveness of Polymers in the Treatment of Nitrocellulose-Manufacturing Wastewater"		3. TYPE OF REPORT & PERIOD COVERED Final Project Report for the period June 1975 to March 1976
7. AUTHOR(s) Lawrence K. Wang, Ray W. Shade, William W. Shuster and Fusun T. Bilgen		6. PERFORMING ORG. REPORT NUMBER RPI - JBA02-1
9. PERFORMING ORGANIZATION NAME AND ADDRESS Rensselaer Polytechnic Institute Troy, New York 12181		8. CONTRACT OR GRANT NUMBER(s) DAAC-53-75-C-0252
11. CONTROLLING OFFICE NAME AND ADDRESS U.S. Army Mobility Equipment R & D Center Fort Belvoir, Virginia 22060		10. PROGRAM ELEMENT, PROJECT, TASK AREA & WORK UNIT NUMBERS JBA02
14. MONITORING AGENCY NAME & ADDRESS (if different from Controlling Office) Department of the Navy Office of Naval Resident Representative 715 Broadway (5th Floor) New York, New York 10003		12. REPORT DATE March 31, 1976
		13. NUMBER OF PAGES 215
		15. SECURITY CLASS. (of this report) Unclassified
		15a. DECLASSIFICATION/DOWNGRADING SCHEDULE
16. DISTRIBUTION STATEMENT (of this Report) This document has been approved for public release and sale. Its dis- tribution is unlimited.		
17. DISTRIBUTION STATEMENT (of the abstract entered in Block 20, if different from Report) This document has been approved for public release and sale. Its distribution is unlimited.		
18. SUPPLEMENTARY NOTES An Appendix is to be published.		
19. KEY WORDS (Continue on reverse side if necessary and identify by block number) Military Wastewater, Nitrocellulose-Manufacturing Wastewater, Wastewater Treatment, Physicochemical Process, Carbon Adsorption, Lime Precipitation, Polyelectrolyte Coagulation, Sand Filtration, Colloid Charge Determination.		
20. ABSTRACT (Continue on reverse side if necessary and identify by block number) The effectiveness of organic polymers in the treatment of two types of industrial wastewaters has been investigated. The experimental study con- sisted of initially performing batch jar tests followed by continuous fil- tration runs with the wastewater, using the results obtained in the jar tests. Six polymers were used in the experiments to determine optimum type and dosage required for effective turbidity removal. Cationic and non-ionic polymers		

(20)

proved to be the most effective in coagulation by the predominant mechanisms of charge neutralization and interparticle bridging, respectively. Bentonite and lime were also used quite effectively as coagulant aids in conjunction with the various polymers.

Two methods of feeding the polymer to the filter were used: 1 - Conventional addition of polymer to the wastewater in a batch unit for coagulation followed by filtration of supernatant, and 2 - Direct addition of polymer to the filter. The latter process, known as contact coagulation-filtration, was not successful in the treatment of the wastewater because of its high turbidity. A thick layer of cake at the surface (formed by the large flocs following coagulation) caused an excessive head loss with an early termination of the filtration operation.

The best method selected for the treatment of wastewater consisted of the addition of 100 mg/l Cat Floe cationic polymer and 100 mg/l of powdered bentonite clay to the wastewater in a batch unit and after sedimentation, filtration of the supernatant at a flow rate of 4 gpm/ sq ft. This treatment yielded a high quality filtrate with a 99.8% reduction in turbidity.

The filtration runs were continued for 3 hours during which periodic samples were taken from the effluent and analyzed for turbidity, net charge, total organic carbon (TOC) and pH. The effect of filtration rate on effluent quality was also investigated, but it was seen that a change in the rate of flow only affected the head loss pattern of the filter.

1(a)

Unclassified

SECURITY CLASSIFICATION OF THIS PAGE (When Data Entered)

ADDITIONAL		
NTIS		✓
DIC		
ONS		
JUL 1975		
<i>AW 1473</i>		
BY		
DISTRIBUTION AVAILABILITY STATEMENTS		
DISC.		
<i>A</i>		

UNCLASSIFIED

INVESTIGATION OF THE EFFECTIVENESS OF
POLYMERS IN THE TREATMENT OF
NITROCELLULOSE-MANUFACTURING WASTEWATER

Final Project Report No. RPI-J3A02-1
for the period 15 June 1975 - 31 March 1976

March 1976

By

Lawrence K. Wang, Ph.D.
Ray W. Shade, Ph.D.
William W. Shuster, D.Ch.E.
Fuson Bilgen, M.Eng.

Prepared for

Department of the Army
U.S. Army Mobility Equipment Research and Development Center
Fort Belvoir, Virginia 22060

Contract No. DAAG-53-75-C-0252

DISTRIBUTION STATEMENT A
Approved for public release;
Distribution Unlimited

Prepared By

Rensselaer Polytechnic Institute
Department of Chemical and Environmental Engineering
Troy, New York 12181

UNCLASSIFIED

ii

DDC
RECEIVED
APR 26 1976
REGULATED
B

TABLE OF CONTENTS

	Page
LIST OF TABLES	vii
LIST OF FIGURES	viii
ACKNOWLEDGEMENT	xii
ABSTRACT	xiii
1. INTRODUCTION	1
2. THEORETICAL CONSIDERATIONS	8
2.1 Basic Concepts of Colloid Chemistry ...	8
2.2 Coagulation Theory	9
2.2.1 Electrical Double-Layer Theory ..	10
2.2.2 Colloid Interactions	12
2.3 Destabilization of Colloids	15
2.4 Mechanisms and Mathematical Models of Filtration	22
2.4.1 Physical Filtration Theories	25
2.4.2 Chemical Filtration Theories	29
3. LITERATURE REVIEW	37
3.1 Early History	37
3.2 Wastewater Applications	39
3.3 The Use of Polyelectrolytes in Filtration	44
4. APPARATUS AND PROCEDURES	51
4.1 Design of Experimental Study	51
4.2 Materials Used	52

	Page
4.2.1 Synthetic Wastewater	52
4.2.2 Actual Wastewater	53
4.2.3 Organic Polyelectrolytes	55
4.2.4 Filter Media	57
4.2.5 Lime and Powdered Carbon	57
4.3 Experimental Apparatus and Procedures	59
4.3.1 Continuous Filtration Apparatus and Procedures	59
4.3.1.1 The Multi-Media Filter	63
4.3.1.2 Start-up and Continuous Operation	65
4.3.2 Jar Test Apparatus and Procedures	69
4.3.2.1 Jar Tests with Polymers and Coagulant Aids	69
4.3.2.2 Jar Tests with Lime	69
4.3.2.3 Jar Tests with Powdered Activated Carbon	70
4.4 Analytical Apparatus and Procedures ...	70
4.4.1 Total Organic Carbon (TOC) Analysis	70
4.4.2 Turbidity Measurement	72
4.4.3 pH Measurement	72
4.4.4 Determination of Colloid Charge ...	74
4.4.4.1 Reagents	75
4.4.4.2 Analytical Procedures	75
4.4.4.3 Calculation of Net Charge	77

	Page
5. RESULTS AND DISCUSSION	79
5.1 Batch Jar Tests	79
5.1.1 Experiments using synthetic wastewater	79
5.1.2 Experiments using actual wastewater	92
5.1.2.1 "Diluted" actual wastewater ...	92
5.1.2.1.1 Tests using coagulant aids	95
5.1.2.2 "Undiluted" actual wastewater	102
5.1.2.2.1 Tests using bentonite as a coagulant aid	102
5.1.2.2.2 Powdered Carbon Adsorption Study	105
5.1.2.2.3 Tests using lime as a precipitant and as a coagulant aid	108
5.2 Continuous Filtration Experiments	112
5.2.1 Filter Effluent Turbidity, Charge and pH	125
5.2.2 Total Organic Carbon(TOC) of Filter Effluent	127
5.2.3 Head Loss Development	128
5.2.4 Effects of Flow Rate	130
5.2.5 Discussion of Various Aspects of the Continuous Runs	131
5.2.5.1 Method of Polymer Addition	131
5.2.5.2 Disadvantages of using lime as a coagulant aid	132
6. CONCLUSIONS	134
7. SUGGESTIONS FOR FURTHER STUDY	137

	Page
8. LITERATURE CITED	139
9. APPENDIX	142

LIST OF TABLES

	Page
Table 2.1 Factors Influencing Coagulation and Flocculation	23
Table 2.2 Modes of Destabilization and their Proposed Characteristics	24
Table 4.1 Analysis of Actual Wastewater	54
Table 4.2 Technical Specifications of Filter Media	58
Table 5.1 Outline of Continuous Filtration Experiments	113
Table A-1 Technical Specifications of Bentonite ...	145
Table A-2 Technical Specifications of Organic Polymers	146

LIST OF FIGURES

		Page
Figure 2.1	Electrical Double-Layer of a Colloid Particle	11
Figure 2.2	Potential Energy of Interaction of Colloidal Particles	14
Figure 2.3	Bridging Model for the Destabilization of Colloids by Polymers	19
Figure 2.4	Effects of Polymers as Filtration Aids	21
Figure 2.5	Particle Transport Mechanisms in Granular Filters	32
Figure 4.1	Flow Diagram of the Continuous Filtration Apparatus	60
Figure 4.2	Overall View of Actual Laboratory Apparatus	61
Figure 4.3	Wastewater Feeding Apparatus	62
Figure 4.4	Polymer Feeding Apparatus	62
Figure 4.5	Diagram of Multi-Media Filter	66
Figure 4.6	Close-up View of Granular Media	67
Figure 4.7	Jar Test Apparatus	71
Figure 4.8	Beckman Carbonaceous Analyzer	71
Figure 4.9	Fisher pH Meter	73
Figure 4.10	Hach Model 2100 A Turbidimeter	73
Figure 5.1	Residual Total Net Charge and pH vs. Polymer Dosage	80
Figure 5.2	Residual Turbidity vs. Polymer Dosage .	80
Figure 5.3	Residual Total Net Charge and pH vs. Polymer Dosage	81
Figure 5.4	Residual Turbidity and TOC vs. Polymer Dosage	81

	Page
Figure 5.5	Residual Total Net Charge vs. Polymer Dosage 82
Figure 5.6	Residual Turbidity vs. Polymer Dosage 82
Figure 5.7	Residual Total Net Charge and pH vs. Polymer Dosage 83
Figure 5.8	Residual Turbidity vs. Polymer Dosage 83
Figure 5.9	Residual Total Net Charge and pH vs. Polymer Dosage 84
Figure 5.10	Residual Turbidity vs. Polymer Dosage 84
Figure 5.11	Residual Turbidity vs. pH 89
Figure 5.12	Residual Turbidity vs. pH 90
Figure 5.13	Residual Turbidity vs. pH 91
Figure 5.14	Residual Turbidity vs. Polymer Dosage 93
Figure 5.15	Residual Turbidity vs. Polymer Dosage 93
Figure 5.16	Residual Total Net Charge and pH vs. Polymer Dosage 94
Figure 5.17	Residual Turbidity vs. Polymer Dosage 94
Figure 5.18	Residual Total Net Charge and pH vs. Polymer Dosage 97
Figure 5.19	Residual Turbidity and TOC vs. Polymer Dosage 97
Figure 5.20	Residual Total Net Charge and pH vs. Polymer Dosage 98
Figure 5.21	Residual Turbidity and TOC vs. Polymer Dosage 98
Figure 5.22	Residual Turbidity vs. Bentonite Dosage 100
Figure 5.23	Residual Total Net Charge and pH vs. Polymer Dosage 101
Figure 5.24	Residual Turbidity vs. Polymer Dosage 101
Figure 5.25	Residual Total Net Charge and pH vs. Polymer Dosage 103

	Page
Figure 5.26 Residual Turbidity and TOC vs. Polymer Dosage	103 .
Figure 5.27 Residual Total Net Charge and pH vs. Polymer Dosage	104
Figure 5.28 Residual Turbidity and TOC vs. Polymer Dosage	104
Figure 5.29 Residual Turbidity vs. Bentonite Dosage	106
Figure 5.30 Residual TOC vs. Powdered Carbon Dosage	107
Figure 5.31 Residual Turbidity and pH vs. Lime Dosage	109
Figure 5.32 Residual pH vs. Polymer Dosage	110
Figure 5.33 Residual Turbidity and TOC vs. Polymer Dosage	110
Figure 5.34 Residual pH vs. Polymer Dosage	111
Figure 5.35 Residual Turbidity and TOC vs. Polymer Dosage	111
Figure 5.36 Effluent Total Net Charge and pH vs. Filtration Time	114
Figure 5.37 Effluent Turbidity and TOC vs. Filtration Time	114
Figure 5.38 Head loss vs. Filtration Time	115
Figure 5.39 Effluent Total Net Charge and pH vs. Filtration Time	116
Figure 5.40 Effluent Turbidity and TOC vs. Filtration Time	116
Figure 5.41 Head loss vs. Filtration Time	117
Figure 5.42 Effluent Total Net Charge and pH vs. Filtration Time	118
Figure 5.43 Effluent Turbidity and TOC vs. Filtration Time	118
Figure 5.44 Head loss vs. Filtration Time	119

	Page
Figure 5.45	Effluent Total Net Charge and pH vs. Filtration Time 120
Figure 5.46	Effluent Turbidity and TOC vs. Filtration Time 120
Figure 5.47	Head loss vs. Filtration Time 121
Figure 5.48	Head loss and pH vs. Filtration Time 122
Figure 5.49	Effluent Turbidity and TOC vs. Filtration Time 122
Figure 5.50	Effluent Total Net Charge and pH vs. Filtration Time 123
Figure 5.51	Effluent Turbidity and TOC vs. Filtration Time 123
Figure 5.52	Head loss vs. Filtration Time 124
Figure A-1	Rotameter Calibration Data 148
Figure A-2	Rotameter Calibration Data 148
Figure A-3	Carbonaceous Analyzer Calibration Curve 149
Figure A-4	Calibration Curve for WT- 2870 Polyelectrolyte 150
Figure A-5	Calibration Curve for Cat Floc T Polyelectrolyte 151

ACKNOWLEDGEMENT

An investigation of the effectiveness of polymers in the treatment of nitrocellulose-manufacturing wastewater was conducted by the Department of Chemical and Environmental Engineering, Rensselaer Polytechnic Institute (RPI), for the U.S. Army Mobility Research and Development Center (USAMERDC), Fort Belvoir, Virginia, under Contract No. DAAG-53-75-C-0252.

This Final Project Report summarizes all of the work done on the project during the period June 1975 to March 1976. The report was reviewed by Mr. Maurice Pressman, Contracting Officer of the USAMERDC. His comments and suggestions are gratefully acknowledged. Mr. W. Fostel of the Department of the Navy, Office of Naval Representative, New York, New York, was the Administrative Contracting Officer. Mr. Fostel's aid and cooperation made this work a reality.

Dr. Lawrence K. Wang, Assistant Professor of RPI, served as the Principal Investigator and the coordinator of the entire research. Dr. Ray W. Shade and Dr. William W. Shuster, Associate Professor and Professor, respectively, were Co-Investigators. Mrs. Fusun T. Bilgen was a former graduate student of RPI where she received her Master Degree in Environmental Engineering. The four authors extend their sincere appreciation and thanks to Mr. Charles Vannier, Chemical Technician of RPI, for his assistance in construction of the filtration pilot plant.

ABSTRACT

The effectiveness of organic polymers in the treatment of two types of industrial wastewaters has been investigated. The experimental study consisted of initially performing batch jar tests followed by continuous filtration runs with the wastewater, using the results obtained in the jar tests. Six polymers were used in the experiments to determine optimum type and dosage required for effective turbidity removal. Cationic and non-ionic polymers proved to be the most effective in coagulation by the predominant mechanisms of charge neutralization and interparticle bridging, respectively. Bentonite and lime were also used quite effectively as coagulant aids in conjunction with the various polymers.

Two methods of feeding the polymer to the filter were used: 1- Conventional addition of polymer to the wastewater in a batch unit for coagulation followed by filtration of supernatant, and 2- Direct addition of polymer to the filter. The latter process, known as contact coagulation-filtration, was not successful in the treatment of the wastewater because of its high turbidity. A thick layer of cake at the surface (formed by the large flocs following coagulation) caused an excessive head loss with an early termination of the filtration operation.

The best method selected for the treatment of wastewater consisted of the addition of 100 mg/l Cat Flocc cationic

polymer and 100 mg/l of powdered bentonite clay to the wastewater in a batch unit and after sedimentation, filtration of the supernatant at a flow rate of 4 gpm/ sq ft. This treatment yielded a high quality filtrate with a 99.8% reduction in turbidity.

The filtration runs were continued for 3 hours during which periodic samples were taken from the effluent and analyzed for turbidity, net charge, total organic carbon (TOC) and pH. The effect of filtration rate on effluent quality was also investigated, but it was seen that a change in the rate of flow only affected the head loss pattern of the filter.

PART 1
INTRODUCTION

A fundamental requirement common to most industrial waste treatment processes is solids-liquid separation. The objective is to remove the suspended solids from the wastewater prior to its discharge or re-use within the plant. Most waste systems contain both colloidal and gross (larger than colloidal size) suspended solids in varying proportions. The solids larger than colloidal size have a settling velocity usually sufficient to assure ultimate settling and can be removed by a conventional sedimentation operation. Those solids in the colloidal size range (1-100 millimicrons) have an enormous surface-to-volume ratio. Their behavior in the waste system is therefore determined largely by the nature of their surface properties and can remain in suspension indefinitely making their removal quite difficult.

The most important property of colloid particles is their electrical charge. The magnitude of the charge may vary and depends on the nature of the colloidal material. Many colloidal dispersions are dependent upon the electrical charge for their stability. Similarly charged colloidal particles repel, thus enabling them to stay apart to prevent agglomeration into larger particles. The electrokinetic properties of colloids are of great importance in sanitary engineering, as the application of these properties is very important in the destruction

of many forms of colloids. When a charged colloid particle is immersed in solution, ions of opposite charge arrange themselves in a layer around the particle. Because of the attraction of these counter-ions to the surface, a concentration gradient is established and diffusion of counter ions takes place between the surface of the particle and the bulk of the solution. The two competing forces, electrostatic attraction and diffusion, distribute the charge over a second diffuse layer. The boundary surface between the fixed ion layer and the solution serves as a shear plane when the particle undergoes movement relative to the solution. The stability of the colloid is generally a function of the zeta potential, ζ , which is defined as the magnitude of charge at the surface of the shear plane.

Presently, electrophoretic mobility studies are being used to determine the charge characteristics of colloidal particles. In this method, the zeta potential is calculated from the migration velocity of the colloidal particles determined by a special instrument. The zeta potential is defined by the equation,

$$\zeta = \frac{4\pi nV}{DE}$$

where n = solvent viscosity

V = measured velocity of the charged particle

D = dielectric constant

E = electric field strength

Many types of colloidal particles can be found in naturally turbid waters and the migration speed of a significant fraction of these particles cannot be measured easily. In this sense, accurate electrophoretic mobility measurements are difficult to carry out. In this research, the application of the colloid titration technique is used to determine colloidal charge. This method yields data similar to the electrophoretic mobility measurements. The method is simple and easy to carry out without the need for specialized equipment and can be used as an alternative to electrophoretic mobility measurements. A more detailed discussion of the method is presented in Part 4 of this report.

It is obvious that the magnitude of the charge on a colloidal particle plays the most important role in its stability. The object of coagulation then is to reduce the charge and destabilize the system to provide particle agglomeration. Coagulation of colloids can be carried out in a number of ways. The most common are the addition of potential determining ions, the addition of chemicals that form hydrolyzed metal ions and the addition of long-chained organic molecules (polymers) to the colloid system. The common objective of these methods is to destabilize the system in a way to promote the coagulation and flocculation of colloid particles.

The use of polyelectrolytes for destabilization of colloidal suspensions is perhaps the most significant recent development in water treatment technology. Their use has

become increasingly important because both laboratory and plant work have demonstrated their effectiveness when used in low concentrations. Polymers may be natural or synthetic. Important natural polymers are of biological origin and are derived from starch products and cellulose derivatives. The other class consists of synthetic, long-chained high molecular weight organic substances. Depending on whether their charge when placed in water is negative, positive, or neutral, these polymers are classified as anionic, cationic, or non-ionic, respectively.

Polyelectrolytes are being used in two main categories in filtration operations. In the first category, polyelectrolytes are applied as primary coagulants neutralizing the charge of the particles to promote coagulation. During the flocculation stage, the organic polymers also act to bridge the particles and aggregates together to form much larger flocs which can easily be removed by sedimentation and filtration. The action of polyelectrolytes are similar to the hydrolyzing inorganic coagulants. However, due to the very long polymer lengths and the number of charged sites along the polymer chains, the organic polymers are much more effective both for neutralizing particle charges and for bridging than the inorganic alum and iron salts. Another advantage of using organic polymers in the conventional clarification process is the considerable reduction in both the weight and the volume of the settled sludge. Non-ionic and anionic polymers

do not neutralize particle charges themselves since in most wastewater systems the suspended colloid particles are negatively charged, but improve the bridging action of the primary coagulation. Since non-ionic and anionic polymers have much larger molecules and longer chain lengths than either inorganic or organic cationic polymers, they are the most effective bridgers or flocculators. Moreover, when the suspended particles are very concentrated or large in size, the particle charge becomes much less important so that a non-ionic or anionic polymer may cause coagulation without neutralizing particle charges. This phenomenon is encountered more frequently in waste treatment than in water treatment.

In the second category, polyelectrolytes are being used as filter aids in wastewater treatment. In this process, called contact coagulation-filtration, the wastewater is pumped directly to the filters and the polymer is introduced prior to entering the filter. This process has gained popularity recently to clarify low turbidity waters since it has the advantage of omitting the sedimentation and flocculation units. The organic polymers as filter aids provide tougher flocs which resist shear, resulting in better turbidity removal and longer filter runs even at high rates of flow. In some cases the filter media can be "preconditioned" with an organic polymer so that removal of turbidity, algae and bacteria can be obtained for a considerable length of time even though no polymer is added to the water during filtration.

The use of polyelectrolytes as filter aids has been made possible with the design of the dual or multi-media filters which provide deeper penetration of the floc into the bed without causing excessive head loss. When a filter composed of a single type of granular medium is used, during backwashing the medium will grade hydraulically, with the finest particles rising to the top of the bed. As a result, most of the material will be removed very near the surface of the bed. Only a small fraction of the total voids in the bed have been used to store particulates and the head loss increases very rapidly at high filter rates or high solids loadings. It is very typical for 75-90% of the head loss to occur in the upper inch of rapid sand beds. It can be seen that the limitations of the single media rapid sand filter result from its behavior as a surface filtration device. In order to increase the effective filter depth, dual media (a layer of coarse coal above a layer of fine sand) is being used. In this way, the storage capacity and the efficiency of removal with depth of the filter is increased. This also makes it possible for higher rates than the once conventional maximum rate of 2 gpm/sq ft to be used, but the selection of the filter rate depends on the characteristics of the raw water and the type of pretreatment.

The objectives of this research were to investigate several treatment methods and their effectiveness on two specific wastewaters: 1- synthetic wastewater and 2- actual wastewater (cellulose nitrate) in the presence of organic polyelectrolytes. The objective was to select the best type of treatment

for the wastewater. The following factors were investigated throughout the research:

- 1- The type of polymer (cationic, anionic, non-ionic) that provided efficient turbidity removal for a given wastewater.
- 2- The optimum dosage of polymer to be used in the treatment.
- 3- The point of addition of polymer to the treatment system as follows:
 - a- Conventional process- Addition of polymer, then coagulation, flocculation, sedimentation in a batch unit, followed by filtration of supernatant.
 - b- Direct addition to the filter.
- 4- Effects of filtration rate on the removal efficiency of the system.
- 5- The use of possible coagulant aids such as bentonite clay or lime in conjunction with the various polymers.
- 6- Effects of treating colloidal wastewater by powdered carbon adsorption and by high-lime precipitation with and without polymers.

To achieve these objectives, batch jar tests and continuous filtration runs were carried out in the laboratory under varying controlled operating conditions. The system efficiency was evaluated by carrying out analyses to determine various physical and chemical variables.

PART 2

THEORETICAL CONSIDERATIONS

2.1 Basic Concepts of Colloid Chemistry

A colloidal system is a two-phase system in which one of the phases is dispersed in the other in the form of finely divided particles or droplets. Various types of disperse systems are known depending on whether the physical nature of the two phases are solid, liquid, or gaseous. Colloid particles normally range in size from 1 to 100 millimicrons and are not visible even with the aid of an ordinary high-powered microscope. Because colloidal particles are so small, their surface area in relation to mass is very great. As a result of this large area, surface phenomena predominate and control the behavior of colloidal suspensions.

There are two general types of colloidal solid particle dispersions in liquids. When water is the solvent, these are called the hydrophobic or "water-hating" and the hydrophilic or "water-loving" colloids. In terms of stability, colloidal systems are again divided into two groups. Thermodynamically stable colloidal systems have been named reversible; thermodynamically unstable colloids are termed irreversible (33). Examples of reversible colloids include soap and detergent micelles, proteins, and starches; examples of irreversible systems include clays, metal oxides and microorganisms. In water and wastewater treatment, coagulation is concerned primarily with the aggregation of thermodynamically unstable

(irreversible) colloids.

All colloidal particles are electrically charged. The charge varies considerably in its magnitude with the nature of the colloidal material and may be positive or negative. The sign and magnitude of the primary charge is also affected by pH and ionic content of the aqueous phase. Surface charge develops mostly through preferential adsorption and ionization but regardless of how it is developed, this stability must be overcome if these particles are to be aggregated into larger particles with enough mass to settle easily.

Colloidal particles are bombarded by molecules of the dispersion medium, and because of their small mass, they move in a random manner under the impact of the bombardment. This is known as Brownian movement.

Because colloidal particles have dimensions greater than the average wavelength of white light, they interfere with the passage of light. As a result, a beam of light passing through a colloidal suspension is visible to an observer at right angles to the beam of light. This phenomenon is known as the Tyndall effect.

2.2 Coagulation Theory

In the field of colloid science, two different theories have been presented (29) to explain the basic mechanisms involved in the stability of colloid systems. The first theory is the chemical theory which assumes that colloids are

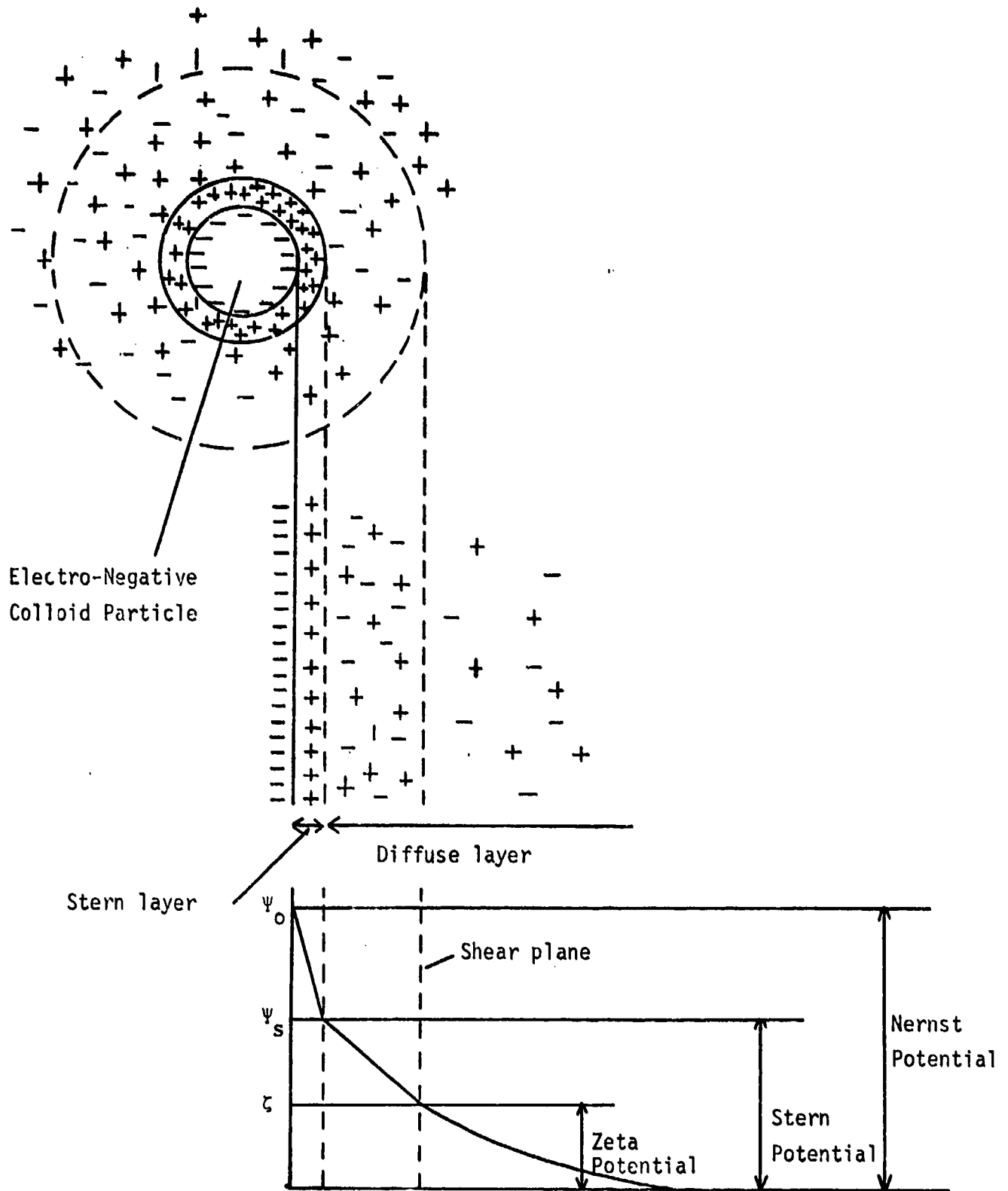
aggregates of definite chemical structural units and emphasizes specific chemical interactions between the coagulant and the colloids. According to this theory, the coagulation of colloids is the result of a precipitation of insoluble complexes that are formed by specific chemical interactions. The second theory—the physical or double-layer theory—emphasizes the importance of the electrical double layers surrounding the colloidal particles in the solutions and the effects of counter-ion adsorption and zeta-potential reduction in the destabilization of colloidal systems. This theory has replaced the older chemical theory and is presented in more detail below. A very recent chemical bridging model has also been proposed as a mechanism in coagulation in the presence of organic polyelectrolytes. This model will be discussed in Section 2.3.

2.2.1 Electrical Double-Layer Theory

The stability of hydrophobic colloids depends on the electrical charge of the particles. Since a colloidal dispersion (the solid and aqueous phases together) does not have a net electrical charge, the primary charge on the particles must be counterbalanced in the aqueous phase. This can be described with the aid of Figure 2.1 (34,17).

When a particle is immersed in aqueous solution, it can develop a surface charge by adsorbing ions denoted as potential determining ions on to its surface. As a result of this surface charge, ions of the opposite charge will be attached to the surface while those of the same sign will be repelled.

Figure 2.1
Electrical Double-Layer of a Colloid Particle



These are known as counter ions and are held there through electrostatic and van der Waals forces. This layer is known as the Stern layer and is of the order of hundreds of angstroms thick which depends on the ionic strength of the solution. The thickness of this layer is such that it contains a sufficient number of counter ions to neutralize the surface charge to preserve electrical neutrality.

Due to the attraction of counter-ions to the surface of the particle, a concentration gradient is formed and there is a diffusion of ions from the surface of the particle toward the bulk of the solution where their concentration is lower. These two competing forces (diffusion and electrostatic attraction) spread the charge over a diffuse layer, within which the excess concentration of counter-ions is highest adjacent to the surface of the particle and decreases gradually with increasing distance from the solid-liquid interface. The overall potential drop between the surface of the particle and the bulk of the solution is the Nernst potential. The potential drop in that part of the diffuse layer between the plane of shear- separating the water bound to the particle from the free water- and the bulk of the solution is called the "Zeta Potential".

2.2.2 Colloid Interactions

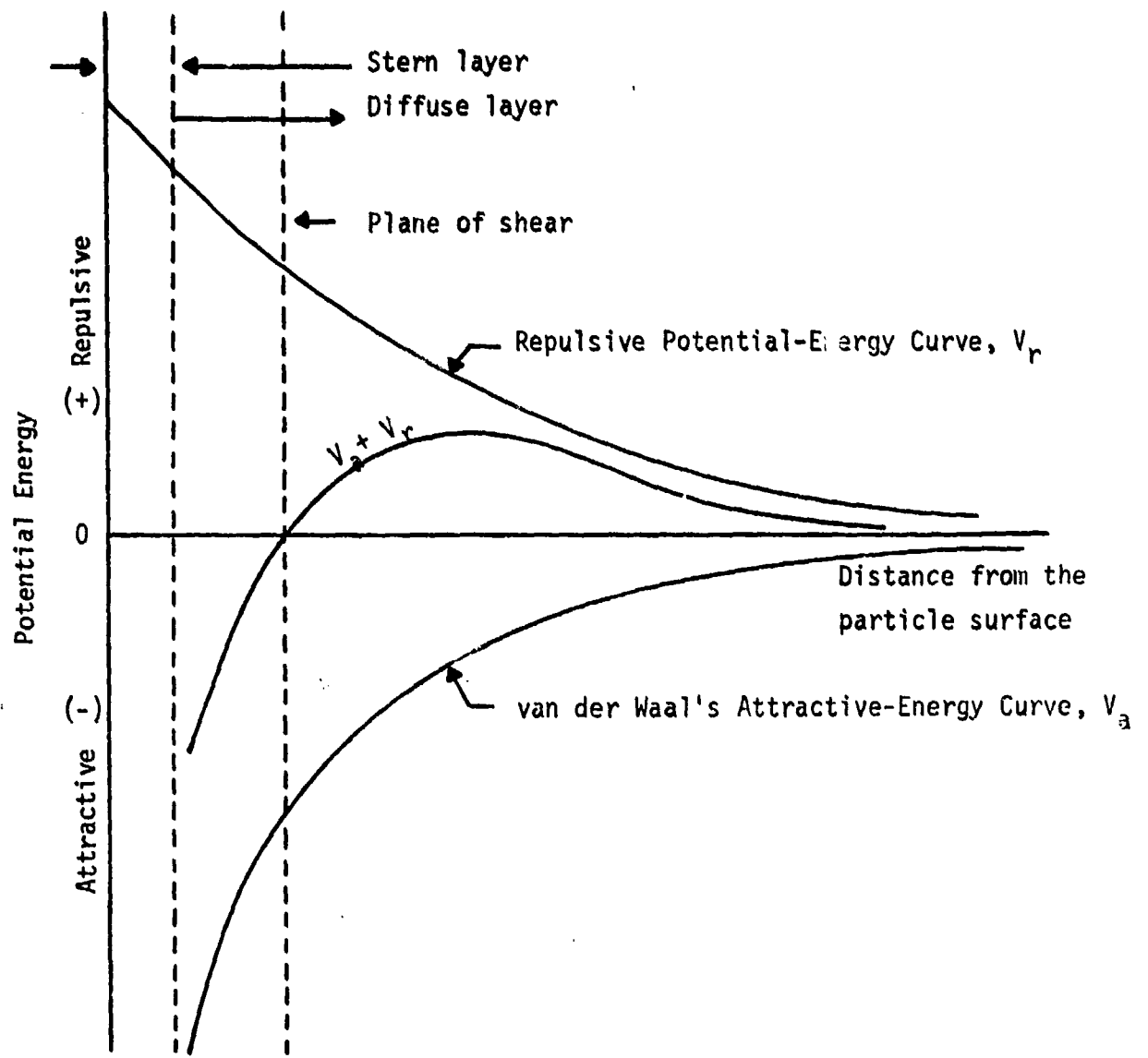
When two colloidal particles having the same sign of charge approach each other, the possibility of their coa-

gulation will depend on the difference in their resultant interaction energy and kinetic energy. The interactions are caused by the electrostatic forces which are repulsive for like charged surfaces and attractive for unlike charged surfaces and the London-van der Waals attraction due to the dipole moments of the materials. These forces operate independently of each other so that their effects are additive. The general form of the potential energy of the particle interaction for two like charged surfaces is shown in Figure 2.2 (34,2).

When two similar colloidal particles approach each other their diffuse layers begin to interact. This electrostatic interaction between particles of similar charge produces a repulsive force. A repulsive potential energy, V_r , arises which increases in magnitude as the distance separating the particles is decreased. There are also the attractive forces that decrease with increasing distance separating the particles which produces the attractive potential energy, V_a . The net interaction energy ($V_r + V_a$) can be determined by summing the repulsive and attractive energies of interaction. This net repulsion can be considered as an activation energy barrier which must be overcome for particle aggregation to occur. As long as the zeta potential is great enough to produce repulsive forces in excess of the van der Waals force, the particles cannot aggregate. The objective of chemical coagulation is to reduce the magnitude of the zeta potential

Figure 2.2

Potential Energy of Interaction of Colloidal Particles



so that repulsive forces between particles are less than the van der Waals forces of attraction. Then coalescence of colloidal particles will occur, and coagulation can be accomplished.

2.3 Destabilization of Colloids

Particle charge reduction and destruction of hydrophobic colloids may be accomplished in the following ways (27):

- 1- Boiling
- 2- Freezing
- 3- Addition of potential determining ions (which will be taken up by or will react with the colloid surface to lessen the surface charge)
- 4- Addition of chemicals that form hydrolyzed metal ions
- 5- Addition of long-chained organic molecules (polymers).

Boiling of a hydrophobic colloidal suspension often results in coagulation of the colloidal particles. This action is not usually attributed to a reduction in the zeta potential but rather to modification in the degree of hydration of the particles, or sometimes to increased kinetic velocities which increases zeta potential requirements to maintain stability. However, boiling is considered to be too expensive for general industrial application.

Freezing is another method for coagulation of colloids. During freezing, due to crystal formation of pure water, the colloidal materials are forced into a concentrated

state. In this way, the zeta potential required to maintain stability increases and at the same time, the concentration of electrolytes increases therefore decreasing the zeta potential. The combined effect is the coagulation of the colloid.

The addition of potential-determining ions will cause them to be taken up and reacted with the colloid surface to lessen the surface charge. An example for this is the addition of strong acids or bases to reduce the charge of metal oxides or hydroxides to near zero, so that coagulation can occur. The addition of electrolytes will reduce the thickness of the diffuse electric layer and thereby reduce the zeta potential.

The trivalent salts of iron and aluminum used in coagulation of water act in several ways. When added to water, these salts ionize to yield trivalent metallic ions, the amount depending on the pH of the water. Some of the trivalent ions neutralize the charge on the colloidal particles but the majority of the trivalent ions form colloidal metallic hydroxides which carry a positive charge. The positive hydrolyzed metal ions are more than sufficient to neutralize the negative charged colloidal particles and the excess remaining is neutralized by the negative ion of the metallic salt. This is a fairly complex process and will not be considered in detail here. For a more complete review on the chemistry of the process, articles by Stumm and Morgan (29) and Stumm and O'Melia (30) are recommended.

Within the last decade, synthetic organic polymers have gained extensive use as destabilizing agents in the treatment of water and wastewater. Although the action of the various polyelectrolytes is quite different, the reason for their use is the same- to improve the removal characteristics of suspended solids. The action of polyelectrolytes as applied to the filtration of wastewater may be divided into two general categories.

In the first category, polyelectrolytes act as coagulants neutralizing the charge of the wastewater particles. Used in this application, polyelectrolytes are considered to be primary coagulants. In principle, once the particle charge has been neutralized, the particles can be flocculated and removed either by settling or filtration or flotation. When polymers are added to the wastewater directly prior to its entry into the filter bed, the upper portions of the filter bed will act as a flocculation basin. By controlling the point of injection, the degree of bed penetration can be varied.

Interparticle bridging is the second mode of action of polyelectrolytes in the application to filtration. Ruehrwein and Ward (26) were the first investigators to propose a polymer-bridging mechanism for the flocculation of highly concentrated clay suspensions. The bridging theory postulates that the polymer molecules attach themselves to the surface of the suspended particles at one or more adsorption site, and that part of the chain extends out into the bulk of the solution. When

these extended chain segments make contact with vacant adsorption sites on other suspended particles, bridges are formed. The particles are bound into small packets that can grow in size limited only by the shear gradient imposed by the degree of agitation.

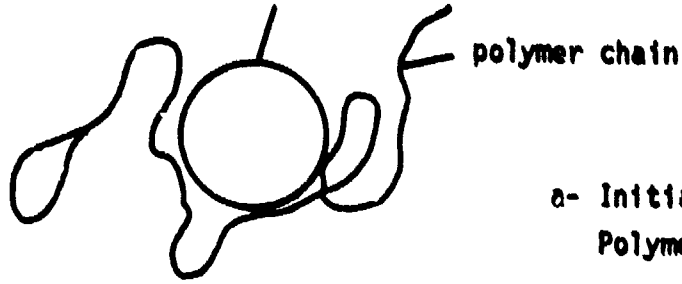
If there is excess polymer in solution, then all the adsorption sites on the particles can be taken up by individual molecules and interparticle bridging will be prohibited because stabilization of the colloid will occur due to the protective adsorbed layer of polymer. This can be understood by the fact that as the concentration increases, more of the available adsorption sites are taken. In order to promote attachment of a suspension particle to a bed particle there must be sufficient free sites on the colloid particle surface so that the free end of a polymer chain attached to the surface of the bed particle can also become attached to the colloid particle. Initially, increasing the polymer concentration promotes the bridging mechanism but when this concentration is too high, adsorption sites are no longer available on either surface of the bed or colloid particles.

Figure 2.3 shows a schematic representation of the bridging model for the destabilization of colloids by polymers. At low polymer concentrations, a large portion of the surface area of each colloidal particle remains exposed, and a given polymer chain can be adsorbed on two or more

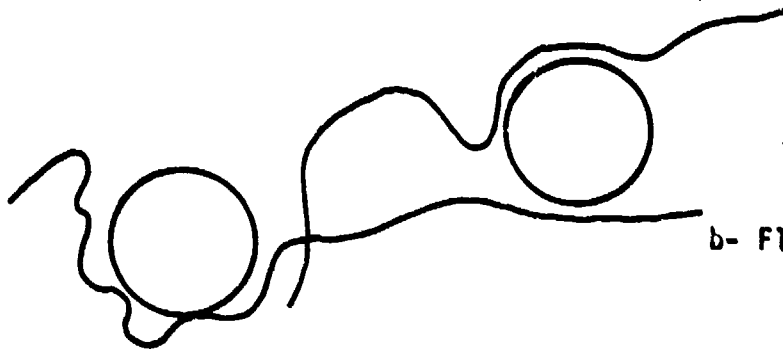
Figure 2.3
Bridging Model for the Destabilization of Colloids
by Polymers

colloid particle

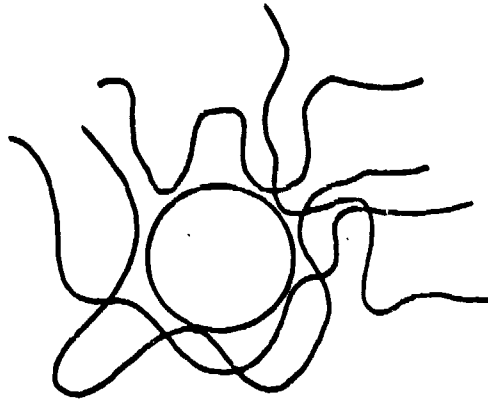
19A



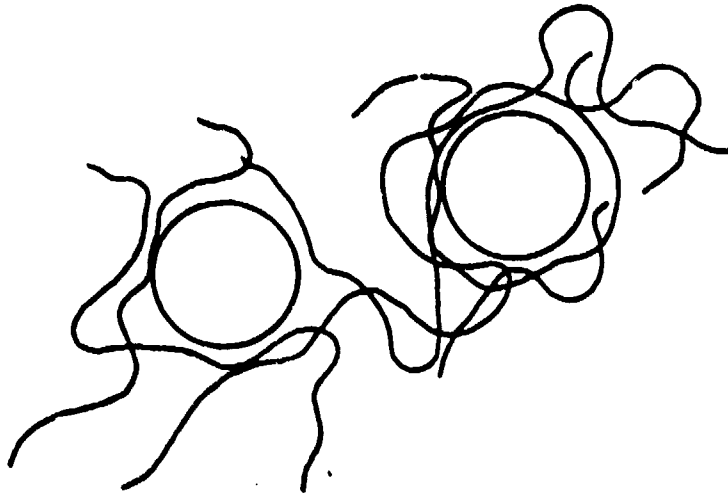
a- Initial Adsorption of
Polymer on Colloid Surface



b- Flocc Formation



c and d- Cases of Overdose of
Polymer (results in
surface coating)

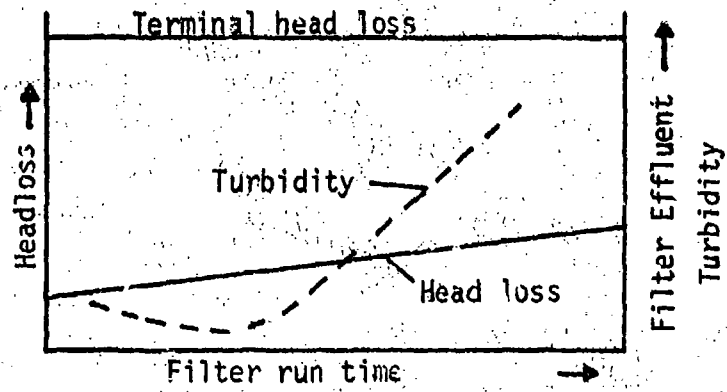


particles (Figure 2.3a and b). Thus, polymer "bridges" are formed which tend to draw the colloidal particles together sufficiently close for the van der Waals attraction between them to become dominant. At higher polymer concentrations, however, each individual colloidal particle becomes covered with polymer chains, and the resultant coatings prevent mutual approach to sufficiently small distances for coagulation to occur (Figure 2.3c and d). In short it can be said that for a given system there is a polymer concentration at which the flocculation efficiency is optimum. Below this concentration, there is insufficient polymer to form bridges, whereas above it the polymer chains coat the particles protectively and floc formation is inhibited.

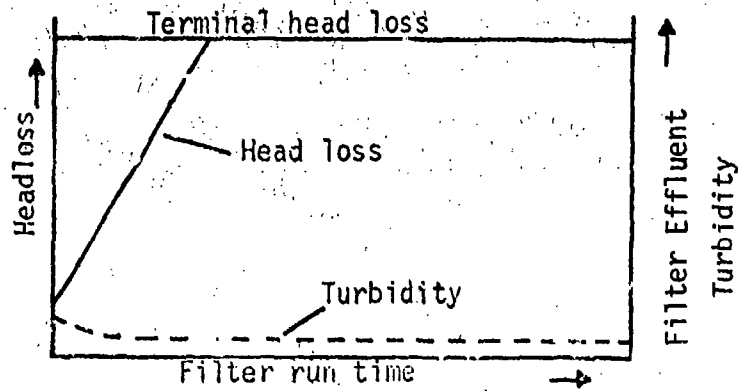
La Mer and Healey (15) have emphasized that the bridging mechanism is more important in forming the flocs than electric-charge effects, for they find that negatively charged polyelectrolytes can be effective in flocculating even negatively charged colloids. They also state that the aggregating action of anionic or non-ionic polyelectrolytes is caused by adsorption (via ester formation or hydrogen bonding) of hydroxyl or amide groups on the solid surfaces with each polymer chain forming bridges between more than one particle.

The effects of polyelectrolytes as filter aids can be seen in Figure 2.4 (4). Figure 2.4.a illustrates the results of a weak floc which penetrates the filter and causes

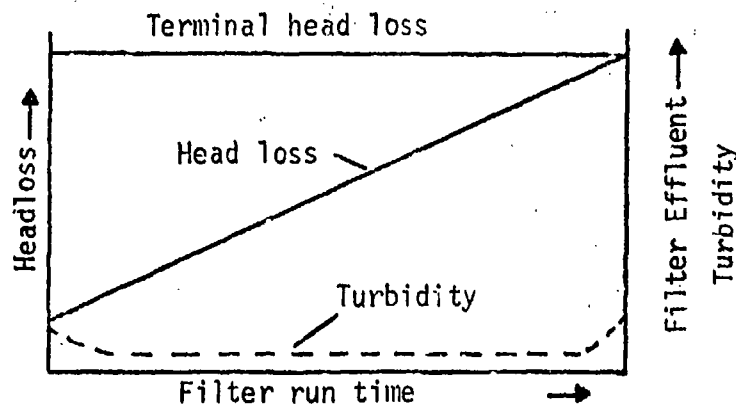
Figure 2.4
Effects of Polymers as Filtration Aids



A- Polymer Dose Inadequate



B- Polymer Dose Excessive



C- Optimum Polymer Dose

termination of the run due to excessive effluent turbidity. If the polymer dose is too high, then the floc is too strong to penetrate through the filter causing a rapidly developing head loss in the upper portion of the filter and the filter run is stopped due to excessive head loss. The optimum polymer dose will cause the terminal head loss to be reached at the same time there is an initial increase in the filter effluent turbidity as can be seen in Figure 2.4.c.

The stabilizing and destabilizing factors influencing coagulation and flocculation of colloids and the characteristics of the two particle destabilization theories discussed in this section are shown respectively in Tables 2.1 (11) and 2.2 (17).

2.4 Mechanisms and Mathematical Models of Filtration

Although water filtration is among the most widely used and extensively investigated process in the field of sanitary engineering, a clear understanding of the mechanisms by which particle removal takes place is not yet available and pilot testing has still remained necessary as a basis for filter design.

The basic theories in filtration can be classified as physical and chemical. Physical filtration theories consider the physical characteristics of the filter bed, its method of operation and the suspension under treatment. These theories deal mostly with media size, filtration rate and

Table 2.1

Factors Influencing Coagulation and Flocculation

<u>Stabilizing Factors</u>	<u>Destabilizing Factors</u>
1- Electric double layer repulsion	1- Reduction of zeta potential to a critical value where attractive forces are predominant
2- Short range hydration repulsion (caused by adsorption of solvent)	2- Bridging of particles with the proper flocculant
3- Protective colloids (adsorption of a protective layer on the particles)	

Table 2.2

Modes of Destabilization and their Proposed Characteristics

<u>Phenomena</u>	<u>Physical Double-Layer Theory</u>	<u>Chemical Bridging Model</u>
Electrostatic interaction	Predominant	Subordinate
Chemical interactions and adsorption	Absent	Predominant
Zeta potential for optimum aggregation	Near zero	Usually not zero
Addition of an excess of destabilizing species	No effect	Restabilization due to complete surface coverage
Relationship between optimum dosage of destabilizing species and the concentration of colloid	Critical coagulant concentration independent of colloid concentration	Stoichiometry, a linear relationship between flocculant dose and surface area
Physical properties of flocs	Dense, great shear strength but poor filtrability in cake filtration	Flocs of three-dimensional structure; low shear strength but excellent filtrability in cake filtration

water temperature. Theories which consider the chemical characteristics of the aqueous phase and the surface characteristics of the suspended particles and the filter media are called chemical filtration theories.

2.4.1 Physical Filtration Theories

The investigations of Ives (11) represent the best available in the field of water filtration theory. He begins with two equations suggested by Iwasaki (13) in 1937:

$$-\frac{\partial C}{\partial L} = \lambda C \quad (1)$$

$$\frac{\partial \sigma}{\partial t} + \frac{v}{1-\epsilon_{\sigma}} \frac{\partial C}{\partial L} = 0 \quad (2)$$

where C = volumetric concentration of material entering
a unit

L = filter depth

λ = coefficient of proportionality (filter coefficient)

t = filtration time

σ = volume of suspended material retained per unit
of filter volume

ϵ_{σ} = porosity of deposited material

v = superficial filtration velocity

Equation 1 states that the removal of suspended particles is proportional to the concentration of particles present in the water. Equation 2 is based upon a mass balance and states that the volume of material accumulated in the filter equals the volume removed from suspension. This assumes

that the density and porosity of the deposited material do not change during the course of a filtration run, and biologic and chemical reactions do not cause soluble materials to either accumulate in the deposits or be released from them.

The filter coefficient (λ) varies with time and depth in the filter and is a function of the specific deposit (σ). Ives has developed a general relationship between λ and σ based on the hypothesis that the filter coefficient is a function of the changing specific filter surface (surface area per unit filter volume) available for deposition and the increasing interstitial velocity. He proposed that:

$$\lambda = \lambda_0 + C\sigma - \frac{\phi\sigma^2}{(\epsilon - \sigma)} \quad (3)$$

where λ_0 , C and ϕ are filter coefficient constants and ϵ is the initial filter bed porosity. Equation 3 is an empirical expression which describes the variation of the filter coefficient with the specific deposit.

Substitution of Equation 3 in Equation 1 yields:

$$-\frac{\partial C}{\partial L} = \left(\lambda_0 + C\sigma - \frac{\phi\sigma^2}{\epsilon - \sigma} \right) C \quad (4)$$

Equations 2 and 4 describe the changes in filtrate quality with depth and time. Equation 4 can only be solved incrementally using a digital computer, but the constants in the equation must first be evaluated empirically which introduces

a number of difficulties. One of the difficulties is that the specific deposit must be expressed in units of volume per unit filter volume. However, water quality at any depth is usually measured in units of mg/l or in turbidity units. The relation between these units and the desired specific deposit units is difficult to obtain.

Fox and Cleasby (6) point out some of the difficulties and deficiencies of the Ives' filtration model. They state that the assumptions made in deriving the model were too general and oversimplifying. These assumptions are:

- 1- The suspended material is a homogeneous, discrete, unisize floc which is more dense than the fluid and about two orders of magnitude smaller than the filter pores.
- 2- The filter medium is granular, homogeneous and unisize.
- 3- The fluid is in laminar flow.

The Ives' filtration equation was developed using the experimental results obtained in the filtration of algae. The authors state that this equation cannot be extended to a floc such as hydrous ferric oxide floc since it is not of uniform size and has low density. In general, it seems that, because so many variables affect the removal of solids in sand filters, all of them cannot be included and correlated in one filtration equation.

Ives has also shown that rate of head loss development

in the filter is a function of specific deposit. The well known Carmen-Kozeny equation for head loss through porous media is as follows:

$$h_f = f' \left(\frac{L}{\phi_s D_p} \right) \left(\frac{1-\epsilon}{\epsilon^3} \right) \left(\frac{\bar{v}_s}{g_c} \right) \quad (5)$$

$$f' = 150 \frac{1-\epsilon}{N_{Re}} + 1.75 \quad (6)$$

where h_f = frictional head loss across bed, (ft)(lb force)/
(lb mass)

L = depth of bed, ft

ϕ_s = particle shape factor, dimensionless

D_p = particle diameter, ft

ϵ = bed porosity, dimensionless

\bar{v}_s = superficial velocity, ft/sec

g_c = Newton's Law conversion factor, (ft)(lb mass)/
(lb force)(sec²)

N_{Re} = Reynold's Number, dimensionless

Beginning with this equation, Ives developed the following expression for the rate of head loss development in the filter:

$$\frac{\partial h_f}{\partial L} = \left(\frac{\partial h_f}{\partial L} \right)_{L=0} + k \quad (7)$$

where k is a head loss constant. Thus the head loss can be approximated by the initial head loss (determined from the Carmen-Kozeny equation) plus a constant times the specific

deposit. Ives reported that integration of this equation through the full filter depth, when the filter concentration is small (less than 5%) of the influent concentration, leads to a linear head loss versus time curve.

In order to use the equation developed by Ives, it is necessary to determine experimentally the set of five coefficients ($\lambda_0, C, \phi, k, \epsilon_0$) for each filter bed, flow rate and pretreatment condition to be used. Ives and Sholji (12) have investigated the effects of certain physical filtration variables on the filter coefficient and have reported that for the particulate suspension used, the filter coefficient is inversely proportional to the filtration rate, the filter grain size and the square of the viscosity of water.

2.4.2 Chemical Filtration Theories

In recent years some investigators have directed attention to the effects of chemical parameters on the filtration process. To some extent these investigations have been motivated by the inability of physical theories to explain observed filtration data or to predict filter performance.

O'Melia (22) and Yao (35), et al. have developed models of filtration focusing on the basic mechanisms involved in suspended solids removal. They state that until now only the physical phenomena were considered in design. The important role of electrochemical phenomena in filtration

and the similarities between it and coagulation are now being realised. Electrokinetic and chemical phenomena are important in filtration because it has been observed that the surface charge of the bed and the particles are significant factors in determining and controlling the removal efficiency of the filter. Efficient filtration is a physical-chemical process involving particle destabilization and particle transport similar to the mechanisms of coagulation. Good coagulants are also efficient filter aids and the processes of coagulation and filtration are inseparable, therefore interrelationships must be considered for best treatment results.

The removal of suspended solids by a granular filter is very complex. Removal of solids by the filter may be primarily at the bed's surface by the formation of a cake of removed solids and is accomplished by a simple mechanical straining mechanism. Removal efficiency should improve with time, but due to the cake's compressibility, an exponential head loss development is observed.

More commonly, however, removal of suspended solids takes place within the filter bed (depth filtration). Efficiency during depth removal depends on a number of mechanisms. Some solids are removed by interstitial straining. Removal of other solids, particularly the smaller solids, depends on other mechanisms outlined below. O'Melia and Stumm (22) present a filtration model by considering that suspended particle removal within a filter bed involves two separate steps:

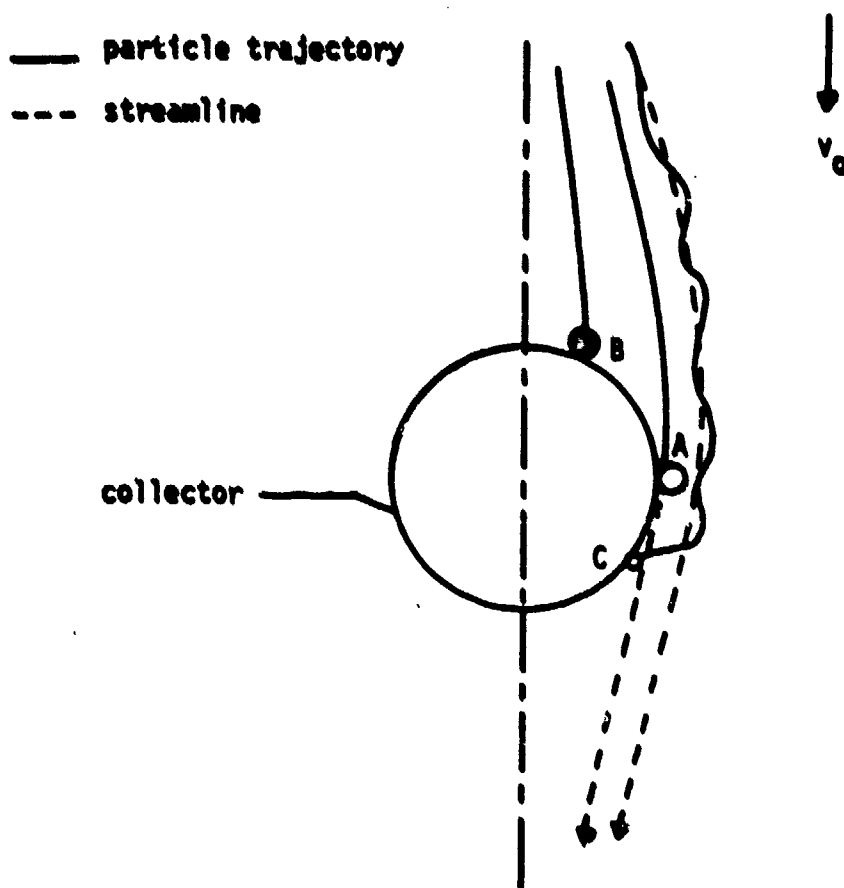
- 1- Transport of the suspended particles to the filter surface,
- 2- Attachment of the particles to the filter media.

Particle transport is a physical-hydraulic process consisting of phenomena such as straining, sedimentation, inertial impingement, interception and Brownian diffusion whereas particle attachment is basically an electrochemical process influenced by both physical and chemical parameters. Both of these steps are rate controlling in water filtration but the predominance of one over the other is dependent on the size of the particles being filtered. For large particles (diameter $> 30\mu$), the physical phenomena control the rate of filtration while for smaller particles (diameter $\leq 1\mu$) the chemical effects are rate controlling. For intermediate particle sizes ($3\mu - 30\mu$) both mechanisms are important.

Figure 2.5 (35) shows the basic transport mechanisms in water filtration. The collector is a single particle of filter media. The main flow direction is that of the gravitational force. A suspended particle following a streamline of the flow may come in contact with the collector by virtue of its own size (case A); this transport process is interception. If the density of the suspended particle is greater than that of water, the particle will follow a trajectory due to the influence of the gravitational field (case B); this process is sedimentation. Finally, a particle in suspension is subject to random bombardment by molecules of the suspending medium resulting in

Figure 2.5

Particle Transport Mechanisms in Granular Filters



Brownian movement of the particle; this mass transport is called diffusion (case C). Transport mechanisms are also affected by physical characteristics such as media size, filtration rate and fluid temperature.

As the particle approaches the surface of the medium or previously deposited solids on the medium, an attachment mechanism is required to retain the particle. Particle attachment, like particle transport, can be accomplished by a number of different mechanisms. The attachment mechanism may involve electrostatic interactions, chemical bridging, or specific adsorption, all of which are affected by the coagulants applied in the pretreatment and by the chemical characteristics of the water and the filter medium.

In actual filtration practice, removal results from a combination of these mechanisms. As a filter run progresses, the dominant transport and attachment mechanisms may change, causing unusual and different patterns of effluent quality and head loss behavior.

O'Melia and Yao, et al. (22,35) developed their model by trying to show the similarities between coagulation and filtration processes. In coagulation, the overall rate of aggregation is evaluated by determining the rate at which collisions occur between particles by fluid motion (orthokinetic flocculation) and by Brownian diffusion (perikinetic flocculation), multiplied by a "collision efficiency factor". It is stated that a similar approach should be used in establishing

a model for filtration processes. In both processes, the particles to be removed are destabilized and must be transported so that contacts can occur. In water filtration transport models are being derived which are based on models developed by investigators in air filtration (8). These models predict that suspended particles larger than about 1 micron are transported to the filter media by settling and interception and smaller particles are transported by Brownian diffusion.

The model is stated in terms of a single collector efficiency, η_c , defined as the rate at which particles strike the collector divided by the rate at which particles flow toward the collector:

$$\eta_c = \frac{\text{rate at which particles strike the collector}}{V_o C_o \left(\frac{\pi d_c^2}{4}\right)} \quad (8)$$

where V_o = velocity of particles

C_o = concentration of particles

Separate equations for each transport mechanism have been developed. For diffusion:

$$(\eta_c)_D = 4.04 \text{ Pe}^{-2/3} \quad (9)$$

where $\text{Pe} = \text{Peclet number}$

$$\left(\frac{v d_c}{D_p}\right)$$

d_c = collector diameter

D_p = particle diffusivity

v = velocity of particle

at an infinite distance
from the collector

For interception:

$$(\eta_c)_I = \frac{3}{2} \left(\frac{d_p}{d_c} \right)^2 \quad (10)$$

where d_p = particle diameter.

For sedimentation (based on Stoke's Law):

$$(\eta_c)_G = \frac{(\rho_s - \rho_l) g d_p^2}{18 \mu v} \quad (11)$$

where ρ_s = mass density of solid particle

ρ_l = mass density of the liquid

μ = viscosity of the liquid

The overall single collector efficiency is approximated by the sum of the individual expressions:

$$\eta_c = (\eta_c)_D + (\eta_c)_I + (\eta_c)_G \quad (12)$$

This expression can be substituted into Iwasaki's Equation 1 with modifications as follows:

$$\frac{\partial C}{\partial L} = - \frac{3}{2} \left[\frac{(1-\epsilon)}{d_c} \right] \eta_c C \quad (13)$$

where η = collision efficiency factor

= number of contacts which succeed in producing adhesion

no. of collisions which occur between particle and media

= 1.0 in completely destabilized system.

Integration of Equation 13 leads to:

$$\ln \frac{C}{C_0} = - \frac{3}{2} (1-\epsilon) n_c \frac{L}{d_c}$$

or,

$$C = C_0 \times \exp \left[- \frac{3}{2} (1-\epsilon) n_c \frac{L}{d_c} \right]$$

Yao et al. (35) concluded that the conventional deep granular filters provide ample contact opportunities for removal of all particles which are applied to them. If filters are not producing efficient removal of suspended solids, the chemical pretreatment should be changed to alter the collision efficiency factor.

PART 3

LITERATURE REVIEW

Until recent years, the principal application of filtration has been in the area of surface and ground water treatment for municipal use therefore most of the information in the literature on the design and operation of granular multi-media filters has been based on experiences in potable water filtration. With the current trend of higher quality standards for wastewater effluents, granular filtration is becoming increasingly more important as a tertiary wastewater treatment operation. The continued use of granular filters for wastewater applications led to the development of new pretreatment methods, an important one being the use of synthetic organic polyelectrolytes as primary coagulants, coagulant aids and as filter aids. While significant advances have been reported, investigations are continuing in order to achieve further improvement in filter operation.

3.1 Early History

The first water filters used were the small sand beds constructed in 1804 by John Gibb in Paisley, Scotland and the large sand beds built by James Simpson in 1828 in London, England (5). These filters were operated at low flow rates of 0.04 to 0.12 gallons per minute per square foot (gpm/sq ft). The first filter of this kind introduced in the United States was in 1872 by James P. Kirkwood on the Hudson

River in Poughkeepsie, N.Y. These filters were not generally successful on American waters due to their relatively higher turbidity and this led to the development of coagulation and sedimentation operations preceding rapid sand filtration (1 to 4 gpm/sq ft).

Slow and rapid sand filters differ not only in the rate of flow of water through the sand bed but also in design, construction and operation. Aside from their low hydraulic loading, some of the distinguishing features of slow sand filters are the small effective size and large coefficient of nonuniformity of the grains and the unstratified grain size distribution of the sand in the filter bed. The penetration of suspended matter is very superficial compared with the rapid sand filter causing surface removal of wastewater suspended solids by mechanical straining within several inches of the top layer of the bed. The length of runs are usually 30-40 days compared with 24-36 hr for a rapid sand filter. Regeneration of the filter bed is also carried out differently for the two types of filters. The slow sand filter is cleaned by scraping and removing from the filter an inch or two of sand from the surface of the bed. The sand is washed and either placed back on the bed immediately or put in the storage bins and replaced after several scrapings and cleanings have accumulated. Because rapid sand filters operate at many times the rate of slow sand filters, they need to be cleaned many times as often. The filter units are washed from below with

previously filtered water, which by fluidizing the bed, dislodges and removes the suspended matter trapped in the sand. After the bed has been washed clean, it settles back into place. This also causes a stratification of the bed. The amount of wash water used in cleaning is 0.2 to 0.6% of filtered water for a slow sand filter and 4 to 6 % of filtered water for a rapid sand filter.

The first sizable, municipal, rapid filter-plant was designed by George W. Fuller for Little Falls, N.J. in 1909. Although the high rates of flow and the backwashing operation complicate the hydraulic design, rapid sand filters have almost totally replaced slow filters in North American practice. This is explained by their convenience in size, adaptability to changing raw-water quality, and over-all economy of construction and operation under North American conditions.

3.2 Wastewater Applications

In advanced wastewater treatment, granular filters are being used for the removal of:

- 1- the biological floc from settled secondary treatment plant effluent,
- 2- the precipitates resulting from alum, iron or lime precipitation of phosphates,
- 3- solids remaining after the chemical coagulation of wastewaters in physical-chemical waste treatment operation.

As an example of the first type of wastewater application stated above, Tchobanoglous (32) has investigated the filtration of an effluent from an activated sludge treatment plant with and without chemical additions. The chemicals used were two different cationic polyelectrolytes which were added as primary coagulants to the settled effluent. He concluded that the effluent filtration without the addition of chemicals is relatively ineffective in terms of turbidity removal and is primarily a function of the grain size of the filter material. For a filtration rate of 5 gpm/sq ft, the removal efficiency varies from 15% for a sand size of 1.0 mm to 40% for a sand size of 0.5 mm. These values represent the removal at 1 inch below the top of the sand and are independent of time. He has reported that other factors which influence the removal efficiency are the rate of filtration and the characteristics of the settled effluent. However, it is indicated that sand size has a more pronounced effect on removal efficiency than the rate of filtration. For a sand size of 0.68 mm, the removal efficiencies at 1 inch below the top of the filter media are 23% and 18% for corresponding flow rates of 2 gpm/sq ft and 10 gpm/sq ft, respectively. Among the important characteristics of the settled effluent stated that affect removal efficiency are the suspended solids concentration, particle size distribution and surface charge.

It was observed that the efficiency of the filtration can be controlled effectively by the quantity and type of polyelectrolyte added to the settled effluent. The effects of adding a cationic polyelectrolyte to wastewater effluent were evaluated using dual medium filter beds which consisted of an anthracite layer of 12 in. placed over a sand layer of 8 in. Typical results obtained in a run are shown in the table below:

Run Data

Column area (sq ft)	0.11
Filtration rate (gpm/sq ft).....	5.15
Length of run (hr)	4.5
Total volume filtered (l)	580
Influent SS concentration (mg/l)	23.5
Polyelectrolyte dosage (mg/l)	20
Effluent SS concentration (mg/l)	1.0

Mass Balance Analysis

Total SS in influent (mg)	13,650
Total SS in effluent (mg)	580
Quantity theoretically removed in column (mg)	13,070

Experimental Data

Suspended solids removed

12,300

It is seen from the table that the calculated theoretical value and the experimental value for the amount of suspended solids removed are very close. With the use of polymers,

it is also observed that the removal of suspended solids is 91%. Results of experiments using cationic polyelectrolytes indicate that the point of zero electrophoretic mobility does not correspond to the condition which produces the best filtration results. In the filtration of settled effluent, best results were obtained when the mobility of the influent particles was in the range of -0.6 to $-0.2 \mu/\text{sec}/\text{v}/\text{cm}$ (microns/second/volt/centimeter).

The advantages and economics of a mixed-media filter for tertiary treatment are discussed by Shireman (28). Filtration is used as a polishing process to remove any solids carried over from secondary or chemical clarifiers used in the preceding treatment of wastewater. The use of filter aids such as lime, alum or polymers are strongly suggested for greater removal efficiency. Typical removals by the mixed media beds at the South Lake Tahoe P.U.D. Wastewater Treatment Plant are reported below. In this process, lime was used as a primary coagulant in a conventional clarifier and recarbonated to pH 7.0 before application to the beds.

<u>Substance</u>	<u>Influent conc.</u>	<u>Effluent conc.</u>	<u>% Removal</u>
Phos.total (mg/l)	0.65	0.05	70-99
Phos.dissolved (mg/l)	0.45	0.05	65-90
Phos.particulate (mg/l)	0.20	0.00	100
COD (mg/l)	23	15	15-50
BOD (mg/l)	9	4	30-80
SS (mg/l)	15	0	80-100
Turbidity (JTU)	7.0	0.2	60-95

It should be noted from the results in the table that the removal of soluble phosphorus by the separation beds is something that could not possibly be achieved in a surface filter. The COD reduction in the beds reduces the COD load applied to the carbon columns and the BOD in the filter influent is low enough to meet strict effluent standards even without further treatment by carbon adsorption.

Treatment of oily wastewater streams generated by refineries, petrochemical complexes, steel finishing mills and machine shops has recently been investigated by Nebolsine (20). Deep bed high rate industrial type filters were used to treat discharges from finishing stands of hot rolling mills of steel plants. The main contaminant that the filters removed consisted of fine mill scale. However, it was found that a large portion of the oils carried by these discharges was also intercepted. This led to the design of filter units especially adapted to treat oily waste streams. The design of these units differed mainly in the backwash mechanism. Air is used for backwashing and in some cases heat is applied to keep the media from getting clogged with oil. The standard filter units were cylindrical steel tanks operated under pressure 6 to 15 ft in diameter and 12 to 20 ft in height, having a filter depth of 5 ft which usually consisted of coarse sand. Under these conditions, it was found that due to the effect of agglomeration, adsorption and straining, up to 95% of the free oils and suspended

solids as well as a part of the emulsified oils could be removed from an influent containing 150 to 500 mg/l of total oils. It was reported that no bulk chemicals were used, but under some conditions the application of small doses of polyelectrolytes as filter aids could be required to achieve the desired degree of oil removal.

3.3 The Use of Polyelectrolytes in Filtration

Polyelectrolytes have been used basically in two distinct areas in filtration operations. These include the use of polyelectrolytes as either a primary coagulant or as a filter aid or in some cases both. Although much work has been carried out in the application of synthetic polyelectrolytes as primary coagulants in the treatment of potable water, only few investigations have been reported in the application of polyelectrolytes as direct filter aids.

Pressman (24) has conducted studies testing the effectiveness of cationic polyelectrolytes as prime coagulants in natural-water treatment. Initially a series of laboratory jar tests were carried out using eight cationic polyelectrolytes, Potomac River water, and, for comparative purposes, natural water from four other area sources. The jar tests revealed that after the polymer was added, the negative charge on the turbidity particles was reduced and increasing flocculation took place and reached its optimum as the zeta potential was reduced to a value near zero (± 5 mV). If the dosage of polymer was increased beyond the optimum, a charge reversal

and dispersion of turbidity particles took place causing the residual turbidity and the zeta potential to increase. Optimum flocculation dosages of polymer were in the range of 2-5 ppm with waters of less than 120 units of settled turbidity. The predominant factor determining the optimum dosage was the nature of the water being treated rather than the specific type of polymer used. It was also noted that lower optimum dosages of polymer were required for lower pH conditions. At a high pH charge reversal took place at increasingly higher dosages of polymer.

Larson et al. (16) have carried out studies using polyelectrolytes in treatment of combined meat-packing and domestic wastes. After various preliminary jar test determinations, it was found that a dual system of ferric chloride and a high-molecular-weight anionic organic polyelectrolyte decreased suspended solids concentration by 100 mg/l and BOD by 140 mg/l, leaving effluent concentrations of 120 mg/l and 550 mg/l, respectively. These results are not the best that could be obtained although the authors state that this system proved to be the most successful. The primary flocculation of the colloidal and fine particles by the ferric chloride produced a small floc that was further increased in size and density by the secondary flocculation of the organic polyelectrolyte, producing a settleable precipitate.

Freese and Hicks (7) report that high-molecular-weight organic polyelectrolytes have been used successfully

to flocculate raw wastewater and to increase the removal of pollutants from the wastewater during primary sedimentation. Three polymers, Dow's anionic A-21*, modified with cationic C-31*, Hercules' cationic Reten 210*, and Calgon's anionic ST 269* were added to raw wastewater for flocculation in a plant with a capacity of 240 million gallons per day (MGD).

Various polyelectrolytes were tested for coagulation of paper mill wastes by Suzuki (31). Nonionic polyacrylamide was the most effective for the purification and up to 80% removal of pulp fiber was obtained in a wide range of pH tested. Anionic polyelectrolytes such as sodium alginate and sodium polyacrylate, however, dispersed the suspension of pulp fiber instead of coagulating it. The use of polyelectrolytes for coagulation of pulp mill waste was advised if the waste contained large fiber colloids.

Another application of polyelectrolytes in coagulation of municipal wastewater was carried out by Mints et al. (18). Sewage was treated with a 1-2% solution of a cationic polyelectrolyte followed by one hour of sedimentation and filtration on sand filters. The content of suspended matter was reduced by 72, COD by 50.5, BOD₅ by 58% before filtration and by 97, 74, and 82% respectively, after filtration. The purified water had a BOD of 20, COD of 60 and suspended matter of 2 mg/l. The presence of heavy metals (Cr⁺⁶, Cu⁺²) and

* commercial designations.

dyes or surface active substances did not affect the purification process.

The effects of polyelectrolytes as a filter aid have been investigated by Garnell (9). Separan NP 10*, anionic potable-water grade, a product of Dow Chemical Co., Midland, Mich. which is a polyacrylamide with a molecular weight of approximately 1,000,000 was used in the experiments. The polyelectrolyte was diluted to a 0.05 per cent concentration in a 50-gallon drum and fed directly to the applied water as it entered the filter. During each test the filtered-water turbidity ranged from 0.3 to 0.4 units. Applied water turbidities varied from 2 to 15 units and water temperature from 33° to 70° F. Filter rates were 2-5 gpm/sq ft and the effective size of the sand 0.60 mm. It was concluded that with dosages of 10-30 ppb applied directly to the filters, polyacrylamide effectively reduced filtered-water turbidity. At a continuous dosage of 20 ppb the effluent turbidity was reduced from 0.5 to less than 0.1 units in about 2 hr. If dosing was discontinued, turbidity reappeared after approximately 2 hr.

Conley and Pitman (3) have conducted filtration tests on Columbia River water using polyelectrolytes as filter aids. It has been determined that various materials can be applied directly to the filters in such a manner as to cause floc particles to adhere to the filter grains very

* commercial designation.

strongly. This process is called filter conditioning. They have observed that the continuous application of a polyacrylamide solution (5-50 ppb) improved the filtrability of alum floc particles and postulated that the polymer bound the floc particles both to the filter and to each other. Filter conditioning also made it possible to filter water at very high rates (10-15 gpm/sq ft) without excessive head loss. The resulting filtered water was very clear with less than 0.01 ppm turbidity.

Conley and Hsiung (10) have reported that the addition of polymers to the filter influent have greatly increased the efficiency of filtration. When a polyelectrolyte coagulant (polyacrylamide) was applied immediately ahead of the filter, the performance of the filtration changed substantially. With an influent of 30 standard turbidity units and a 24" multi-media bed operated at a rate of 5 gpm/sq ft without polyacrylamide, the effluent turbidity was 17 JTU at the end of 4 hr. The effluent turbidity was 0.2 JTU under the same conditions, when 0.1 mg/l of polyacrylamide was applied directly to the filter. The head loss changed from 3 to 6 ft when using the polyacrylamide as a filter aid for the same length of filter run.

Robeck et al. (25) conducted pilot plant studies with turbid water from the Little Miami River (Cincinnati, Ohio). They used activated silica in many runs, but also made a run using a synthetic polyelectrolyte (Purifloc, by Dow Chem. Co.)

which was fed into one of two filter influents. Although the raw water turbidity was low, the filter with no polyelectrolyte added to the filter influent had a breakthrough after 16 hr at a head loss of 2 ft. With a dosage of 0.08 mg/l of polyelectrolyte in the other filter, excellent quality water was produced for 22 hr with a 4 ft head loss. Thus, it was noted that head loss is greater when a polyelectrolyte is used.

O'Melia (21) has carried out research to determine how destabilizing chemicals such as polyelectrolytes function in improving the effectiveness of filtration processes, and to consider selected applications of destabilizing chemicals in filtration for wastewater treatment. The investigations included laboratory experiments using polymers and latex suspensions; laboratory and pilot plant experiments using alum, polymers and calcium phosphate suspensions. Five homologs of polyethylenimine (PEI series, Dow Chem.Co.) with molecular weights of 600, 1200, 1800, 40-60,000 and 50-100,000 were used. It was reported that overdosing of polymers can occur due to restabilization of the suspended particles. For the cationic polymer series investigated, the optimum polymer dosage was independent of the molecular weight of the polymer, but the removal efficiency of filters operated at this optimum dosage increased with increasing molecular weight.

Adin and Rebhun (1) have carried out the most recent investigation of the application of polyelectrolytes to the filtration process. They have proposed a direct, high-rate

filtration system for low turbidity waters thus eliminating the need for costly flocculation and sedimentation basins. Contact-flocculation-filtration, as it is called, is carried out by feeding the flocculant into the suspension immediately before it enters the filter, to bring about a strong attachment of the particles to the grains, and to take optimal advantage of the capacity of the bed. A cationic polyelectrolyte, polydialkyl-dimethylammonium halide, was used as flocculant and polymer doses of 0.05-0.06 mg/l gave the best removal in filtration for an influent suspended solids concentration of 20 mg/l. It has been concluded that this process of contact flocculation-filtration allows particulate removal from dilute suspensions without the need for separate flocculation and settling units.

PART 4

APPARATUS AND PROCEDURES

4.1 Design of Experimental Study

The experimental investigations can be divided into two groups: 1- batch jar tests and 2- continuous filtration experiments. Batch jar tests were initially carried out to test the effectiveness (efficient turbidity removal) of various polymers on the wastewater being tested. Six polymers were used in the experiments to determine optimum type and dosage. In some of the tests, optimum pH for the particular polymer was also determined. The parameters measured in the jar test studies were residual turbidity, residual pH, residual net colloidal charge and in some cases total organic carbon (TOC). The effects of coagulant aids such as bentonite clay and lime with and without the addition of polymers were also investigated. Powdered carbon adsorption studies were carried out using the jar test apparatus. The continuous filtration runs were based mainly on the results obtained in the jar tests. Optimum polymer type, optimum dosage and the most effective coagulant aid were selected to be used in the filtration runs. Two types of continuous filtration runs were carried out: 1- Conventional treatment- the coagulant aid and polymer were added to the wastewater. After initial rapid mixing and flocculation, the system was allowed to settle and the supernatant was pumped directly to the filter. 2- Direct addition of polymer- the wastewater and polymer were pumped

separately and contact occurred just prior to entering the filter media. The effluent from the filter was analyzed for TOC, turbidity, pH and colloidal charge. Head loss measurements were taken at periodic intervals. The effect of filtration rate on the effluent quality and head loss was also investigated.

4.2 Materials Used

4.2.1 Synthetic Wastewater

Synthetic wastewater was prepared for the initial experiments to study the basic mechanisms of polymer action in turbidity removal. It had the advantage of having a supply of wastewater constant in concentration and characteristics.

The following components were used:

1- Bentonite clay (USP Volclay- supplied by American Colloid Company, Stokie, Illinois).

Concentration: 500 mg/l

2- Laundry detergent (Tide, manufactured by Procter and Gamble, Cincinnati, Ohio).

Concentration: 100 mg/l

3- Motor oil (Penetrex W-30, Non-detergent, manufactured by Quaker Oil Corporation, St. Louis, Missouri).

Concentration: 50 mg/l

4- Tap water (Laboratory tap water at RPI, Troy, N.Y.)

Technical data on bentonite clay can be found in the Appendix (Table A-1).

According to the formulation of the wastewater, the measured amounts of clay, detergent and oil were placed in a 55 gallon polyethylene tank with tap water and mixed rapidly with a heavy duty mixer for 15 minutes. The mixture was always mixed again rapidly before any samples were taken for jar tests to ensure uniformity. No temperature or pH adjustments were made.

4.2.2 Actual Wastewater

The actual colloidal wastewater was supplied by the U.S. Army Radford Ammunition Plant in Radford, Virginia. The wastewater was generated from a nitrocellulose process and was termed the "alcohol rectification waste". A brief look at the nitrocellulose process where the waste is generated can be helpful.

Nitrocellulose (cellulose nitrate) is made by treating cotton linters or wood pulp cellulose with mixed nitric and sulfuric acids at 30-34°C for about 25 minutes. After this treatment, most of the acid is removed by "drowning" the material in water. This product is then treated with boiling dilute sulfuric acid for 70 hours. Following this, the product is beaten and cut in alkaline water to remove the residual acid and to reduce the average fiber length. It is then washed and screened to remove the water. Nitrocellulose powder is a highly flammable material and therefore should be handled with appropriate precautions.

The wastewater was shipped from Radford, Virginia

Table 4.1

Analysis of Actual Wastewater

pH	7.0
COD, mg/l	2915
TOC, mg/l	875
Nitrates, mg/l	565
Sulfates, mg/l	16
Alkalinity, mg/l	225
Suspended solids, mg/l	1800
Dissolved solids, mg/l	2716
Color, units	1050

in 55-gallon drums. Prior to the major shipment, a 5 gallon sample of the wastewater was obtained to permit some preliminary experimental evaluations. This sample was diluted with tap water to one-fifth its original concentration for use in the initial jar tests. This is termed "actual diluted" wastewater. The large shipment was used without dilution and is designated as "actual undiluted" wastewater. The wastewater had a turbid appearance and a brownish yellow color. An approximate analysis for this wastewater was supplied by the Army Ammunition plant and is presented in Table 4.1.

4.2.3 Organic Polyelectrolytes

The following polyelectrolytes were used in the experimental study:

- 1- Cat Flocc T (cationic)- manufactured by Calgon Corporation, Pittsburgh, Pa.

Cat Flocc T is a liquid cationic polyelectrolyte used as a primary coagulant in water clarification. It is accepted by the EPA for treating drinking water supplies at concentrations not exceeding 5 ppm.

- 2- WT-2870 (cationic)- manufactured by Calgon Corporation, Pittsburgh, Pa.

WT-2870 is a clear-white to yellow viscous liquid, cationic polyelectrolyte. It is completely soluble in water and can be used as a primary

coagulant, or in combination with inorganic primary coagulants.

- 3- Cat Flocc (cationic)- manufactured by Calgon Corporation, Pittsburgh, Pa.

Cat Flocc is a clear water-white to pale yellow viscous liquid, cationic polyelectrolyte. It is completely soluble in water and is accepted by the U.S. Public Health Service for use in the treatment of drinking water supplies.

- 4- WT-2690 (non-ionic)- manufactured by Calgon Corporation, Pittsburgh, Pa.

Calgon WT-2690 is an off-white flake-like, non-ionic polyelectrolyte which is completely soluble in water.

- 5- WT-2700 (anionic)- manufactured by Calgon Corporation, Pittsburgh, Pa.

Calgon WT-2700 is an off-white, flake-like anionic polyelectrolyte. It is viscous but highly soluble in water and can be used as a coagulant or in combination with inorganic primary coagulants.

- 6- Purifloc A-21 (anionic)- manufactured by Dow Chemical Co. Midland, Michigan.

Purifloc A-21 is an off-white, flake-like anionic polyelectrolyte. It is highly soluble in water.

Technical specifications for these polymers are presented in Table A-2 in the Appendix.

Special care must be taken for the preparation of stock solutions of organic coagulants. In general, the polymer solutions were prepared by adding the polymer to the vortex of approximately 500 ml of rapidly agitated distilled water. Thirty minutes were allowed for complete dissolution. The stock solutions and the polymers were stored in a dry area at room temperature.

4.2.4 Filter Media

The filter media used in the filter consisted of gravel, sand and anthracite. The gravel and sand was supplied by Northern Gravel Co. Muscatine, Iowa. Anthracite filter media was obtained from Carbonite Filter Corporation, Delano, Pa. Technical information provided by the suppliers on the media is presented in Table 4.2.

The thickness of each layer of media and filling procedure is described in Section 4.3.1.1.

4.2.5 Lime and Powdered Carbon

Certified calcium hydroxide (C-97) distributed by the Fisher Scientific Co. was used in the high lime precipitation studies. The powdered activated carbon used was Darco S-51, supplied by the Atlas Chemical Industries, Inc., Wilmington, Delaware.

Table 4.2
Technical Specifications of Filter Media

Anthracite Coal

Hardness	3.0 Mohs scale
Specific Gravity	1.6
Solubility in alkaline and acid water	none
Size	0.9 to 1.5 mm
Uniformity coefficient	1.5 or less
Porosity (void fraction)	0.45

Torpedo Sand

Effective size	0.80 to 1.20 mm
Uniformity coefficient	1.7 or less
Porosity (void fraction)	0.36

Gravel

Type 1	1/8" to 10 mesh
Type 2	1/4" to 1/8"
Type 3	1/2" to 1/4"
Type 4	3/4" to 1/2"

4.3 Experimental Apparatus and Procedures

4.3.1 Continuous Filtration Apparatus and Procedures

The flowsheet for the continuous filtration apparatus is presented in Figure 4.1.

The wastewater for the filtration unit was stored in a 55-gallon polyethylene feed tank and was mixed continuously with a single-speed "Lightnin" stirrer (Mixing Equipment Co., Rochester, N.Y.) This stirrer is capable of mixing low-viscosity fluids in quantities up to 50 gallons and lesser volumes of high viscosity. It operates at 1725 rpm, 1/8 HP and has a 3 blade propeller of 2³/₄" diameter on a 24 inch stainless steel shaft. A mounting clamp permits clamping to any open vessel or to a separate support. The wastewater was conveyed to a Manostat Varistaltic Pump through a ¹/₂" I.D. flexible Tygon tubing. The pump was supplied by Fisher Scientific Co. and had a capacity of 15-4500 ml/min. with $\pm 3\%$ reproducibility. The pumping action consisted of two rollers squeezing flexible tube against the wall of a horseshoe shaped housing, thereby producing a peristaltic effect. The pump used tubing of 1/8" to 3/8" I.D. with 1/16" thick walls. (See Figures 4.2, 4.3 and 4.4 for overall views of the actual laboratory apparatus).

The wastewater was pumped to the filter at the various desired flow rates. The rotameters for flow measurement used in the study were manufactured by Brooks Instruments, Hatfield, Pa. They were the Sho-Rate "150"

Figure 4.1

Flow Diagram of the Continuous Filtration Apparatus

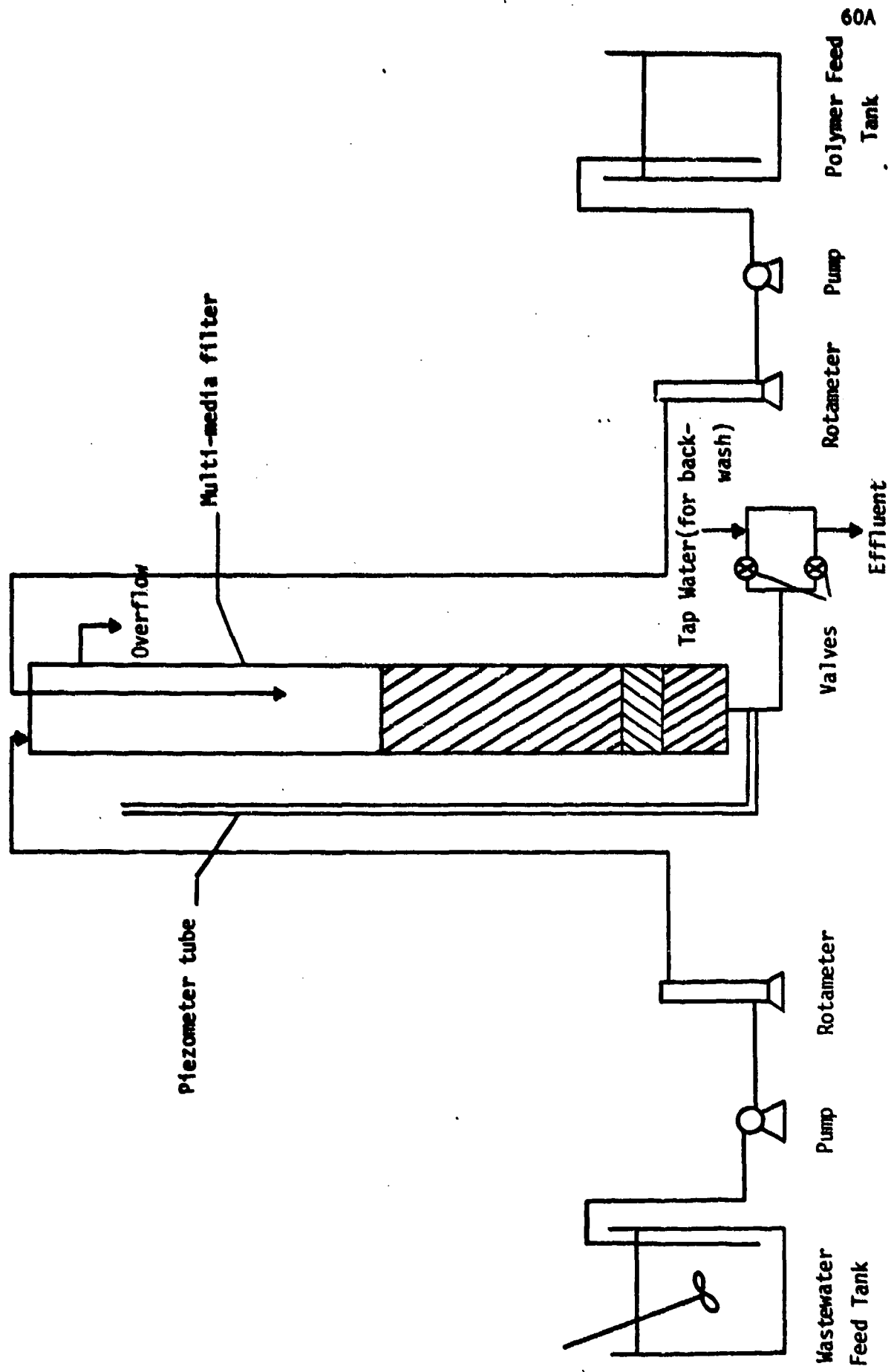


Figure 4.2
Overall View of Actual Laboratory Apparatus

61A

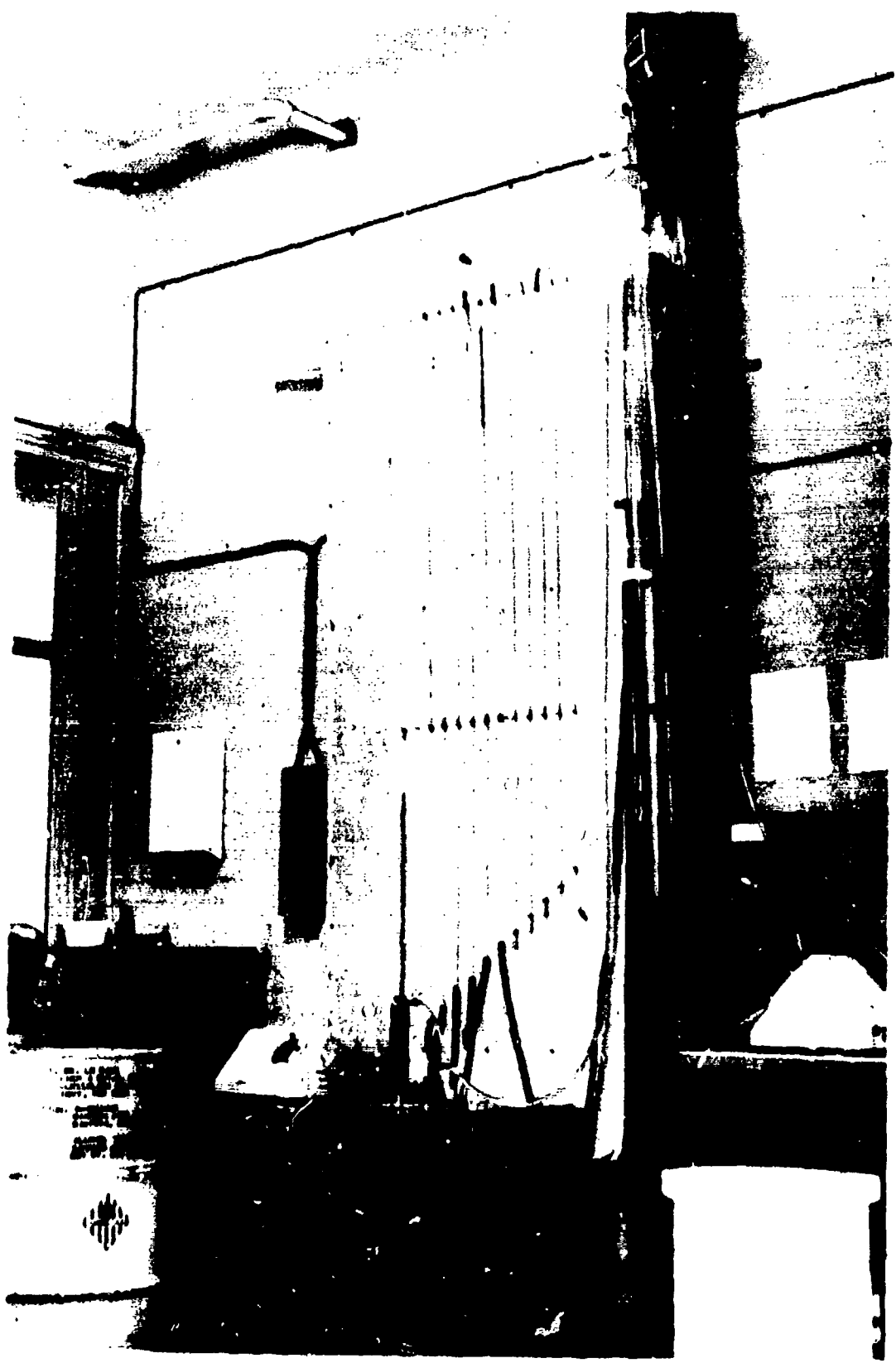


Figure 4.3

Wastewater Feeding Apparatus

Figure 4.4

Polymer Feeding Apparatus

62A



flowmeters having a range of flow of 0.5 cc/min to 2060 cc/min of water. Reproducibility was within $\frac{1}{4}\%$ of instantaneous reading and maximum operating conditions were 200 psig and 250°F. The range of flow could be changed easily by changing the float material in the tube. Float materials that were available for use were glass, sapphire, stainless steel, carboloy and tantalum. Calibration curves for the flowmeters are given in Figures A-1 and A-2 in the Appendix.

The polymer feed solution was stored in a 15-gallon polyethylene drum and fed to the filter by a Manostat Vari-staltic pump similar to the one used for feeding the wastewater. The same type of flowmeter with a different flow range was also used for the polymer. The solution was pumped through a $\frac{3}{8}$ " I.D. flexible Tygon tubing. This tubing extended into the filter by means of a pulley system at the top of the filter and the polymer solution was discharged at approximately 1 ft above the filter media.

4.3.1.1 The Multi-Media Filter

The multi-media filter was constructed of tubular Cadco Cast Acrylic (Cadillac Plastic and Chemical Co., Albany, N.Y.) having an inside diameter of 3 in. and outside diameter of $3\frac{1}{4}$ in. The height was 10 ft to provide sufficient head for the filter. The filter was constructed by connecting two pieces of acrylic tubing, one 6 ft, the other 4 ft. The connection was made with a 2-inch ring of acrylic tubing having an I.D. of $3\frac{1}{4}$ in. that slipped around the joint and

was sealed by using a Plexiglas solvent (1,2 dichloro ethane). The bottom end of the column was closed off with a $\frac{1}{2}$ -inch Plexiglas plate having a $\frac{1}{2}$ -inch outlet for the wastewater located at the midpoint. The bottom endplate was sealed to the filter by using dental cement. A $\frac{1}{2}$ -inch diameter overflow line was located 10 in. from the top of the filter. Tygon tubing of $\frac{1}{2}$ -inch I.D. was used to connect the overflow line to the drain. The filter column rested on a wooden plate that projected from the laboratory wall, and was maintained in position by several braces along the height of the column.

Two valves were located on the effluent line of the filter. As can be seen in Figure 4.1, during operation, the tap water inlet valve (used for backwashing) was closed and the effluent valve was opened. A piezometer tube was located on the effluent line to measure the total head loss of the filter.

The granular media (see Section 4.2.4) used in the filter consisted of anthracite, fine sand and a gravel support. The thickness of each layer from top to bottom was:

Anthracite	21 in.
Fine Sand	4 in.
Gravel (Type 1)	2 in.
Gravel (Type 2)	2 in.
Gravel (Type 3)	2 in.
Gravel (Type 4)	2 in.

The filter configuration can be seen in detail in Figures 4.5 and 4.6. Packing the filter with the media was carried out by filling the empty filtration column with tap water and dropping the media from the top until the desired height was achieved. After this was completed, the filter was back-washed to remove any dust or foreign particles and to ensure even settling and stratification of layers.

4.3.1.2 Start-up and Continuous Operation

The continuous filtration unit was operated in two ways: 1- Conventional treatment and 2- Direct addition of polymer to the filter.

In the first process, the required amount of polymer and coagulant aid were added to the wastewater in a 55-gallon polyethylene drum. The suspension was stirred rapidly for 2 minutes to achieve complete mixing to provide contact for coagulation. The flocculated wastewater was then allowed to settle for 2 hours. A sample of the supernatant was taken for analysis of various parameters. The supernatant was pumped to the filter at the desired flow rate and was allowed to fill the column to a certain height. At this point, the effluent valve was opened and the filtration run was started.

The second method of continuous filtration was carried out by pumping the polymer solution directly to the filter at a flow rate that would give the desired concentration of polymer in the wastewater. The wastewater, mixed

Figure 4.5
Diagram of Multi-Media Filter

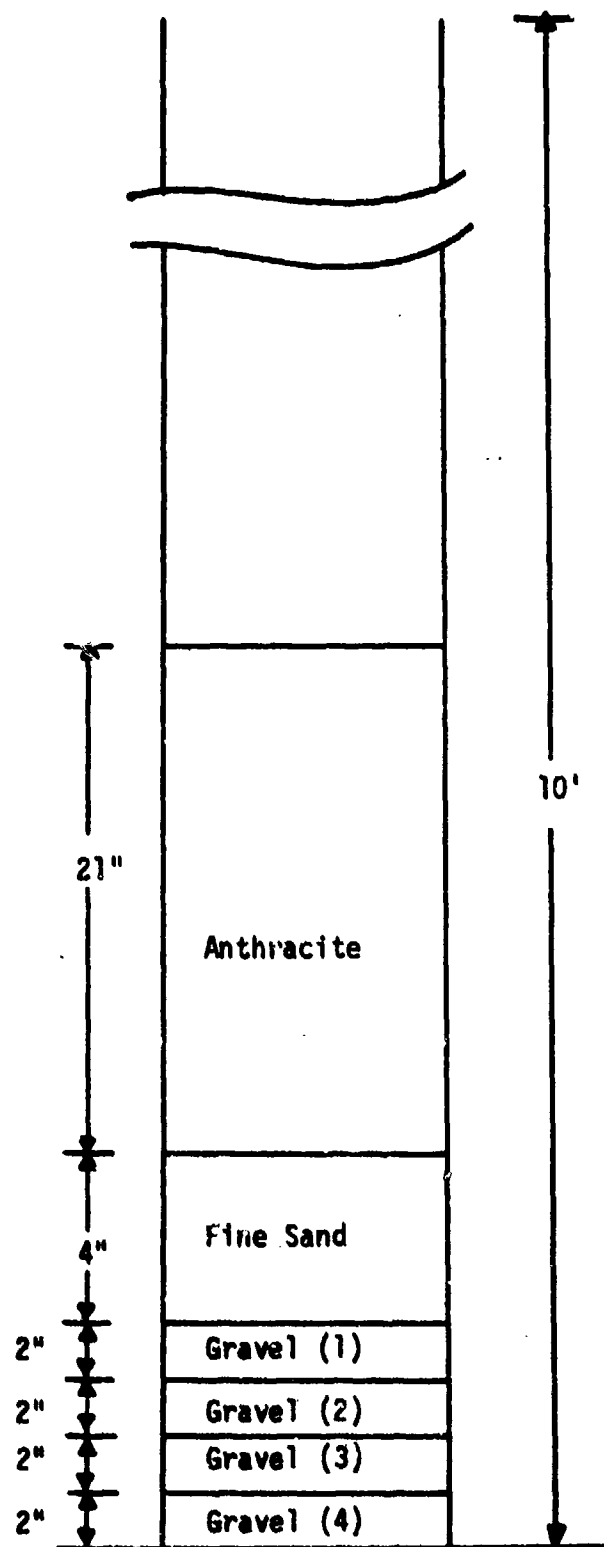
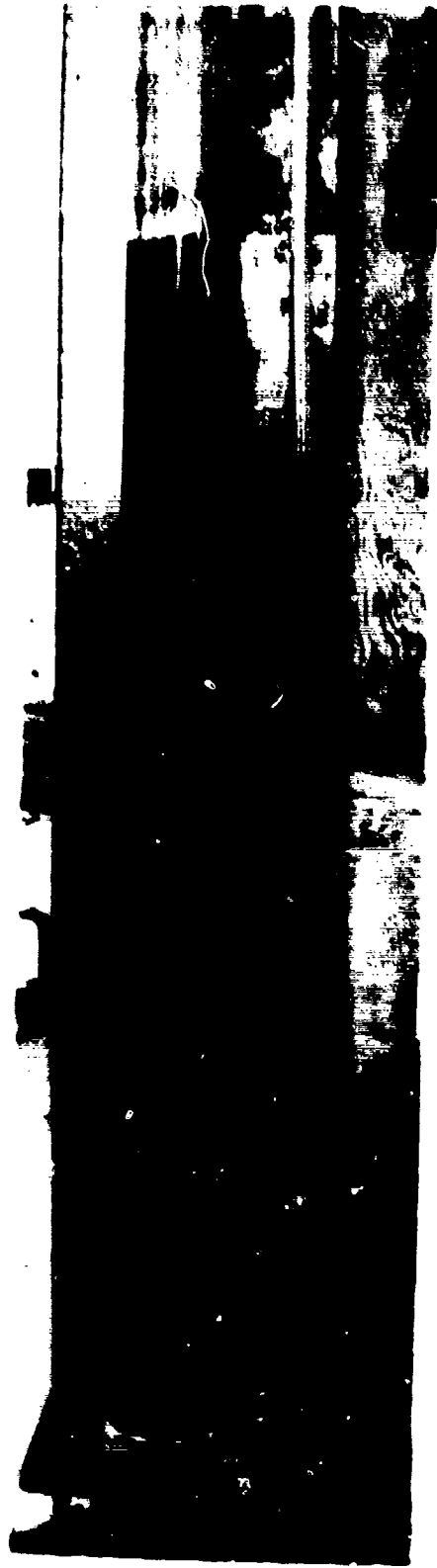


Figure 4.6
Close-up View of Granular Media

01A



with the coagulant aid, was pumped separately to the column and contact occurred at about 1 ft above the filter media.

The filter was operated on a constant rate (constant water level) basis. To achieve this, the effluent valve was manually controlled to keep the water level in the filter at a constant level. As the run proceeded, the effluent valve had to be opened slowly to maintain the same water height. This was due to the accumulation of solids in the filter media. The headloss increase with time was noted by observing the water level in the Piezometer tube.

The filtration runs were usually terminated at 3 hours. Only one of the runs was made for 9 hours to see any long term effects in the effluent quality and other variables. During the length of the run, samples were taken from the effluent at periodic intervals. These were analyzed for various parameters discussed in detail in Section 4.4.

After the end of each run, the filter was backwashed to remove completely the solids accumulated in the filter media. Backwashing procedure consisted of closing the effluent valve and opening the valve for the tap water to start bed fluidization. The bed expansion was about 100%. The backwashing was stopped when the turbidity in the overflow line reached a low limit (approximately the turbidity of tap water). The tap water valve was closed and the effluent valve opened to permit drainage of the water to a level above the filter media. The wastewater and polymer feed lines

were also flushed with tap water to remove any residue and to make the unit ready for a new set of operating conditions.

4.3.2 Jar Test Apparatus and Procedures

The laboratory jar test apparatus (see Figure 4.7) consisted of a multiple stirring unit manufactured by Phipps and Bird Inc., Richmond, Virginia. The unit was equipped with six 2-in. by 3-in. stirrers and a variable transformer that provided speeds from 10 to 100 rpm. The stirrers were driven by a 1/30 HP motor. The entire unit was mounted in an elongated, cast aluminum housing, supported 9½ inches above the bench.

4.3.2.1 Jar Tests with Polymers and Coagulant Aids

Eight hundred milliliter quantities of wastewater in 1-liter beakers were placed on the mixing stand. The polymer solution of specified volume was pipetted to the beaker and mixing was started at 100 rpm for 30 seconds. Then the mixture was flocculated for 20 minutes at 30 rpm. The flocculated sample was allowed to stand undisturbed for 30 minutes. Physical and chemical analyses were carried out on the settled liquid sample (supernatant). When coagulant aids were used, they were first added to the wastewater and mixed completely at 100 rpm before the polymer was added to the mixture.

4.3.2.2 Jar Tests with Lime

A similar procedure was carried out in the jar

tests when lime was being used. The lime was added to 800 ml of wastewater at appropriate dosages and rapid mixing was started at 100 rpm for 1 minute. After this the mixing was stopped and the mixture was allowed to settle for 30 minutes.

4.3.2.3 Jar Tests with Powdered Activated Carbon

Eight hundred milliliters of the wastewater were placed in a 1-liter glass beaker. Powdered activated carbon of specified quantity was then added to the wastewater sample and thoroughly mixed at 100 rpm for 5 minutes. A mixed sample of 40 ml was taken and immediately filtered with a Whatman No.2 filter paper. The filtrate was analyzed for total organic carbon.

4.4 Analytical Apparatus and Procedures

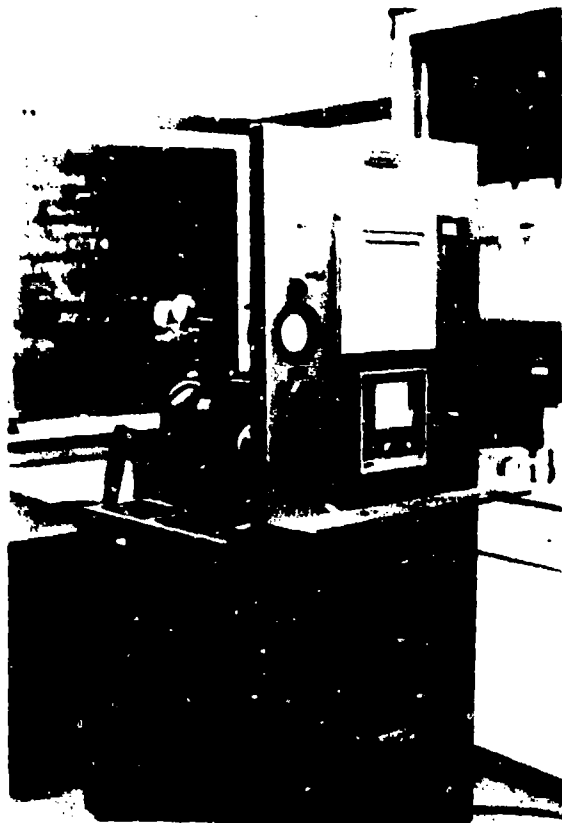
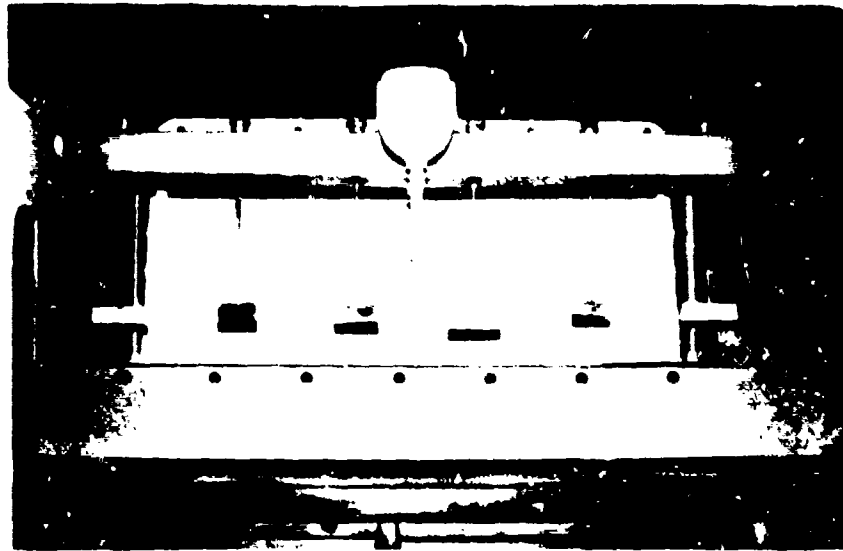
4.4.1 Total Organic Carbon (TOC) Analysis

A Beckman Carbonaceous Analyzer was used for measuring carbon content of the sample (see Figure 4.8). The analysis system consists essentially of a panel on which are mounted a Beckman Model IR-315 Infrared Analyzer, a Leeds and Northrup Type "H" Model "S" Strip-Chart Recorder, and a special sampling system. The carbonate alkalinity in the sample was removed by addition of 4N HCl to convert it to CO₂, then bubbling nitrogen gas to remove the CO₂. In this way, the total organic carbon content of the sample is measured.

Figure 4.7
Jar Test Apparatus

Figure 4.8
Beckman Carbonaceous Analyzer

71A



Twenty microliters of the sample was injected into the combustion tube with a hypodermic syringe. The combustion tube was heated to 950°C and received a 150 cc/min stream of oxygen. The heated oxygen oxidized any organic material yielding carbon dioxide which was detected by a Model IR-315 Infrared Analyzer. A calibration curve was prepared (see Figure A-3 in the Appendix) using various concentrations of carbon (0-100 mg/l). The standards were made from oxalic acid. Appropriate dilutions were made for samples that had a higher organic carbon content than 100 mg/l.

4.4.2 Turbidity Measurement

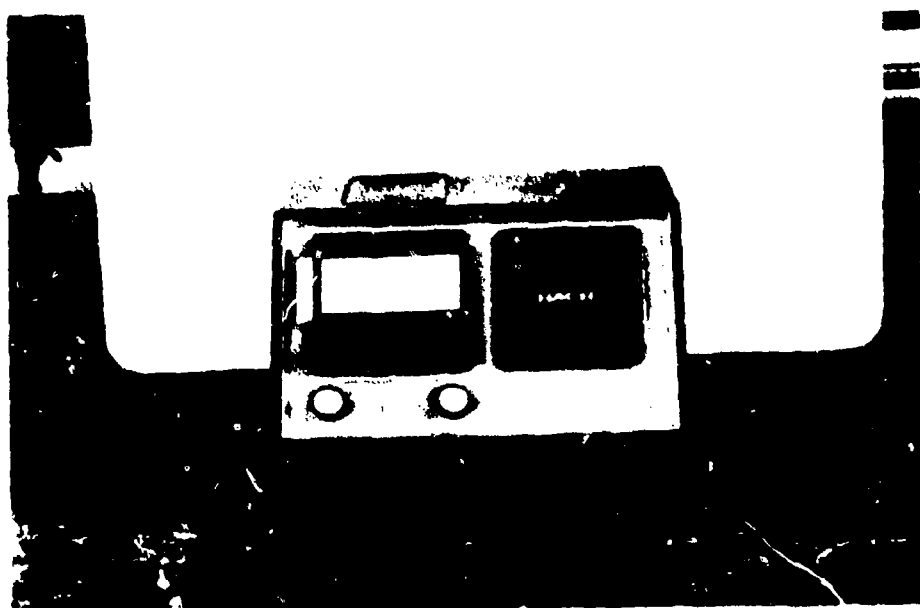
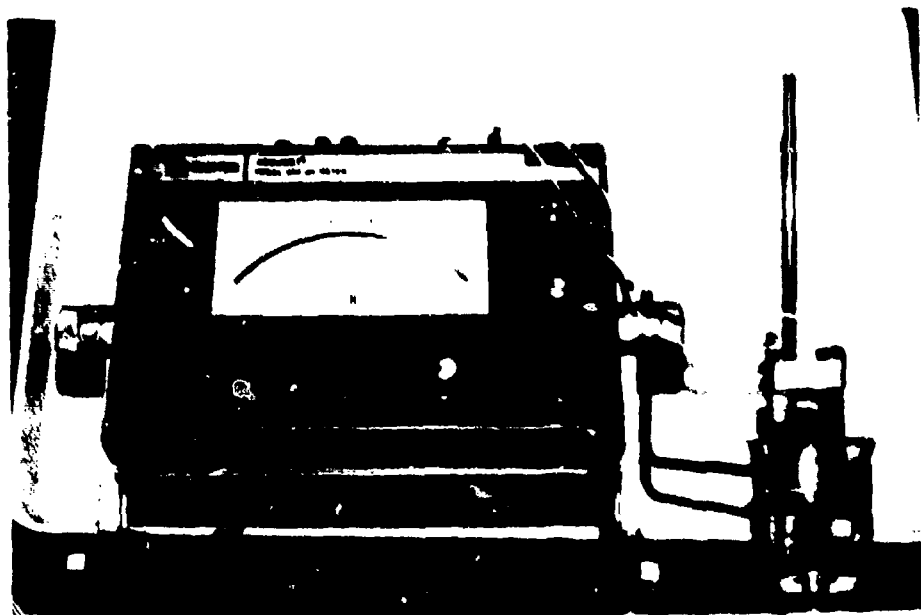
The turbidity of the samples were measured using a Model 2100 A Hach Turbidimeter manufactured by Hach Chemical Co., Ames, Iowa (see Figure 4.10). Turbidity standards of 0.61, 10, 100 and 1000 FTU (Formazin Turbidity Units which are equivalent to JTU) were available to be used with the instrument. The 10,100,1000 FTU standards were suspensions of polystyrene latex in water and the 0.61 FTU standard was a chlorobenzene solution.

4.4.3 pH Measurement

pH was measured by a Fisher Accumet Model 220 General Purpose pH meter manufactured by Fisher Scientific Co., Pittsburgh, Pa.

Figure 4.9
Fisher pH Meter

Figure 4.10
Hach Model 2100 A Turbidimeter



4.4.4 Determination of Colloid Charge

Colloid charge was measured using an application of the colloid titration method initially developed by Kawamura and Hanna (14), and modified by Wang and Shuster (36). The principles, reagents, and analytical and calculation procedures of Wang and Shuster's new method are presented below.

This method is able to measure low concentrations of polyelectrolytes and colloids and in turn the charge of the constituent can be calculated from these measurements. The basic principle involved in the improved direct titration method is that a neutralization reaction occurs between cationic and anionic polyelectrolytes. In titration of cationic polyelectrolytes, poly(vinyl sulfuric acid) potassium (PVSAK) is used as the standard anionic titrant. The cationic polyelectrolytes show a light blue color in the presence of toluidine blue-0 dye, and the blue color turns to bluish purple when the titration end point is reached. In titration of anionic polyelectrolytes, 1,5-dimethyl-1,5-diazaundecamethylene polymethobromide (DDPM) is used as the standard cationic titrant. The anionic polyelectrolytes show a bluish purple color in the presence of toluidine blue-0 dye, and the purple color turns to light blue when the titration end point is reached.

Calibration curves should be prepared for each polyelectrolyte to be used. The calibration curves for WT-2870 and Cat Floe T are presented in Figures A-4 and A-5 in the Appendix.

4.4.4.1 Reagents

- 1- Toluidine blue-0 solution (TBO)- 1000 mg/l (Eastman Organic Chemicals, Rochester, N.Y., Cat. No. C 1756)
- 2- Stock poly (vinyl sulfuric acid) potassium (PVSAK) solution, 0.01 N (Eastman Organic Chemicals, Rochester, N.Y., Cat.No. 8587)
- 3- Stock 1,5-dimethyl-1,5-diazaundecamethylene polymethobromide (DDPM) solution, 0.01 N (Aldrich Chemical Co. Inc., Cedar Knolls, New Jersey, Cat.No. 10768-9)
- 4- Sodium hydroxide (NaOH) solution, 0.1 N
- 5- Hydrochloric acid (HCl), 0.1 N

4.4.4.2 Analytical Procedures

- 1- Measure 50 ml of sample into a 250 ml Erlenmeyer flask.
- 2- If the pH of the sample is not in the range of 3 to 9, adjust the pH by NaOH or HCl addition.
- 3- Add 3 drops of TBO solution to the flask containing the sample and mix well. If the color is blue, the sample contains cationic or no polyelectrolyte; then follow procedures C4 through C6. If the color is purple, the sample contains anionic polyelectrolyte; procedures A4 through A6 should be followed.
- C4- Titrate the blue-colored water sample with PVSAK solution (dilute if necessary) until the color of water sample turns from light blue to bluish purple. Record the amount of PVSAK solution used in titration.

- C5- A blank is run by the same procedures from 1 to C4 using distilled water.
- C6- Determine the cationic polyelectrolyte concentration from the calibration curve prepared previously.
- A4- Titrate the purple-colored sample with DDPM solution (dilute if necessary) until the color turns from bluish purple to light blue. Record the amount of DDPM solution used in titration.
- A5- A blank is run by the same procedures using distilled water.
- A-6 Determine the anionic polyelectrolyte concentration from the calibration curve prepared previously.

A slight modification of the procedure is necessary when the concentration or net charge of an anionic sample is being measured in the presence of suspended colloid particles (negatively charged). These particles tie up the cationic toluidine blue-0 dye causing an interference in the titration. To overcome this, the anionic sample is first made cationic in nature by adding a known amount of excess cationic reactant. The procedure for this is as follows: A known amount of cationic reactant and toluidine blue-0 dye are added to the sample. If the color turns blue then this means there is a sufficient amount of excess cationic reagent in the system. If the color turns purple, this is an indication that not enough cationic reactant was added and the procedure has to be repeated until there is excess cationic reagent in the sample. Then the excess

cationic reactant is back titrated to determine the amount that reacted with the anionic sample.

4.4.4.3 Calculation of Net Charge

A calibration curve for a specific polyelectrolyte in routine analysis is suggested but is not absolutely necessary since by knowing the sample size, the concentration of the standard titrant and the volume of titrant used, the concentration of polyelectrolyte in the sample can be calculated by the following equation:

$$N_1 V_1 = N_2 V_2$$

where N_1 = normality of sample, eq/l
 V_1 = sample volume, l
 N_2 = normality of standard titrant, eq/l
 V_2 = volume of titrant used, l

Knowing the normality and the mono-molecular weight, the concentration of the polyelectrolyte in mg/l or the polyelectrolyte's net charge in meq/l can be calculated.

In the case where excess cationic polyelectrolyte is added to an anionic sample and back titration is carried out, the following equation can be used to determine the concentration of the original polyelectrolyte sample:

$$N_1 V_1 = N_2 V_2 + N_3 V_3$$

where N_1 = normality of excess cationic polyelectrolyte solution, eq/l
 V_1 = volume of excess cationic polyelectrolyte added, l
 N_2 = normality of anionic sample, eq/l
 V_2 = sample size, l
 N_3 = normality of standard anionic titrant, eq/l
 V_3 = volume of anionic titrant used, l

This method, however, does not differentiate between two cationic or two anionic polyelectrolytes. The measurement in this case is expressed as "meq/l of net colloid charge". It is concluded that the direct titration method presented measures the "free" or "dissolved" polyelectrolytes, or the "net charges" of colloidal matters.

PART 5
RESULTS AND DISCUSSION

5.1 Batch Jar Tests

5.1.1 Experiments using synthetic wastewater

A synthetic wastewater was used for the initial jar test experiments to ensure invariant concentration and characteristics. This uniformity was desirable in the initial tests to aid in understanding the basic mechanisms and principles involved in effective coagulation with polymers. Five polymers (Purifloc A-21, wt-2700, WT-2690, Cat Flocc T, WT-2870) (see Section 4.2.3) were used as coagulants to determine effectiveness in turbidity removal. The data obtained in these experiments are presented in Figures 5.1 through 5.10. Residual turbidity, total net charge and pH were plotted as a function of polymer dosage. In one experiment using cationic polymer WT-2870, the residual TOC as a function of polymer dosage was also analyzed.

The first general observation that can be made from these figures was that an optimum dosage of polymer for turbidity removal exists and both underdosing and overdosing could occur in the system. For the cationic and anionic polymers that were effective in turbidity removal, the optimum dosage was around 50 mg/l. The single non-ionic polymer investigated gave an optimum dosage of 10 mg/l. It has been reported that non-ionic polymers usually have a larger molecule

Figure 5.1

Residual Total Net Charge and pH vs. Polymer Dosage

Figure 5.2

Residual Turbidity vs. Polymer Dosage

Experimental Conditions

Wastewater: Synthetic

Initial Turbidity = 120 JTU (33 JTU after settling)

Initial pH = 9.9

Initial Charge = $-1550 * 10^{-4}$ meq/l

Polymer: Cat Floc T (cationic)

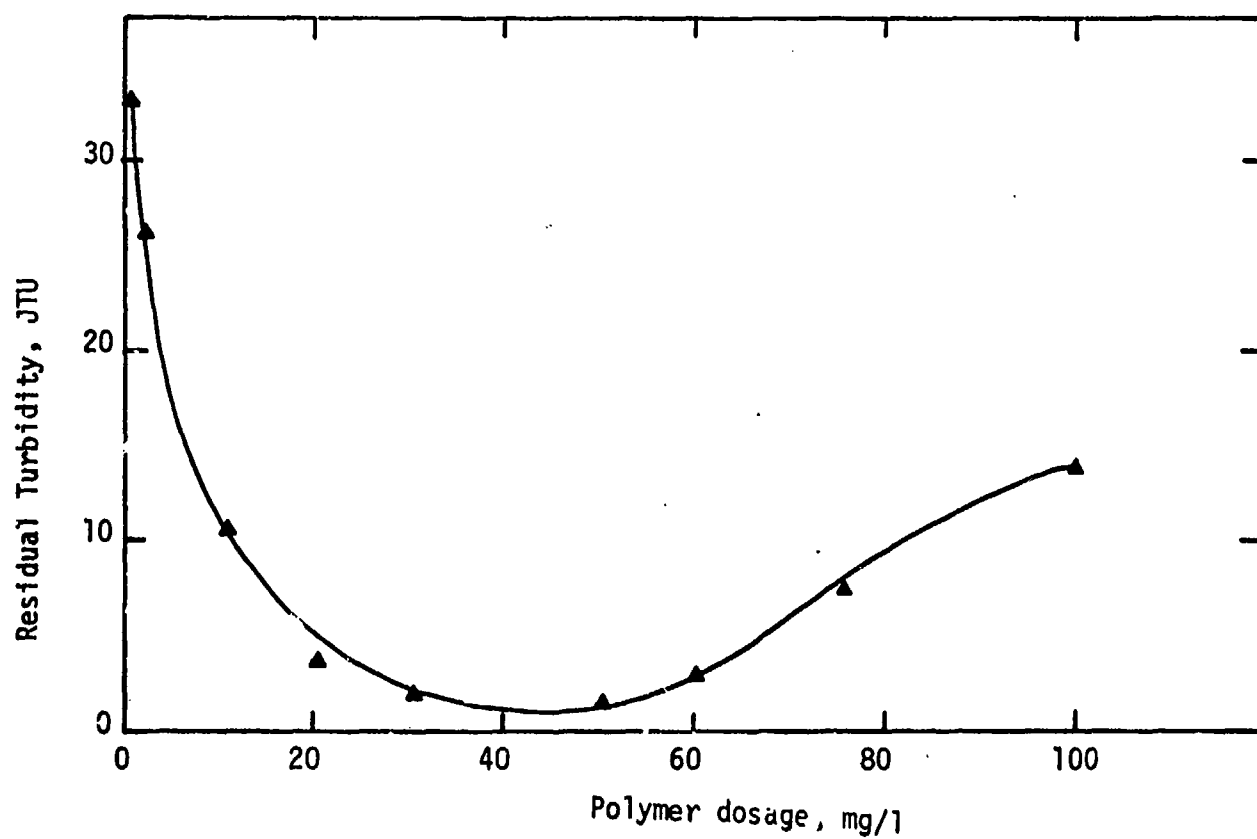
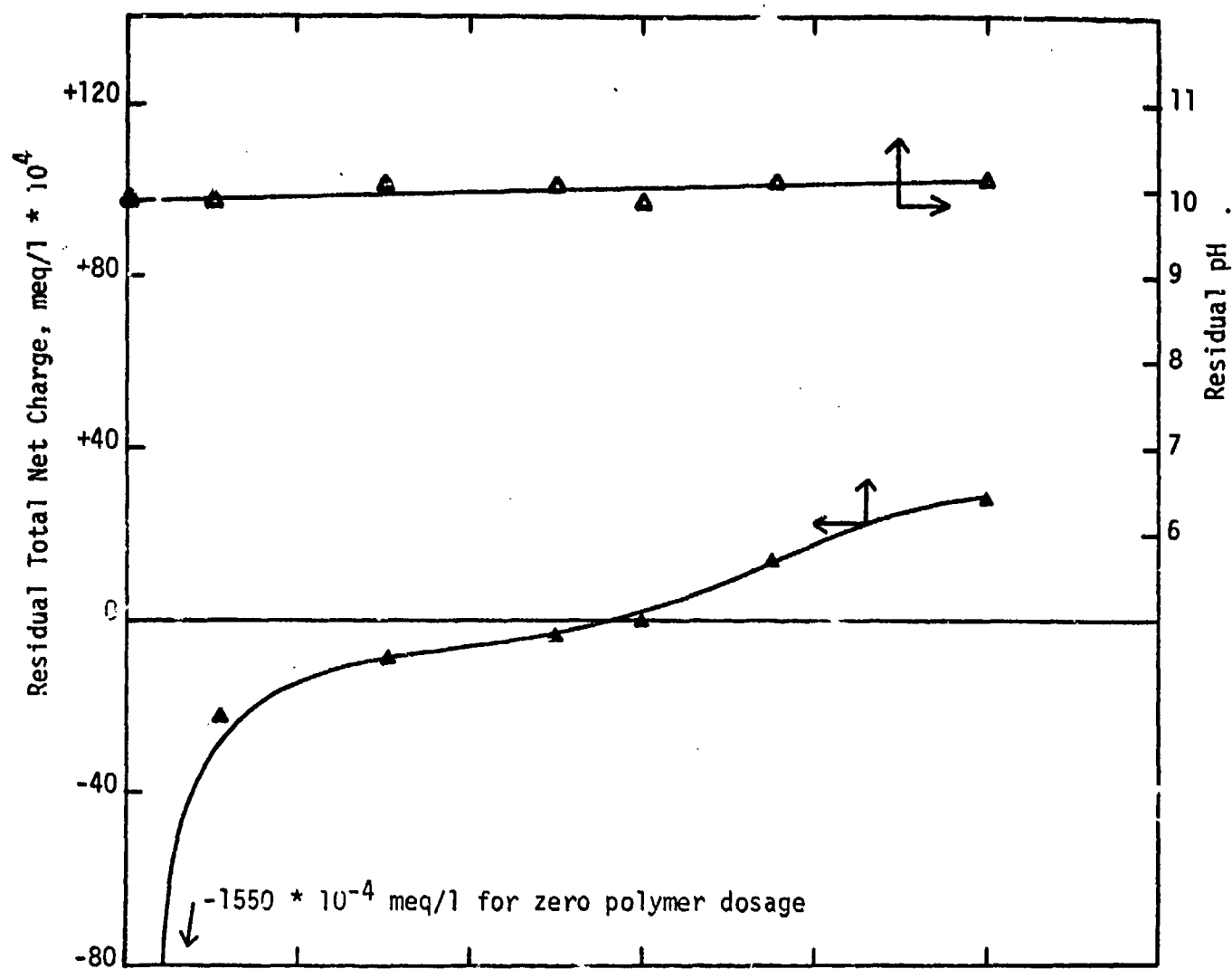


Figure 5.3

Residual Total Net Charge and pH vs. Polymer Dosage

Figure 5.4

Residual Turbidity and TOC vs. Polymer Dosage

Experimental Conditions

Wastewater: Synthetic

Initial Turbidity = 110 JTU (32 JTU after settling)

Initial pH = 10.0

Initial Charge = $-1600 * 10^{-4}$ meq/l

Initial TOC = 39 mg/l

Polymer: WT-2870 (cationic)

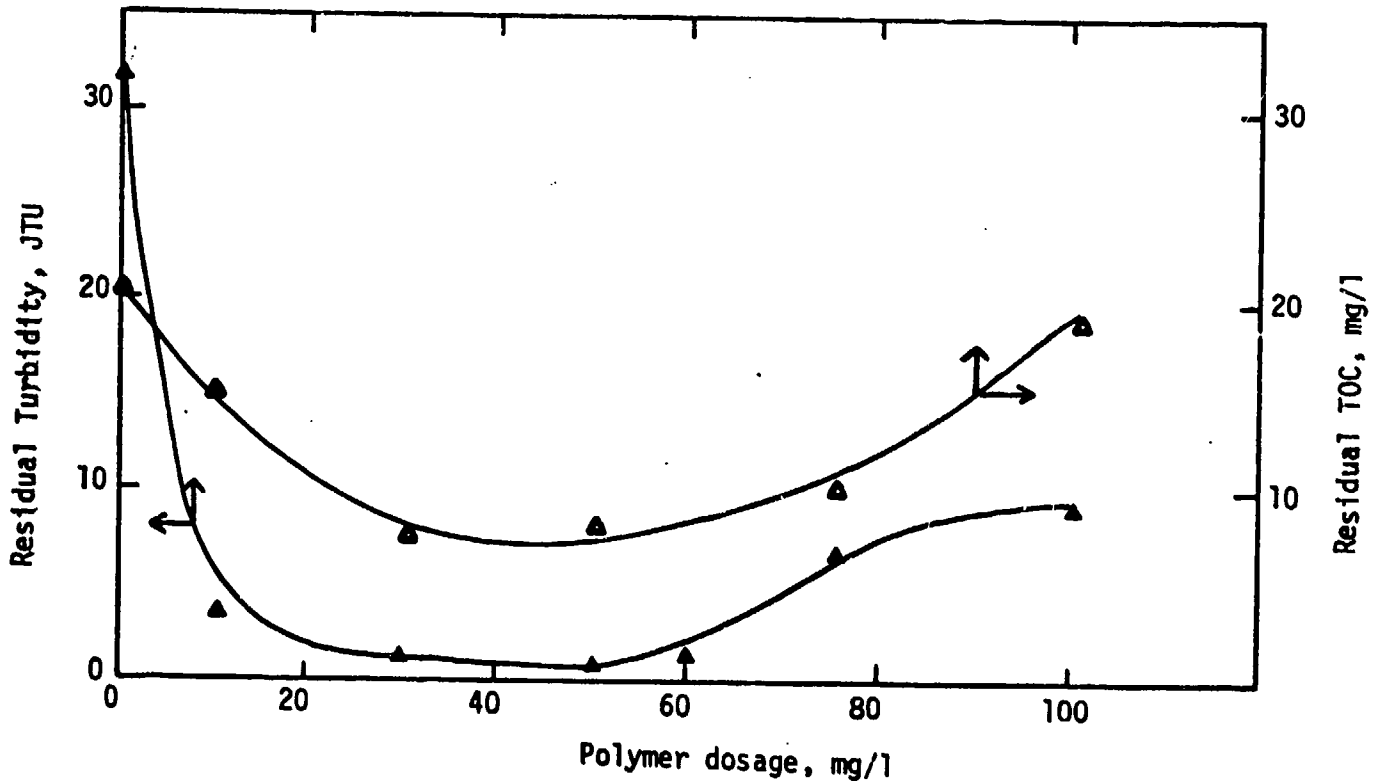
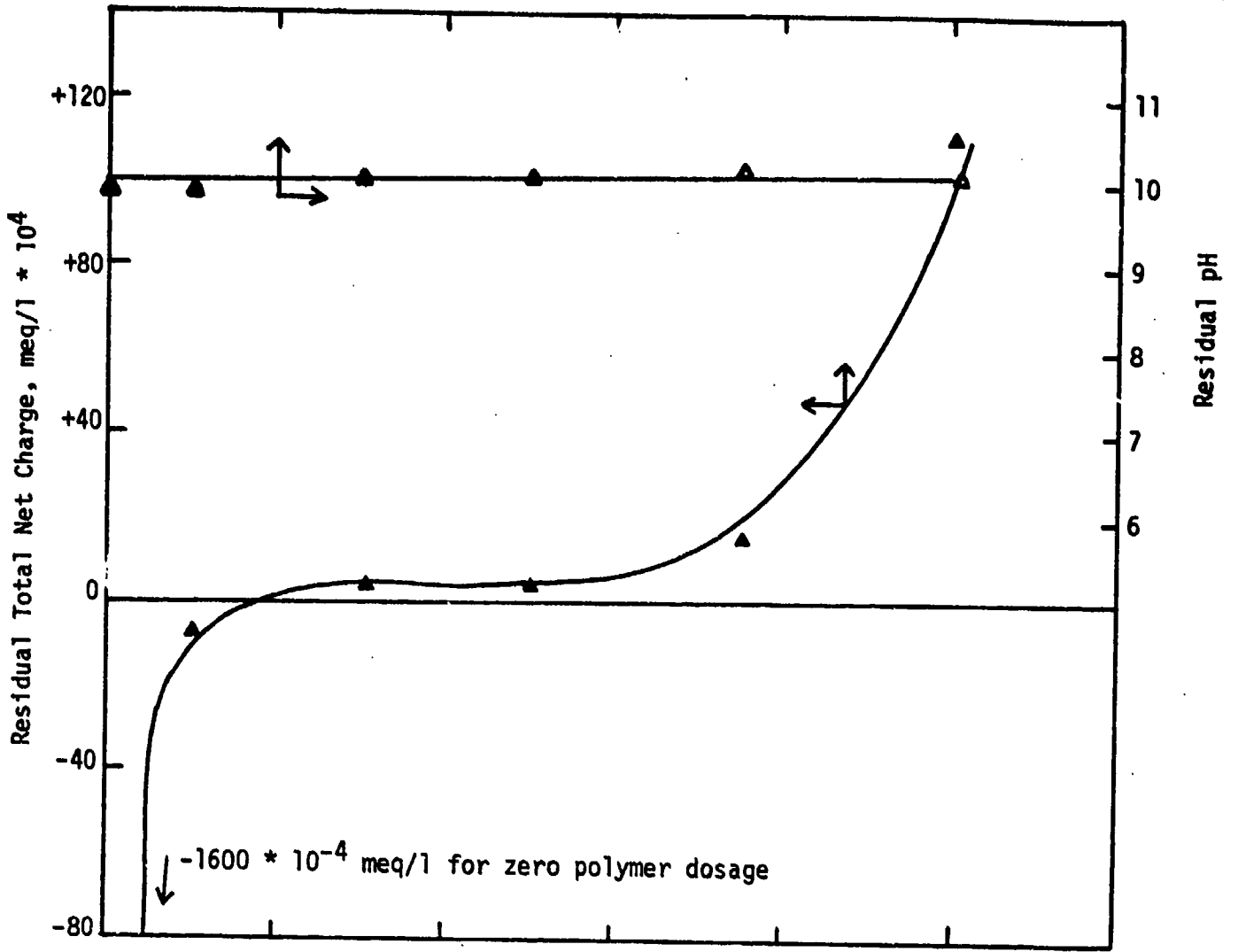


Figure 5.5

Residual Total Net Charge and pH vs. Polymer Dosage

Figure 5.6

Residual Turbidity vs. Polymer Dosage

Experimental Conditions

Wastewater: Synthetic

Initial Turbidity = 110 JTU (33 JTU after settling)

Initial pH = 7.4

Initial Charge = $-1600 * 10^{-4}$ meq/l ($-1200 * 10^{-4}$ meq/l
after settling)

Polymer: WT-2690 (Non-ionic)

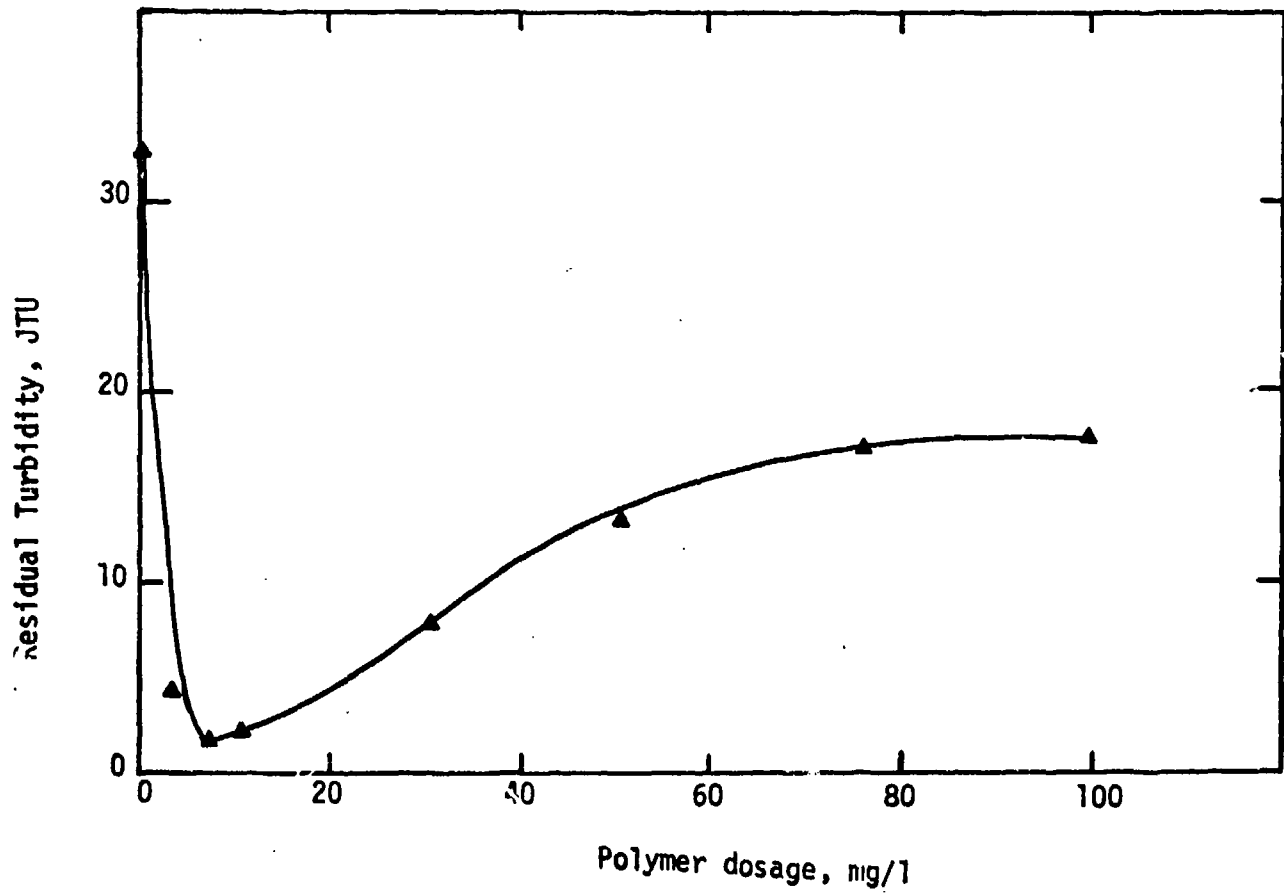
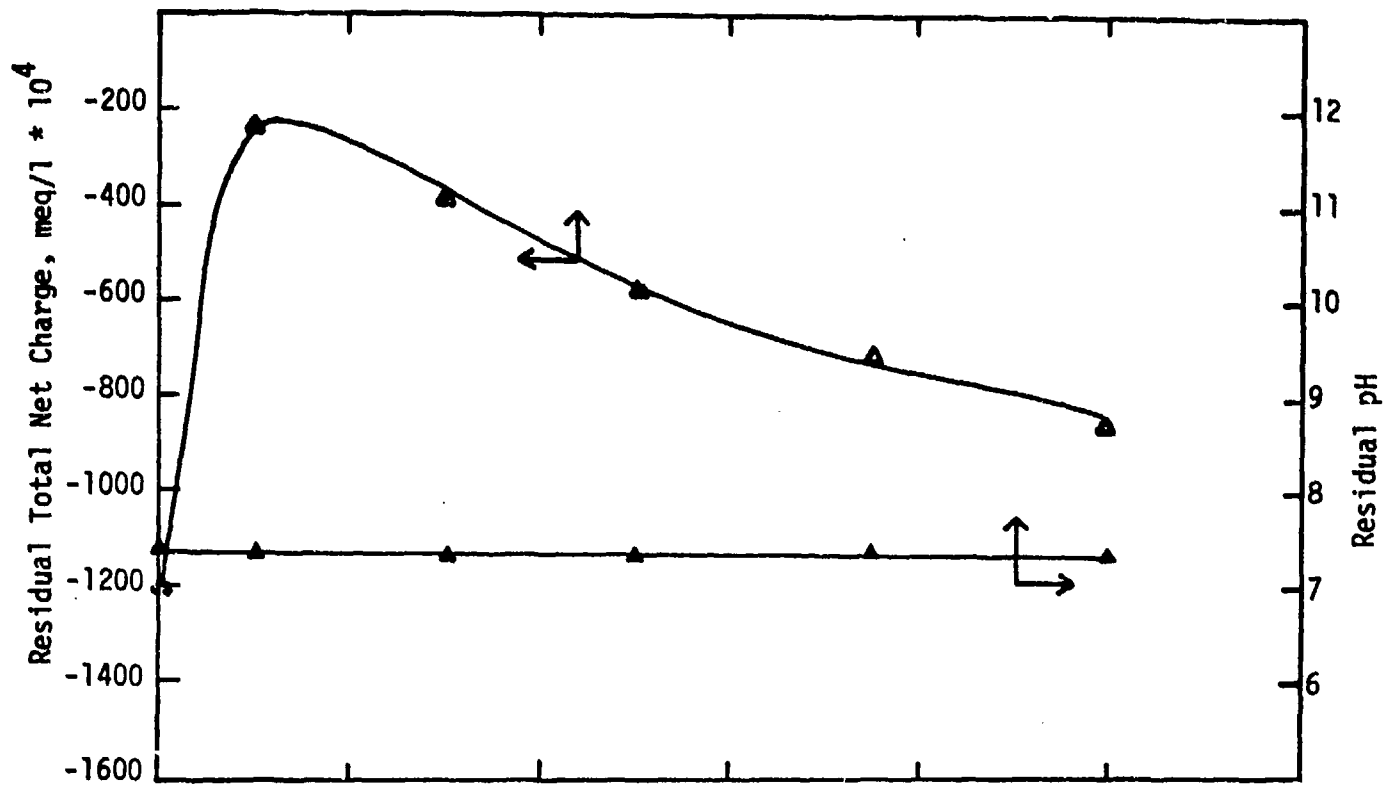


Figure 5.7

Residual Total Net Charge and pH vs. Polymer Dosage

Figure 5.8

Residual Turbidity vs. Polymer Dosage

Experimental Conditions

Wastewater: Synthetic

Initial Turbidity = 120 JTU (31 JTU after settling)

Initial pH = 8.2

Initial Charge = $-1400 * 10^{-4}$ meq/l ($-1250 * 10^{-4}$ meq/l
after settling)

Polymer: Purifloc A-21 (anionic)

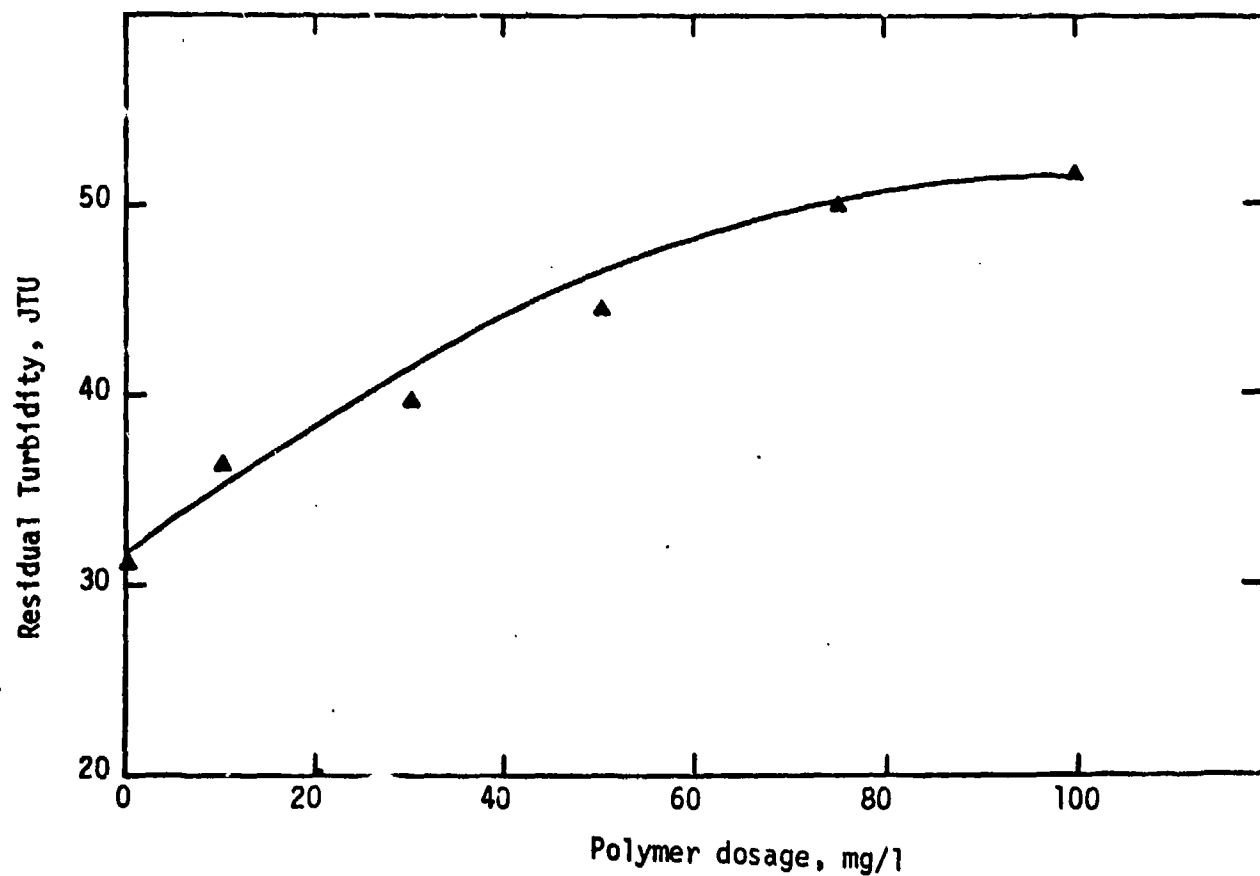
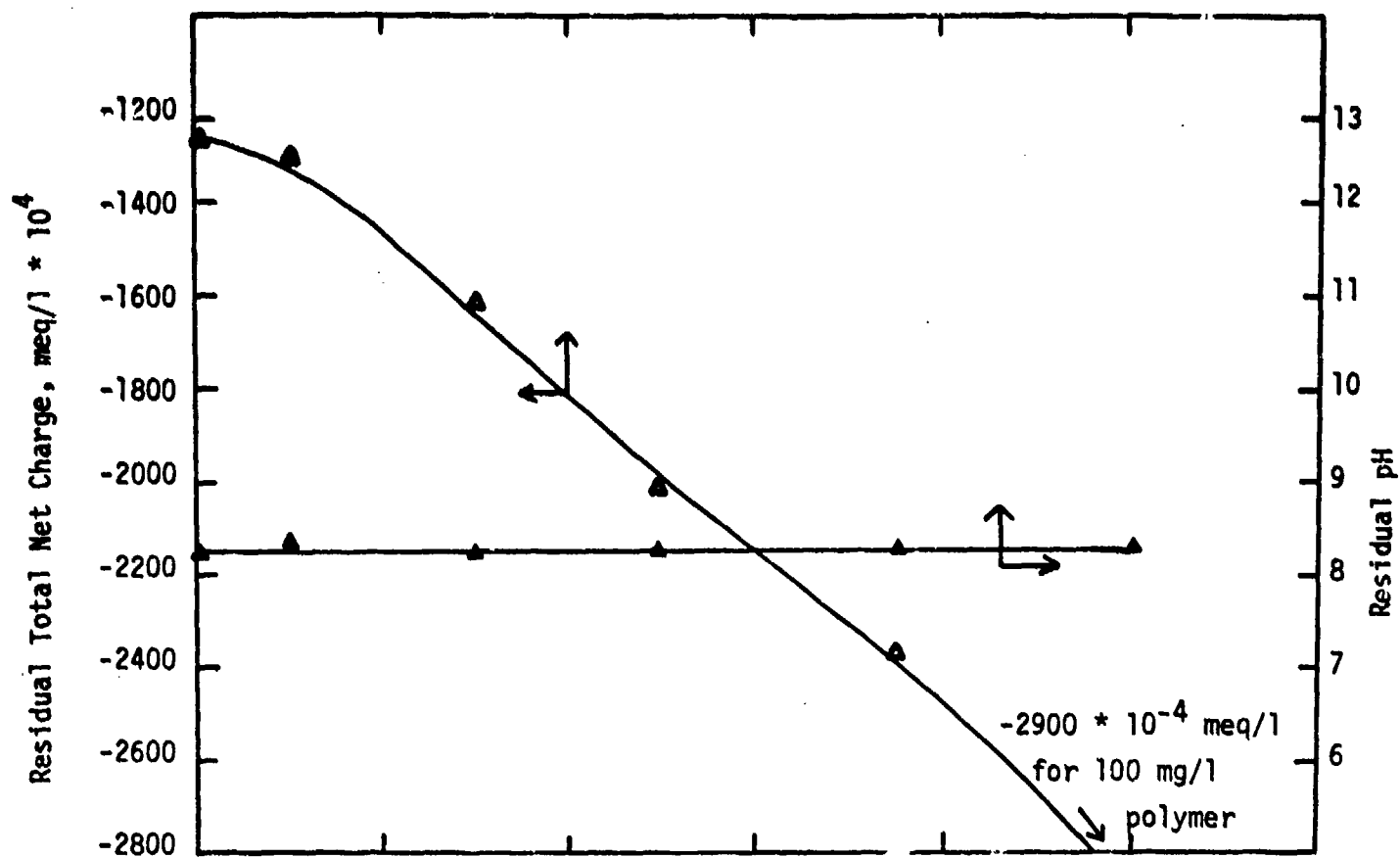


Figure 5.9

Residual Total Net Charge and pH vs. Polymer Dosage

Figure 5.10

Residual Turbidity vs. Polymer DosageExperimental Conditions

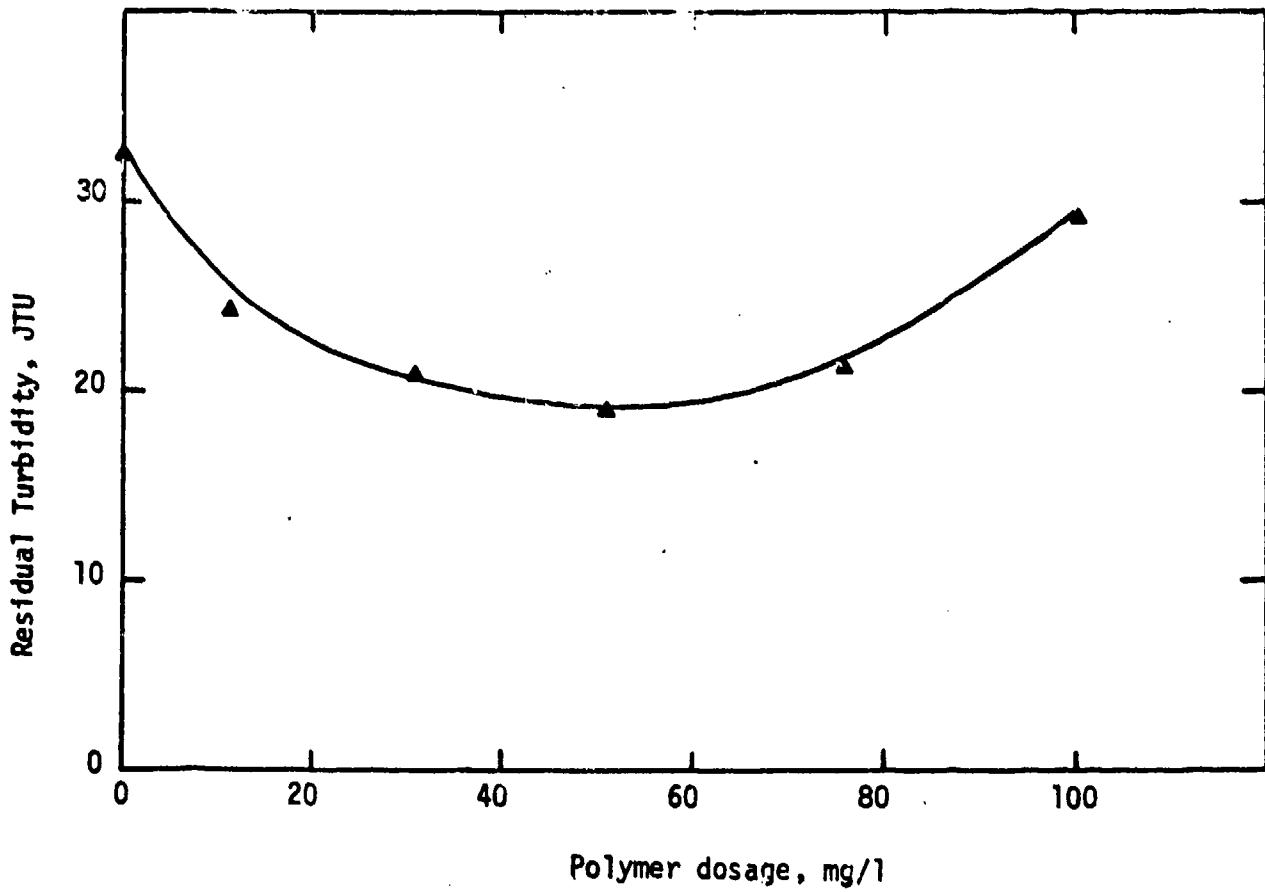
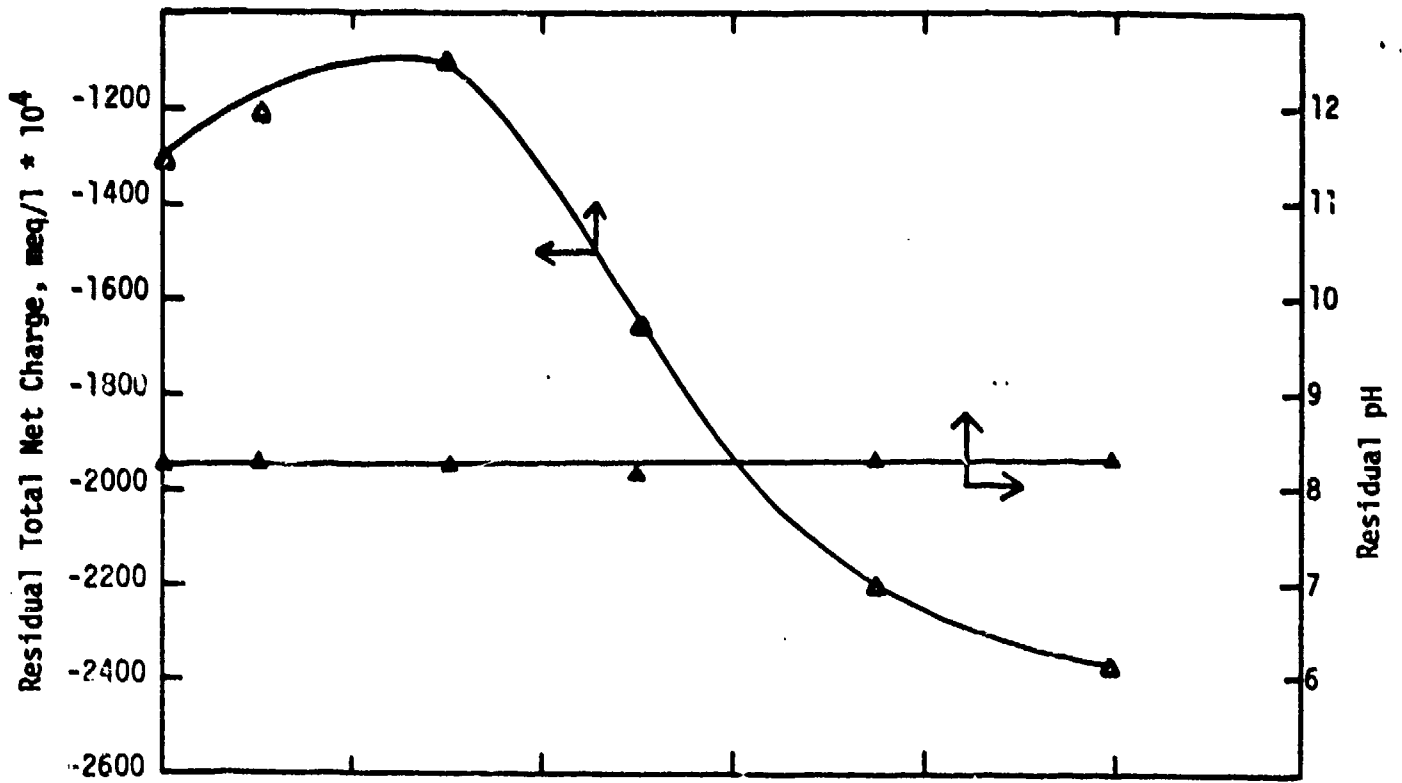
Wastewater: Synthetic

Initial Turbidity = 115 JTU (33 JTU after settling)

Initial pH = 8.3

Initial Charge = $-1500 * 10^{-4}$ meq/l ($-1300 * 10^{-4}$ meq/l
after settling)

Polymer: WT-2700 (anionic)



size and a longer chain length than cationic polymers (19). For this reason, they can extend outside the electrical double layer of the suspended colloidal particle to bring about coagulation and flocculation by an effective bridging mechanism. The amount of non-ionic polymer needed is usually less than that of a cationic polymer. Experimental observations also showed that larger flocs were formed with the non-ionic polymer than with the cationic polymers. This concept also supports the effective bridging mechanism (8,9) that took place during flocculation.

In Figures 5.1 to 5.4, the relation between charge neutralization and optimum turbidity removal can be seen. Charge neutralization, like the bridging model, is another mechanism in coagulation and flocculation with polymers. It is usually dominant when the wastewater and the polymer to be used are opposite in charge. In these experiments, the wastewater was anionic in nature due to the negatively charged colloidal bentonite particles and the anionic surfactant in its composition. Cationic polyelectrolytes, therefore, were expected to give the best turbidity removal, with the mechanism of charge neutralization being predominant. This is verified in the experimental data. The results show that the total net charge is highly anionic initially and then a reduction in the net negative charge takes place as the polymer dosage approaches its optimum value. The most effective removal in turbidity corresponds to a point where the net charge

is near zero. This shows that effective turbidity removal (at the optimum polymer dosage) corresponds to nearly complete neutralization of the colloidal particles. It can be concluded that coagulation by charge neutralization is a dominant mechanism for cationic polymers when the wastewater is oppositely charged although some bridging action may also be observed.

Charge neutralization, however, was not a dominant mechanism for non-ionic and anionic polymers since the wastewater used in the experiments was negatively charged. This does not imply that all of these polymers were completely ineffective in turbidity removal. In Figures 5.5 and 5.6, it can be seen that the non-ionic polymer was quite effective in turbidity removal although some charge reduction took place. The removal could be predominantly brought about by an effective bridging mechanism and the reduction in charge was caused not by charge neutralization but by the removal of the negatively charged colloid particles in the supernatant where the charge measurement was made. It is noted that the non-ionic polymer is effective in a very narrow range and overdosing of polymer results in a high residual turbidity due to the protective coating of polymer surrounding the colloidal particles preventing coagulation. It is also seen that beyond the optimum polymer dosage the net negative charge increases correspondingly with the increasing residual turbidity.

A point of interest is that although the initial turbidity of the synthetic wastewater is 110 JTU, the residual turbidity of the settled sample where no polymer addition is made is 33 JTU. This means that a 70% reduction in turbidity takes place just by allowing the wastewater sample to settle for 30 minutes and indicates that most of the suspended particles in the wastewater were larger than colloidal size. Therefore the effectiveness rating of the polymer in turbidity removal should be based on an initial "colloidal" turbidity of 33 JTU and not 110 JTU.

The effect of anionic polymers in removing turbidity of the synthetic wastewater can be seen in Figures 5.7 to 5.10. When WT-2700 was used as coagulant, (Figures 5.9 and 5.10) a slight removal in turbidity was observed with the optimum polymer dosage being 50 mg/l. In correspondence with this turbidity removal, the net negative charge first decreased slightly (due to the removal of negatively charged colloidal particles from the supernatant) then increased beyond the initial net charge of the wastewater due to the addition of increasing amounts of anionic polymer. The turbidity removal that took place was slight and was not due to charge neutralization. Bridging between particles was the dominant mechanism in the system. Another anionic polymer, Purifloc A-21 (Figures 5.7 and 5.8) was not effective at all in coagulating the synthetic wastewater. The addition of polymer in increasing dosages only resulted in an increasing residual turbidity and increasing negative charge. Even the

slight turbidity reduction brought about by the other anionic polymer WT-2700 was not possible with Purifloc A-21. This could be due to the difference in their structure, size and chain length since these characteristics play an important role in effective bridging and flocculation.

The addition of the anionic polymer in this system increased the repulsion forces between the negatively charged suspended colloidal particles. This effect prevented the particles to come into contact and agglomerate into flocs which could be removed by settling. The overall result was the increase in residual turbidity with increasing dosage of anionic polymer. The increase in the net charge was due to the additive effects of the charge of the colloidal particles and the anionic polymer.

In the data presented so far, the residual pH did not change significantly with polymer dosage. To further test the effect of pH on this system, the following experiments were conducted: Jar tests were carried out by using a constant polymer dosage and varying pH for the wastewater samples. The polymer dosage used was the optimum dosage determined previously. These tests were made to see if an optimum pH existed in coagulation of the wastewater. Data obtained in these experiments are presented in Figures 5.11 through 5.13.

A general look at the data indicates that the dependence of turbidity removal on pH is not very significant

Figure 5.11

Residual Turbidity vs. pH

Experimental Conditions

Wastewater: Synthetic

Initial Turbidity = 110 JTU (32 JTU after settling)

Polymer: WT-2690 (Non-ionic)

Polymer Dosage: 10 mg/l

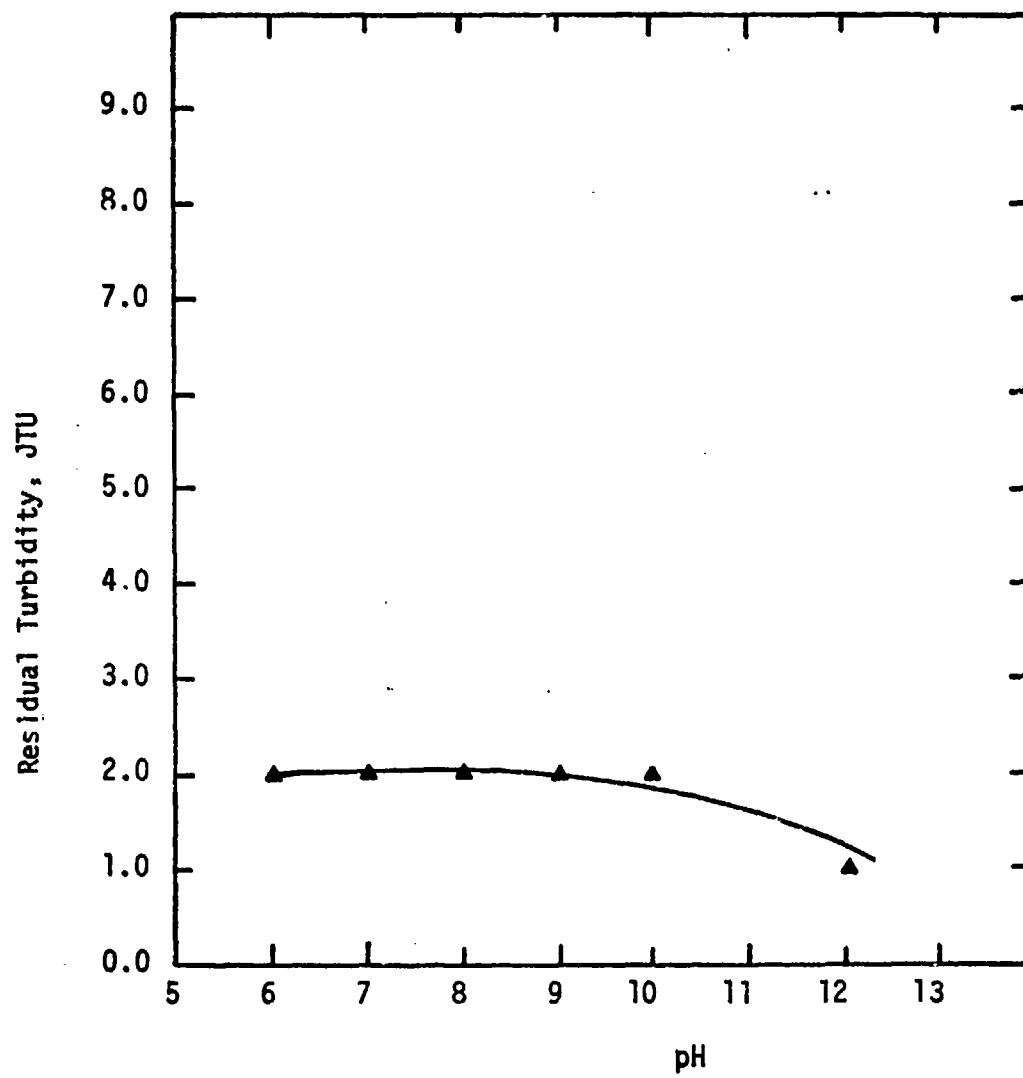


Figure 5.12

Residual Turbidity vs. pHExperimental Conditions

Wastewater: Synthetic

Initial Turbidity = 120 JTU (32 JTU after settling)

Polymer: Wt-2870 (cationic)

Polymer Dosage: 50 mg/l

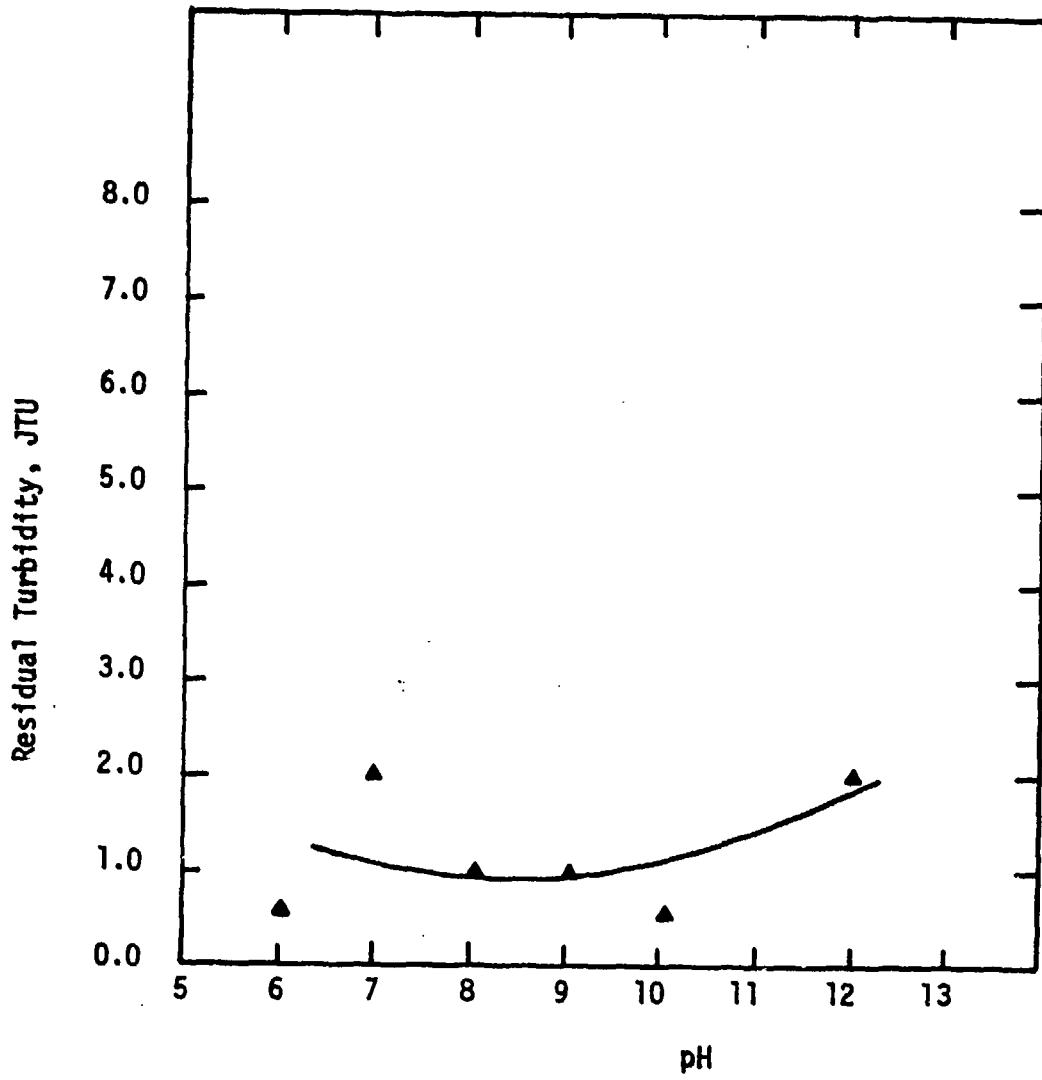


Figure 5.13

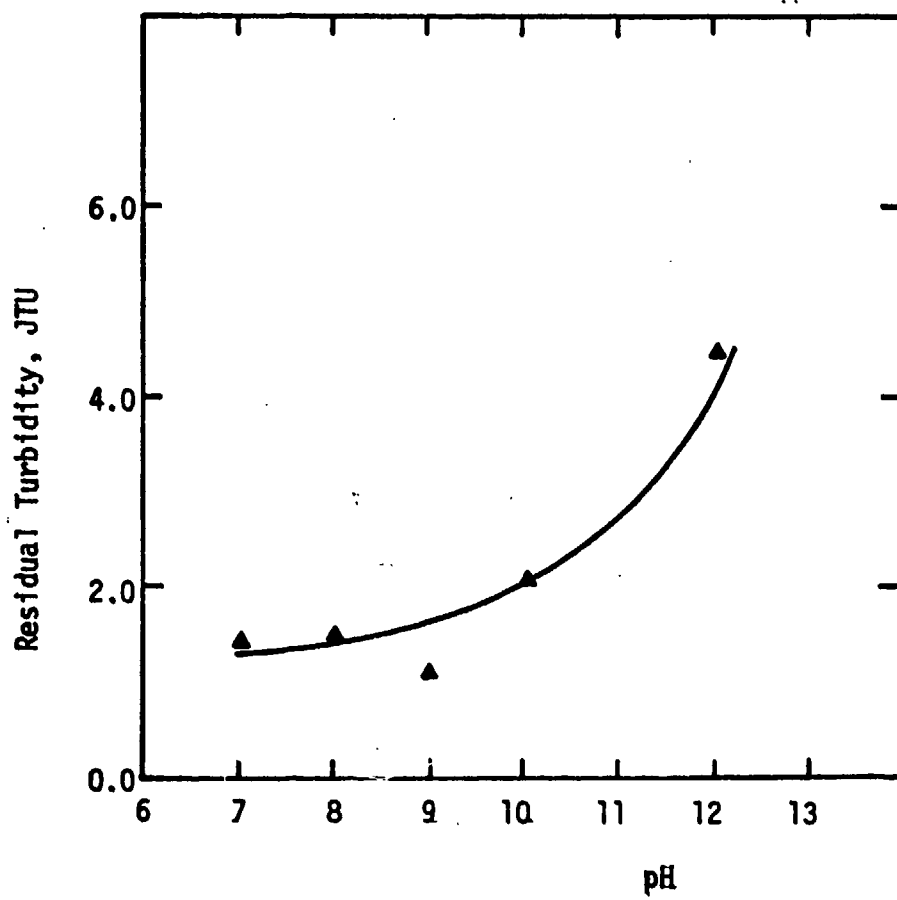
Residual Turbidity vs. pHExperimental Conditions

Wastewater: Synthetic

Initial Turbidity = 115 JTU (32 JTU after settling)

Polymer: Cat Floc T (cationic)

Polymer Dosage: 50 mg/l



with the possible exception of Figure 5.13. Although there is some variation in the data points, the residual turbidity range under consideration is so low that it is probable the variation is due to errors in experimental measurement.

During the course of the experiments with the synthetic wastewater, a gradual decrease in pH was observed which could not be explained.

5.1.2 Experiments using actual wastewater

5.1.2.1 "Diluted" actual wastewater

The initial shipment of wastewater from the Radford Army Ammunition plant was 5 gallons. This wastewater was diluted 5:1 (16.7% of original concentration) with tap water to carry out the initial experiments.

A colloid net charge determination of the wastewater indicated that it was slightly positive. Therefore, first the anionic polymers were tested as coagulants in the jar tests since they were of opposite charge. The non-ionic polymer was also used as a coagulant for the actual wastewater. Results obtained from these initial jar tests are presented in Figures 5.14 through 5.17.

The results show that the anionic and non-ionic polymers were not effective in coagulating the wastewater. To test a wide range of polymer dosages, the dosage was varied from 0.2 to 100 mg/l for the anionic polymers (see Figures 5.14 and 5.15). This was done to ensure that the system was

Figure 5.14

Residual Turbidity vs. Polymer Dosage

Experimental Conditions

Wastewater: Actual "diluted"

Initial Turbidity = 255 JTU

Polymer: WT-2700 (Anionic)

Figure 5.15

Residual Turbidity vs. Polymer Dosage

Experimental Conditions

Wastewater: Actual "diluted"

Initial Turbidity = 250 JTU

Polymer: Purifloc A-21 (Anionic)

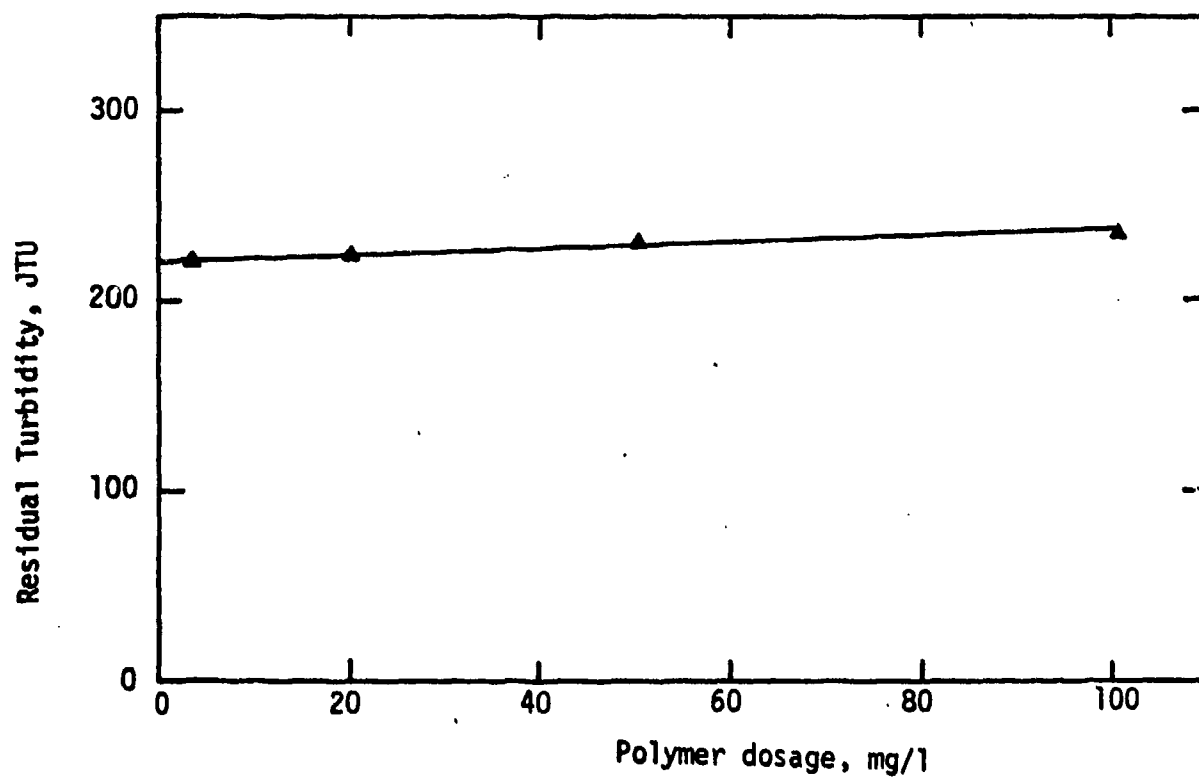
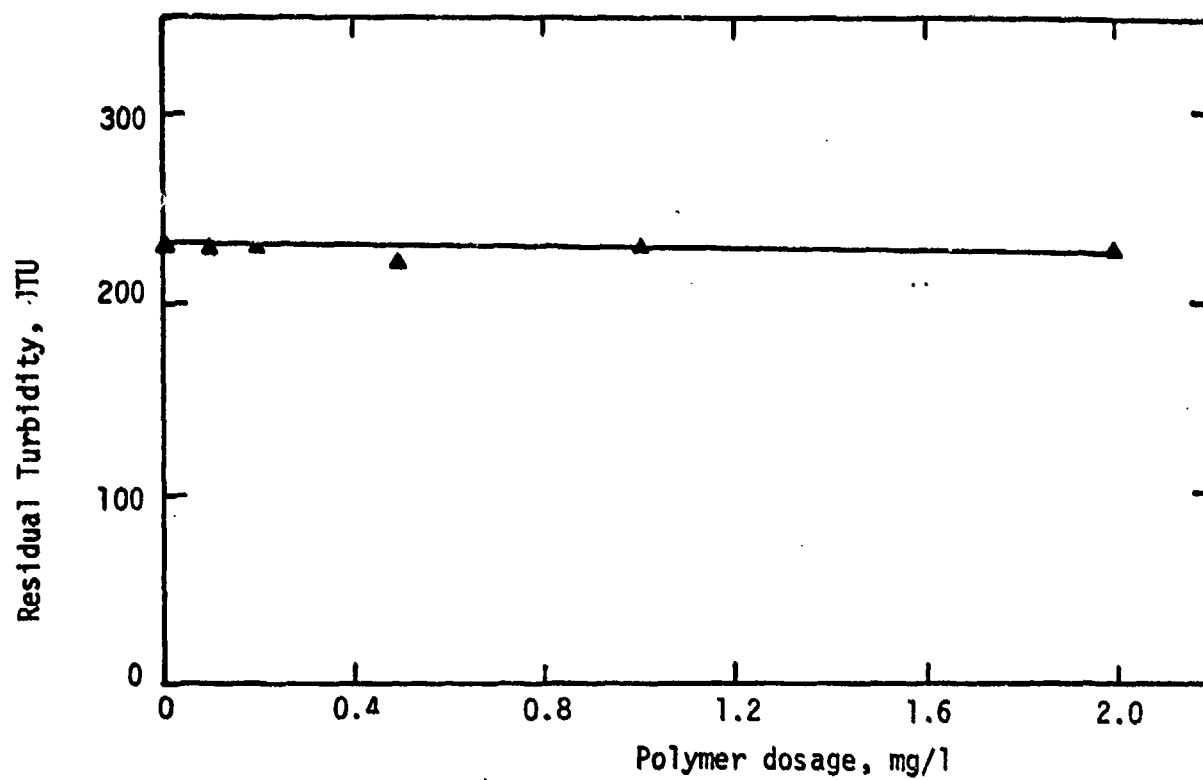


Figure 5.16

Residual Total Net Charge and pH vs. Polymer Dosage

Figure 5.17

Residual Turbidity vs. Polymer Dosage

Experimental Conditions

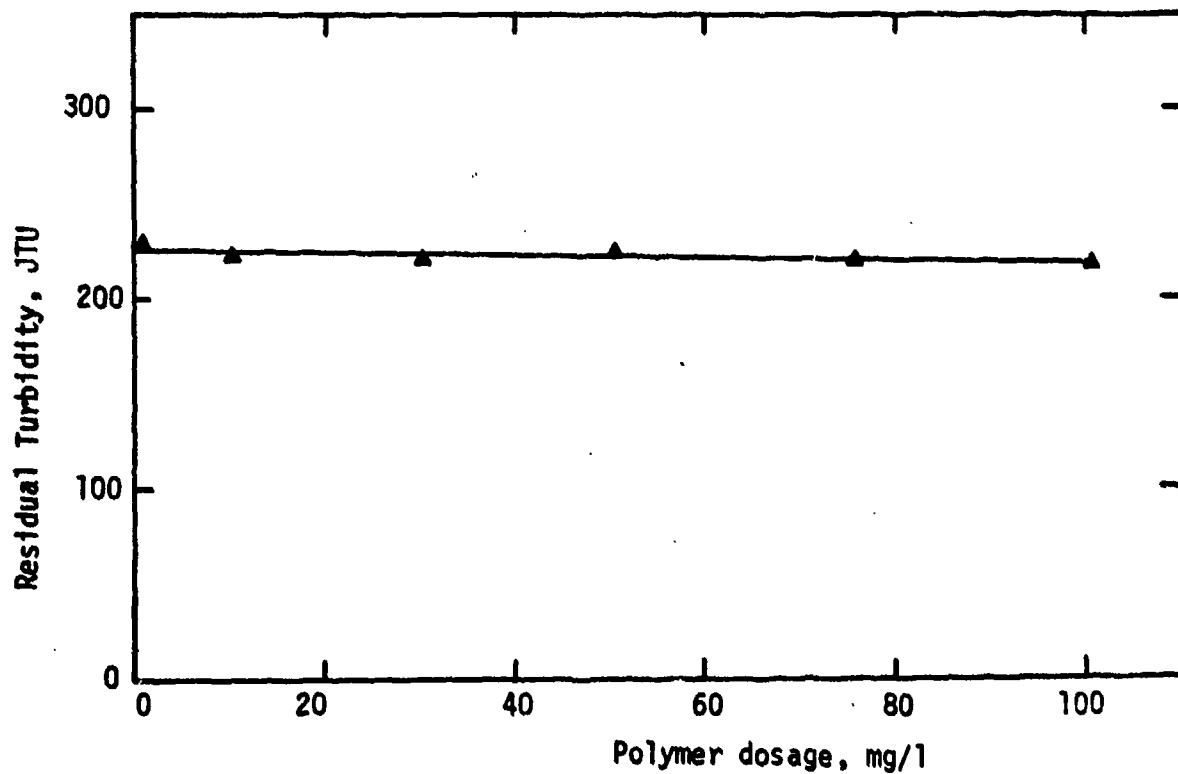
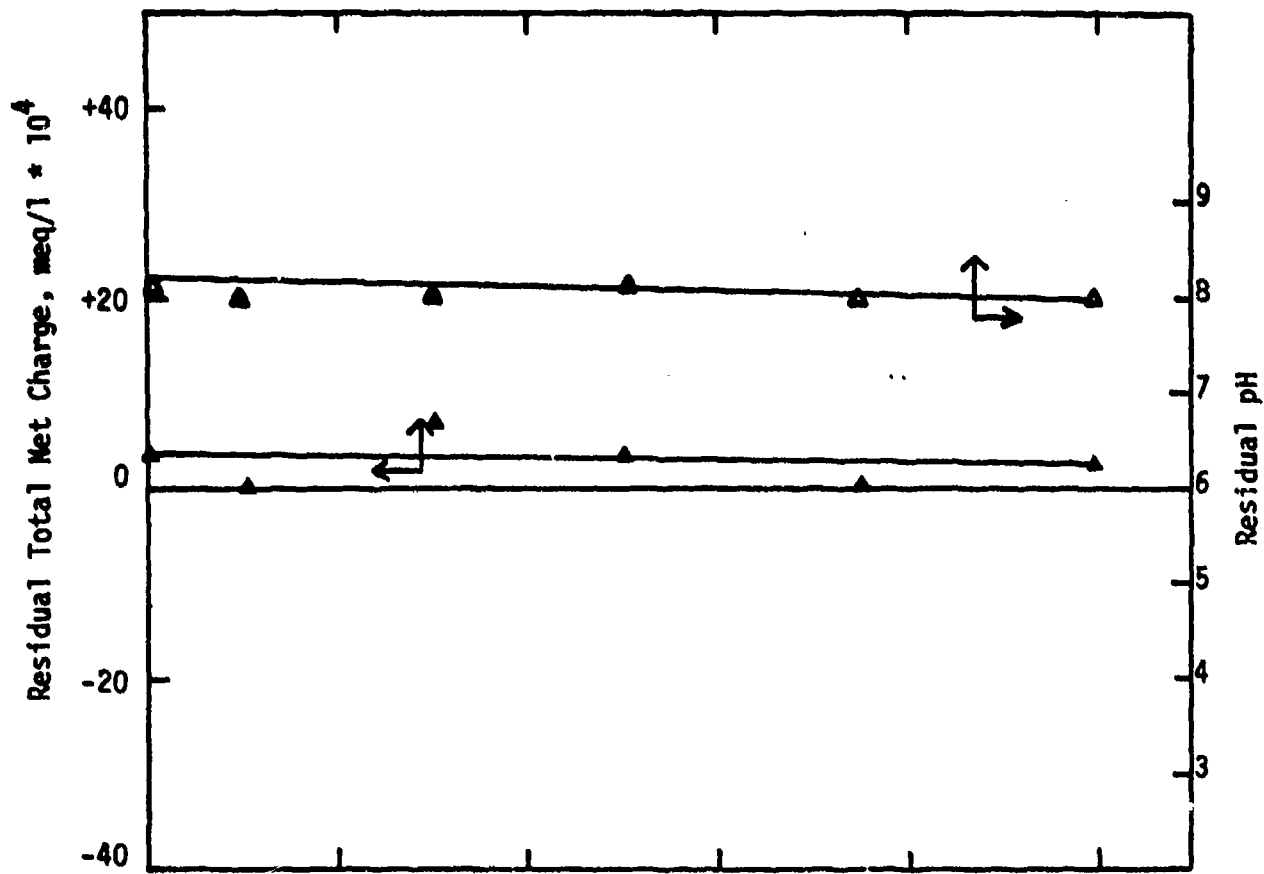
Wastewater: Actual "diluted"

Initial Turbidity = 255 JTU

Initial pH = 8.2

Initial Charge = $+12 \cdot 10^{-4}$ meq/l

Polymer: WT-2690 (Non-ionic)



not "underdosed" or "overdosed" with polymer. However, as can be seen from the results, all of the polymer dosages tested did not give any turbidity removal. One reason for this was the very slight positive charge of the wastewater. This net charge was probably made up of positively and negatively charged colloid solids in the wastewater. The overall net charge was positive. However, this positive charge was so low that coagulation by charge neutralization could not be made possible. In Figure 5.16, the total net charge vs. polymer dosage curve is nearly close to zero in the first place, therefore charge neutralization could not be effective in coagulation. It should be noted that although the non-ionic polymer was effective in turbidity removal for the synthetic wastewater, (see Figure 5.6) the same action could not be seen in the actual "diluted" wastewater. It was mentioned previously that the non-ionic polymer's coagulating action was due mainly to interparticle bridging. This mechanism depends largely also on the characteristics of the wastewater. One possible explanation is that the bentonite particles in the synthetic wastewater were larger than the colloidal suspended particles in the actual wastewater, thus the bridging mechanism was much more effective in the synthetic wastewater than in the actual wastewater.

5.1.2.1.1 Tests using coagulant aids

At this point in the research, it was decided that the characteristics of the wastewater had to be changed in

some way to improve the coagulation process. From the previous experiments it was known that the cationic polymers worked quite effectively on the highly anionic synthetic wastewater. Jar tests were then carried out by adding a certain dosage of bentonite to the system before the polymer was added. Results of these tests are presented in Figures 5.18 through 5.21.

The addition of bentonite (negatively charged) neutralized the slightly positive charge of the wastewater and made it highly anionic in nature. Cationic polymers acted on this anionic system predominantly by charge neutralization to bring about effective turbidity removal. It can be seen in Figures 5.18 and 5.20 that the net charge of the system is reduced to near zero at the point of highest turbidity removal. This indicates that coagulation took place predominantly by the mechanism of charge neutralization. The residual TOC of the supernatant was also measured in these jar tests. The results show that TOC removal took place in correspondence with the turbidity removal. The TOC removal was due to the removal of suspended solids in the system; the remaining TOC was due to the dissolved organic solids in the wastewater which could not be removed.

The bentonite added to the system as a coagulant aid acted not only to make the wastewater anionic in nature but also to provide sites for particle attachment that would allow the colloidal particles to grow in size. This action is termed the nuclei effect. The following test was carried

Figure 5.18

Residual Total Net Charge and pH vs. Polymer Dosage

Figure 5.19

Residual Turbidity and TOC vs. Polymer Dosage

Experimental Conditions

Wastewater: Actual "diluted"

Initial Turbidity = 270 JTU

Initial pH = 8.9

Initial Charge = $+12 * 10^{-4}$ meq/l ($-920 * 10^{-4}$ meq/l
after bentonite addition)

Initial TOC = 145 mg/l

Polymer: Cat Flocc T (Cationic)

Coagulant aid and dosage: Bentonite, 1.25 g/l

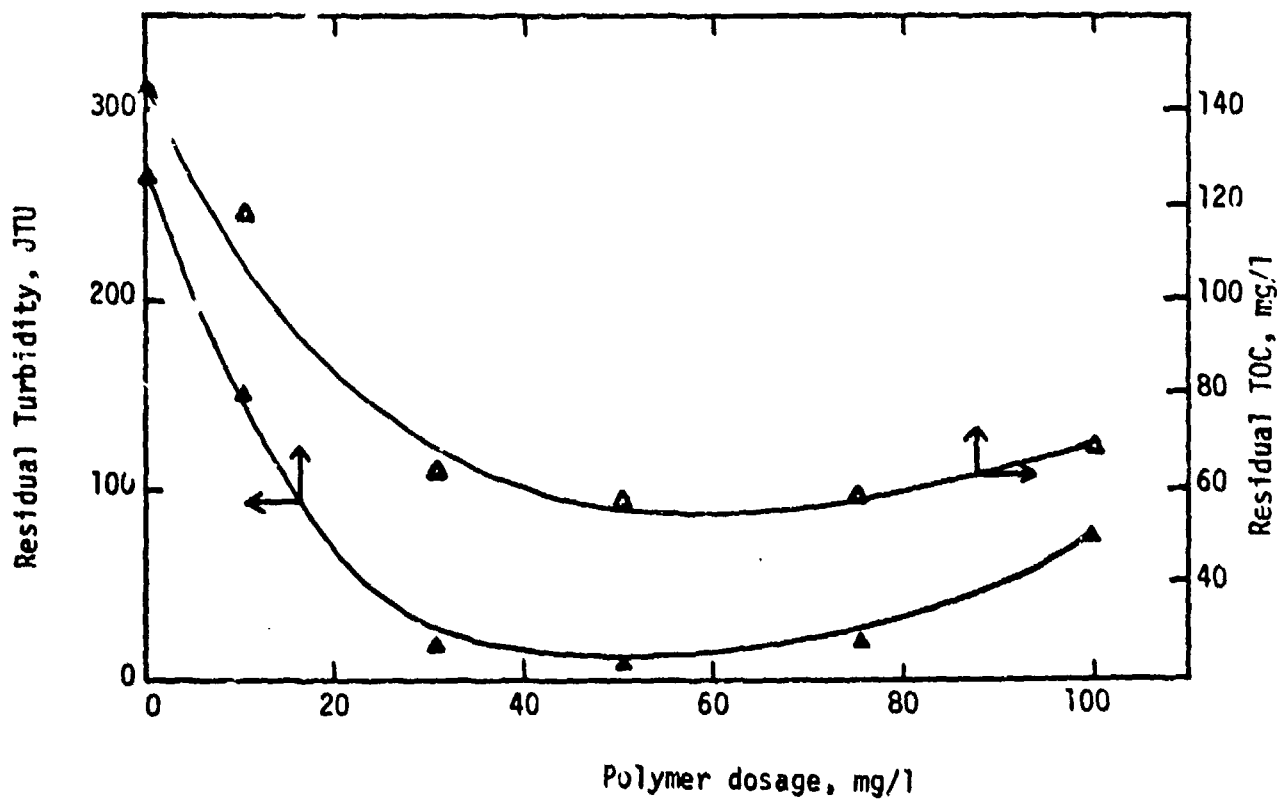
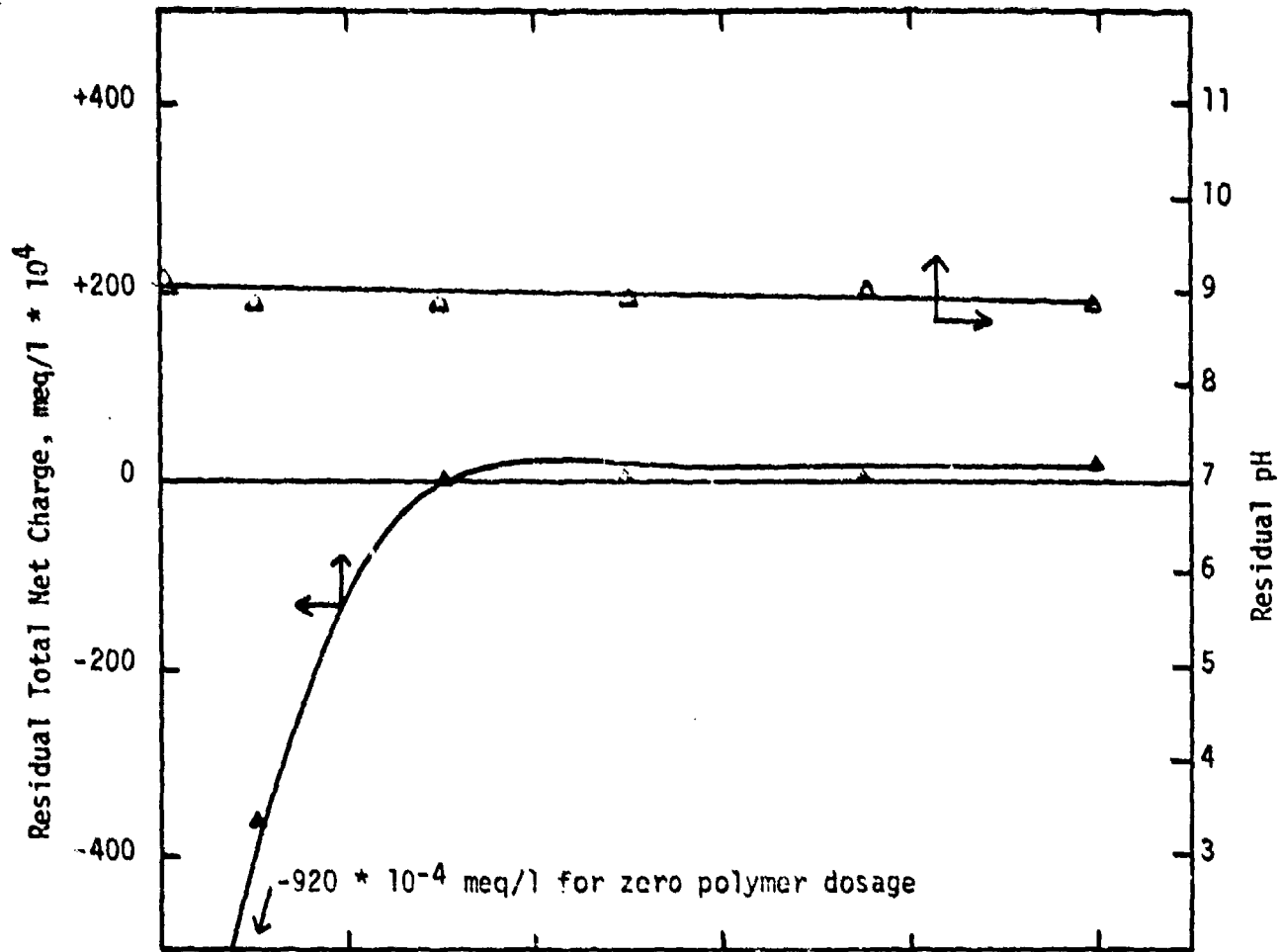


Figure 5.20

Residual Total Net Charge and pH vs. Polymer Dosage

Figure 5.21

Residual Turbidity and TOC vs. Polymer DosageExperimental Conditions

Wastewater: Actual "diluted"

Initial Turbidity = 260 JTU

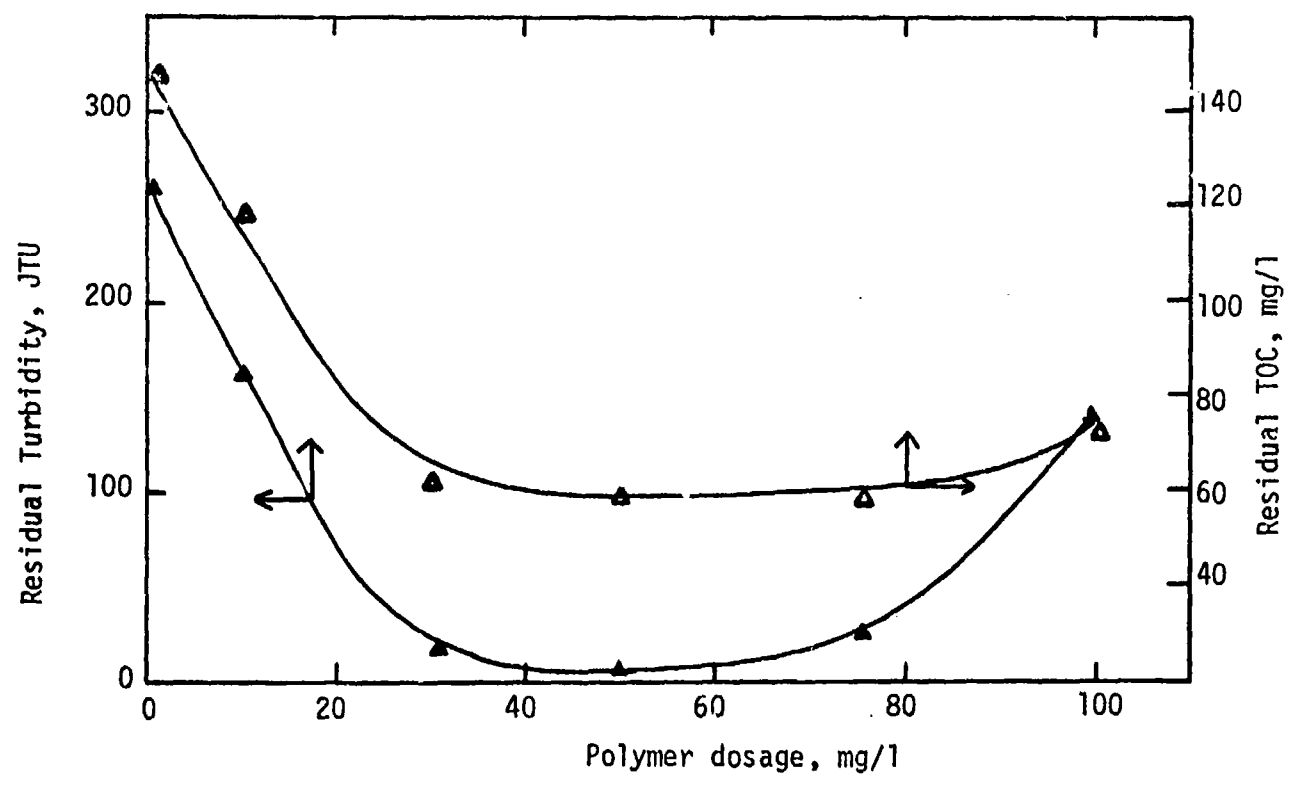
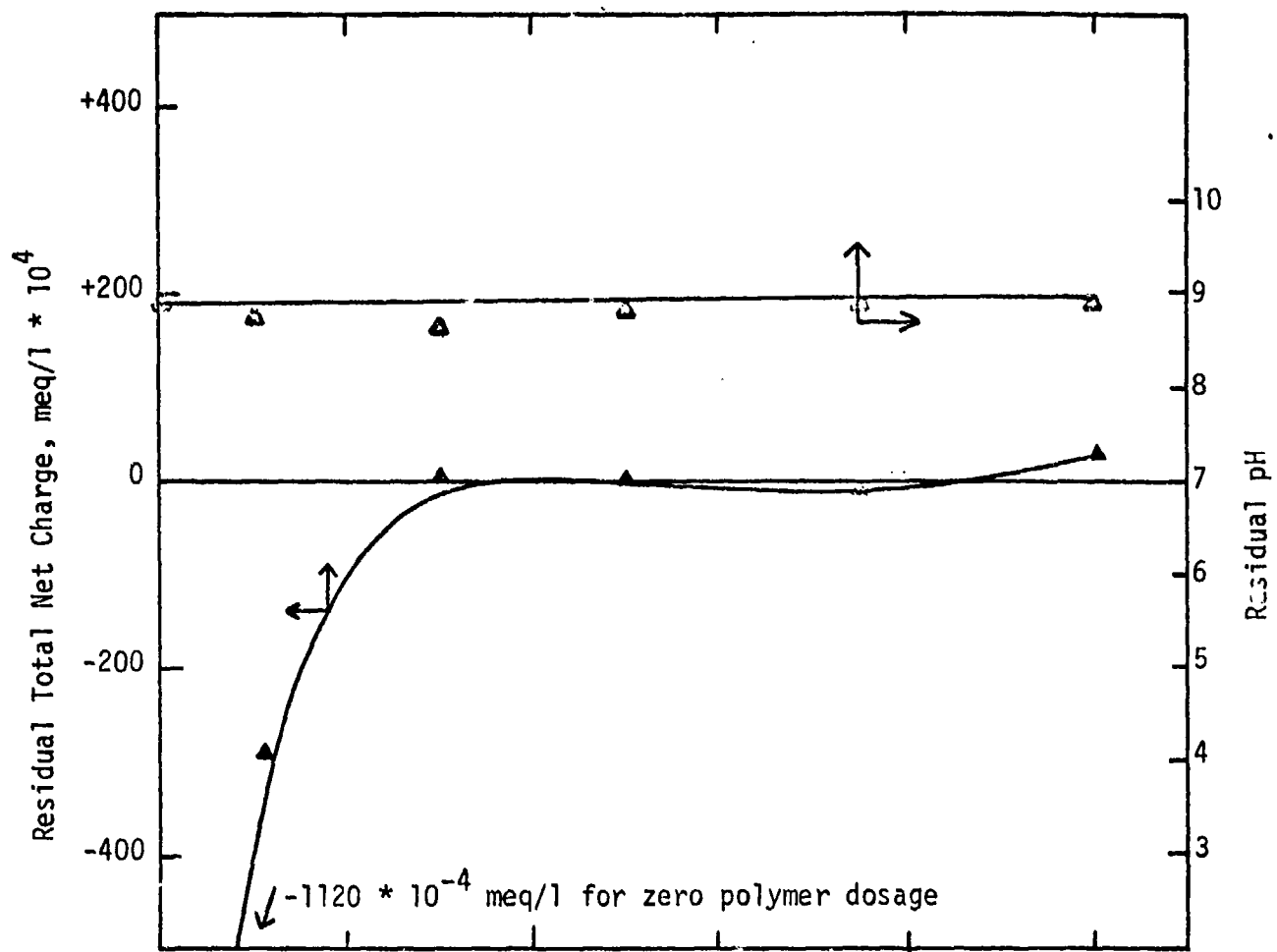
Initial pH = 8.9

Initial Charge = $+12 * 10^{-4}$ meq/l ($-1120 * 10^{-4}$ meq/l
after bentonite addition)

Initial TOC = 145 mg/l

Polymer: WT-2870 (Cationic)

Coagulant aid and dosage: Bentonite, 1.25 g/l



out to see if the dosage of bentonite could be reduced without changing its favorable effect in turbidity removal. A jar test was conducted where Cat Flocc T polymer was added at a constant dosage of 50 mg/l to the wastewater samples. Varying dosages of bentonite were added and residual turbidity of the supernatant was measured. The data obtained can be seen in Figure 5.22. It was observed that even with 0.1 g/l of bentonite, a 91.6 % reduction in turbidity could be achieved. As the bentonite dosage was increased, the turbidity removal also increased. In an actual treatment process a compromise would have to be made between the turbidity removal desired and the amount of sludge formation due to the increased amounts of bentonite. From the experimental data, it was assumed that a bentonite concentration of 0.5 g/l would give a balanced compromise.

A test was conducted with the wastewater and anionic polymer WT-2700 using the optimum dosage of 0.5 g/l bentonite as a coagulant aid. Figures 5.23 and 5.24 show the data obtained from the test. The results indicate that this system did not work effectively and very little turbidity removal was achieved. The increase in the negative net charge was due to the increased amounts of anionic polymer. The reason why the anionic polymer did not work was because both the wastewater containing bentonite clay and the coagulant were negatively charged and the magnitude of the repulsion forces between the like-charged particles prevented contact so that

Figure 5.22

Residual Turbidity vs. Bentonite DosageExperimental Conditions

Wastewater: Actual "diluted"

Initial Turbidity = 250 JTU

Polymer: Cat Flocc T (Cationic)

Polymer Dosage: 50 mg/l

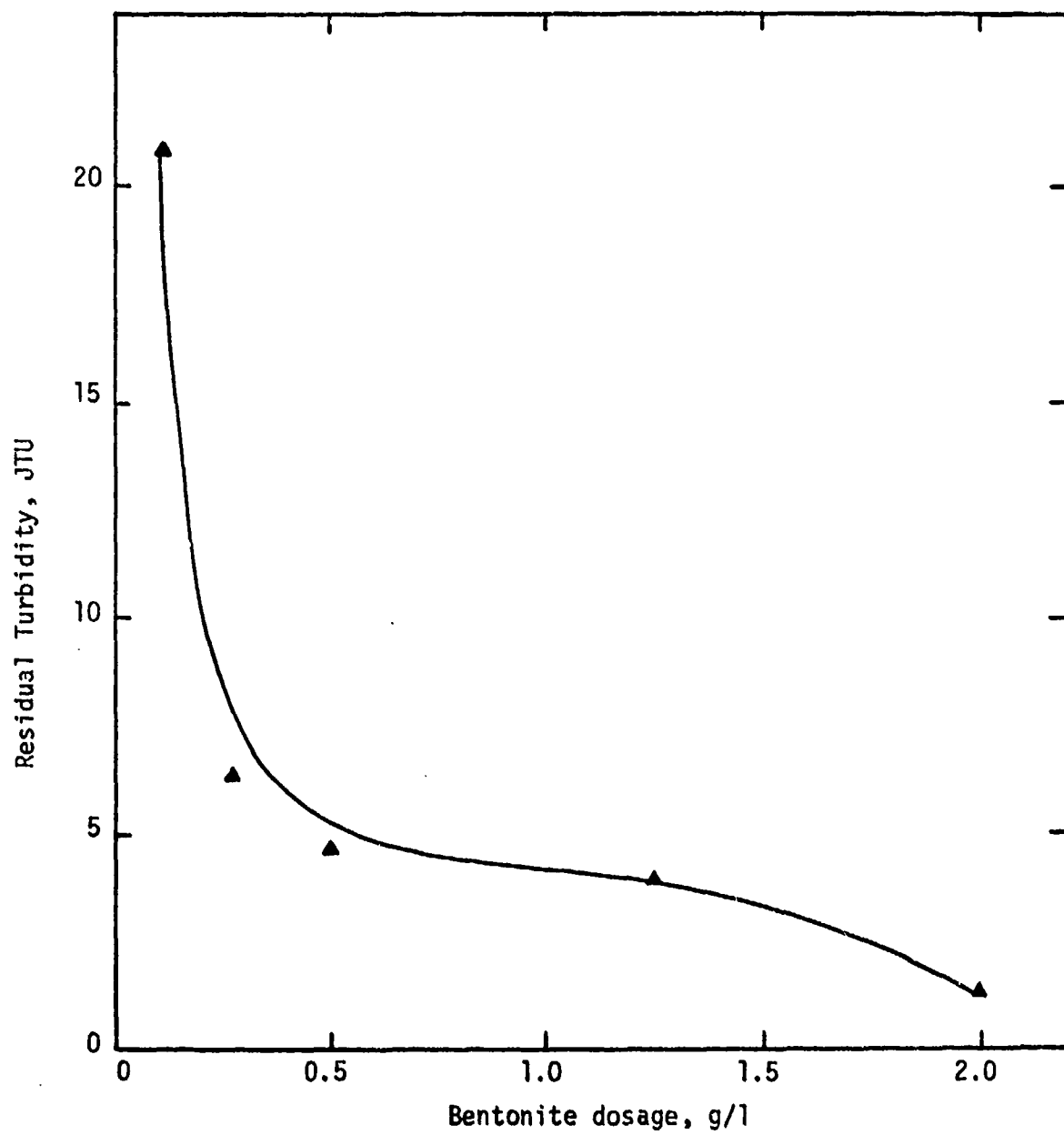


Figure 5.23

Residual Total Net Charge and pH vs. Polymer Dosage

Figure 5.24

Residual Turbidity vs. Polymer DosageExperimental Conditions

Wastewater: Actual "diluted"

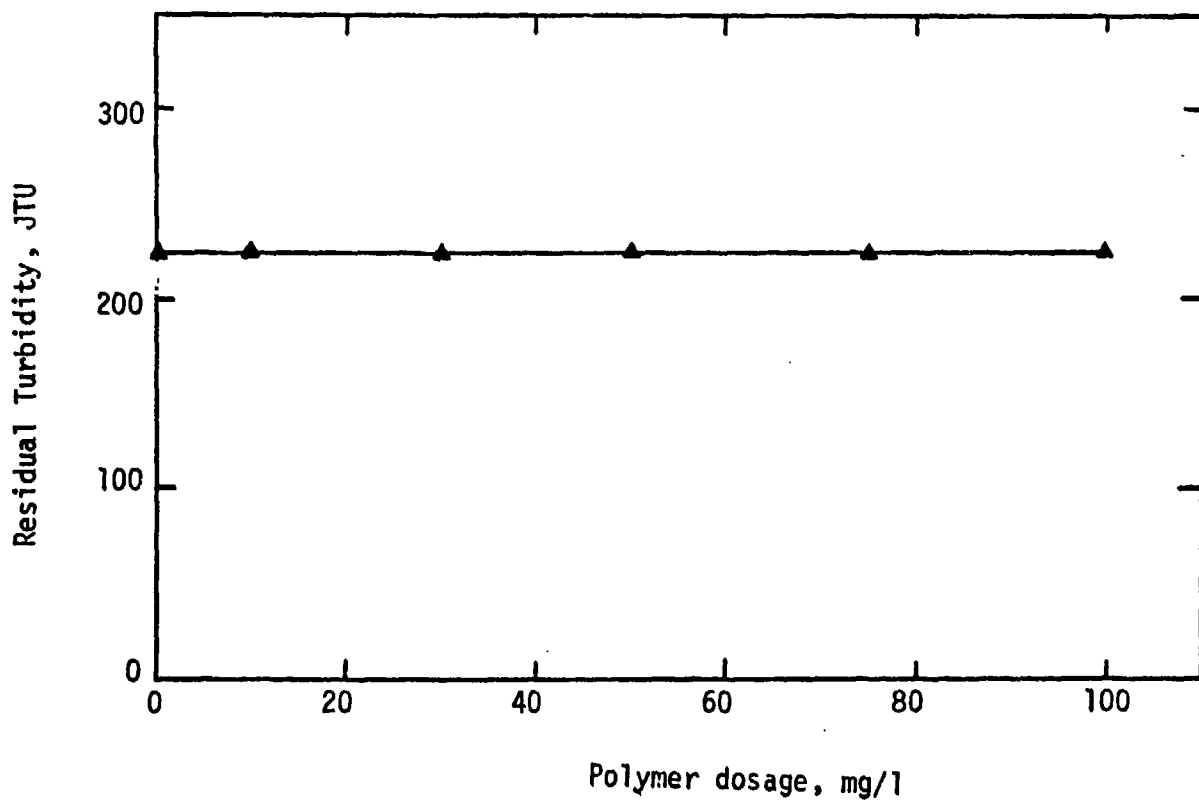
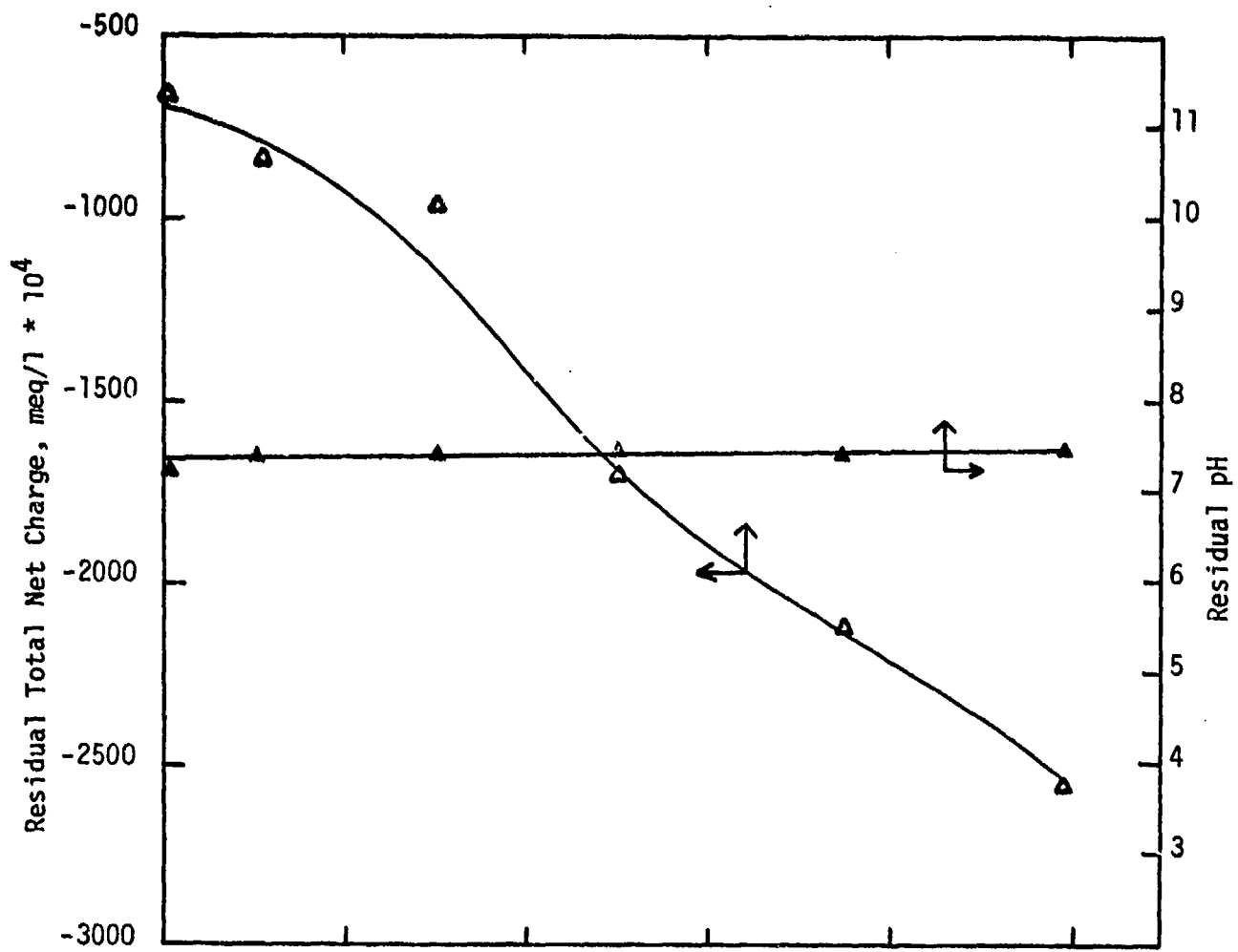
Initial Turbidity = 250 JTU

Initial pH = 7.2

Initial Charge = $+12 * 10^{-4}$ meq/l ($-624 * 10^{-4}$ meq/l
after bentonite addition)

Polymer: WT-2700 (Anionic)

Coagulant aid and dosage: Bentonite, 0.5 g/l



no bridging action was possible.

5.1.2.2 "Undiluted" actual wastewater

The experiments were continued when 15 55-gallon drums of actual wastewater were shipped from the Radford Army Ammunition plant. Since there was adequate wastewater to continue the experiments, no dilutions were made. Unfortunately, the two shipments of wastewater did not possess the same concentration and characteristics, therefore direct comparison of the results obtained from the two batches of actual wastewater could not be made.

5.1.2.2.1 Tests using bentonite as a coagulant aid

Initially two jar tests were conducted using cationic polymers Cat Floe and WT-2870 and powdered bentonite clay as a coagulant aid. The two polymers gave good results in terms of turbidity removal (see Figures 5.25 through 5.28). The optimum polymer dosage was around 100 mg/l for both polymers. In tests with the synthetic wastewater, the optimum polymer dosage for the cationic polymers was around 50 mg/l. Higher dosage of polymer was required for the actual wastewater because the concentration of the suspended colloid particles were greater than in the synthetic wastewater. The higher concentration required greater amounts of polymer. The data also shows that near the point of optimum turbidity removal nearly complete charge neutralization has taken place and the residual net charge is close to zero. This indicates

Figure 5.25

Residual Total Net Charge and pH vs. Polymer Dosage

Figure 5.26

Residual Turbidity and TOC vs. Polymer DosageExperimental Conditions

Wastewater: Actual "undiluted"

Initial Turbidity = 245 JTU

Initial pH = 7.1

Initial Charge = $+200 * 10^{-4}$ meq/l ($-980 * 10^{-4}$ meq/l
after bentonite addition)

Initial TOC = 610 mg/l

Polymer: Cat Flocc (Cationic)

Coagulant aid and dosage: Bentonite, 1.25 g/l

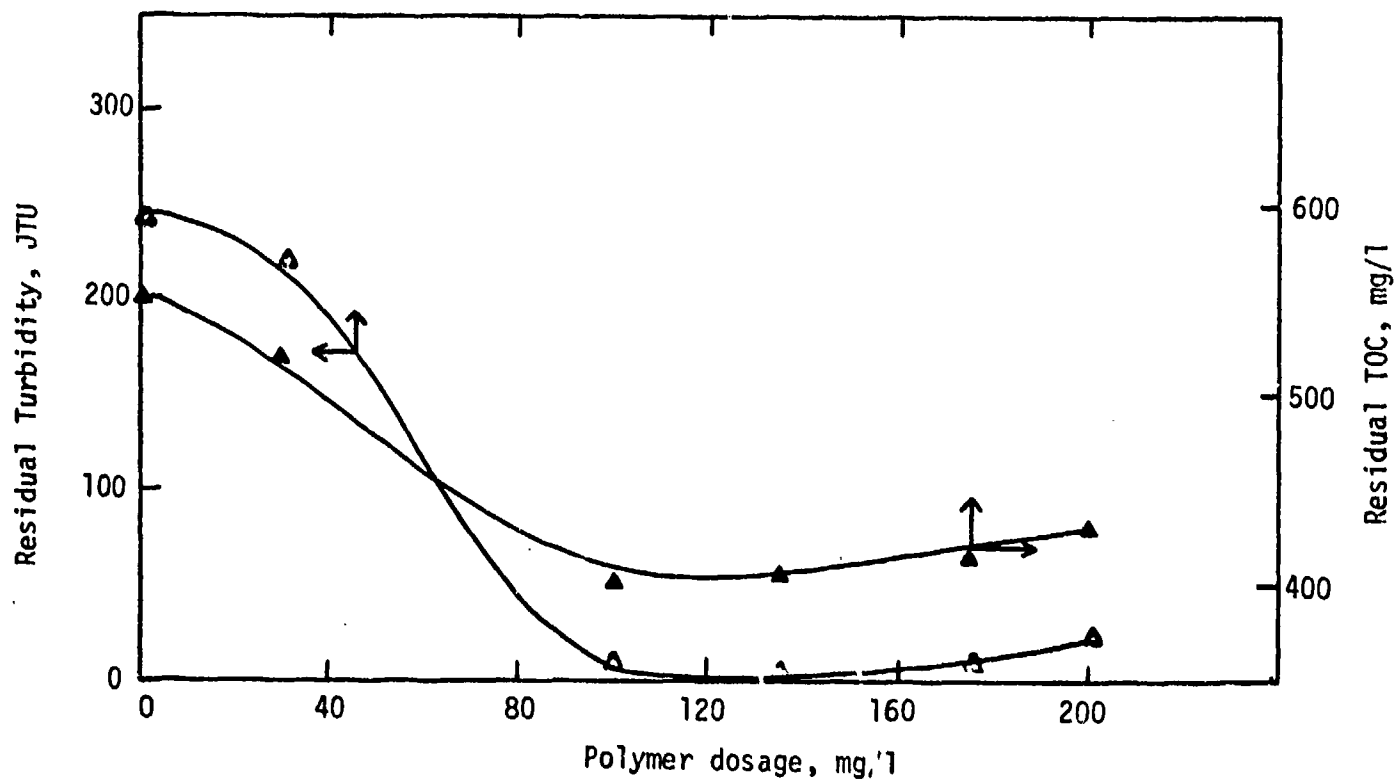
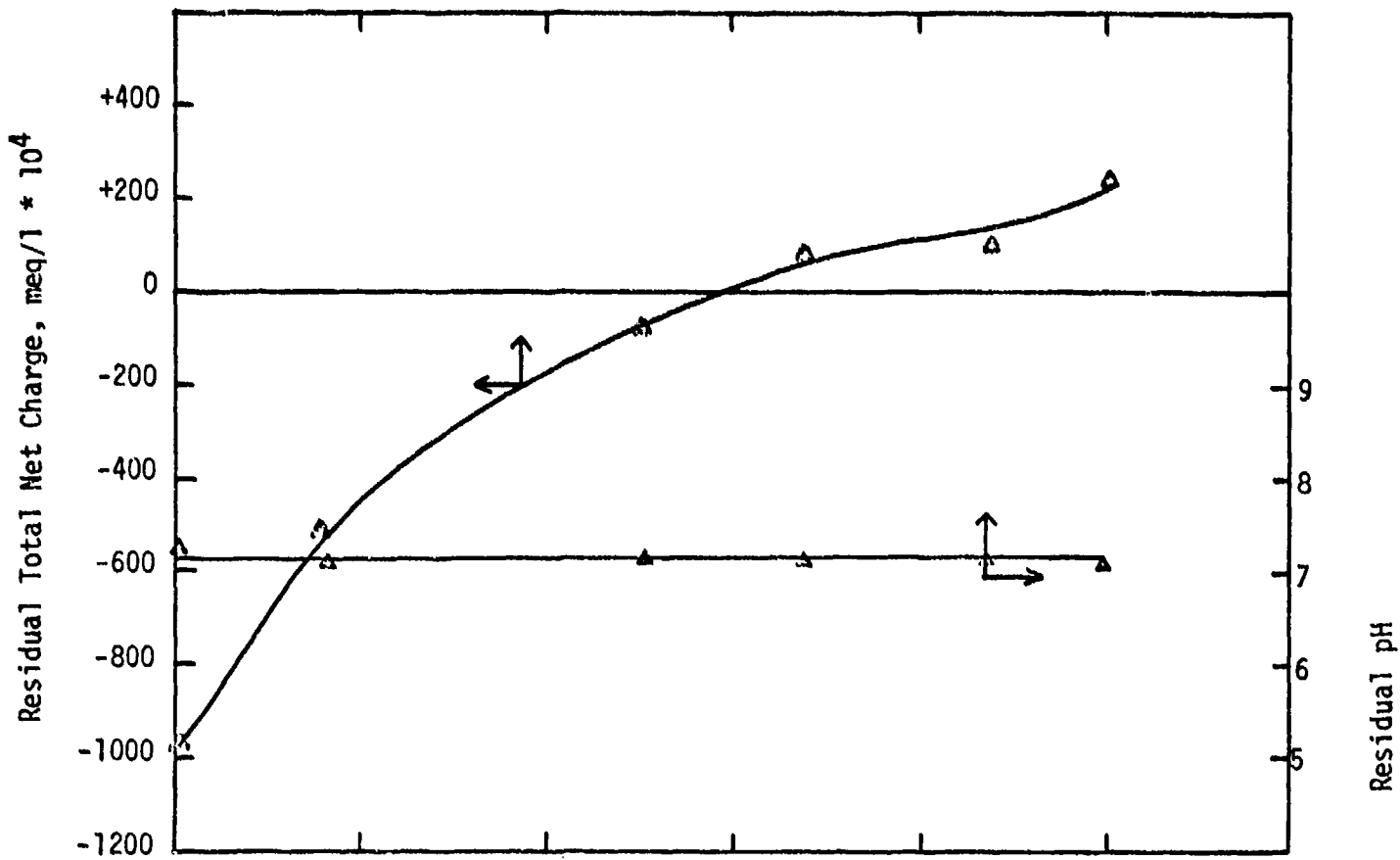


Figure 5.27

Residual Total Net Charge and pH vs. Polymer Dosage

Figure 5.28

Residual Turbidity and TOC vs. Polymer Dosage

Experimental Conditions

Wastewater: Actual "undiluted"

Initial Turbidity = 245 JTU

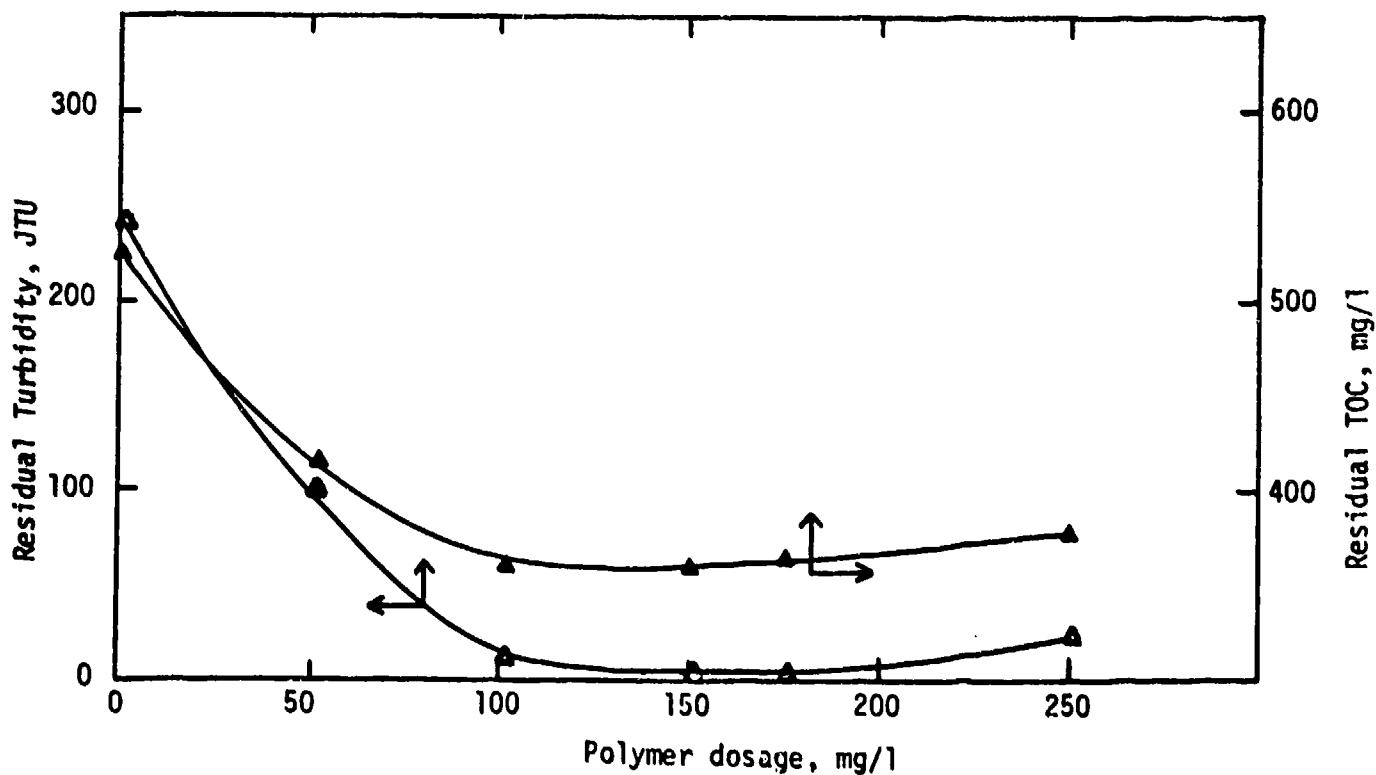
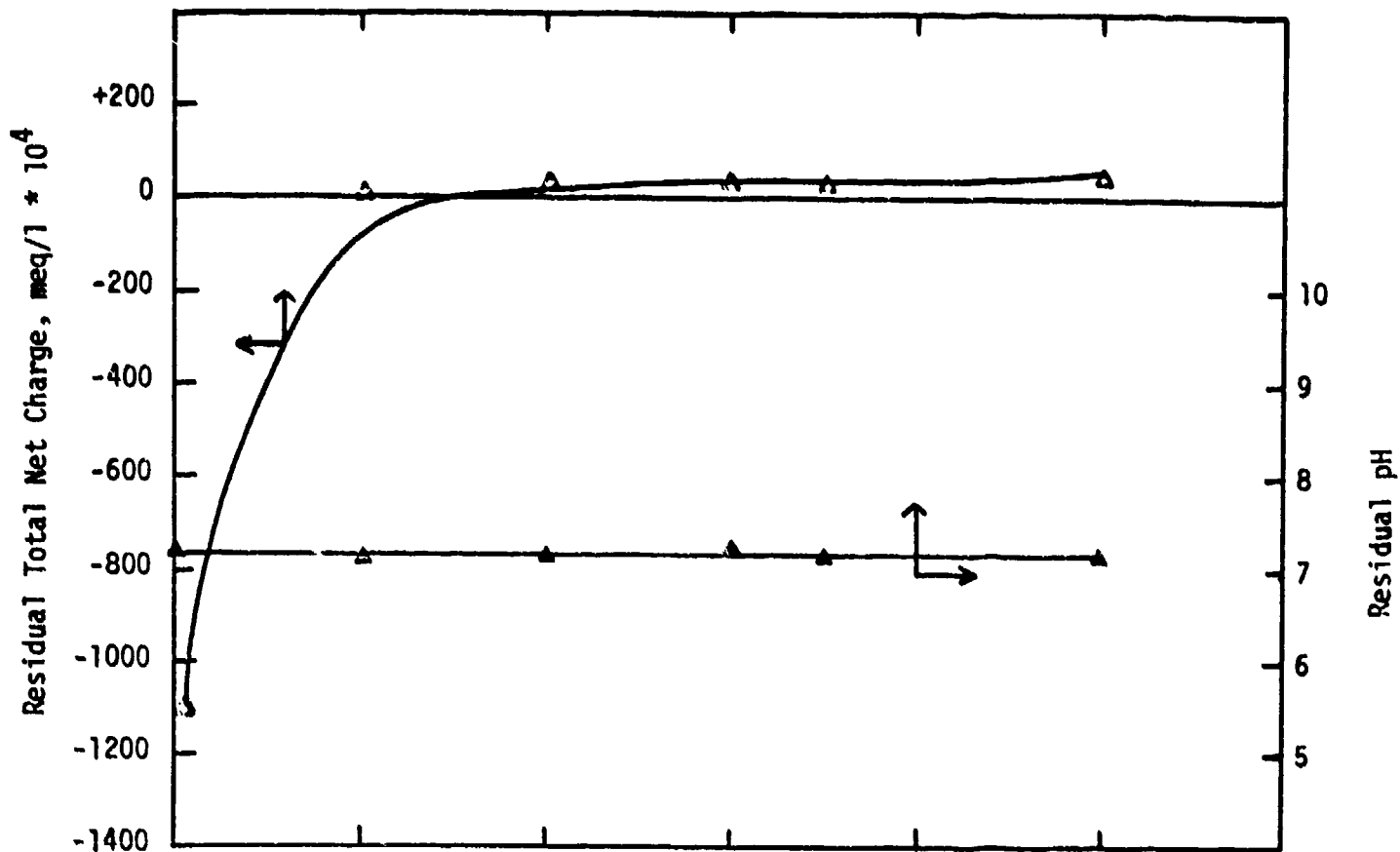
Initial pH = 7.1

Initial Charge = $+200 * 10^{-4}$ meq/l ($-1100 * 10^{-4}$ meq/l
after bentonite addition)

Initial TOC = 610 mg/l

Polymer: WT-2870 (Cationic)

Coagulant aid and dosage: Bentonite, 1.25 g/l



again that the dominant mechanism for coagulation of negatively charged wastewater with a cationic polymer is charge neutralization. The TOC removal is due to the colloidal suspended solids removed in coagulation and flocculation and the remaining TOC is accounted for in the dissolved organic solids left in the supernatant.

Since the two nitrocellulose-manufacturing wastewaters that were shipped were different in concentration and characteristics, it was necessary to repeat the determination of the effect of bentonite dosage on turbidity removal with the second shipment of wastewater. In this jar test, Cat Flocc was used as the coagulant at a constant dosage of 100 mg/l with varying dosages of bentonite clay. The results of this experiment are presented in Figure 5.29. It is seen that a bentonite clay dosage of 0.1 g/l was quite sufficient in bringing about a 98% reduction in turbidity. The much smaller dosage of bentonite that was required in this case could be due to the different polymer and a high polymer dosage being used and also due to the different wastewater being tested.

5.1.2.2.2 Powdered Carbon Adsorption Study

Jar tests were conducted to test the effect of carbon adsorption in removing organic impurities in the wastewater. Powdered activated carbon was added in varying dosages to the wastewater samples and the residual TOC of the samples were measured. The data obtained has been graphed in Figure 5.30. The TOC removal was not significant. Even when

Figure 5.29

Residual Turbidity vs. Bentonite DosageExperimental Conditions

Wastewater: Actual "undiluted"

Initial Turbidity = 240 JTU

Polymer: Cat Flocc (Cationic)

Polymer dosage: 100 mg/l

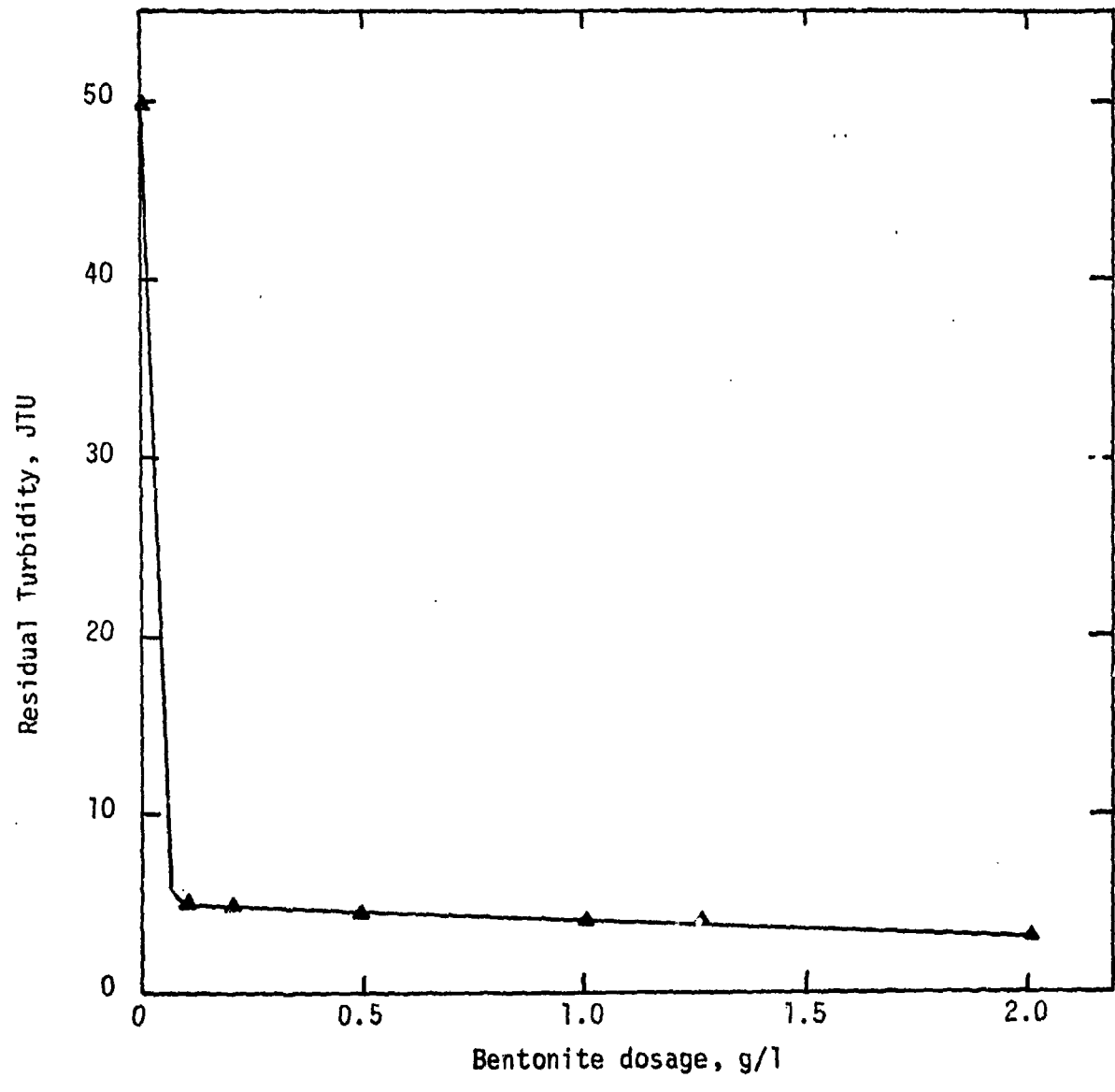


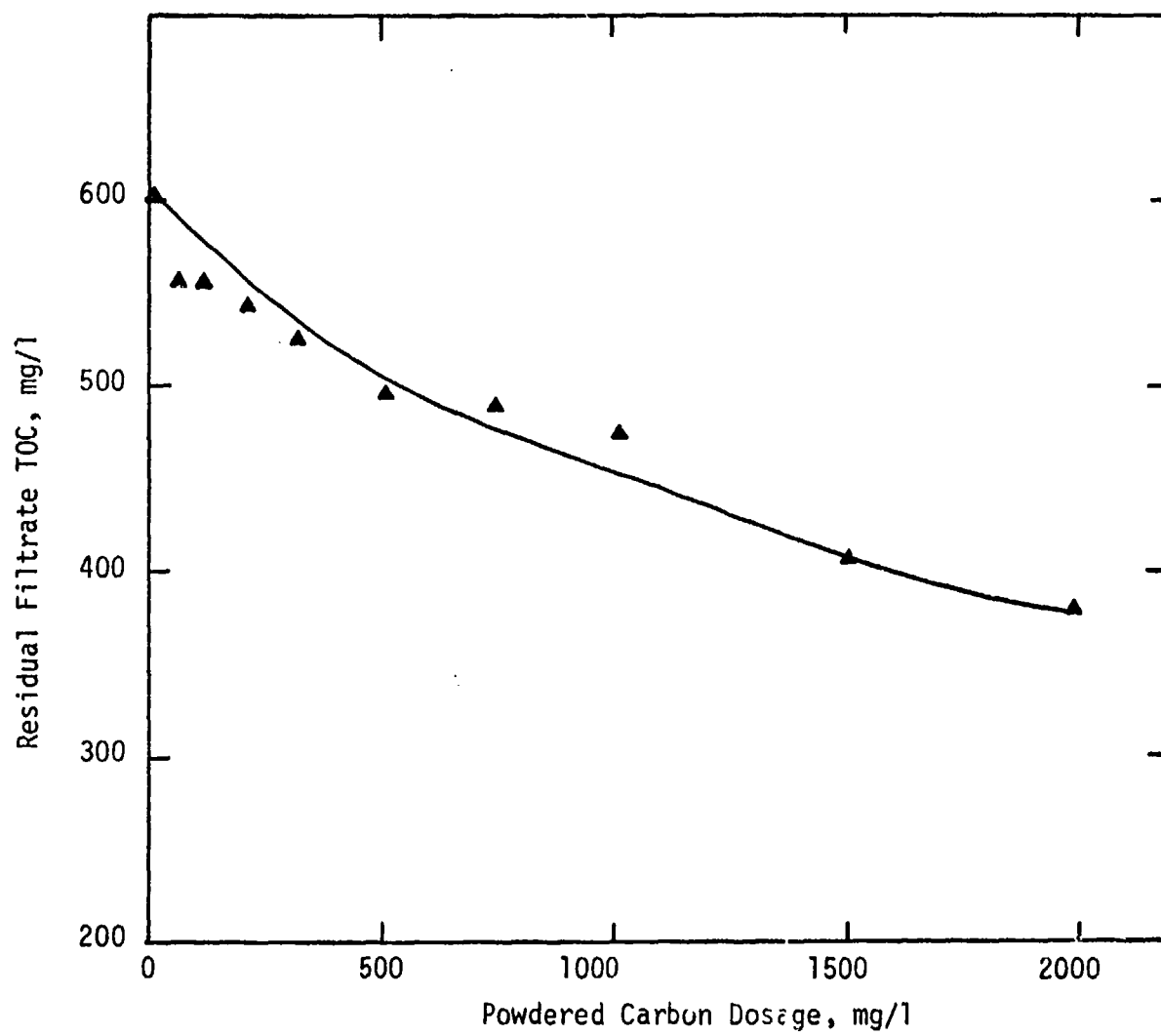
Figure 5.30

Residual TOC vs. Powdered Carbon DosageExperimental Conditions

Wastewater: Actual "undiluted"

Initial TOC = 600 mg/l

Contact time = 5 minutes



a carbon dosage of 2000 mg/l was applied, the TOC removal was 37%. Therefore, further tests with powdered carbon and various polymers were not carried out. The ineffectiveness of this test was probably due to the short contact time of 5 minutes.

5.1.2.2.3 Tests using lime as a precipitant and as a coagulant aid

High-lime precipitation was performed on the wastewater to observe its effectiveness in turbidity removal. The wastewater samples were dosed with varying amounts of calcium hydroxide and after initial mixing and sedimentation, the residual turbidity and pH of the samples were measured. (see Figure 5.31). Observation of the data reveals that high-lime precipitation is effective in turbidity removal. A lime dosage of 3 g/l gave a 82.4% turbidity reduction. The pH increase was due to the increasing hydroxide ion concentration. The effectiveness of lime in removing colloidal suspended solids was due to the enmeshment of these colloidal particles in the precipitate formed by the addition of lime (23).

It was decided to test lime in conjunction with other polymers to see if further turbidity reduction of the wastewater would be achieved. The lime dosage of 3 g/l was used since it was the lowest dosage which gave a significant turbidity removal (see Figure 5.31). Two polymers - cationic Cat Flocc and anionic Purifloc A-21- were used as coagulants. Significant reduction in the turbidity was obtained (see Figures 5.32 through 5.35).

Figure 5.31

Residual Turbidity and pH vs. Lime DosageExperimental Conditions

Wastewater: Actual "undiluted"

Initial Turbidity = 245 JTU

Initial pH = 7.1

Polymer: None

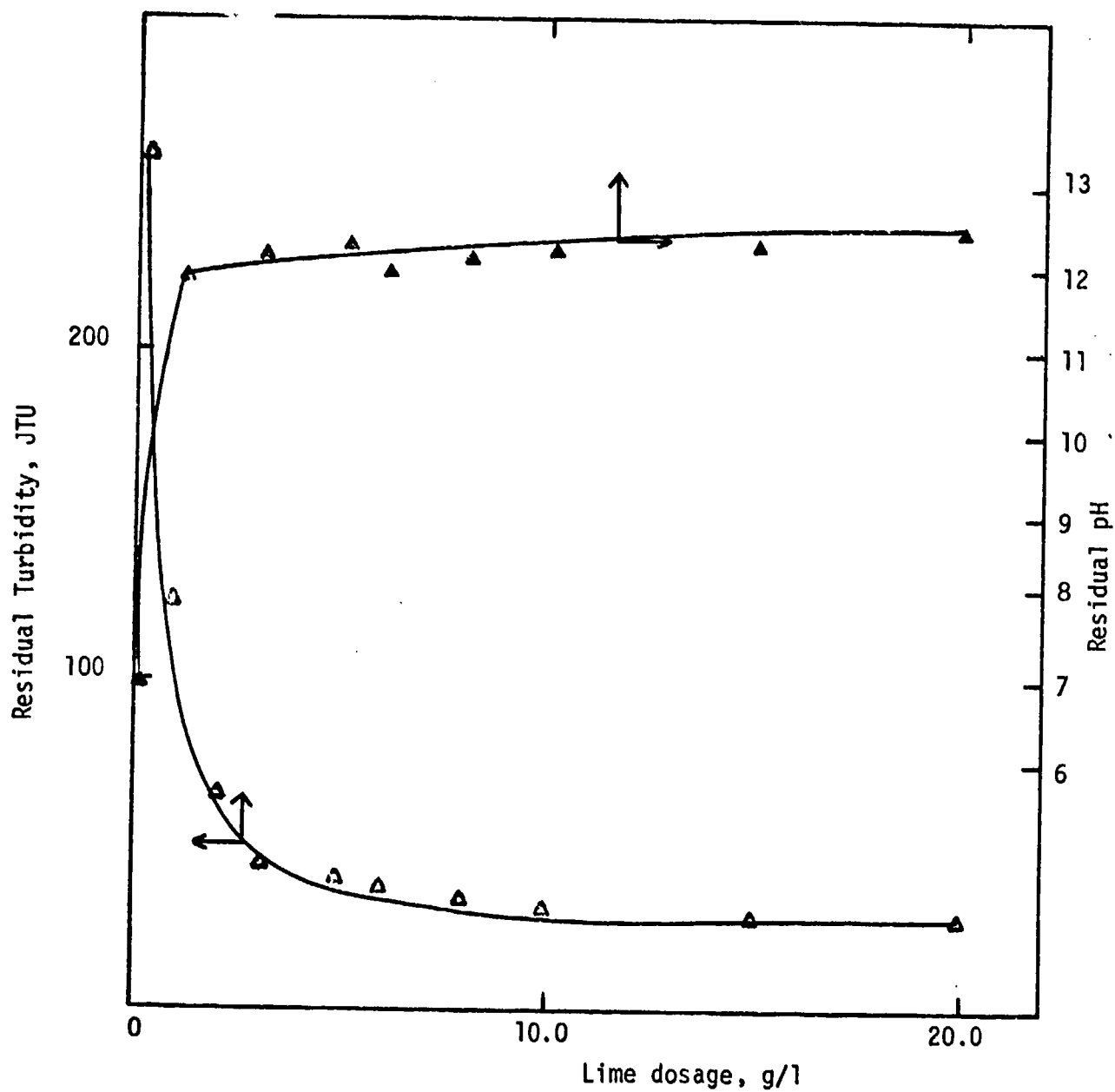


Figure 5.32

Residual pH vs. Polymer Dosage

Figure 5.33

Residual Turbidity and TOC vs. Polymer DosageExperimental Conditions

Wastewater: Actual "undiluted"

Initial Turbidity = 245 JTU

Initial TOC = 600 mg/l

Initial pH = 7.1

Polymer: Cat Flocc (Cationic)

Coagulant aid and dosage: Lime, 3 g/l

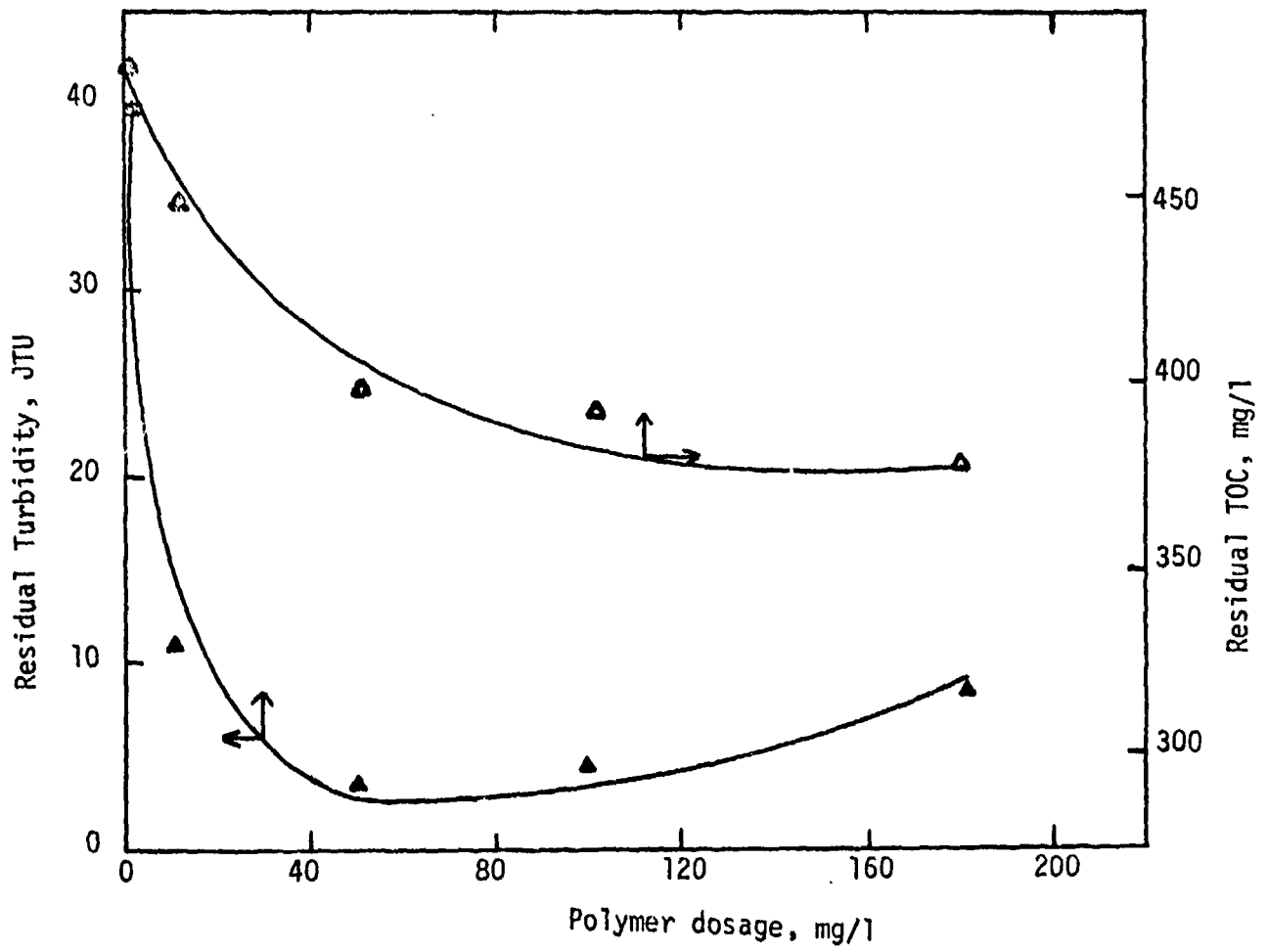
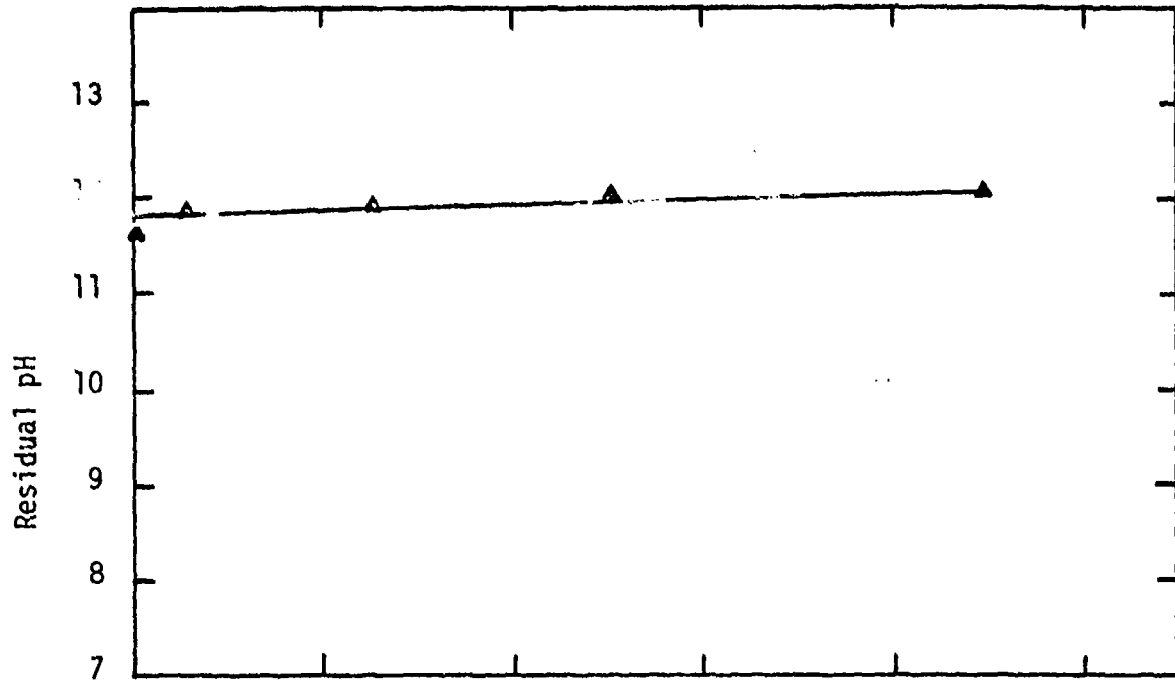


Figure 5.34

Residual pH vs. Polymer Dosage

Figure 5.35

Residual Turbidity and TOC vs. Polymer DosageExperimental Conditions

Wastewater: Actual "undiluted"

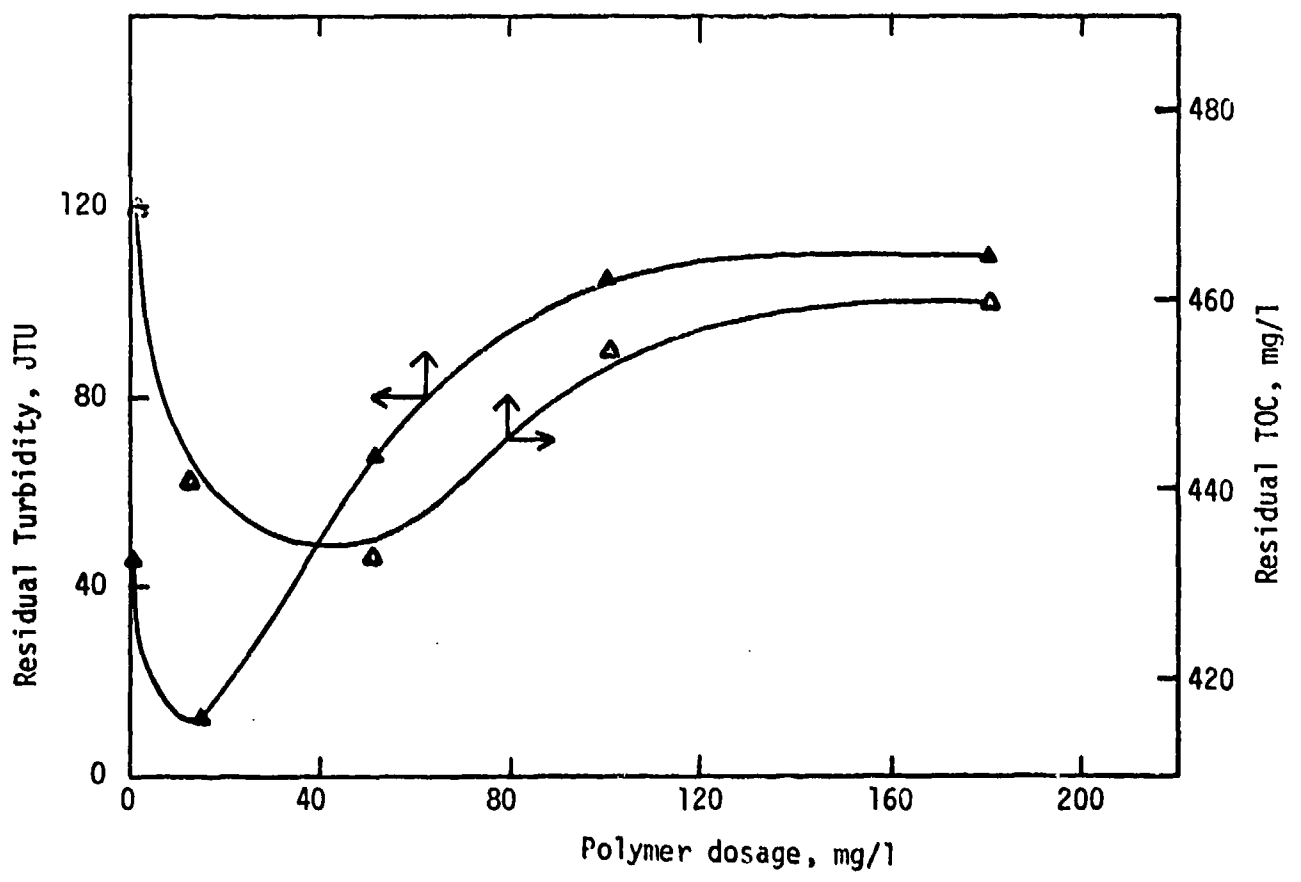
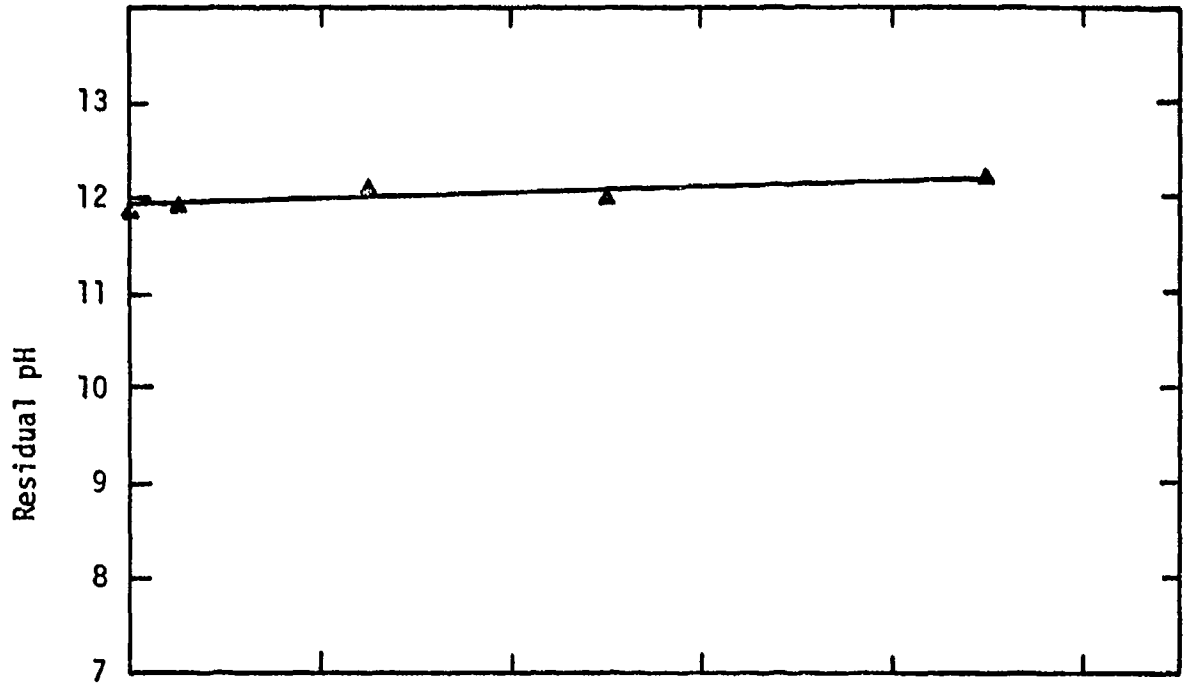
Initial Turbidity = 250 JTU

Initial TOC = 610 mg/l

Initial pH = 7.2

Polymer: Purifloc A-21 (Anionic)

Coagulant aid and dosage: Lime, 3 g/l



It was observed that when no polymer was added, the lime was able to reduce the turbidity from 250 JTU to 42 JTU. The additional turbidity removal was brought about by the coagulating action of the polymer. It should be noted that although the anionic polymer, Purifloc A-21, did not work effectively with the synthetic wastewater, it worked quite well with the actual wastewater. This was due to the fact that the synthetic wastewater was negatively charged and the actual wastewater had a positive charge of about $200 * 10^{-4}$ meq/l. The positive charge of the actual wastewater and the anionic nature of the polymer brought about charge neutralization, and turbidity removal could be achieved. The high pH was due to the presence of lime in high concentration. However, it should also be observed that when lime was used as a coagulant aid instead of bentonite, the optimum polymer dosage required was considerably lower. High-lime precipitation was able to reduce the TOC by 22% without any polymer addition. The addition of polymer increased this removal only to 31%. This indicates that most of the TOC was present in dissolved form.

5.2 Continuous Filtration Experiments

Six continuous filtration experiments were conducted with the actual undiluted wastewater using the information obtained in the jar tests. These runs have been outlined in Table 5.1. The experimental data has been graphed and is presented in Figures 5.36 through 5.52.

Table 5.1
Outline of Continuous Filtration Experiments

	<u>Run No.</u>					
	1	2	3	4	5	6
Flow rate (gpm/sq ft.)	2	2	2	4	2	2
Polymer used	None	Cat Floc	Cat Floc	Cat Floc	Cat Floc	Cat Floc
Method of Polymer Addition	-	Direct	Conventional	Conventional	Conventional	Conventional
Polymer Dosage (mg/l)	-	100	100	100	50	100
Coag.aid Used	None	Bentonite	Bentonite	Bentonite	Lime	Bentonite
Coag.aid Dosage (mg/l)	-	100	100	100	3000	100
Filtration Time (min.)	180	53	180	180	120	480

Figure 5.36

Effluent Total Net Charge and pH vs. Filtration Time

Figure 5.37

Effluent Turbidity and TOC vs. Filtration Time

Experimental Conditions

Wastewater: Actual "undiluted"

Initial Turbidity = 240 JTU

Initial TOC = 530 mg/l

Initial Charge = $+200 * 10^{-4}$ meq/l

Initial pH = 7.5

Flow rate = 2 gpm/sq ft

Polymer: None

Coagulant aid: None

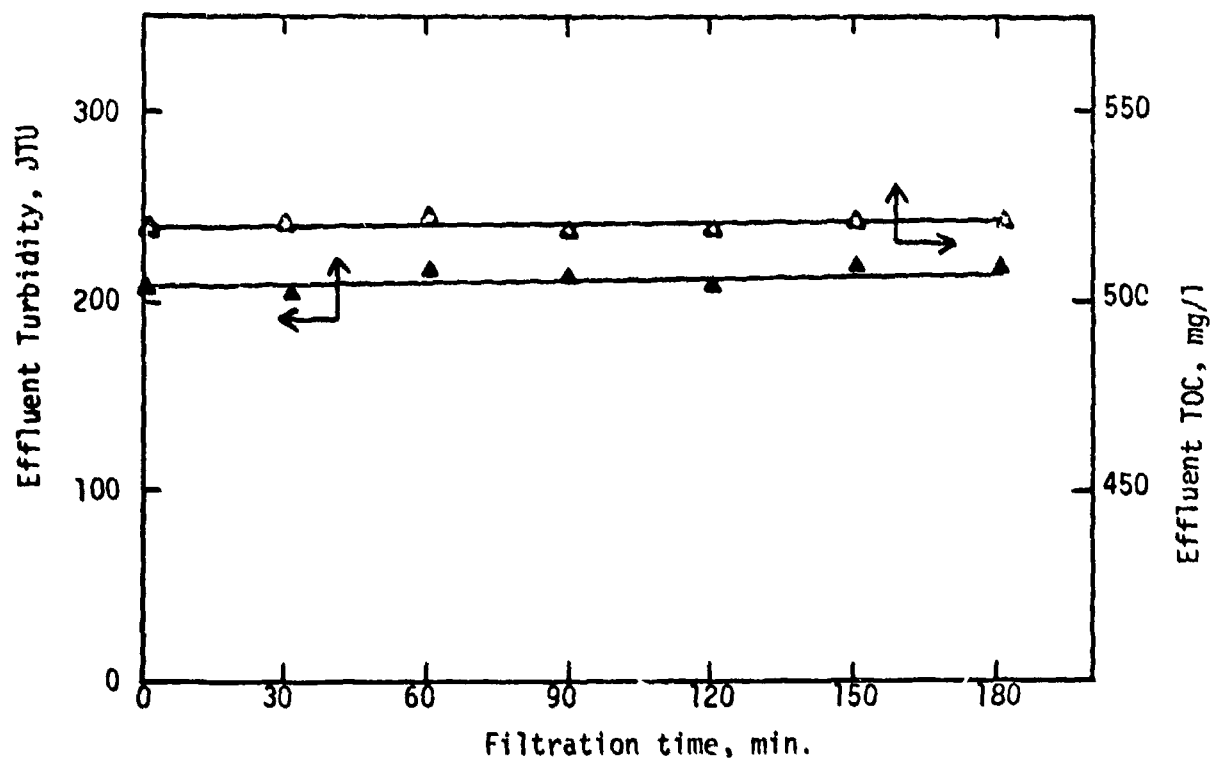
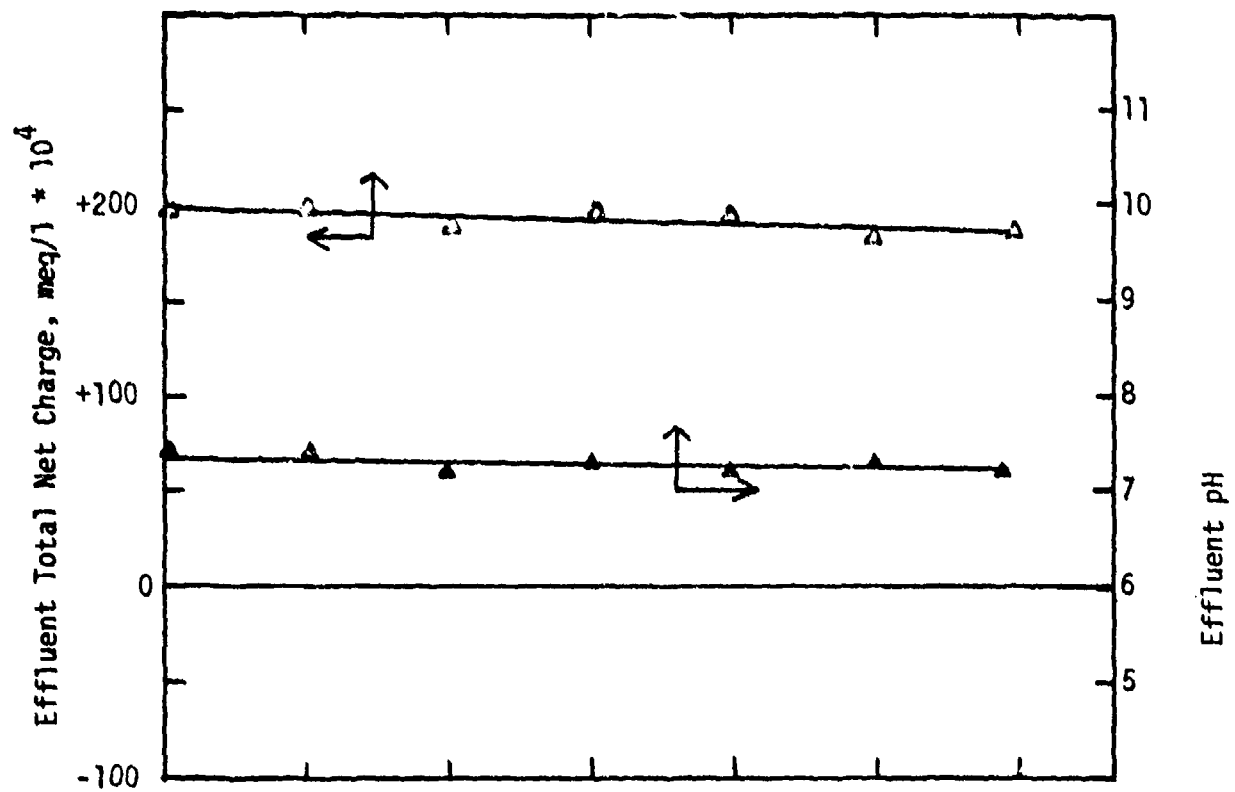


Figure 5.38

Head loss vs. Filtration TimeExperimental Conditions

Wastewater: Actual "undiluted"

Initial Turbidity = 240 JTU

Initial TOC = 530 mg/l

Initial Charge = $+200 * 10^{-4}$ meq/l

Initial pH = 7.5

Flow rate = 2 gpm/sq ft

Polymer: None

Coagulant aid: None

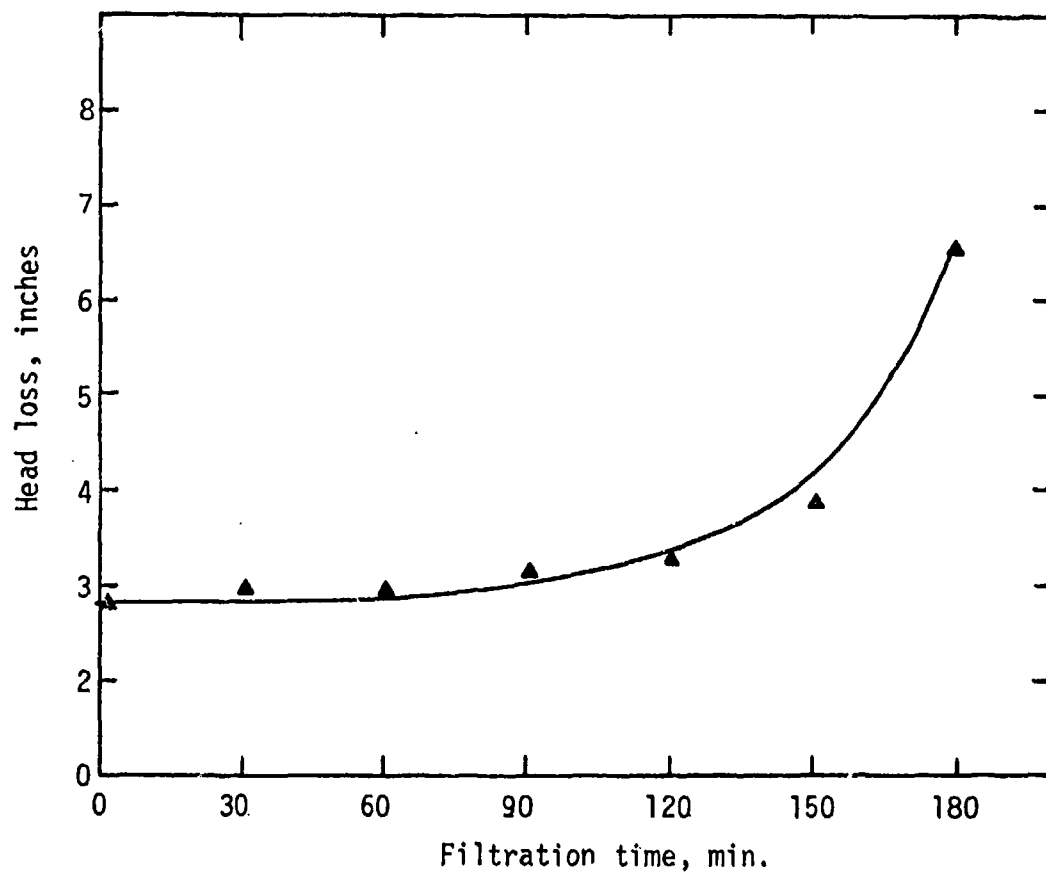


Figure 5.39

Effluent Total Net Charge and pH vs. Filtration Time

Figure 5.40

Effluent Turbidity and TOC vs. Filtration TimeExperimental Conditions

Wastewater: Actual "undiluted"

Initial Turbidity = 260 JTU

Initial TOC = 530 mg/l

Initial Charge = $+200 * 10^{-4}$ meq/l ($-380 * 10^{-4}$ meq/l
after bentonite addition)

Initial pH = 7.5

Flow rate = 2 gpm/sq ft

Polymer and dosage: Cat Floc, 100 mg/l

Method of polymer addition: Directly to the filter

Coagulant aid and dosage: Bentonite, 100 mg/l

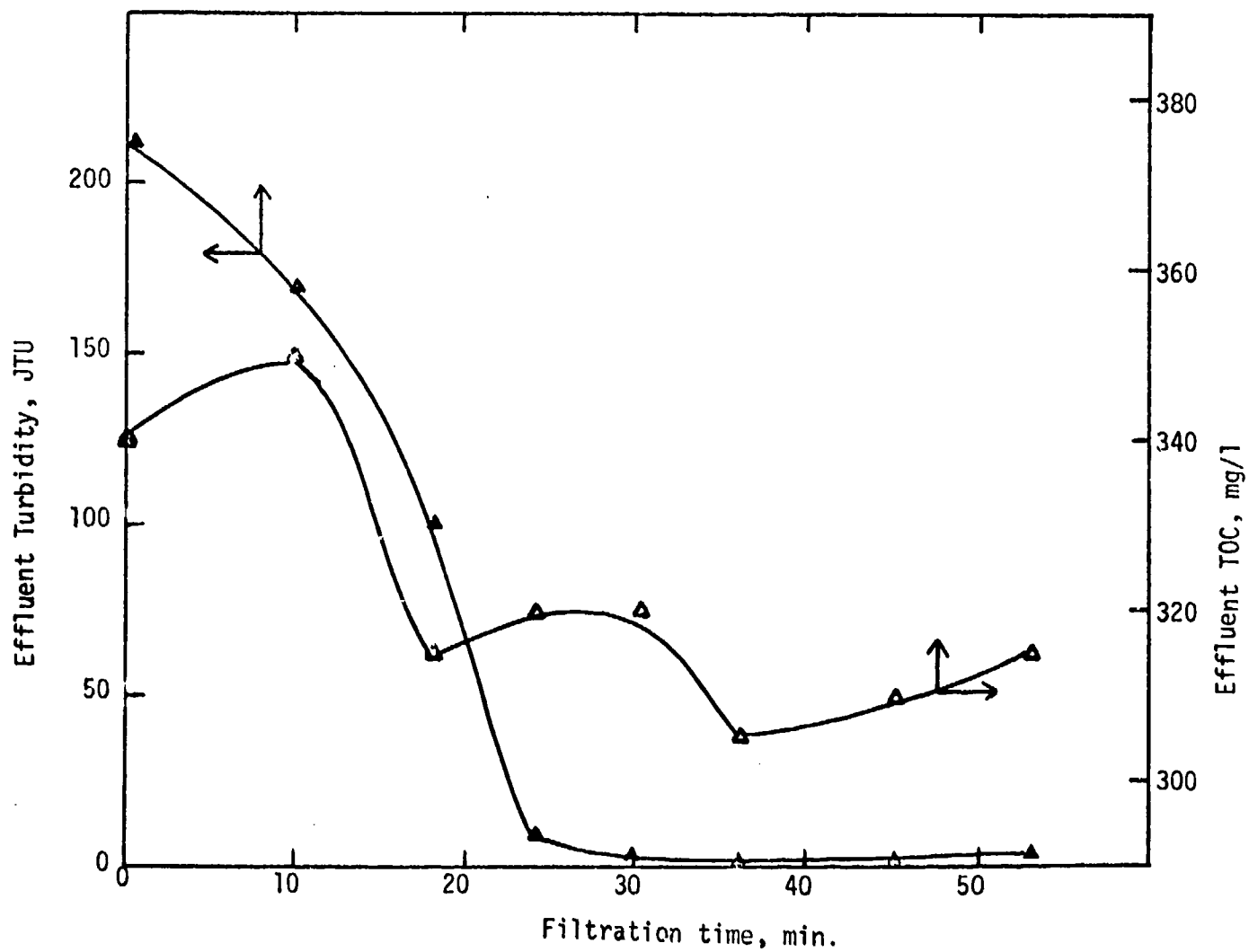
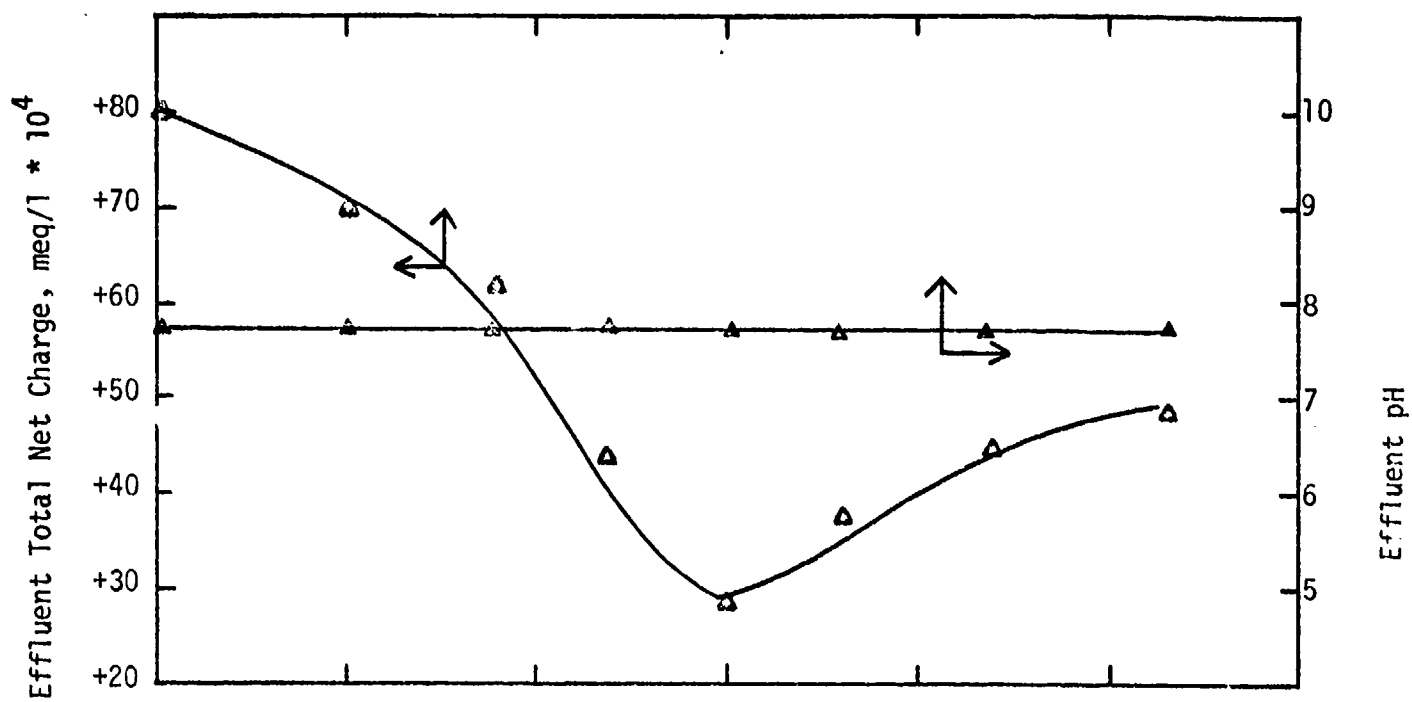


Figure 5.41

Head loss vs. Filtration TimeExperimental Conditions

Wastewater: Actual "undiluted"

Initial Turbidity = 260 JTU

Initial TOC = 530 mg/l

Initial Charge = + 200 * 10⁻⁴ meq/l (-380 * 10⁻⁴ meq/l
after bentonite addition)

Initial pH = 7.5

Flow rate = 2 gpm/sq ft

Polymer and dosage: Cat Floc, 100 mg/l

Method of polymer addition: Directly to the filter

Coagulant aid and dosage: Bentonite, 100 mg/l

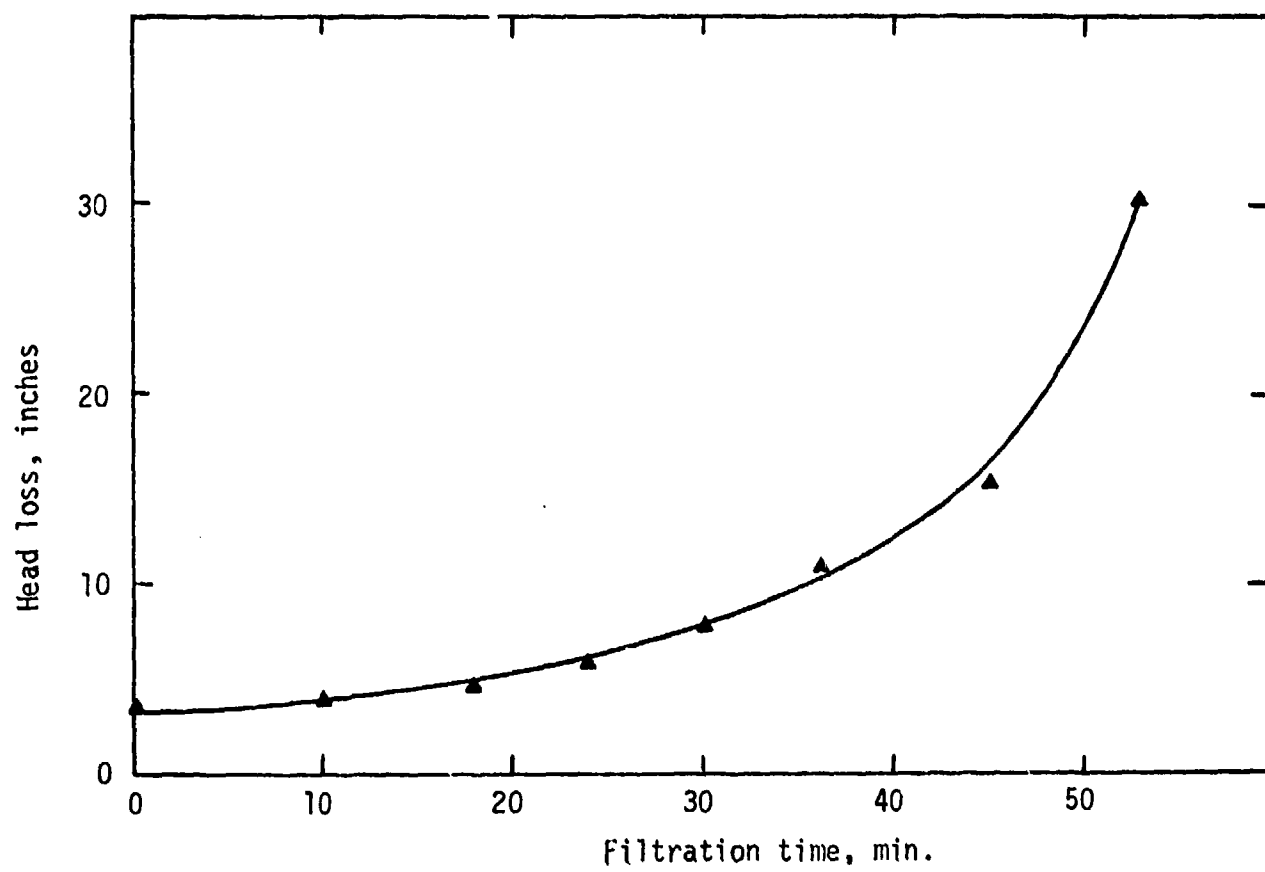


Figure 5.42

Effluent Total Net Charge and pH vs. Filtration Time

Figure 5.43

Effluent Turbidity and TOC vs. Filtration TimeExperimental Conditions

Wastewater: Actual "undiluted"

Flow rate = 2 gpm/sq ft

Polymer and dosage: Cat Floc, 100 mg/l

Method of polymer addition: Conventional process

Coagulant aid and dosage: Bentonite, 100 mg/l

Supernatant Turbidity = 5 JTU (after coagulation)

Supernatant TOC = 365 mg/l (after coagulation)

Supernatant Charge = $+48 * 10^{-4}$ meq/l (after coagulation)

Supernatant pH = 7.7 (after coagulation)

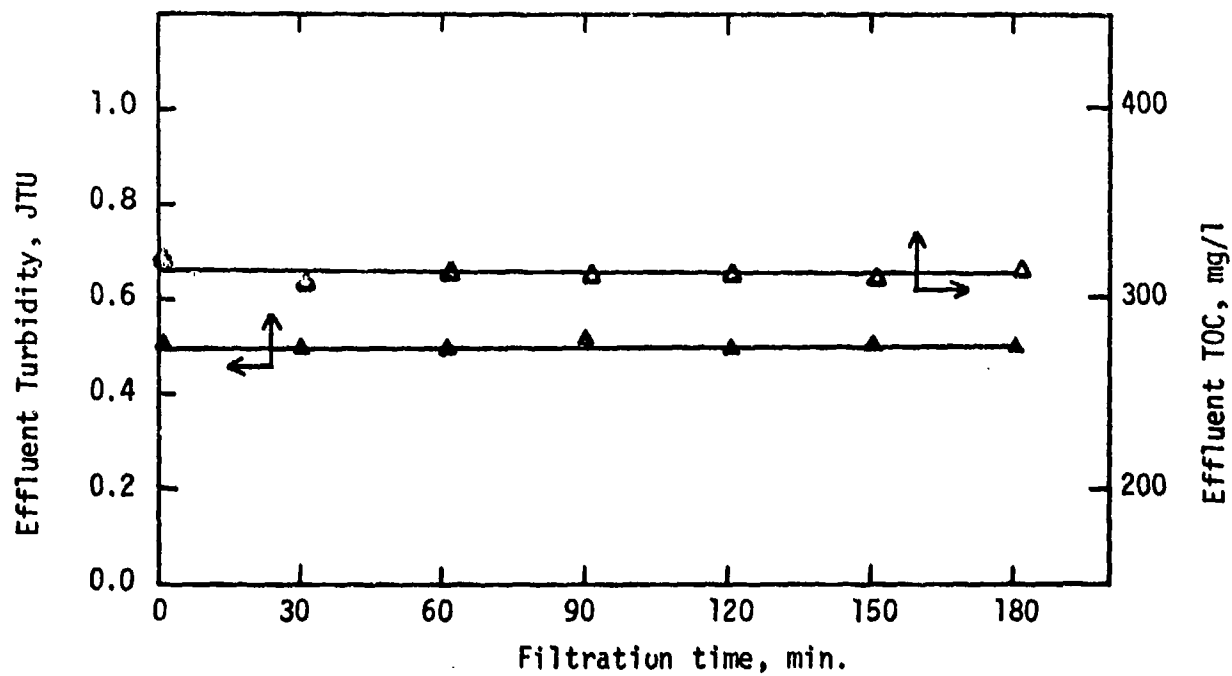
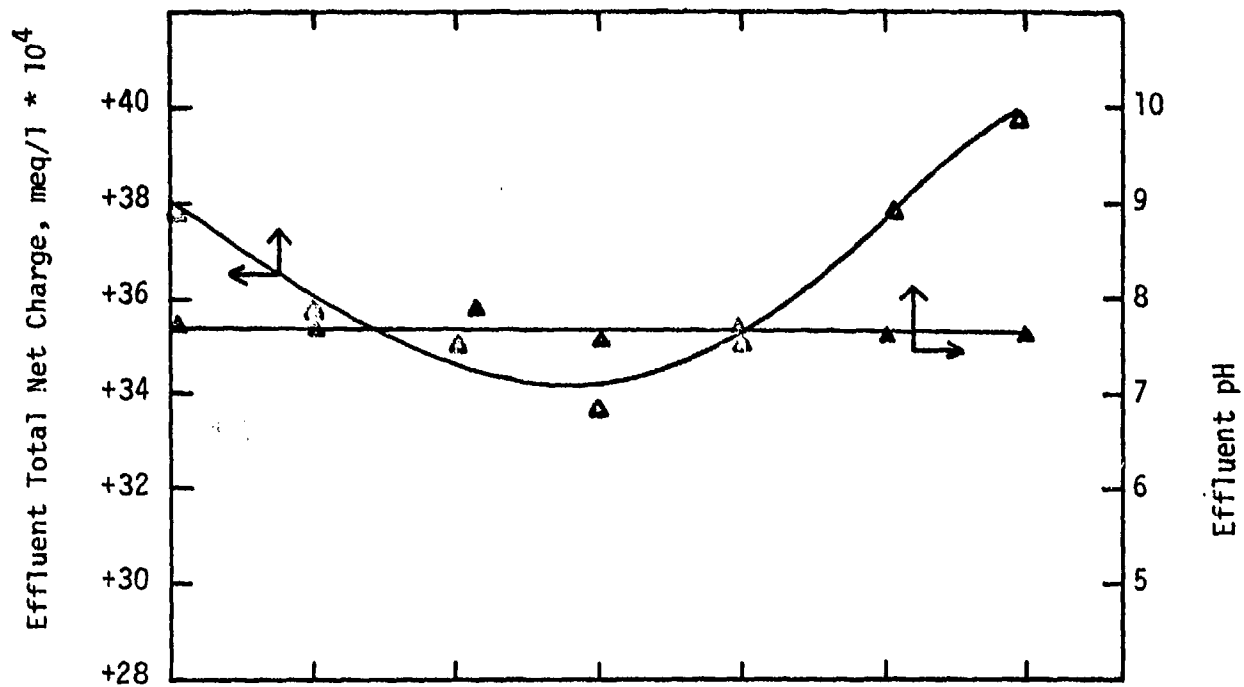


Figure 5.44

Head loss vs. Filtration TimeExperimental Conditions

Wastewater: Actual "undiluted"

Flow rate = 2 gpm/sq ft

Polymer and dosage: Cat Floc, 100 mg/l

Method of polymer addition: Conventional process

Coagulant aid and dosage: Bentonite, 100 mg/l

Supernatant Turbidity = 5 JTU (after coagulation)

Supernatant TOC = 365 mg/l (after coagulation)

Supernatant Charge = $+48 * 10^{-4}$ meq/l (after coagulation)

Supernatant pH = 7.7 (after coagulation)

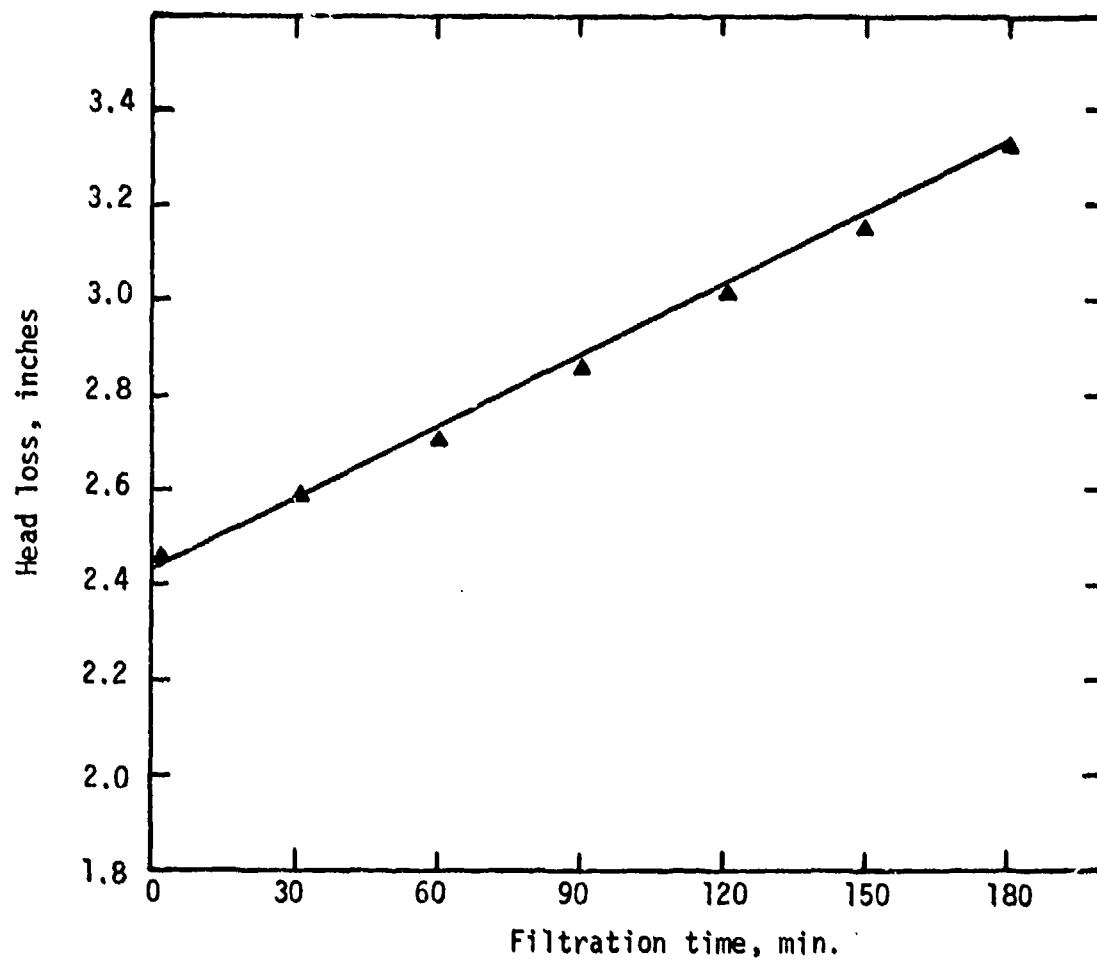


Figure 5.45

Effluent Total Net Charge and pH vs. Filtration Time

Figure 5.46

Effluent Turbidity and TOC vs. Filtration TimeExperimental Conditions

Wastewater: Actual "undiluted"

Flow rate = 4 gpm/sq ft

Polymer and dosage: Cat Floc, 100 mg/l

Method of polymer addition: Conventional process

Coagulant aid and dosage: Bentonite, 100 mg/l

Supernatant Turbidity = 4.5 JTU (after coagulation)

Supernatant TOC = 355 mg/l (after coagulation)

Supernatant Charge = $+52 * 10^{-4}$ meq/l (after coagulation)

Supernatant pH = 7.5 (after coagulation)

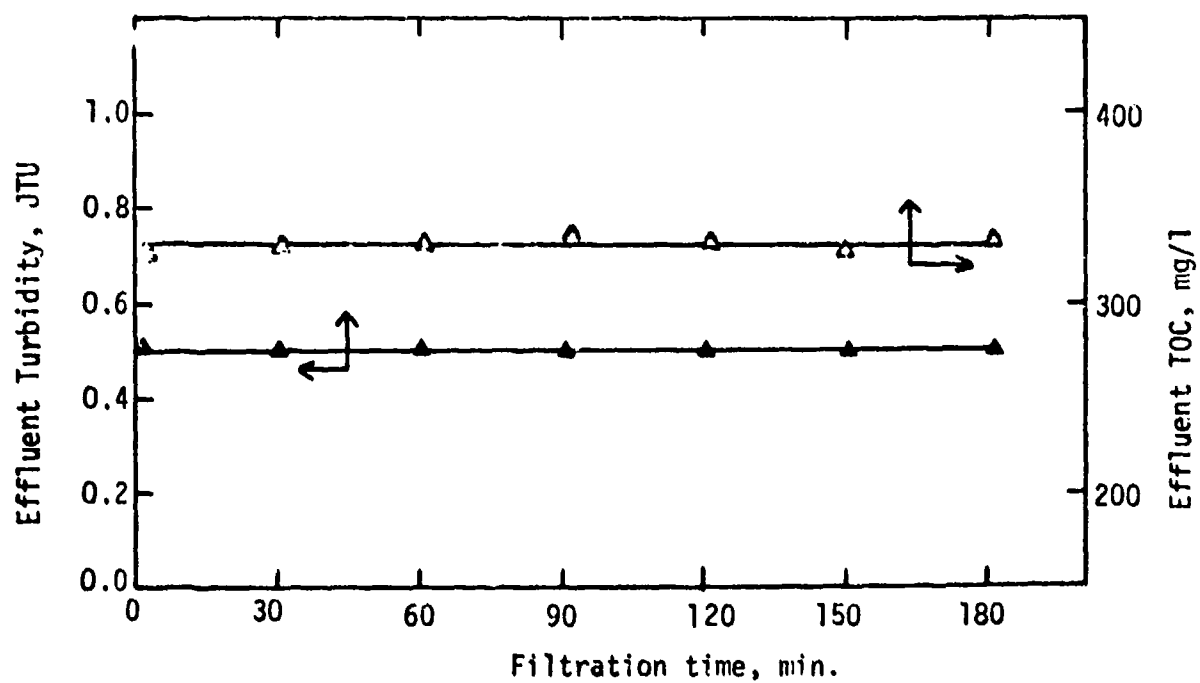
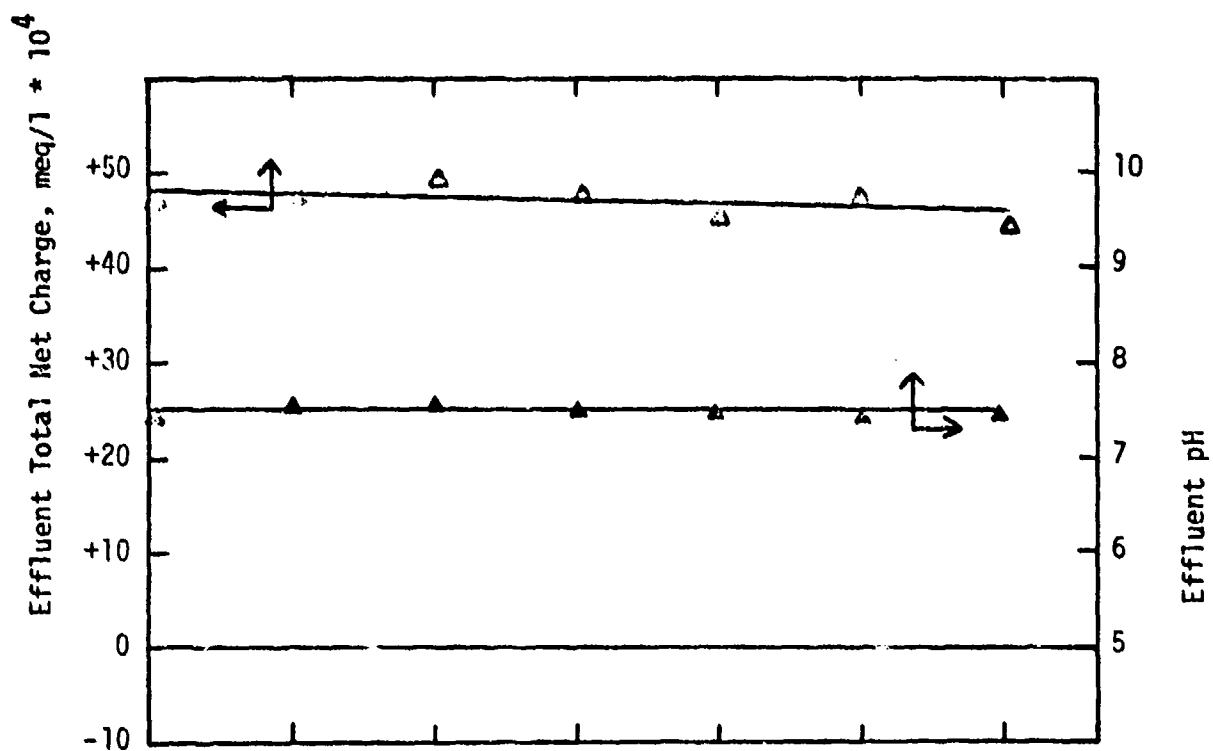


Figure 5.47

Head loss vs. Filtration TimeExperimental Conditions

Wastewater: Actual "undiluted"

Flow rate = 4 gpm/sq ft

Polymer and dosage: Cat Floc, 100 mg/l

Method of polymer addition: Conventional process

Coagulant aid and dosage: Bentonite, 100 mg/l

Supernatant Turbidity = 4.5 JTU (after coagulation)

Supernatant TOC = 355 mg/l (after coagulation)

Supernatant Charge = $+52 * 10^{-4}$ meq/l (after coag.)

Supernatant pH = 7.5 (after coagulation)

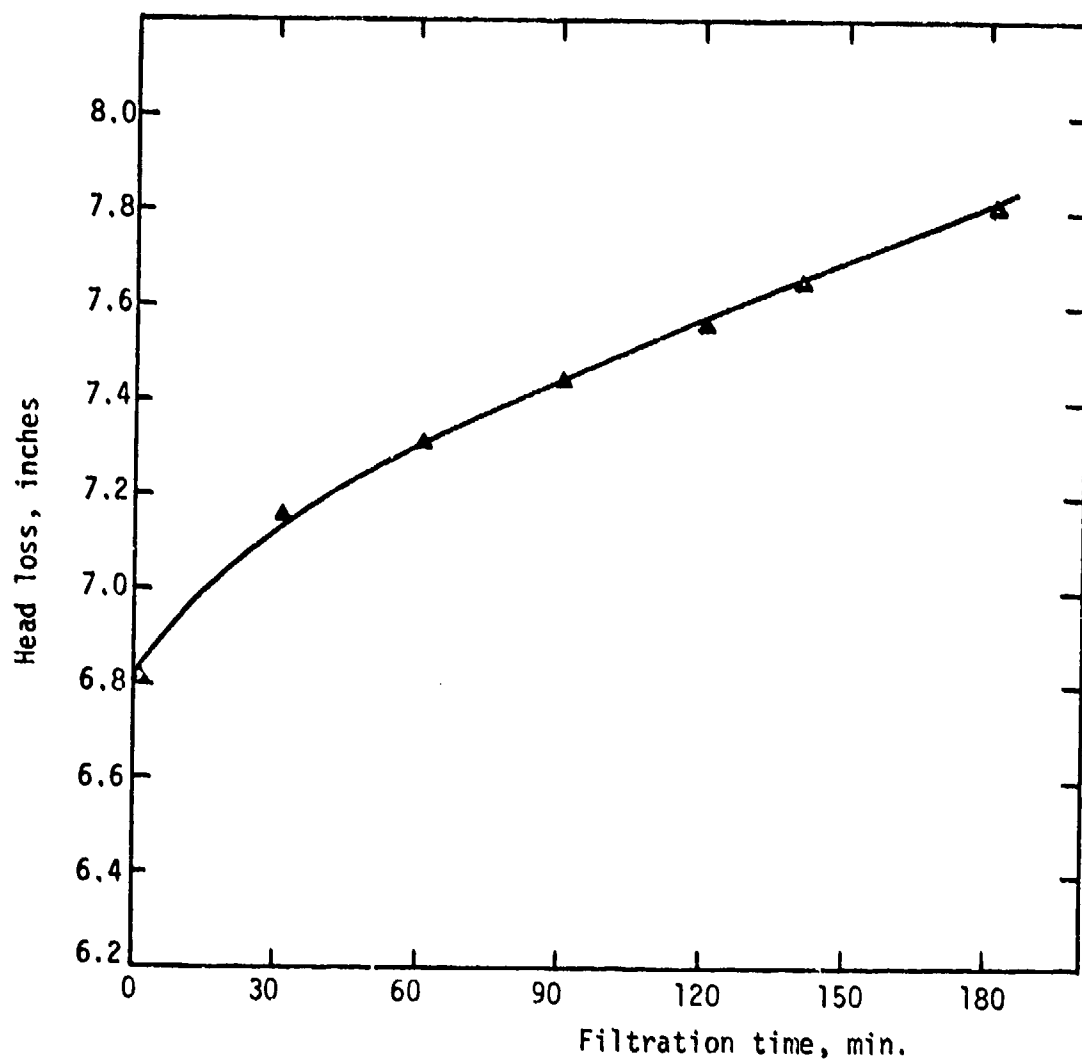


Figure 5.48

Head loss and pH vs. Filtration Time

Figure 5.49

Effluent Turbidity and TOC vs. Filtration TimeExperimental Conditions

Wastewater: Actual "undiluted"

Flow rate = 2 gpm/sq ft

Polymer and dosage: Cat Floc, 50 mg/l

Method of polymer addition: Conventional process

Coagulant aid and dosage: Lime, 3 g/l

Supernatant Turbidity = 7 JTU (after coagulation)

Supernatant TOC = 375 mg/l (after coagulation)

Supernatant pH = 11.8 (after coagulation)

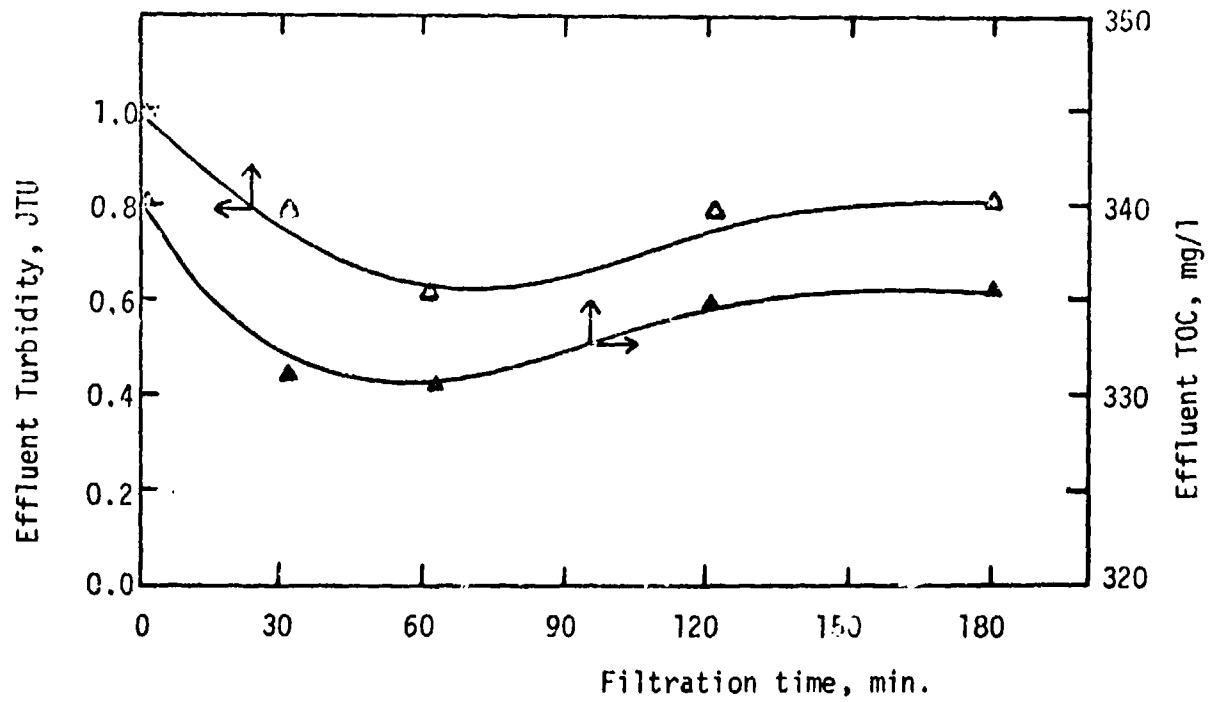
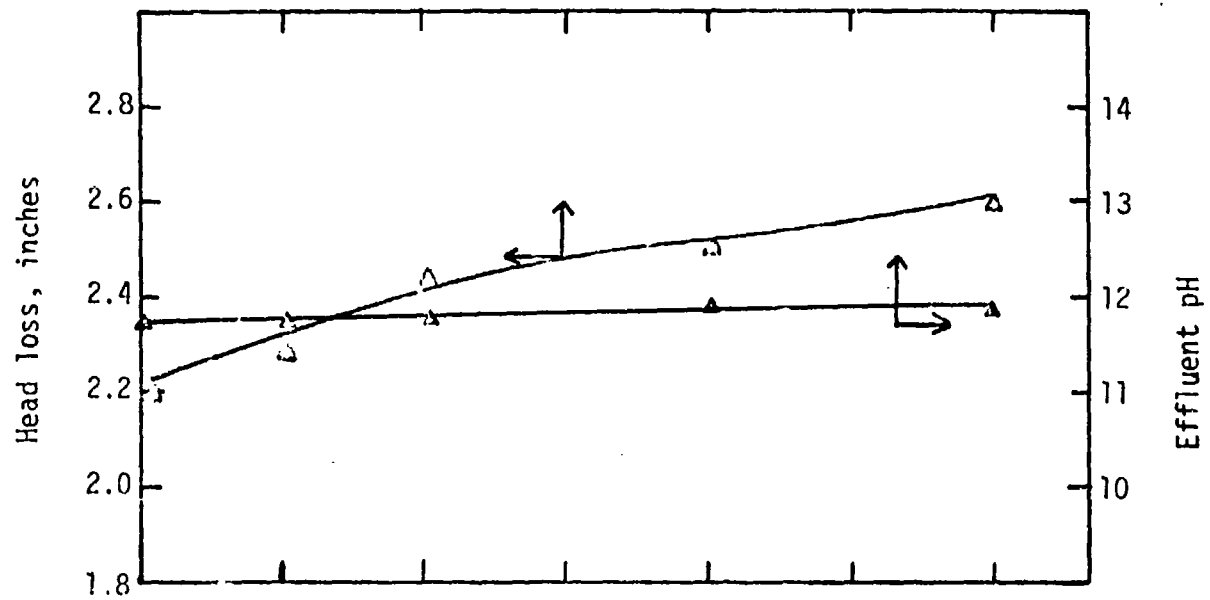


Figure 5.50

Effluent Total Net Charge and pH vs. Filtration Time

Figure 5.51

Effluent Turbidity and TOC vs. Filtration TimeExperimental Conditions

Wastewater: Actual "undiluted"

Flow rate = 2 gpm/sq ft

Polymer and dosage: Cat Floc, 100 mg/l

Method of polymer addition: Conventional process

Coagulant aid and dosage: Bentonite, 100 mg/l

Supernatant Turbidity = 3.5 JTU (after coagulation)

Supernatant TOC = 375 mg/l (after coagulation)

Supernatant Charge = $+52 * 10^{-4}$ meq/l (after coagulation)

Supernatant pH = 7.7 (after coagulation)

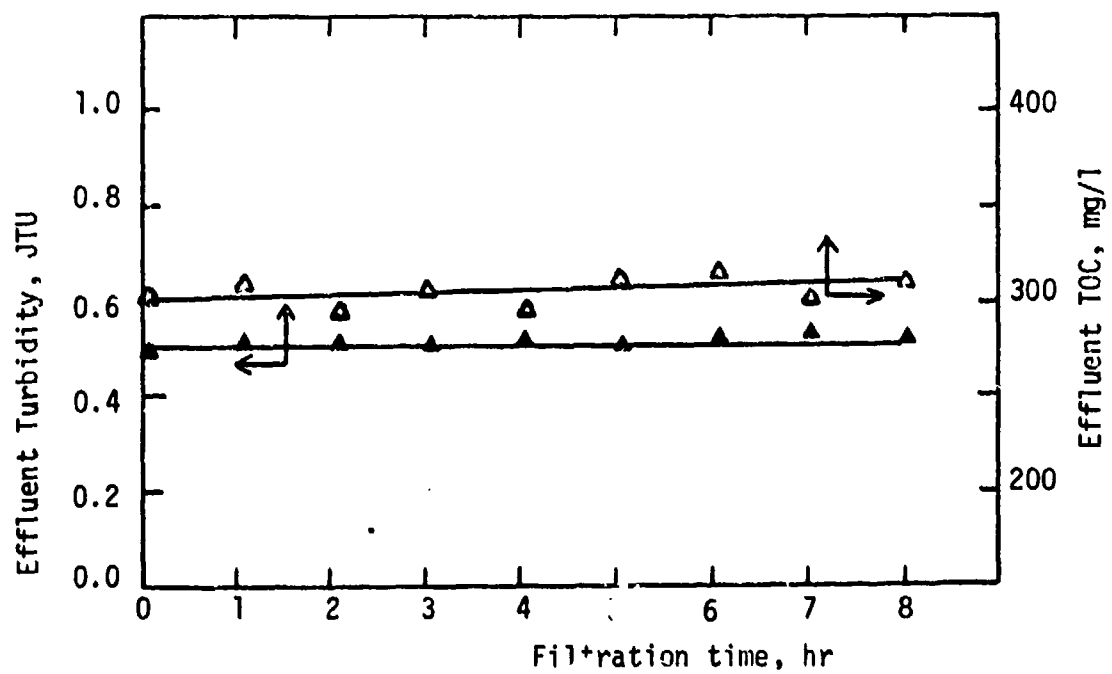
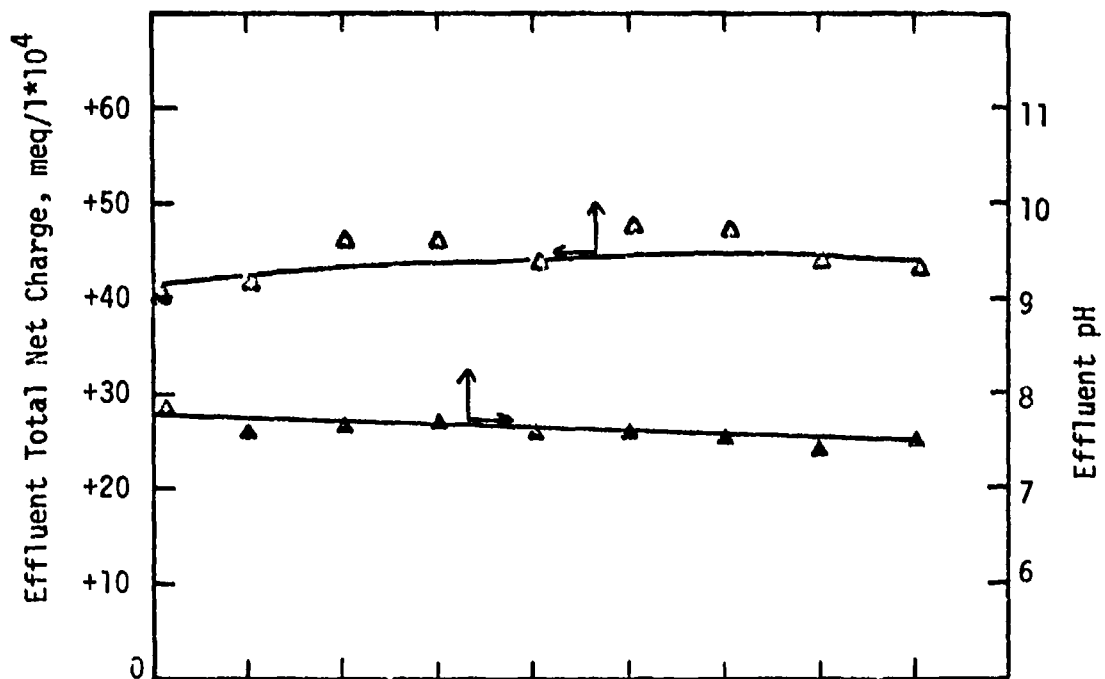


Figure 5.52

Head loss vs. Filtration TimeExperimental Conditions

Wastewater: Actual "undiluted"

Flow rate = 2 gpm/sq ft

Polymer and dosage: Cat Floc, 100 mg/l

Method of polymer addition: Conventional process

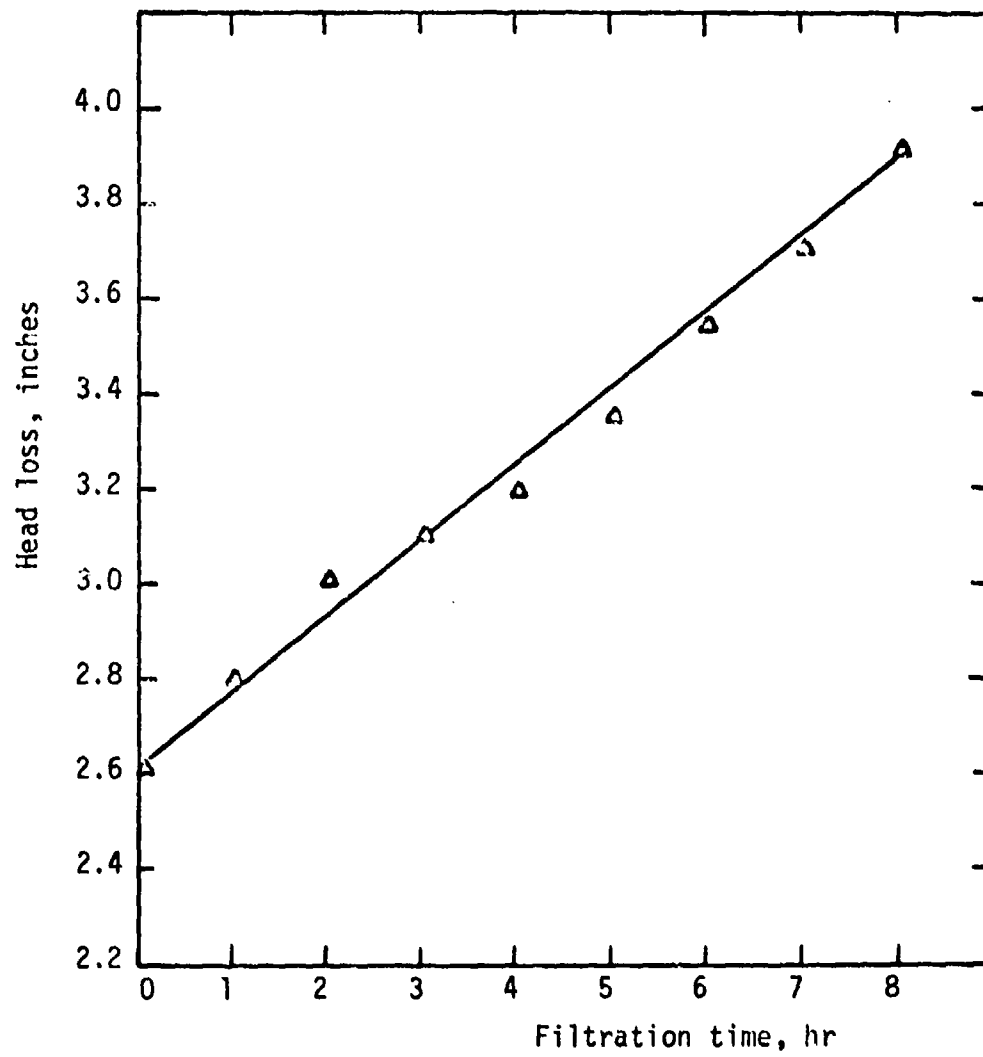
Coagulant aid and dosage: Bentonite, 100 mg/l

Supernatant Turbidity = 3.5 JTU (after coagulation)

Supernatant TOC = 375 mg/l (after coagulation)

Supernatant Charge = $+52 * 10^{-4}$ meq/l (after coag.)

Supernatant pH = 7.7 (after coagulation)



5.2.1 Filter Effluent Turbidity, Charge and pH

Figures 5.36 through 5.38 present the experimental data obtained in the first continuous filtration experiment. This run was performed as a control run therefore no coagulant aid or polymer was added to the actual wastewater. The initial turbidity of the wastewater in the filter influent was 240 JTU. As can be seen in Figure 5.37, the effluent turbidity was in the range 235-240 JTU. This indicates that negligible turbidity removal was achieved in the filter. This was due to the very small size of the colloidal suspended particles in the wastewater; the size was small enough to pass through the pores in the filter media. It is also observed that the pH and net charge of the effluent are nearly constant. Since the net charge was not changed, it was an indication that no particle neutralization or attachment took place within the filter media and the wastewater simply passed through the filter without any changes taking place.

The second continuous run was performed by directly adding the polymer continuously within the filter (see Section 4.3.1.2 for procedures). This process is a recent development in wastewater treatment and is called contact flocculation-filtration (1). Some of its advantages and disadvantages are discussed in Section 5.2.5.1. The effluent turbidity in this operation was quite different from the other continuous runs. Initially, the turbidity was quite high (200 JTU), then at a filtration time of about 20 minutes

it decreased suddenly to a low value of 1.0 JTU (see Figure 5.40). This was due to the fact that at the beginning of the run there was no time for flocculation to take place with initial contact of the wastewater and polymer and the effluent turbidities in the earlier stages of the filtration were high. An approximate calculation shows that about 15 minutes are required for the wastewater to flow through the column. Therefore, even if coagulation took place at initial contact this amount of time would be required to affect the quality of the effluent. As time elapsed, flocculation took place, the large flocs were held up in the filter and the effluent turbidity was lower. A sharp decline in the net charge also indicates that at that point, the removal of solids was increased. No pH changes could be observed throughout the run.

In the remaining filtration runs, the conventional method of pretreatment of wastewater was used (see Section 4.3.1.2). This meant that the wastewater was already coagulated, flocculated and settled prior to filtration and the clear supernatant was pumped to the filter. For this reason, the turbidity of the wastewater in the filter influent was quite low (approximately 5 JTU). In nearly all of the following runs, the filter effluent had a constant turbidity of about 0.5 JTU (see Figures 5.42 through 5.52). The last filtration run was carried for 8 hrs instead of the usual 3 hrs to see if there would be any degradation of effluent quality with time. The results show that the effluent

turbidity did not change during this time. This was due to the low turbidity of the wastewater entering the filter. The suspended solids concentration was so low that clogging of the filter and degradation of effluent quality would probably take a few days instead of a few hours.

The net charge and pH of the filter effluent were also quite constant. Some variations occurring in the value of the net charge were not significant since charge magnitudes were expressed in terms of 10^4 . The small variations could also have been due to errors in analytical measurement.

5.2.2 Total Organic Carbon (TOC) of Filter Effluent

In the control filtration run with only the actual wastewater passing through the filter, negligible TOC removal was achieved (see Figure 5.37). The influent TOC was 530 mg/l and the effluent value averaged to be 510 mg/l. Since an insignificant turbidity removal took place, the TOC removal in the form of suspended solids was small and most of the remaining TOC was in dissolved form.

The TOC removals in the remaining filtration runs were also not very significant. The highest removal achieved was close to 50%. When the conventional treatment of wastewater was used, most of the TOC (40%) was removed in the batch coagulation, flocculation, sedimentation process before the wastewater entered the filter. Only up to 5% additional TOC removal took place within the filter itself. In

conclusion, it was noted that the TOC removal was achieved in correlation with the turbidity reduction taking place. The suspended solids being removed also caused a partial reduction in the TOC. The remaining TOC was due to the dissolved organic matter which could not be removed by the filter. Some graphical variations are present in the TOC values, however, the range of TOC in consideration is very small to make these variations significant and essentially the measurements can be considered to be close in magnitude.

5.2.3 Head Loss Development

The head loss taking place in the filter was measured periodically with the aid of a piezometer tube. These values were graphically represented as inches of head loss vs. filtration time (see Figures 5.38, 5.41, 5.44, 5.47, 5.48 and 5.52).

Head loss curves reveal considerable information on how suspended solids removal took place in a filter. Granular filters remove suspended solids in one of the following ways (33): 1- Removal of suspended solids at the surface by the media at the top of the filter, 2- Depth removal of suspended solids within the voids of the media and 3- Combination of surface removal and depth removal.

Solids removal may take place at the surface if the filter media is too small or if the filtration rate is low. Surface removal of a compressible solid results in a

head loss curve that is exponential. Increasing the terminal head loss will not increase production per filter run with this type of head loss pattern.

If removal of solids occurs within the filter media, the head loss curve (of head loss vs. total volume filtered) will be quite linear. Increasing the filtration rate will increase the initial head loss but the head loss curves will still be parallel with increasing filtration rates. Increasing the terminal head loss increases both the run length and the production per run since the curves are nearly linear. This pattern is the most common pattern observed in coarse-to-fine filtration.

When the solids are partly removed on the surface and partly in the depth of the filter, surface removal will predominate at low filtration rates. With higher rates, the solids are carried deeper into the granular medium and more filtrate is produced before the surface cake forms. The rate may become high enough to prevent surface cake formation and the head loss will then be controlled only by depth filtration.

The experimental data for the first continuous filtration run showed that the head loss curve was linear in the earlier parts of the run and then it became exponential (see Figure 5.38). This indicates that initially for the first 2 hrs, surface cake formation did not become significant and suspended solids removal in the filter was

small. The exponential section of the curve indicates the formation of a surface cake at the top of the filter media.

In the second filtration run, the polymer was added directly to the filter and coagulation and flocculation took place in the upper portions of the filter. The flocs that were formed were larger than the coarsest filter media (anthracite) and therefore formed a thick cake at the top of the filter media. The head loss curve for this run was a typical exponential curve as was predicted theoretically (33) (see Figure 5.41). The filtration run lasted only 53 minutes and had to be terminated due to the excessive increase in head loss.

The remaining filtration experiments were carried out by the conventional process, (see Section 4.3.1.2) therefore the turbidity of the wastewater entering the filter was quite low. The low concentration of suspended solids prevented surface cake formation and the removal took place predominantly in the filter bed. This type of removal resulted in nearly linear head loss patterns.

5.2.4 Effects of Flow Rate

All of the continuous filtration runs with the exception of one were carried out at a filtration rate of 2 gpm/sq ft. The other flow rate used was 4 gpm/sq ft. Although only one run was repeated at two different flow rates, the experimental data still revealed considerable information on the effect of flow rate on physical and chemical parameters.

The initial head loss of the filter with the higher flow rate was approximately 3 times greater than the initial head loss at the lower flow rate (see Figures 5.44 and 5.47). Theoretically, this ratio should have been 4:1 since the head loss is proportional to the square of the velocity, as shown in the equation by Carmen-Kozeny. Doubling the velocity should have given a head loss four times as great. The inconsistency results from the limitations of the Carmen-Kozeny equation to describe the dynamics of a multi-media granular filter.

Parameters such as effluent turbidity, TOC, net charge and pH were not affected by the increase in flow rate as can be seen by comparing Figures 5.42 and 5.43 with Figures 5.45 and 5.46.

5.2.5 Impacts of Various Parameters on the Performance

5.2.5.1 Impact of Polymer Addition

In this investigation, polymer addition to the wastewater was accomplished in two different ways- the direct addition of polymer to the filter and the conventional type of treatment of wastewater. These methods have been described in detail in Section 4.3.1.2.

The direct addition of polymer to the filter is a recent trend in water treatment technology and also is applied in the filtration of low turbidity wastewaters. The advantage of this "contact coagulation-filtration process is the omission of costly flocculation and sedimentation

units. This process, however, did not work efficiently in the present investigation. The main reason for the ineffectiveness was the high turbidity of the wastewater. Suspended solids concentration was so high that when coagulation and flocculation took place in the filter, the flocs that were formed were too large in size to enter the voids in the filter media. A thick surface cake developed and the run had to be terminated in 53 minutes due to excessive head loss. Backwashing of the filter also caused some problems since the larger flocs (3-4 mm) could not be removed completely and total regeneration of the filter could not be achieved. In conclusion, the method of directly adding the polymer to the filter did not work effectively for wastewaters of high turbidity.

The conventional process of adding the polymer to the wastewater in a pretreatment system provided very low turbidity wastewater for the filter influent. Since the suspended solids concentration in the influent was low, the head loss build up over a period of time was not excessive and longer filtration runs could be achieved. On the other hand, because of the low turbidity in the filter influent, significant changes were not observed experimentally in the relatively short term filtration runs (3 hr).

5.2.5.2 Disadvantages of using lime as a coagulant aid

In some of the tests conducted, lime was used as a precipitant and a coagulant aid to provide effective

turbidity removal. The following disadvantages were noted when using lime:

- 1- Due to the very high concentration of lime required (3000 mg/l = 12.5 tons/million gal.), considerable amounts of sludge were formed.
- 2- The addition of lime increased the pH of the system to nearly 12. This brings about the requirement for a neutralization process to reduce the pH of the effluent before re-use or discharge to a stream.
- 3- The problem of calcium carbonate formation was encountered due to the reaction of calcium with dissolved carbonates in the system.

The reasons pointed out above show that lime is not very practical as a coagulant aid in the treatment of wastewater. None of these disadvantages were encountered when using powdered bentonite clay as a coagulant aid. The concentration that was effective was 100 mg/l (0.4 ton/million gal.) and the pH of the system was not altered during coagulation. In conclusion, bentonite clay is recommended as a coagulant aid in the treatment of the actual wastewater since it is more effective and does not have any of the disadvantages associated with lime treatment.

PART 6
CONCLUSIONS

The following conclusions were drawn from the results of the experimental investigations:

- 1- An optimum dosage of polymer exists in turbidity removal and underdosing and overdosing can occur. The optimum polymer dosage depends on the properties of the wastewater.
- 2- Cationic polyelectrolytes are quite effective in treating a negatively charged synthetic wastewater by the mechanism of charge neutralization. The optimum dosage was around 50 mg/l.
- 3- Anionic polymers did not provide significant turbidity removal for the anionic synthetic wastewater because of the magnitude of the repulsive forces present in the system.
- 4- The non-ionic polymer gave a high turbidity removal for the synthetic wastewater at a lower optimum dosage than the cationic polyelectrolytes. Turbidity removal was accomplished by a bridging action rather than charge neutralization.
- 5- The dependence of optimum polymer dosage on the pH of the system is not significant.
- 6- The polymers tested for the coagulation of the actual nitrocellulose-manufacturing wastewater

are not effective by themselves primarily due to the very low net positive charge of the wastewater. Charge neutralization can not be a dominant mechanism in turbidity removal because of the insignificance of the charge of the wastewater.

- 7- Bentonite is a successful coagulant aid when used in conjunction with the cationic polymers in coagulation of the actual nitrocellulose-manufacturing wastewater. With a bentonite concentration of 1.25 g/l and a polymer dosage of 50 mg/l, a 98.5% removal in turbidity can be achieved.
- 8- The TOC removals in the jar tests, due to the coagulation and removal of suspended solids, are not significant since most of the TOC is in dissolved form.
- 9- A stoichiometry exists between the optimum polymer dosage and the concentration of solids in the wastewater; higher polymer dosages are required for more turbid wastewater.
- 10- High-lime precipitation (3000 mg/l) by itself reduces the turbidity of the actual wastewater by 84%.
- 11- Lime is also an effective coagulant aid when used with the polymers in the treatment of the actual wastewater. With a lime dosage of 3 g/l and a cationic polymer dosage of 50 mg/l, a 98.7% turbidity removal is achieved. However,

- the use of lime brings about several disadvantages such as high pH, large amounts of sludge formation and CaCO_3 precipitation problems.
- 12- Without the addition of a coagulant aid or polymer, direct continuous filtration of the actual wastewater is very ineffective in terms of turbidity removal.
 - 13- The process of contact coagulation-filtration where the polymer is added continuously directly to the filter is not successful for the actual wastewater due to its very high turbidity. Surface removal is predominant giving an excessive head loss that causes early termination of the run.
 - 14- The conventional pretreatment process using the optimum dosages of coagulant aid and polymer obtained in the jar tests is successful in giving a high quality filter effluent.
 - 15- Head loss increase with time is a linear relationship if in-depth removal of suspended solids is taking place. The head loss pattern is exponential if the particles are being removed predominantly by mechanical surface straining.
 - 16- The increase in flow rate causes only an increase in the head loss and does not affect parameters such as effluent turbidity, TOC, net charge and pH.

PART 7

SUGGESTIONS FOR FURTHER STUDY

- 1- The polymers used in this study consisted of three cationic, two anionic and one non-ionic in nature. More experiments are needed with non-ionic polymers to support the results obtained in this investigation.
- 2- The filtration apparatus can be constructed in a way to provide sampling along the filter bed. Samples taken from these ports will give a better indication of how removal of suspended solids changes with the depth of the filter. Head loss measurements taken at various depths will also provide more detailed head loss patterns and will indicate the type of removal taking place in the filter.
- 3- Filtration should be further studied under different types, sizes and depths of filter media.
- 4- In this investigation, the polymer addition in the continuous filtration runs was carried out by two different methods. These methods did not include initially "precoating" the filter bed with a concentrated solution of polymer before filtration of the wastewater. Another possible treatment method to be studied is the continuous flow of polymer to the filter in addition to "precoating" the filter bed. The point of injection of the polymer in the filter column can also be varied to obtain different effluent quality.

- 5- Only few tests have been performed to examine the effect of filtration rate on effluent quality. More investigations should be carried out with different flow rates to verify the data obtained in this study.
- 6- Suspended solids analyses (in mg/l) should be made and correlated with the turbidity values obtained for the samples.
- 7- Powdered activated carbon adsorption studies should be made with longer contact times to ensure complete adsorption of organic particles.
- 8- The duration of the filtration runs in this study was 3 hr. Only one run was carried out for 8 hr and no change in effluent quality was observed during this time. Longer runs should be performed to observe the operation and characteristics of filtration normally associated with actual long term operation.
- 9- From the viewpoint of the treatment of the actual wastewater, reducing the TOC of the filter effluent should be considered. Biological treatment or granular carbon adsorption can be studied as possible treatment methods.

PART 8

LITERATURE CITED

- 1- Adin, A. and Rebhun, M., "High-Rate Contact Flocculation-Filtration with Cationic Polyelectrolytes", Jour. Amer. Water Works Assoc., pp.109-117, Feb. (1974).
- 2- Committee Report, "State of the Art of Coagulation- Mechanisms and Stoichiometry", Jour. Amer. Water Works Assoc., 63, 99 (1971).
- 3- Conley, W.R. and Pitman, R.W., "Innovations in Water Clarification", Jour. Amer. Water Works Assoc., 52:1319 (1960).
- 4- Culp, R.L. and Culp, G.L., "Advanced Wastewater Treatment", Van Nostrand Reinhold Co., New York, N.Y., (1971).
- 5- Fair, G.M. and Geyer, J.C., Okun, D.A., "Water and Wastewater Engineering", Vol.2, John Wiley and Sons, Inc., N.Y.
- 6- Fox, D.M. and Cleasby, J.L., "Experimental Evaluation of Sand Filtration Theory", Jour. San. Eng. Div. , Amer. Soc. of Civil Eng., 92, SA5. 61, (1966).
- 7- Freese, P.V. and Hicks, E., "Full-Scale Raw Wastewater Flocculation with Polymers", NTIS PB Rep. No. 211240, (1970).
- 8- Fiedlander, S.K., Ind. Eng. Chem. 50, pp. 1161-64 (1958).
- 9- Garnell, M.A., "Effects of a Polyelectrolyte as a Filter Aid", Jour. Amer. Water Works Assoc., pp. 597-601 (1963).
- 10- Hsiung, K. and Conley, W.R., "Design and Application of Multi-Media Filters", Jour. Amer. Water Works Assoc. pp.97-102, (1969).
- 11- Ives, K.J., "Rational Design of Filters", Paper 6414, Inst. Civil Eng., London, Eng., 1960 with summary in Proc. Inst. Civ. Eng., London, Eng., 16, 189, (1960).

- 12- Ives, K.J. and Sholji, J., "Research on Variables Affecting Filtration", Jour. San. Eng. Div., Amer. Soc. Civ. Eng., 91 SA4, 1, (1965).
- 13- Iwasaki, T., "Some Notes on Sand Filtration", Jour. Amer. Water Works Assoc., 29, 1591, (1937).
- 14- Kawamura, S. and Tanaka, Y., Water and Sewage Works, 113 (9), 348 (1966).
- 15- La Mer, V.K. and Healey, T.W., "Adsorption-Flocculation Reactions of Macromolecules at the Solid-Liquid Interface", Rev. Pure and Applied Chem., 13:112 (1963).
- 16- Larson, K.D., et al., "Use of Polyelectrolytes in Treatment of Combined Meat-Packing and Domestic Wastes", Jour. Water Pollution Control Fed., pp.2218, Nov. (1971).
- 17- Metcalf and Eddy, Inc., "Wastewater Engineering", McGraw-Hill Book Company, New York, N.Y., p.337 (1972).
- 18- Mints, D.M., et al., "Physicochemical Method of Purifying City Wastewater using Cationic Polyelectrolytes", Chem. Abs. 80, 52058w, (1974).
- 19- Municipal Water Treatment with Polyelectrolytes, Public Works Magazine, v104, N 10 p.80(3), (1973).
- 20- Nebolsine, R., "New Methods for the Treatment of Oily Wastewater Streams", Proc. 25th Ind. Waste Conf. Purdue Univ., pp.885-891, (1970).
- 21- O'Melia, C.R., "The Role of Polyelectrolytes in Filtration Processes", NTIS Rep. PB-233 271/6WP, April (1974).
- 22- O'Melia, C.R. and Stumm, W., "Theory of Water Filtration", Jour. Amer. Water Works Assoc., 59, 1393, (1967).
- 23- Packham, R.F., "Some Studies of the Coagulation of Dispersed Clays with Hydrolyzing Salts", Jour. Colloid Sci. 20, pp.81-92, (1965).

- 24- Pressman, M., "Cationic Polyelectrolytes as Prime Coagulants in Natural-Water Treatment", Jour. Amer. Water Works Assoc., pp.169-181, Feb. (1967).
- 25- Robeck, G.G. and Dostal, K.A., "Studies of Modification in Water Filtration", Jour. Amer. Water Works Assoc. 56, 2, 198, Feb. (1964).
- 26- Rueschwein, K.A. and Ward, D.W., "Mechanisms of Clay Aggregation by Polyelectrolytes", Soil Science, 73:485, (1952).
- 27- Sawyer, C.N. and McCarty, P.L., "Chemistry for Sanitary Engineers", McGraw-Hill Inc., New York, N.Y. (1967).
- 28- Shireman, H.C., "Filtration Boosts Tertiary Treatment", Water Wastes Eng. 9, No.4, pp.34-37, (1972).
- 29- Stumm, W. and Morgan, J.J., "Chemical Aspects of Coagulation" Jour. Amer. Water Works Assoc., 54:8, 971, Aug. (1962).
- 30- Stumm, W. and O'Melia, C.R., "Stoichiometry of Coagulation", Jour. Amer. Water Works Assoc., Vol. 60, p. 514, (1968).
- 31- Suzuki, S., "Coagulation of Paper Mill Wastes by Polyelectrolytes", Chem. Abstracts, 78, 7539b (1973).
- 32- Tchobanoglous, G., "Filtration Techniques in Tertiary Treatment", Jour. Water Pollution Control Fed., pp.604-623, (1970).
- 33- Weber, W. Jr., "Physicochemical Processes for Water Quality Control", Wiley-Interscience, New York, N.Y. (1972).
- 34- Wnek, W., "Electrokinetic and Chemical Aspects of Water Filtration", Filtration and Separation, p.237 May-June (1974).
- 35- Yao, K., Habibian, M.T. and O'Melia, C.R., "Water and Wastewater Filtration", Environ. Sci. and Tech., v5, N11, p.1105 (8), (1971).
- 36- Wang, L.K., and Shuster, W.W., "Polyelectrolyte Determination at Low Concentration", Industrial and Engineering Chemistry, Vol. 14, p. 312-314, (1975).

PART 0
APPENDIX

LIST OF ABBREVIATIONS AND SYMBOLS

BOD	Biochemical Oxygen Demand
°C	degrees Centigrade
cc	cubic centimeter
cm	centimeter
COD	Chemical Oxygen Demand
cu	cubic
eq	equivalents
°F	degrees Fahrenheit
FTU	Formazin Turbidity Units
ft	foot
gpm	gallons per minute
HP	horsepower
hr	hour
I.D.	inside diameter
in.	inch
JTU	Jackson Turbidity Units
l	liter
lb	pound
meq	milliequivalents
mg	milligrams
MGD	million gallons daily
min	minute
ml	milliliter
mm	millimeter
mV	millivolt

mp	millimicron
O.D.	outside diameter
ppb	parts per billion
ppm	parts per million
pH	negative logarithm of the hydrogen ion concentration
psia	pounds per square inch, absolute
rpm	revolutions per minute
sec	second
sq	square
SS	suspended solids
TOC	Total Organic Carbon
μ	micron
V_n	attractive potential energy
V_r	repulsive potential energy
ζ	zeta potential
ψ_o	Nernst potential
ψ_s	Stern potential

Table A-1

Technical Specifications of Bentonite

Grade:	USP Dust Grade Volclay Bentonite	
Composition:	Bentonite- a hydrous silicate of alumina comprised essentially of the clay mineral montmorillonite	
Purity:	Montmorillonite content about 99.75 minimum. Contains small portions of feldspar, biotite, selenite, etc.	
Chemical composition:	Silica	63.02% as SiO ₂
	Aluminum	21.08% as Al ₂ O ₃
	Iron (ferric)	3.25% as Fe ₂ O ₃
	Iron (ferrous)	0.35% as FeO
	Magnesium	2.67% as MgO
	Sodium & Potassium	2.57% as Na ₂ O
	Calcium	0.67% as CaO
	Crystal water	5.64% as H ₂ O
	Trace elements	0.72%
Formula:	A tri-layer expanding mineral structure of approximately: (Al, Fe _{1.67} , Mg _{0.33}) Si ₄ O ₁₀ (OH) ₂ Na ⁺ Ca ⁺⁺ _{0.33}	
Moisture content:	Minimum 5%, maximum 8% as shipped	
Size:	99.75% minimum finer than 325 mesh (44 micron)	
pH:	2% suspension 9.5 to 10.5	
Swelling:	2 gms. allowed to swell freely- 24 ml minimum swollen volume	
Packaging:	Multiwall paper bags, 50 lbs. net	

Table A-2

Technical Specifications of Organic Liquid PolymersCat Flocc T

appearance	clear to pale yellow
solubility	highly soluble in water
weight/gallon	8.6 lb
viscosity	35 cps (minimum) at 25°C
pH (as supplied)	3.5 ± 0.2
flash point	above 200°F
freezing point	27°F

WT-2870

appearance	clear pale yellow liquid
solubility	highly soluble in water
specific gravity	avg. 1.022
viscosity	2000 cps at 25°C maximum
pH (as supplied)	4.2 ± 0.5
flash point	above 200°F
freezing point	27°F

Cat Flocc

appearance	water-white to pale yellow liquid
solubility	highly soluble in water
specific gravity	avg. 1.022
viscosity	2000 cps at 25° C max.
pH (as supplied)	4.2 ± 0.5
flash point	above 200°F
freezing point	27°F

Table A-2 (continued)WT-2690

appearance	off-white, dry flake
solution viscosity	75 cps at 25°C for 0.8% concentration
pH of 0.5% solution	7.0
bulk density (avg.)	27 lbs/cu ft
particle size	100% through 10 mesh 60% through 30 mesh

WT-2700

appearance	off-white, dry flake
solution viscosity	1800 cps at 25°C for 0.5% concentration
pH of 0.25% solution	7.5
bulk density	20-25 lbs/cu ft
particle size	100% through 12 mesh 60% through 30 mesh

Figure A-1

Rotameter Calibration Data

Tube No: R-2-15-B

Float material: Glass

Metering Temperature: 70°F

Metering Pressure: 14.7 psia

Figure A-2

Rotameter Calibration Data

Tube No: R-6-15-B

Float material: Stainless steel 316

Metering Temperature: 70°F

Metering Pressure: 14.7 psia

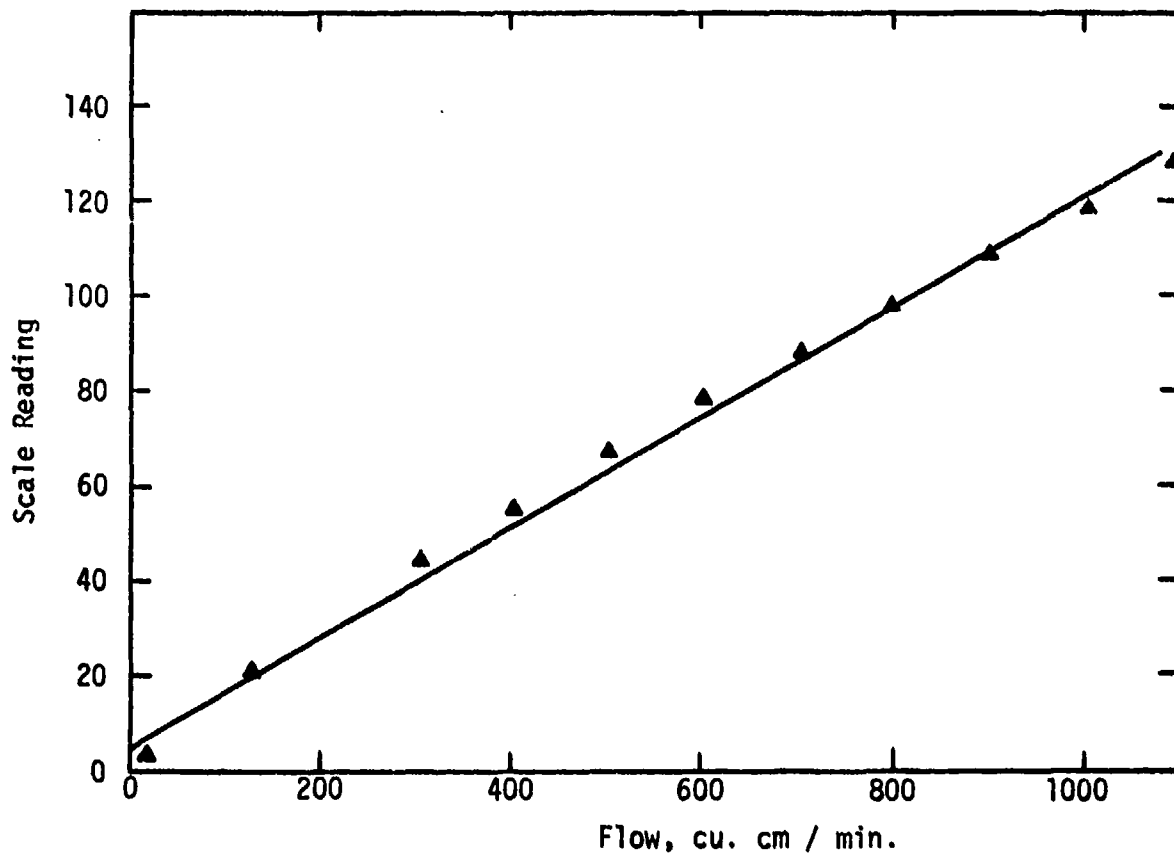
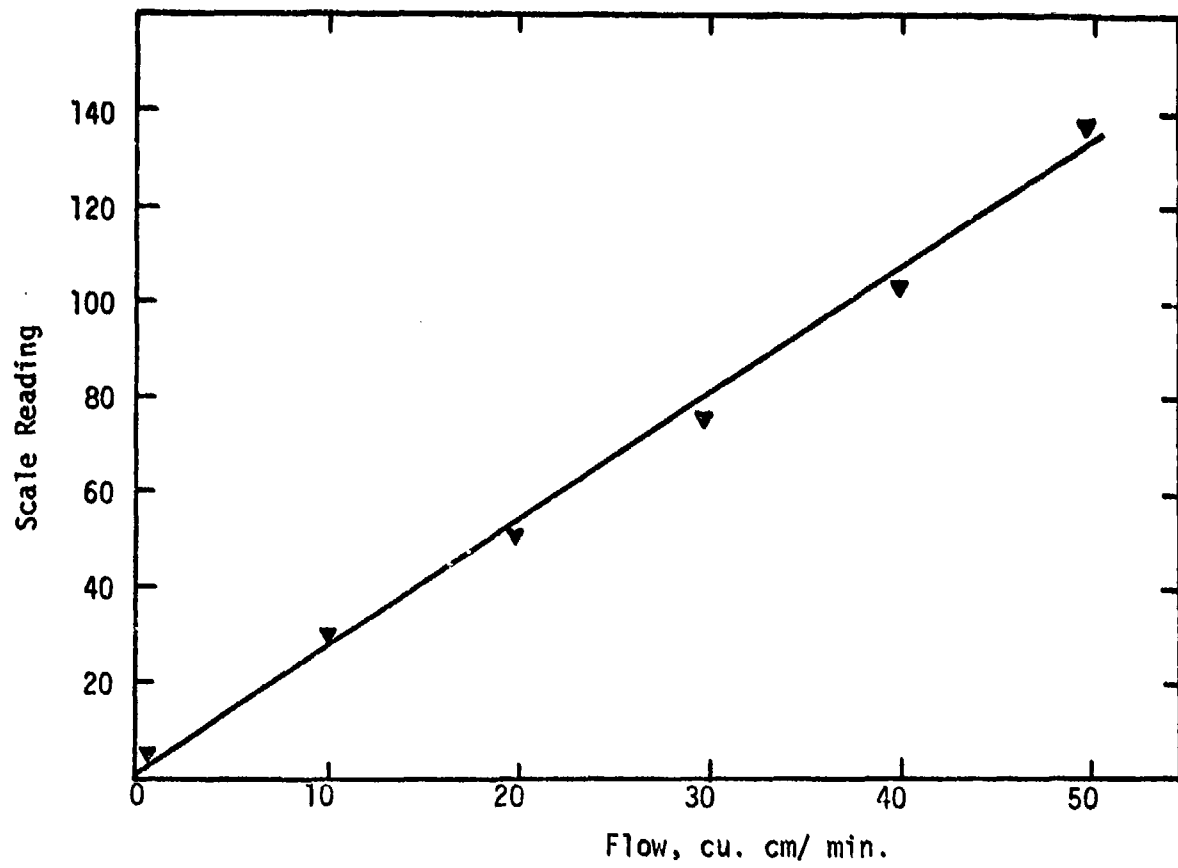


Figure A-3
Carbonaceous Analyzer Calibration Curve

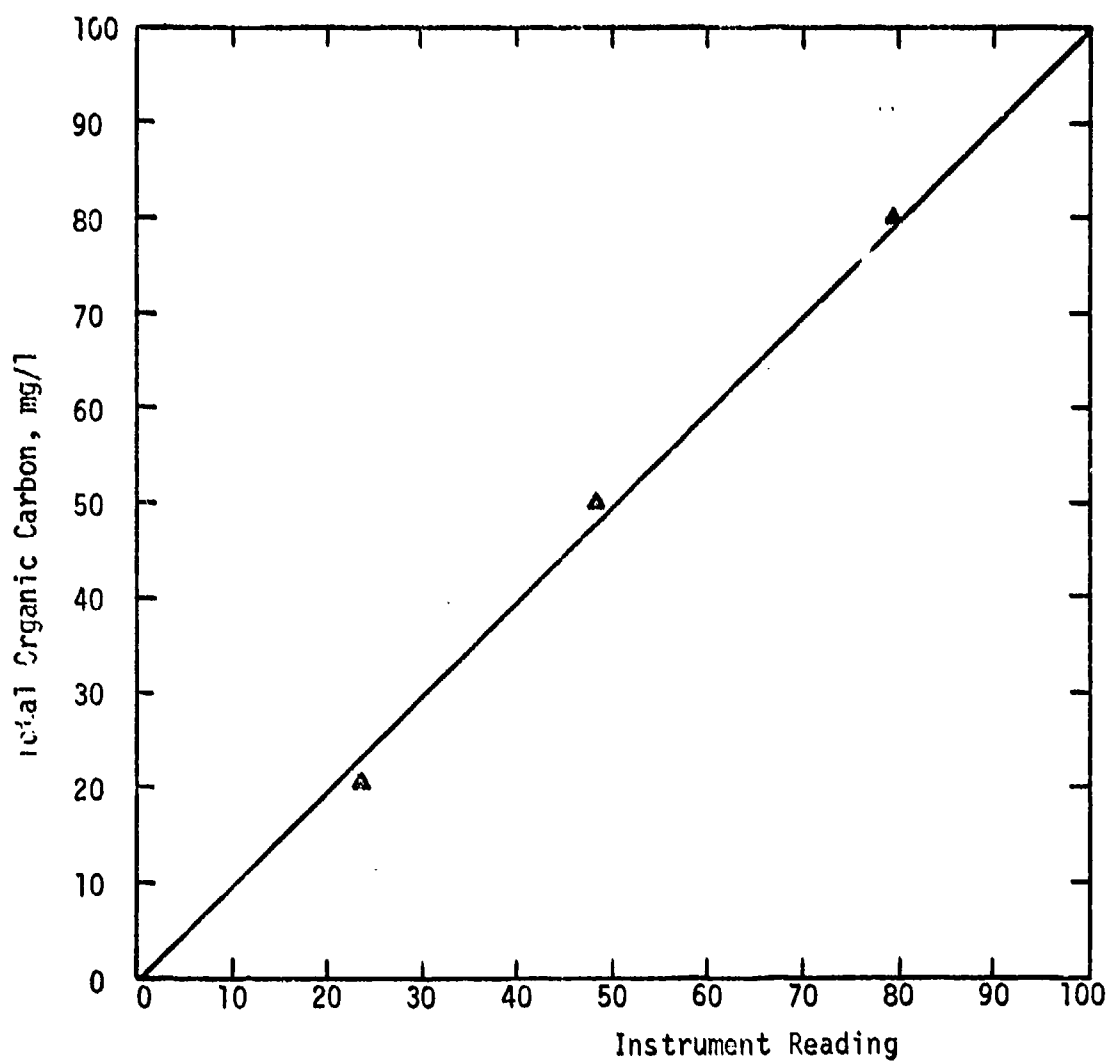


Figure A-4

Calibration Curve for WT-2870 Polyelectrolyte

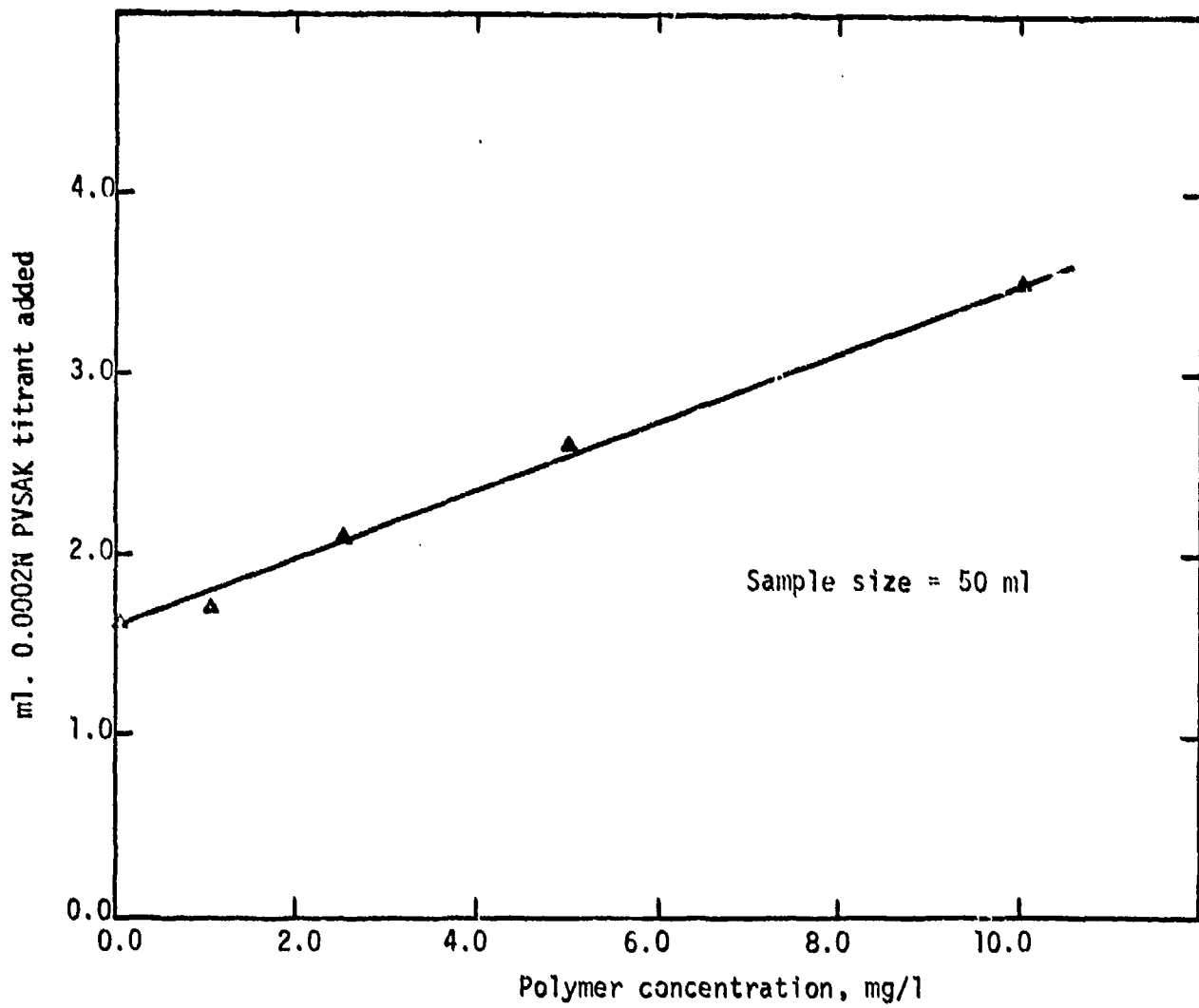
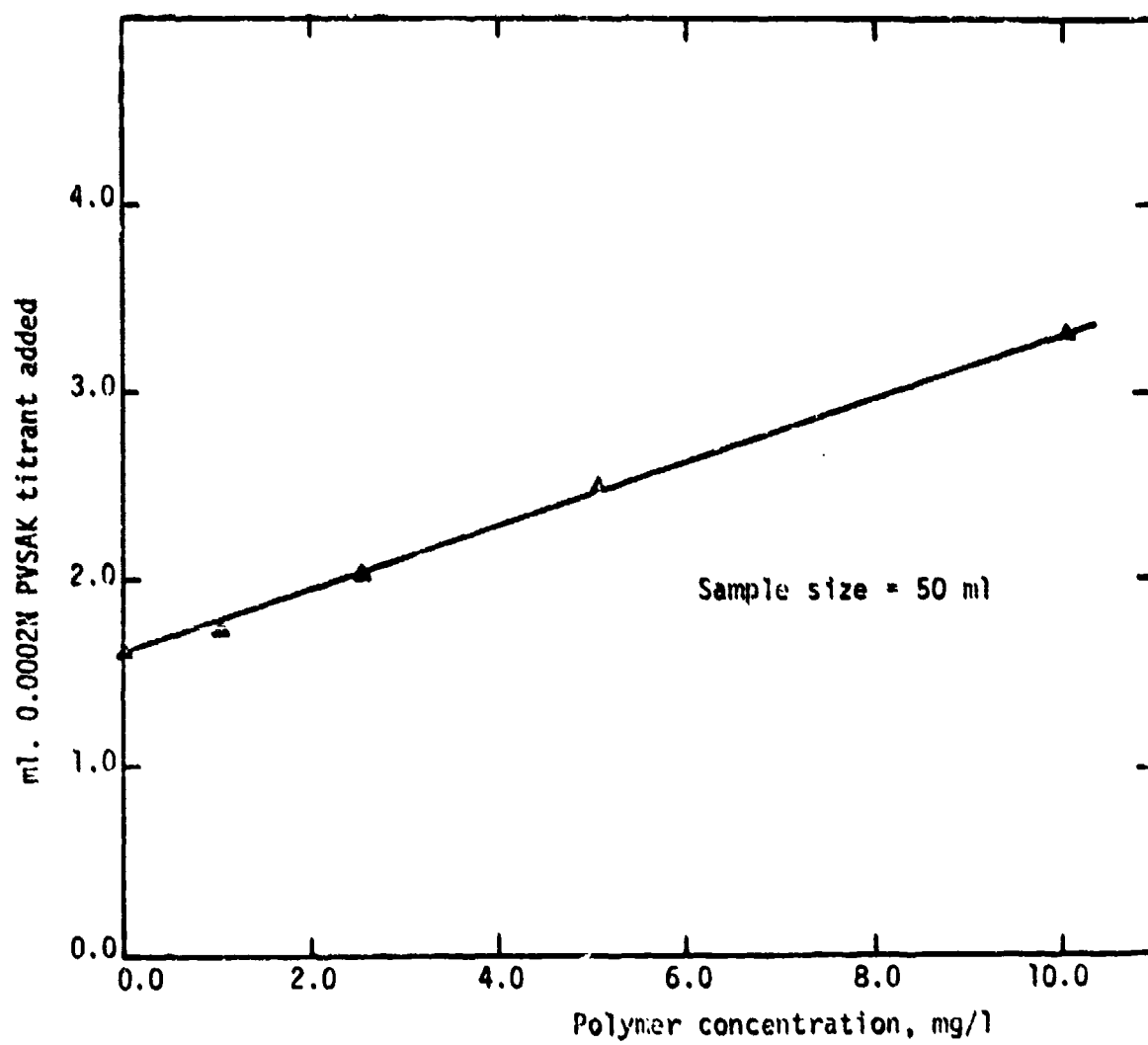


Figure A-5

Calibration Curve for Cat Floe T Polyelectrolytic



KEEP UP TO DATE

Between the time you ordered this report—which is only one of the hundreds of thousands in the NTIS information collection available to you—and the time you are reading this message, several new reports relevant to your interests probably have entered the collection.

Subscribe to the **Weekly Government Abstracts** series that will bring you summaries of new reports as soon as they are received by NTIS from the originators of the research. The WGA's are an NTIS weekly newsletter service covering the most recent research findings in 25 areas of industrial, technological, and sociological interest—invaluable information for executives and professionals who must keep up to date.

The executive and professional information service provided by NTIS in the **Weekly Government Abstracts** newsletters will give you thorough and comprehensive coverage of government-conducted or sponsored re-

search activities. And you'll get this important information within two weeks of the time it's released by originating agencies.

WGA newsletters are computer produced and electronically photocomposed to slash the time gap between the release of a report and its availability. You can learn about technical innovations immediately—and use them in the most meaningful and productive ways possible for your organization. Please request NTIS-PR-205/PCW for more information.

The weekly newsletter series will keep you current. But learn what you have missed in the past by ordering a computer **NTISearch** of all the research reports in your area of interest, dating as far back as 1964, if you wish. Please request NTIS-PR-186/PCN for more information.

WRITE: Managing Editor
5285 Port Royal Road
Springfield, VA 22161

Keep Up To Date With SRIM

SRIM (Selected Research in Microfiche) provides you with regular, automatic distribution of the complete texts of NTIS research reports *only* in the subject areas you select. SRIM covers almost all Government research reports by subject area and/or the originating Federal or local government agency. You may subscribe by any category or subcategory of our WGA (**Weekly Government Abstracts**) or **Government Reports Announcements and Index** categories, or to the reports issued by a particular agency such as the Department of Defense, Federal Energy Administration, or Environmental Protection Agency. Other options that will give you greater selectivity are available on request.

The cost of SRIM service is only 45¢ domestic (60¢ foreign) for each complete

microfiche report. Your SRIM service begins as soon as your order is received and processed and you will receive bi-weekly shipments thereafter. If you wish, your service will be backdated to furnish you microfiche of reports issued earlier.

Because of contractual arrangements with several Special Technology Groups, not all NTIS reports are distributed in the SRIM program. You will receive a notice in your microfiche shipments identifying the exceptionally priced reports not available through SRIM.

A deposit account with NTIS is required before this service can be initiated. If you have specific questions concerning this service, please call (703) 451-1558, or write NTIS, attention SRIM Product Manager.

This information product distributed by

NTIS U.S. DEPARTMENT OF COMMERCE
National Technical Information Service
5285 Port Royal Road
Springfield, Virginia 22161

AD A 023 606

A SEAKEEPING COMPARISON BETWEEN THREE MONOHULLS, TWO SWATHS, AND A COLUMN-STABILIZED CATAMARAN DESIGNED FOR THE SAME MISSION

NAVAL SHIP RESEARCH AND DEVELOPMENT CENTER

Bethesda, Md. 20884

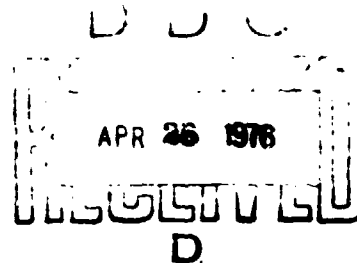


1

A SEAKEEPING COMPARISON BETWEEN THREE MONOHULLS, TWO SWATHS, AND A COLUMN-STABILIZED CATAMARAN DESIGNED FOR THE SAME MISSION

by

A. E. Baitis
W. G. Meyers
D. A. Woolaver
and
C. M. Lee



APPROVED FOR PUBLIC RELEASE: DISTRIBUTION UNLIMITED

SHIP PERFORMANCE DEPARTMENT
RESEARCH AND DEVELOPMENT REPORT

REPRODUCED BY
NATIONAL TECHNICAL
INFORMATION SERVICE
U.S. DEPARTMENT OF COMMERCE
SPRINGFIELD, VA. 22161

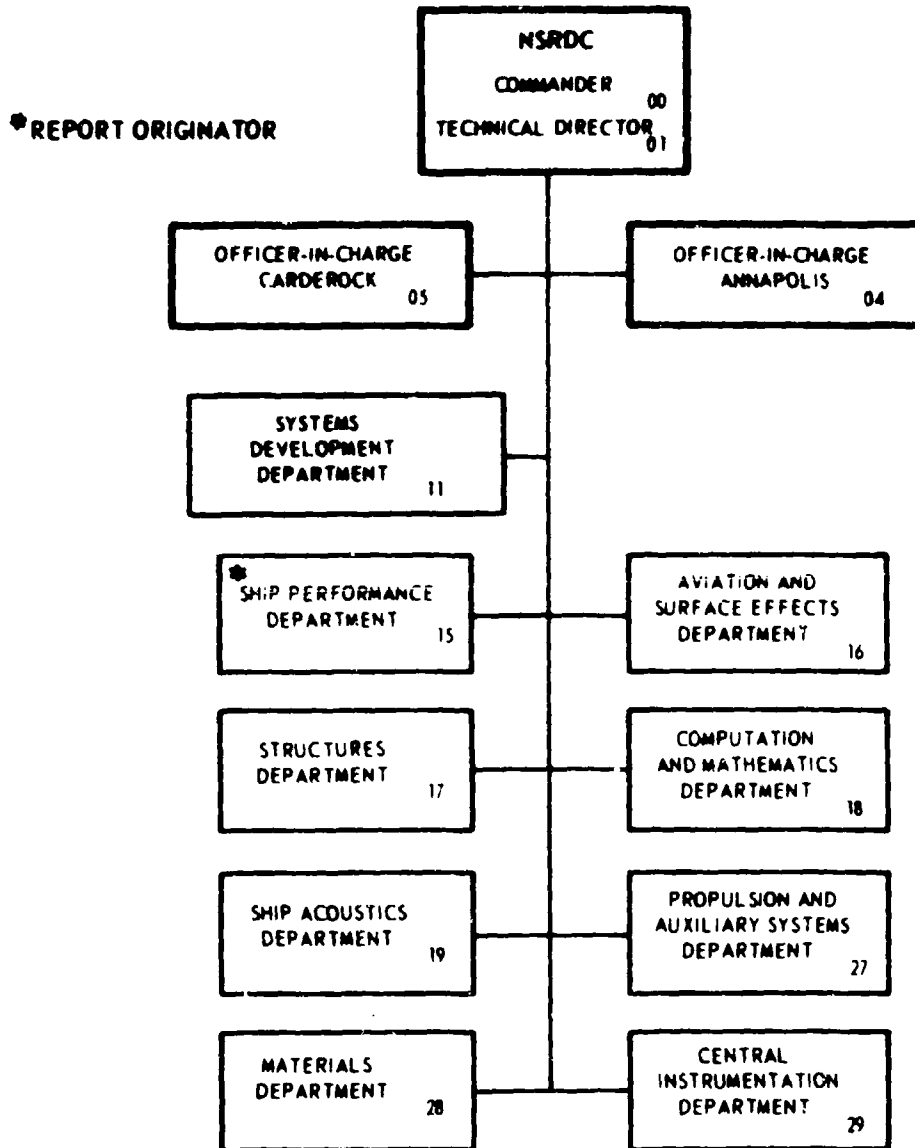
July 1975

Report SPD-622-01

The Naval Ship Research and Development Center is a U. S. Navy center for laboratory effort directed at achieving improved sea and air vehicles. It was formed in March 1967 by merging the David Taylor Model Basin at Carderock, Maryland with the Marine Engineering Laboratory at Annapolis, Maryland.

Naval Ship Research and Development Center
Bethesda, Md. 20814

MAJOR NSRDC ORGANIZATIONAL COMPONENTS



UNCLASSIFIED

SECURITY CLASSIFICATION OF THIS PAGE (When Data Entered)

REPORT DOCUMENTATION PAGE		READ INSTRUCTIONS BEFORE COMPLETING FORM
1 REPORT NUMBER SPD - 622 - 01	2 GOVT ACCESSION NO.	3 RECIPIENT'S CATALOG NUMBER
4 TITLE (and Subtitle) A SEAKEEPING COMPARISON BETWEEN THREE MONOHULLS, TWO SWATHS, AND A COLUMN- STABILIZED CATAMARAN DESIGNED FOR THE SAME MISSION	5 TYPE OF REPORT & PERIOD COVERED Final	
	6 PERFORMING ORG. REPORT NUMBER	
7 AUTHOR(s) A.E. Battis, W.G. Meyers, D.A. Woolaver, and C.M. Lee	8 CONTRACT OR GRANT NUMBER(s)	
9 PERFORMING ORGANIZATION NAME AND ADDRESS Naval Ship Research and Development Center Ship Performance Department Code 1568 Bethesda, Md. 20084	10 PROGRAM ELEMENT PROJECT TASK AREA & WORK UNIT NUMBERS Project 45016 Work Unit 1-1170-083	
11 CONTROLLING OFFICE NAME AND ADDRESS Naval Ship Research and Development Center Systems Development Department Code 117 Bethesda, Md. 20084	12 REPORT DATE July 1975	
	13 NUMBER OF PAGES 66	
14 MONITORING AGENCY NAME & ADDRESS (if different from Controlling Office)	15 SECURITY CLASS (of this report) UNCLASSIFIED	
	15a DECLASSIFICATION DOWNGRADING SCHEDULE	
16 DISTRIBUTION STATEMENT (of this Report) APPROVED FOR PUBLIC RELEASE: DISTRIBUTION UNLIMITED		
17 DISTRIBUTION STATEMENT (of the abstract entered in Block 20, if different from Report)		
18 SUPPLEMENTARY NOTES SUBJECT TO L...		
19 KEY WORDS (Continue on reverse side if necessary and identify by block number) Monohull and SWATH Seakeeping Performance Criteria for Seakeeping Performance Comparisons Sea Representation Workboat Feasibility Candidates		
20 ABSTRACT (Continue on reverse side if necessary and identify by block number) The seakeeping characteristics of six basically different ship designs were evaluated to determine their comparative effectiveness as a U.S. Navy workboat. Three of the designs represent conventional monohulls with different size and speed capabilities. Ship A represents the currently employed torpedo retriever boat, and Ships B and C represent larger versions of A with expanded capabilities. Two designs (Ships D and E) represent small waterplane vehicles which have the same mission capabilities as B and C. (See reverse side)		

UNCLASSIFIED

SECURITY CLASSIFICATION OF THIS PAGE (When Data Entered)

Block 20 (Continued)

Again, Ships D and E differ primarily in their speed capabilities. The remaining candidate design represents a vehicle which has two distinct operating characteristics. In the **transiting condition**, this ship is essentially an oceangoing catamaran and is denoted as Ship F. Once the working station is reached, this ship floods down and becomes a very small waterplane area vehicle. The submerged catamaran hulls are connected to the superstructure by four slender elliptical vertical struts. In this configuration, the ship is designated as Ship G. Based on the weighed characteristics of all ship candidates in transit as well as in the stationkeeping mode, it was established that Ship F (a 20-knot, small **waterplane area twin hull** SWATH design) is the most suitable for the defined mission of a **Navy workboat**. This conclusion is based entirely on the seakeeping responses of the candidate designs without reference to construction or operating costs.

UNCLASSIFIED

SECURITY CLASSIFICATION OF THIS PAGE (When Data Entered)

TABLE OF CONTENTS

	Page
ABSTRACT	1
ADMINISTRATIVE INFORMATION	1
INTRODUCTION	1
PREDICTION PROCEDURE	2
OVERVIEW	2
SHIP AND PREDICTION PARTICULARS	3
SEA REPRESENTATION	5
SEA CONDITIONS IN OPERATING AREA	8
CALCULATION OF ROLL	10
CRITERIA FOR COMPARATIVE PERFORMANCE	11
CALCULATION OF RELATIVE BOW MOTIONS IN TIME DOMAIN	12
PRESENTATION OF RESULTS	13
RESPONSES PER UNIT SIGNIFICANT WAVE HEIGHT	14
CRITICAL SIGNIFICANT WAVE HEIGHTS FOR SLAMMING OR DECK WETNESS	18
TIME DOMAIN RESULTS FOR SLAMMING AND DECK WETNESS	19
INFLUENCE OF DAMPING DEVICES ON SWATH RESPONSES IN HEAD SEAS	20
INFLUENCE OF BILGE KEELS ON SHIP RESPONSES IN BEAM SEAS	21
CONCLUSIONS AND RECOMMENDATIONS	22
ACKNOWLEDGMENT	23
APPENDIX A DEFINITION OF RELATIVE BOW MOTION	24
APPENDIX B WAVE-EXCITING FORCES AND MOMENTS FOR WORK- BOAT CANDIDATES AND FEASIBILITY OF ACTIVE FIN STABILIZERS	29
REFERENCES	33

LIST OF FIGURES

1	Ship Particulars	35
2	Comparison of Candidate Ship Types	36
3	Computer Fit of Body Plans for Candidate Ship Types	37
4	Data Channels and Ship Locations for Which Responses Were Calculated	38
5	Theoretical Wave Spectra Used to Represent Sea Conditions	39

	Page
6 Summary of Calculation Conditions	40
7 Relative Frequencies at Which Individual Wave Systems or Combined Systems Occur	41
8 Influence of Modal Sea Period on the Significant Single Amplitude Pitch and Heave of Ship Candidates	42
9 Influence of Modal Sea Period on the Significant Single Amplitude Relative Bow Motion and Vertical Accelerations of the Ship Candidates	43
10 Influence of Ship Speed and Modal Sea Period on the Significant Single Amplitude Relative Bow Motion and Comparable Absolute Vertical Motion of the Candidate Ships	45
11 Influence of Ship Speed and Modal Sea Period on Significant Wave Height Levels Critical for Various Ship Candidates	46
12 Influence of Ship Speed and Modal Sea Period on the Mission-Interrupting Events	48
A.1 Definition of Relative Bow Motion on Ship Centerline	27
A.2 Summary of Relative Bow Motion Calculations	28
B.1 Wave-Exciting Forces and Moments for the Ship Candidates	32

LIST OF TABLES

1 - Definition of Sea States	50
2 - Constants for Single-Amplitude Statistics and Equation for Two-Parameter Bretschneider Spectrum	51
3 - Yearly Average Statistics of Four Major Hawaiian Wave Systems	52
4 - RMS Responses of Ship A, 85-Foot Hardchine Monohull	53
5 - RMS Responses of Ship B, 15-Knot Monohull	54
6 - RMS Responses of Ship C, 20-Knot Monohull	55
7 - RMS Responses of Ship D, 15-Knot SWATH with and without Bilge Keels	56
8 - RMS Responses of Ship E, 20-Knot SWATH	58
9 - RMS Responses of Ship F, Column Stabilized Up	59
10 - RMS Responses of Ship G, Column Stabilized Down	60
11 - Beam Sea RMS Accelerations and Roll of Candidate Ships	61

NOTATION

C	Clearance between the calm water surface and the ship cross structure or freeboard at longitudinal location L_c
D	Draft at L_c
GM_L	Longitudinal metacentric height
GM_T	Transverse metacentric height
$H_{1/3}(\tilde{\xi}_w)_{1/3}$	Significant wave height, average of the 1/3 highest waves
L_A	Lateral acceleration in g
L_c	Longitudinal location for which relative motion between ship and water surface was predicted
L_{PP}	Length between perpendiculars
L_V	Vertical acceleration in g
RAO	Response amplitude of operator
RBM	Relative bow motion at L_c
RMS	Root mean square, square root of variance
T_Z	Natural heave period, period corresponding to maximum value of beam-sea, zero-speed heave RAO
T_ξ	Natural roll period, period corresponding to maximum value of beam-sea, zero-speed roll RAO
T_θ	Natural pitch period, period corresponding to maximum value of head-sea, zero-speed pitch RAO

ABSTRACT

The seakeeping characteristics of six basically different ship designs were evaluated to determine their comparative effectiveness as a U.S. Navy workboat. Three of the designs represent conventional monohulls with different size and speed capabilities. Ship A represents the currently employed torpedo retriever boat, and Ships B and C represent larger versions of A with expanded capabilities. Two designs (Ships D and E) represent small waterplane vehicles which have the same mission capabilities as B and C. Again, Ships D and E differ primarily in their speed capabilities. The remaining candidate design, a column-stabilized catamaran, represents a vehicle which has two distinct operating characteristics. In the transiting condition, this ship is essentially an oceangoing catamaran and is denoted as Ship F. Once the working station is reached, this ship floods down and becomes a very small waterplane area vehicle. The submerged catamaran hulls are connected to the superstructure by four slender elliptical vertical struts. In this configuration, the ship is designated as Ship G.

Based on the weighed characteristics of all ship candidates in transit as well as in the station-keeping mode, it was established that Ship E (a 20-knot small waterplane area twin-hull (SWATH) design) is the most suitable ship for the defined mission of a Navy workboat. This conclusion is based entirely on the seakeeping responses of the candidate designs without reference to construction or operating costs.

ADMINISTRATIVE INFORMATION

This work was conducted at the Naval Ship Research and Development Center (NSRDC) by Ship Performance Department Code 1568 at the request of NSRDC's Systems Development Department. The work reported herein was funded under Work Unit 1-1170-083.

INTRODUCTION

The U.S. Navy has been employing a small 85-foot hardchine boat in its Hawaiian operations. This boat has been found to be far from ideal as a workboat in its present role because of its limited size and the associated seakeeping characteristics. NSRDC was requested to perform a feasibility design for a workboat that is more suitable for present and projected tasks in the Hawaiian area. The seakeeping analysis undertaken for this feasibility design is the subject of the present report.

Ship motions, including accelerations, and the relative ship to water motions were predicted in long-crested, irregular seas for a series of six ships of basically different design.

Five represent competing feasibility designs for a workboat to be used by the Navy, and the other represents the existing workboat. Since the five competing feasibility designs all have the same mission, motion predictions were made for a series of realistically related ships by using a variety of documented and undocumented ship motion computer programs.

Three aspects of these prediction procedures were somewhat unusual for this type of motion investigation. The first was the use of four distinct wave spectra to represent sea conditions at a specific sea state or wave height level. The second was that ship responses were evaluated for ship mission-oriented conditions, i.e., transiting in head seas to the work site and stationkeeping at the work site. The third aspect was that their effectiveness was evaluated by considering how well the various candidates meet specific ship response criteria for the two operating conditions.

PREDICTION PROCEDURE

OVERVIEW

Four basic computer programs or groups of programs were used to develop ship responses. Two programs developed the responses in the frequency domain, and the other two developed and reduced these responses in the time domain.

The first program developed the response amplitude operators (RAOs) and the second program calculated the responses of the various ships for a series of four distinct sea conditions selected from the intended operating area of the workboat. The third program converted the results of the first program into the time domain, and the fourth program computed the critical wave heights at which ship performance would be degraded by mission-interrupting events such as slamming or deck wetness. It is pointed out that the results of the second program were used primarily to check the time domain ship responses of the third computer program.

Three different computer programs were used to calculate the RAOs which characterize ship responses for particular load, speed, and heading conditions. Monohull RAOs were obtained from the NSRDC Ship Motion and Sea Load Program.^{1,2} Both head and beam sea

¹Meyers, W.G., et al. "Manual NSRDC Ship Motion and Sea Load Computer Program." NSRDC Report 3376 (1975). A complete listing of references is given on page 33.

²Salvesen, N., et al. "Ship Motions and Sea Loads." *SSAME Trans.*, Vol. 78, pp. 250-287 (1970).

RAOs were obtained for the monohulls from this program. RAOs from SWATH and column-stabilized catamarans in head seas were obtained from an undocumented, modified version of the Frank Close-Fit Ship Motion Computer Program.^{3,4} In turn, the beam sea RAOs for these ships were calculated by using an undocumented computer program as well as roll damping coefficients measured during SWATH model experiments.

The RAOs calculated by the various programs were converted to a single consistent coordinate system prior to their use as input to the third or time domain conversion program. The time domain conversion was performed by using the procedures of several investigators.⁵⁻⁷

The relative bow motions calculated in the fourth program were developed according to the procedure given in Appendix A. Simple level crossing techniques were employed to establish the number of critical events (slamming, deck wetness or cross-structure impacts) that would interrupt ship mission during 30 minutes of operation in the selected seaways. It should be noted that all ships were subjected to exactly the same seaway time history at a particular modal wave period and speed condition. Thus the responses of the individual candidate vehicles are directly comparable at the various conditions.

SHIP AND PREDICTION PARTICULARS

Figure 1 presents the particulars of the seven configurations for which response predictions were made. Ship A, a small 85-foot hardchine boat, was included because it represents a workboat whose response characteristics as a Navy workboat are already known. The objectionable characteristics of this boat when transiting to the work site (slamming, wetness) as well as during stationkeeping at the site (excessive roll) thus represent response levels against which the new workboat candidates can be compared.

Both the cross sections of the candidate boats at a longitudinal location L_c and the location of L_c on the calm-water waterplane area are shown in Figure 1. L_c was the

³ Frank, W. and N. Salvesen, "The Frank Close-Fit Ship-Motion Computer Program," NSRDC Report 3289 (1970).

⁴ Jones, H.D., "Catamaran Motion Prediction in Regular Waves," NSRDC Report 3700 (1972).

⁵ Zarnick, I.E. and J.A. Diskin, "Modeling Techniques for the Evaluation of Anti-Roll Tank Devices," Third Ship Control Symposium, Bath, England (Sep 1972).

⁶ Withrington, J.K., "Analytical Methods for Verifying the Structural Integrity of LNG Carriers," Third International Conference on Liquefied Natural Gas, Washington, D.C. (Sep 1972).

⁷ Batts, A.E. et al., "LNG Cargo Tanks - A Ship Motions Analysis of Internal Dynamic Loadings," GASTECH 74, International LNG and LPG Congress, Amsterdam (Nov 1974).

location at which relative motions between the ship and the water were computed for all ships in head seas. The reasons for this choice of location are discussed later. Both size and arrangement of the waterplane area of the candidate boats are shown in order to demonstrate their significant differences. Two points should be noted in this regard. First, the waterplane areas essentially represent a measure of the static restoring force potential of the different ships, i.e., the tons per inch immersion. The three monohulls (Ships A, B, and C), for example, respectively require 2.72, 8.69, and 10.49 tons to increase draft by 1 inch. On the other hand, the 15- and 20-knot SWATHs (Ships D and E) respectively require only 2.78 and 3.20 tons to increase the draft by 1 inch. The column-stabilized ship requires an increase of 8.96 tons per inch of draft in the surfaced condition (Ship F) even though it has essentially twice the displacement of the monohull with equal 15-knot design speed. Once the hulls of the column-stabilized catamaran are submerged (Ship G), only 1.64 tons are required to increase draft by 1 inch. This, of course, is even less than the very much smaller Ship A although ballast pumping would alleviate this very low extra payload-carrying capacity. The key point to note is that monohulls are much less sensitive to payload increase than are SWATHs. Thus, one of the significant differences between these two types is their sensitivity to payload increases. It is important to recognize this fundamental difference in the payload growth potentials of the two types.

The basic motion behavior in seaways represents a second major difference between the ship types. The small waterplane area SWATH and the column-stabilized catamaran both have very large natural motion periods, particularly for angular ship responses. The natural periods shown in tabular form (Figure 1) were obtained from the zero-speed, beam-sea, roll and heave RAOs and the zero-speed, head-sea pitch RAOs. The importance of the long natural periods is that motion responses due to seas generated by local winds are thus lower for the SWATHs than for the monohulls or the catamaran (Ship F).

The major ship dimensions and particulars are given in Figures 1 and 2. Figure 3 was prepared to demonstrate in detail the specific input to the various computer programs that produced ship motion RAOs. Note that these programs consider only the below-the-waterline hull form. Forward sections are shown on the right-hand side and aft sections on the left-hand side of the figure. The large difference in the beam and drafts of the various ship types is clearly demonstrated. Monohulls (Ships A, B, C) clearly have both the most shallow drafts and the largest waterplane areas whereas the SWATHs (D and E) and Ship F/G have the deepest drafts and the greatest beam and deck areas.

Ship responses were calculated for operating conditions which represent two specific elements of the ship mission, namely the in-transit and stationkeeping operating modes. Stationkeeping was considered to consist of head and beam sea responses at 0 and 5 knots. The in-transit operating mode was considered to be represented by head sea responses at

speeds up to the design speeds of the candidate ships, i.e., 15 and 20 knots. It should be noted that Ship G, the column-stabilized catamaran in the submerged condition, has a top speed of 5 knots and thus response predictions were made for 0 and 5 knots in head seas.

Figure 4 summarizes the individual responses predicted for the various craft in head and beam seas. Head sea responses were developed for essentially four different locations on the ships and beam sea responses for only two locations. It was considered that head sea or in-transit ship responses could best be represented by vertical accelerations at three longitudinal locations as well as by pitch and the relative motion at a critical longitudinal location L_C (Point 4). Points 1 and 3 represent the furthest practical forward and aft locations at which ship mission-related work might be required during the in-transit operating mode. Point 2 represents the location of the center of gravity (CG) at the main deck level.

Beam sea responses were calculated only to amplify the head sea stationkeeping responses at 0 and 5 knots. Only roll, lateral, and vertical acceleration at the CG (Point 1) were calculated in beam seas at 0 knots. The vertical and lateral accelerations were calculated at the aftmost, outboard location on the decks of the various ships, i.e., Point 2. These acceleration predictions were made on the assumption that Point 2 would be the furthest aft, practical location at which such mission-related work as launch and retrieval of buoys could be made. The transverse distance from the centerline is tabulated as B in Figure 1. The furthest practical forward acceleration responses may be assumed to be essentially identical to the Point 2 predictions.

Figure 5 presents the range of theoretical wave spectra used to represent the range of irregular sea conditions which the workboats are expected to encounter during operation. Figure 6 indicates the various ship and sea conditions for which ship response predictions are made. The sea representation is described in greater detail in the following section.

SEA REPRESENTATION

Realistic seas are composed of a mixture of locally generated wind waves and swell from distant storms. Swell differs from locally generated waves primarily in that waves due to swell are very much longer and somewhat more regular or periodic than short, choppy wind-generated waves. The mixture of such seas can result in waves whose spectra may have two or more distinct modal periods or spectral peaks depending on the differences in the modal periods of the local sea and the swell as well as on their characteristic wave heights. Several

authors have noted⁸⁻¹² that the variability of realistic sea spectra cannot be adequately accounted for by means of a single-parameter Pierson-Moskowitz wave spectrum formulation.¹³

At present, there are two basic schools of thought as to how the accuracy and realism of the sea description can be improved for purposes of predicting ship response. One^{9,11} favors some type of idealized spectral family and the other^{8,10} favors use of a weighted set of real, measured spectra. Baitis et al.⁷ have demonstrated the equivalence of these two approaches for design purposes.

Simulation techniques, such as those recently employed by Baitis et al.,* can be employed to generate any arbitrary set of realistic waves. Their recent sea simulation considered both swell and wind-driven seas together with their relative directions and their respective characteristic wave heights. However, consideration of all possible combinations of the relevant seaway parameters would result in an extremely large data base, at least as large as that from all previously measured wave spectra. Simplification of such a complex sea model is obviously desirable.

Fortunately, the matching of any particular realistic wave spectrum with an idealized spectrum is of little importance in ship motion-related design because any particular wave spectrum is not likely to be encountered by a ship. It is of the utmost importance, however, to develop sea models which will accurately define the *range* of ship responses that are likely to be produced by the almost limitless set of real sea conditions (spectra) a ship may encounter. By definition, such a range must include all possible responses that can occur due to widely different, real seas.

⁸Hadler, J.B. and T.H. Sarchin, "Seakeeping Criteria and Specifications," SNAME Seakeeping Symposium, Webb Institute of Naval Architecture, Glen Cove, N.Y. (Oct 1973).

⁹Baitis, A.E. et al., "Design Acceleration and Ship Motions for LNG Cargo Tanks," Tenth Symposium on Naval Hydrodynamics (Jun 1974).

¹⁰Cummins, W.E., "Prediction of Seakeeping Performance," 17th American Towing Tank Conference State of the Art Report—Seakeeping (Jun 1974).

¹¹Hoffman, D., "Analysis of Measured and Calculated Spectra," International Symposium on the Dynamics of Marine Vehicles and Structures in Waves, University College, London (Apr 1974).

¹²Hoffman, D., "Environmental Condition Representation," 17th American Towing Tank Conference State of the Art Report—Seakeeping (Jun 1974).

¹³Pierson, J.W. and L. Moskowitz, "A Proposed Spectral Form for Fully Developed Wind Seas Based on the Similarity Theory of S.S. Kitaigorodskii," J. Geophys. Res., Vol. 69, No. 24 (1964).

*Reported informally by A.E. Baitis et al., in NSRDC Evaluation Report 563-H-01 (May 1974)

This range of ship responses was obtained here by the use of a series of two-parameter wave spectra (significant wave height and modal period) of the form developed by Bretschneider.¹⁴ Table 1 defines sea conditions in terms of significant wave heights and presents the associated modal wave periods of seas generated by purely local winds. Thus, the table gives essentially the normally accepted definition of sea states in terms of wave height as well as the shortest modal period waves associated with a particular wave height. It is to be noted, of course, that when the addition of swell is considered, longer modal wave periods may occur as sea and swell mix.

Table 2 presents the statistical constants by which the RMS wave height or ship responses may be related to statistical levels such as the average, the average of the 1/3 highest amplitudes, etc. It should be noted that this average of the 1/3 highest amplitudes is generally referred to as the *significant response* or wave amplitude. Double amplitudes or wave height statistics are obtained from the RMS values by multiplying the single-amplitude constants by 2.

In the present investigation, the seas were represented by four different modal wave period spectra. Modal periods of 6, 8, 10, and 14 seconds were chosen because they represent the range of sea and swell conditions which typically occur (see Table 3) at the anticipated work site. Typical characteristics of the seas in this locality, taken from recent references, are discussed in somewhat more detail in the following section.

Figure 5 illustrates the Bretschneider wave spectra used to represent the range of local sea conditions. These wave spectra are shown for a 1-foot significant wave height. Table 2 presents the statistical constants as well as the equation for the Bretschneider spectra in terms of the significant wave heights and modal periods which are related to the various sea states defined in Table 1.

Two important results come about because of this choice of sea spectral representation. The first is related to the linearity of the responses and the second to the physical interpretation of the range of responses associated with the four distinct modal periods. Since ship responses are linear for engineering purposes, responses can then be determined for any wave height from the results of the unit or 1-foot significant wave height.

The physical interpretation of the range of responses varies somewhat with wave height. The given modal period wave spectra represent different mixtures of sea and swell at the various wave height levels. When considered for a significant wave height of 2 feet, the

¹⁴Bretschneider, C.L., "Wave Variability and Wave Spectra for Wave Generated Gravity Waves," Department of the Army, Corps of Engineers Technical Memorandum 118 (1959).

8-second period spectrum, for example, represents a very gentle, local wind-generated sea with a minor swell at 8 seconds. For these same conditions but a significant wave height of 4 feet, both the wind-generated local sea and the 8-second swell increase in severity, the latter somewhat more than the local sea. As the significant wave height is increased to about 8 feet, this spectrum represents a fully developed wind-generated sea without swell. If the significant wave height is again increased to, say, 12 feet, the 8-second spectrum now represents the steepest, partially developed, hurricane-generated sea commonly found in the open ocean. Further increases in significant wave height at this modal period tend to produce very rare, steep seas which can occur only in land-locked bays or lakes.^{15,16} Certainly at steepness ratios (significant wave height/wavelength corresponding to modal wave period) of greater than 1/9 or 1/8, the wave spectrum becomes physically unrealizable.

The most important fact to note in the discussion of sea representation is that this series of different modal period wave spectra establishes the range of the motion responses that can be expected due to the variability of the seas.

SEA CONDITIONS IN OPERATING AREA

Sea conditions in the ocean area (Hawaiian islands) in which the workboat is to operate were recently analyzed both for short-term and long-term characteristics.¹⁷ Based on measured and observed wave data,^{18,19} the analysis indicated that seas in the operating area can be grouped into four basic sets according to their independent generation mechanisms: (1) waves generated by northeast trade winds, (2) waves generated by the local Kona storms, (3) swell originating in the North Pacific, and (4) southern swell. The Kona wind waves and the trade wind waves are mutually exclusive; all other combinations of swell and wind waves may or may not occur simultaneously.

For each of the basic wave systems, the analysis¹⁷ presents the frequency of occurrence, the direction from which the waves originated, the average yearly significant wave heights,

¹⁵Pore, N.A. et al., "Wave Climatology for the Great Lakes," Nat. Ocean Atmosp. Admin. Technical Memorandum NWS TDL-40 (Fe) 1971).

¹⁶Floeg, J., "Wave Climate Study Great Lakes and Gulf of St. Lawrence," SNAME T & R Bulletin 2-17 (1971).

¹⁷St. Denis, M., "The Winds, Currents, and Waves at the Site of the Floating City Off Waikiki," Univ. Hawaii Report 7 (Dec 1974).

¹⁸Ho mer, P.S., "Characteristics of Deep Water Waves in Oahu Area for a Typical Year," Report prepared by Marine Advisers, LaJolla, California, for Board of Commissioners, State of Hawaii, under Contract 5772 (1964).

¹⁹Ho F.P. and L.A. Sherretz, "A Preliminary Study of Ocean Waves in the Hawaiian Area," Univ. Hawaii, Hawaii Inst. Geophys. Report H 16-69-16 (1969).

and the average significant wave periods. The significant wave periods may be regarded as equivalent to the modal periods of the waves/wave spectra. The results, summarized in Table 3, demonstrate that the modal periods of the local sea conditions range from about 6 to 14 seconds, i.e., the range of periods for which ship motion predictions were made.

It is also of interest to know the relative frequencies at which individual wave systems or combinations thereof occur. These frequency results were therefore prepared from the data of Table 3 and are presented as Figure 7 in the form of a Venn diagram. The frequency of occurrence of individual wave systems is represented by the total area within the circle labeled by the name of the system. For example, northeast trade wind seas are represented by a circle (75.3 percent) composed of four distinct areas of wave system combinations. In turn, each area represents a different combination of wave systems. For example, northeast trade wind seas and calm seas occur together only 9.2 percent of the time, northeast trade wind seas and southern swell occur together only 10.4 percent of the time, the combination of these two with North Pacific swell occurs 29.5 percent of the time, and the combination of northeast trade wind seas and North Pacific swell occur 26.2 percent of the time.

Several important points are demonstrated by these frequency results:

1. The scarcity of single direction or single wave system seas, i.e., pure* wind-generated seas ($9.2 + 1.3 = 10.5$ percent) and pure swell seas ($5.0 + 2.0 = 7.0$ percent).
2. The scarcity (5.7 percent) of pure** multidirectional swell in the absence of wind waves.
3. The large percentage ($29.5 + 4.0 = 33.5$ percent) of wind seas and two-component swell seas of nearly the same period, i.e., about 13 to 14 seconds.
4. The predominance of a mixture of sea and swell (75.1 percent)

This fourth point emphasizes the importance of using a sea representation model of the type selected here for an analysis of comparative seakeeping capability.

Thus the occurrence of pure wind-generated seas is expected to affect the response of monohulls, especially the small one, more severely than the other ship types. Conversely, the occurrence of pure swell seas consisting of either a single swell or two different swells of nearly equal periods is expected to be of greater importance for the seakeeping of the SWATH ships and the column-stabilized catamaran than for the monohulls.

Some comments on the relative importance of various combinations of wave systems are relevant here. St. Denis,¹⁷ calculated that the yearly average significant wave height due to sea and swell from all directions was equal to 6.25 feet and that the average significant

* Wind seas or calm seas, swell or calm seas.

** Here the term pure implies wind seas without background swell, and, inversely, swells without the presence of local winds and wind seas.

wave period of these seas was equal to 11.45 seconds. He also presented the expected yearly maximum values of significant wave heights: about 5 feet for the southern swell, 12 feet for the Kona storm waves, 15 feet for the trade wind waves, and 19 feet for the North Pacific swell. It is clear from these data that southern swell is not likely to attain heights that will make operation difficult when they augment the heights of waves for other directions. Thus southern swell is not likely to cause difficulties for workboat seakeeping. On the other hand, the combination of extreme Kona winds with North Pacific swell is likely to produce occasional difficulties. Finally, the combination most likely to produce difficulties is the extreme northeast trade wind waves and North Pacific swell.

Based on the above results, it has been concluded that a yearly average wave height of 6.25 feet (due to all waves) will not often be exceeded. More specifically, the wave height due to all seas will be greater than 7 feet only about 13 percent of the time and greater than 10 feet only about 3 percent of the time. Therefore, it has been concluded on the basis of these local sea characteristics that the behavior of the candidate ships in waves up to 6 feet high is of primary importance in establishing their comparative seaway performance. Consequently their survival capabilities have not been examined to any significant extent in comparing the feasibility of designs.

CALCULATION OF ROLL

As mentioned earlier, the monohull responses were calculated in head and beam seas by using the NSRDC Ship Motion and Sea Load Program. The responses were calculated both with and without bilge keels in accordance with standard procedures that are incorporated as part of that program.

The roll motions of the SWATH ships were calculated according to the procedures of Lee and unpublished damping data from recent NSRDC model experiments. The simplified program (unpublished) developed by Lee was used to predict roll/heave motions of the SWATHs in beam seas. This program essentially considers the ship as a constant cross-section body with length and mass equivalent to the actual ship. Experimental roll damping was used to limit the predicted roll response to realistic values.

The experimental roll damping was obtained from a model whose geometric proportions were similar (but not identical) to those of Ships D, E, and F. Model motion decay experiments had been conducted both with the bare hull and with a variety of damping devices such as fixed fins, blisters* near the waterline, and bilge keels; results have not yet been published. Bilge keels resulted in the largest damping increase above the base hull.

*Blisters are appendages added to the hull at/near the waterline to increase the restoring buoyancy forces that result when the hull is depressed below its waterline.

The measured percentage increase in hull damping due to bilge keels was then used to increase the bare hull SWATH hull damping. In determining the motions of a SWATH with bilge keels, this approach considers that the measured damping modifications are applicable to Ships D, E, and F despite differences in geometry, that is, measured damping increases are considered to be physically realizable with reasonable, though unspecified, bilge keels.

The predicted roll RAOs are considered to be inaccurate primarily in the frequency range where resonance occurs, i.e., inaccuracies are associated with the damping. However, since the RAOs are intended for use in predicting roll in seas whose modal periods are far removed from those of resonant roll, the predicted roll is considered adequate for establishing a relative ranking of the various ship candidates.

A similar procedure was employed to predict the effect of bilge keels on the SWATH heave responses in beam seas and the SWATH pitch, heave, and acceleration responses in head seas.

CRITERIA FOR COMPARATIVE PERFORMANCE

The assumption was made that the consequences of excessive relative motions at section L_C would be exactly the same for all ship types, namely, interruption of mission, and therefore that such motions constituted a criterion for comparative performance. More specifically, it was assumed that when a particular statistical level* of relative motions exceeded the clearance or draft of the ship at L_C , the mission would be interrupted by keel emergence or slamming and deck wetness in the case of monohulls and by cross-structure impacts in the case of SWATHs. Figure 2 was prepared to demonstrate the plausibility of this assumption.

All response predictions were made, of course, by assuming linearity, i.e., a 1-foot wave would yield one-third of the response of a 3-foot wave of identical period. The applicability of the linearity assumption to predict the magnitudes of extremes of responses (e.g., occurrence of deck wetness, keel emergence, or slamming) is, of course, highly questionable. However, it was considered that an accurate, relative ranking of the performance of the candidate ships could be established in terms of such mission-interrupting events by extending the relative motion responses linearly to the draft or clearance (freeboard).

The average of the 1/10 highest single amplitudes of relative motion was selected as the criterion for exceeding draft/clearance because this measure ensures that within a practical

*Average of the 1/10 highest single amplitude of relative motion at L_C .

time span of ship operation (e.g., 30 minutes) a motion cycle will be sufficiently severe so that either disruptive mission-interrupting slamming or deck wetness results. The greater precision attainable by specifying extreme response levels inherent in the use of such concepts as threshold velocities for slamming or variations in the statistical motion level (e.g., the average of the 1/3 highest or some other level) is not warranted. Neither the response characteristics at these nonlinear ranges nor the specific consequences of exceeding particular relative motions is known for the different ship types. Moreover, it is emphasized that these specific in-transit ship response criteria were selected in order to achieve a fair, accurate ranking of the candidate ships during this feasibility design stage. However, to resolve the aforementioned limitations of the predictions and to examine ship behavior under survival conditions, it will be necessary to conduct model experiments for two candidates that our predictions indicate are best suited as Navy workboats.

CALCULATION OF RELATIVE BOW MOTIONS IN TIME DOMAIN

The calculation of relative bow motion was based on the difference between the wave at the longitudinal location L_C and the absolute motion of the ship at that location. No correction was included in the calculation for trim or sinkage due to forward speed; these factors have insufficient impact on the accuracy of the calculations to alter the relative ranking of the different ship candidates. A precise definition of the relative bow motion calculation is given in Appendix A.

It should be noted that the prediction for relative bow motion is made in the time domain developed from the spectral representation of the sea. Each relevant sea condition was converted^{5,6} from the frequency domain into the time domain for every modal period wave spectrum by decomposing the wave spectrum into about 100 evenly spaced (in frequency) sine waves whose amplitudes are related to the ordinates of the modeled wave spectrum. Random phases were assigned by means of a random number generator to each of the 100 component frequencies. The wave at L_C was obtained from the wave at the origin by shifting the phase of each sine wave by the product of the wave number and the distance $|q|$. Figure A.1 of Appendix A illustrates the relative locations of the waves and presents a simple summary of how the various component time histories were combined to yield the relative bow motion.

The pitch and heave RAOs were defined with an interpolation routine for exactly the same frequencies as the components of the wave spectrum. The product of the sine wave components of the wave, the response at the appropriate frequencies, and the appropriate phases were summed for all frequencies to yield the resultant time histories. The appropriate

phase at each frequency was defined as the sum of the random phase and the phase associated with the particular response. This procedure of time-history generation which associates the random phases with the wave time history thus made it possible to expose all candidate ships to exactly the same wave time history.

After the component time histories of the absolute motion at L_C had been generated, the absolute motion time history at L_C was obtained simply from the sum of the heave time history and the product of l times the pitch time history; see Figure A.1. Finally, the relative bow motion at L_C was obtained by subtracting the wave at L_C from the absolute motion at L_C . These arithmetic operations were performed for each instant in time.

PRESENTATION OF RESULTS

The various ship and sea conditions for which predictions are made have been summarized in Figure 6.

Tabulated results (Tables 4-11) were utilized to prepare three basic groups of graphs (Figures 8-12).

The first group presents ship responses at various modal period seas for significant wave heights of 1 foot (Figures 8 and 9) and 6 feet (Figure 10).

The second group (Figures 11a and 11b) presents the significant wave height level at which mission-interrupting events are expected from linear ship motion theory (see the discussion of linearity given in the section on criteria for comparative performance). Thus these figures enable a simple ranking of the candidates in terms of the seas which limit their in-transit operating mode. The higher the limiting sea state, the more capable the ship is to fulfill the defined mission.

The third group (Figures 12a and 12b) presents the results of the time domain representation of ship responses. The actual number of times that the relative motions are expected to exceed either the draft at location L_C or the freeboard or cross-structure clearance was calculated by a level crossing subroutine in the time-history-generating computer program. It was considered appropriate to perform these calculations at the average yearly significant wave height that typifies the intended work site area.¹⁷

The basic graphical format is identical for all three groups of figures and was developed to facilitate a visual comparison of the different ship types. Thus each figure consists of at least three graphical frames, one for each basic ship type (monohull, SWATH, and column-stabilized catamaran). Response magnitudes of each ship are plotted as vertical lines at each of the four modal wave periods. Thus variations in the response of each ship due to the variations in the modal period, or—equivalently—the harmonic content of the sea, are presented as a cluster of four vertical lines representing from left to right the response in the 6-, 8-, 10-, and 14-second modal periods.

Although the tables present the results in RMS form in a sea with a 6-foot significant wave height, the first group of figures presents the results in terms of significant single-amplitude responses. These are equal to twice the RMS values and were selected for presentation because these statistical response levels are generally considered representative of the responses experienced or noted by the crew of Ship A. It has been found that ship operators generally quote angular motions as single amplitudes and translational responses, such as heave, as double amplitudes. The statistical constants which relate the RMS responses to particular statistical response levels such as the average, the average of 1/3 highest or significant, or the highest expected response in N amplitudes are given in Table 2.

RESPONSES PER UNIT SIGNIFICANT WAVE HEIGHT

Figure 8a presents the significant single-amplitude pitch and heave responses for the various candidate ships operating in head seas at 0 knots. It is quite evident that Ship F (the 170-foot, 1032-ton, column stabilized catamaran) generally has the worst pitch motions of any candidate for the new workboat. In fact, its motions are expected to be nearly as bad as those of the presently employed Ship A, which is very much smaller (85-foot, 74-ton hardchine torpedo retriever boat). However, once the column-stabilized catamaran has ballasted down (Ship G) to become essentially transparent to the seas, it will have essentially the lowest pitch responses. This clearly demonstrates the virtue of the dual-operation mode.

Pitch responses for the monohulls (Ships B and C) will not have the undesirably sharp increases in the vicinity of their pitch resonance exhibited by the small or low waterplane candidates (Ships D, E, and G). Such behavior is one of the greatest potential shortcomings of SWATH. However, its practical importance can be negligible provided this pitch resonance condition can be avoided. For example, assuming that operational requirements during the stationkeeping portion of the mission allow such action, the SWATH can avoid pitch resonance by altering its encounter frequency through slight speed or heading changes. Note that Ship E (17.4-second pitch resonance period) is clearly superior to Ship D (comparable period of 12.5 seconds) because it entirely avoids the problem of large responses in swell during stationkeeping. Local sea data for the workboat operating site indicate that 17.4-second swells do not occur with practical frequency. The difference in pitch response levels for these two designs indicate the control that the feasibility ship designer can exert.

Salvesen²⁰ has given a far more comprehensive discussion of the comparative seakeeping qualities of monohulls and SWATHs; see Sections IVb and c of his paper for an explanation of the differences.

(Because the undesirable nature of such sharply tuned behavior has been amply demonstrated by recent Navy experience with an oceangoing catamaran, the effectiveness of passive damping devices, such as bilge keels, for this mode of operation was included in the present study. This aspect is covered in a later section of the report.)

Heave responses at zero speed are quite good for the various monohulls; only the submerged column-stabilized catamaran (Ship G) can be expected to have lower heave responses. The two SWATH candidates will have the highest heave responses.

At design speeds (Figure 8b), the SWATHs showed the lowest pitch of the candidates and the column-stabilized catamaran (Ship F) the worst pitch. In fact, at design speed, Ship F has the worst pitch and heave of all candidates. Thus if the comparison is strictly on the basis of these motions rather than their consequences, Ship F is clearly the least attractive candidate in its present configuration; even the small current workboat (Ship A) has lower ship responses. These particular points are emphasized with reference to Ship F motion responses because they illustrate the care that the feasibility designer must exercise to ensure that the consequences of such motions do not result in unacceptable mission-limiting events. Weight or displacement allowances and ballast pumping capacity must clearly be tightly controlled in order to avoid a critical loss of clearance between the cross structure and the water surface.

Significant differences in the motion response levels between the 15- and 20-knot SWATHs were again evident at the design speed. These results demonstrate clearly that substantial differences in the responses of different SWATH ships are possible with relatively minor basic alterations. Ship E (the 20-knot SWATH) is considered superior to Ship D (the 15-knot SWATH) so far as heave and pitch responses are concerned, both during the station-keeping and in-transit operating modes.

Other measures of seakeeping performance of the various candidates at zero speed emphasize the consequences of large SWATH heave motions. As shown in Figure 9a, Ships D and E definitely have the largest relative bow motions at section L_C of all the candidates. Monohulls have the lowest relative bow motions, and the smallest monohull (Ship A) has the lowest of all. Thus, the monohulls are superior for such tasks as launching and retrieving buoys and for similar work which requires low relative motions. Using the criterion of relative motions at zero speed, the ranking in order of decreasing effectiveness is Ship A, B, C, E, and D.

²⁰Salvesen, N., "A Note on the Seakeeping Characteristics of Small-Waterplane-Area-Twin-Hull Ships," Advance Marine Vehicles Meeting, Annapolis, Maryland; J. Hydromechanics, Vol. 7, No. 1, pp. 3-10 (Jan 1973).

When the vertical acceleration levels at three typical longitudinal positions on the decks of the various ships are considered (see Figures 4 and 9a), the monohulls are very similar to the SWATHs, except that Ship F is notably better than the others. The ranking is Ship E, C, D, B, A, and F. Vertical accelerations are generally lower over wider or larger deck areas than over the longer but narrow decks of monohulls. However, none of the acceleration levels appears to be objectionably high.

A similar acceleration comparison at design speeds (Figure 9b) however, demonstrates the clear superiority of the SWATHs over the monohulls during the in-transit operation mode. This is particularly noticeable for the column-stabilized catamaran, Ship F. Ranking for the ships is E, D, B, C, A, and finally F. The differences between the in-transit acceleration response levels of the SWATHs, monohulls, and the catamaran are on the order of factors of 2 or greater and are important. Significant vertical accelerations which exceed the 0.2- to 0.25-g level tend to become somewhat uncomfortable. Thus, in average 6-foot-high seas, the SWATH acceleration levels would be below these levels, the monohull accelerations would fall at the beginning of the uncomfortable range, and the catamaran accelerations would substantially exceed this uncomfortable range. Should Ship F avoid these uncomfortable accelerations by ballasting down to become Ship G, the rather low maximum speed of 5 knots would strongly penalize this candidate.

The comparison of relative motions during the in-transit operation mode indicates that Ship F has the largest responses and that the SWATH and monohull candidates have lower but quite similar responses. On the basis of the combined results, it is concluded that in its present form, the column-stabilized catamaran* is the least desirable of the three basic types of ships under consideration.

To provide an additional seakeeping comparison between the different ship candidates, their absolute and relative bow motions are presented for average 6-foot seas at speeds ranging from 0 to design speed (see Figure 10). The absolute bow motions are comparable for the monohulls represented by Ships B and C. It is noteworthy, however, that for these 6-foot significant seas, there is no noticeable reduction in bow motion with increase in monohull size. Thus, even the largest 741-ton, 20-knot monohull experiences essentially the same absolute bow motions as the presently employed 74-ton, 20-knot hard-chine boat.

*Substantial improvements in the seakeeping performance of the column-stabilized catamaran can be expected if a large damping foil of the type installed on the T-AGOR and the ASR-21 and -22 were to be installed on the present Ship F/G design. There would of course be a drag penalty associated with such a modification, but this should not be serious.

When comparing the absolute bow motions of the monohulls and the SWATH candidates at 0 and 5 knots, it becomes evident that the monohulls are equal to or better than the SWATHs at these low speeds. The column-stabilized catamaran in the submerged condition (Ship G), however, has the lowest absolute bow motion. It is quite evident from these results that the trends of the absolute bow motions with forward speed are substantially different for the ship types. Bow motions of monohulls tend to increase very slightly with increasing forward speed, those for the catamaran in the surfaced condition (Ship F) increase quite strongly with forward speed, and those of the SWATHs actually decrease with increasing forward speed.

The different ship types also have different trends of relative motion with speed. Relative motions of monohulls are quite low at zero speed and increase somewhat more than the absolute motions with increasing speed. Relative bow motions for the catamaran also strongly increase with increasing speed, and those for SWATHs decrease very slightly with forward speed. This behavior of the SWATHs is regarded as quite favorable from the seakeeping point of view. The trend suggests that if a SWATH is satisfactory at zero speed, then it will be satisfactory during the in-transit condition.

Thus a fundamental difference in the seakeeping performance characteristics of SWATHs (Ships D, E, G) on the one hand and monohulls and catamarans (Ships A, B, C, F) on the other hand is their basic response with speed. This trend was also noted by Salvesen.²⁰ To ease ship responses in severe seas, monohulls and catamarans must slow down but apparently SWATHs must increase speed. (Severe seas are regarded here as seas which produce responses that threaten ship survival.)

It should be noted that even though *absolute* motions and accelerations are important in determining the comfort level on board ship, once *relative* motions exceed specific values, they produce mission-interrupting impacts or deck wetness. This consideration is equally important especially during the in-transit operating mode.

If the mission of these ships is to include extended operations in the open ocean without retreating to a nearby harbor, their survival characteristics must be examined. This would require model experiments to investigate ship responses in severe seas at both zero and design speeds.

If, on the other hand, the ships are to be deployed in the open ocean with the option to retreat from extreme sea conditions, then only zero speed model experiments between the last two basic ship types are indicated.

It is again concluded at this point that in its present configuration, the column-stabilized ship is the worst of the three basic types investigated. It should be noted, however, that this ship apparently has the best survival capabilities of all. For comparative purposes, the

results for Ships F and G will continue to be presented, but this ship candidate is considered as essentially eliminated from the competition.

The following section will compare the candidate ships on the basis of their in-transit performance limits.

CRITICAL SIGNIFICANT WAVE HEIGHTS FOR SLAMMING OR DECK WETNESS

The significant wave height at which mission is disrupted by slamming, deck wetness, or cross-structure impacts is considered a fair measure of the seaway performance of the different ship types. This critical wave height thus represents the limits of ship performance in realistic seas. In waves much higher than those predicted by our linear theory, all ships are expected to encounter such severe disruptions that alterations in ship course and/or speed become mandatory. Inherent in our approach is the assumption of accuracy in the relative ranking of ships by means of their critical wave heights. Model experiments in extreme waves are recommended to verify this assumption for the best two candidate ship types.

Figure 11a presents the influence of speed and modal sea period on the actual wave height that cancels operation because of bow emergence, i.e., slamming. The higher this wave height, the better the candidate ship is in both the in-transit and stationkeeping modes.

For the sake of convenience, sea states are indicated on the right-hand side of the graphs. As in the earlier figures, the vertical lines represent the critical significant wave heights. The dashed portion of the vertical lines represent wave height conditions at the particular modal periods that are very steep; these are exceedingly rare and tend to occur only in land-locked bodies of water.^{14,15}

These results indicate that in average 6-foot seas, none of the candidate vehicles will encounter mission-limiting keel emergence during stationkeeping. As expected from the relative motion data of the previous figures, the monohulls (Ships B and C) are essentially equal to the SWATHs (Ships D and E) so far as these seaway performance limits are concerned. The small, presently used monohull (Ship A) is essentially the worst from this viewpoint because of its performance in local-wind-generated, 6-second modal period seas.

At design speeds, the SWATH ships are superior to the monohull candidates so far as mission-limiting keel emergence is concerned. The 20-knot SWATH (Ship E) appears to be the best and the column-stabilized catamaran (Ship F) the worst of the candidates unless the large speed loss inherent in its operation as Ship G is accepted without penalty.

This ranking alters somewhat when the ships are compared in terms of when their relative bow motions will exceed freeboard or cross-structural clearance; see Figure 11b. During the stationkeeping and in-transit operating modes, the monohulls are substantially superior to the other candidates. However, none of the ships is really unsatisfactory since all can operate in seas up to State 4, i.e., seas which occur the majority of the time. It must be noted that as far as the wave height indicated for Ship F is concerned, this is the height at which deck wetness of the lower catamaran hulls occurs at section L_C . This is not considered to be a condition which limits the operation of the ship. Ship responses which result in relative motions greater than this lower hull freeboard are inaccurate because the RAO computer programs assume that the basic above-water hull form is wall-sided. Thus relative bow motions are inaccurate, that is, computer predictions are larger than would be expected from model/full-scale experiments.

The ranking established by these performance-limiting wave heights tends to favor the monohulls for most combinations of performance measures and operating mode. The SWATH ships, however, have better in-transit performance both because they have lower in-transit accelerations and higher in-transit sea state capabilities. In other words, they can operate in higher seas for a given motion or acceleration response level. Based on the above considerations, Ship E is considered to be the ship with the best seakeeping characteristics.

Before we proceed to the time domain results, it should be noted that the above ranking of the candidate ships was obtained by equally weighting the responses at each modal wave period. This is not entirely realistic, of course, but ranking made on the basis of responses weighed by the frequency of occurrence of the particular modal period is beyond the scope of this limited project. It is recommended that such ranking be performed once the candidate ship type has been selected.

TIME DOMAIN RESULTS FOR SLAMMING AND DECK WETNESS

The number of times that relative motions can be expected to exceed either the draft at location L_C (see Figures 1, 2) or the available freeboard cross-structure clearance was calculated from the relative motion time histories for all ships. These head sea events were calculated for the yearly average seas with 6-foot significant wave height (see Reference 17).

Figure 12a indicates the likelihood that draft will be exceeded or that slamming will occur. The vertical lines represent the number of times that relative bow motions will exceed the draft at L_C for the various ships. It is evident from these results that only the small, presently employed workboat should experience difficulties in transiting 6-foot seas to the work site. Ship G, of course, also shows some keel emergences in these relatively mild seas.

Similar information on the likelihood of deck wetness is presented in Figure 12b. The extent of such wetness for the individual catamaran hulls is not considered to represent operational difficulties for Ship F. The presently used workboat (Ship A) appears to have some minor deck wetness at the transiting speeds. Again, all other ships are not likely to encounter deck wetness difficulties in these typical seas.

In the absence of reliable information on the levels of ship response that hinder workboat operation while in the stationkeeping mode, it is impossible to establish a comparison of the percentage and number of times that the individual ship candidates will exceed such values. It is recommended that operators of the present Navy workboat be questioned (1) as to what specific levels* of ship responses and (2) what *particular* ship responses most hinder their work while on station. Once such values are given, the productivity of the different workboat candidates can be readily established from the available stored time histories of ship response.

INFLUENCE OF DAMPING DEVICES ON SWATH RESPONSES IN HEAD SEAS

The zero speed pitch response of the SWATHs, especially Ship D, was regarded as potentially unsatisfactory because of the sharp increase in pitch as the modal sea period approached the natural pitch period. This pitch behavior near resonance is of concern not only because the zero speed behavior is potentially unsatisfactory but also because it suggests large pitch responses in sea conditions which contain sufficient energy at low frequencies near pitch resonance. Thus, the SWATH might incur very large pitch responses both in quartering and following seas at speeds which result in low frequencies of encounter as well as in swell. These large motions may unnecessarily limit the operational ship speed/heading.

Active fins would not be expected to provide sufficient pitch moment at zero speed to adequately reduce the potentially unsatisfactory pitch at resonance. At forward speed, of course, active fins can successfully limit the near-resonance motion behavior of SWATHs, as has been demonstrated with the U.S. Navy Semisubmerged Platform (SSP). The pitch and roll excitation moments are presented in Appendix B together with the heave excitation force per unit of wave height to enable estimates of comparative fin sizes.

* Such as ± 5 degrees of roll, ± 5 feet of relative bow motion, etc.

At any rate, active* fins are obviously a costly last resort and the addition of large bilge keels was considered to be the most practical method of modifying the zero-speed, near-resonance pitch. The effect of the additional damping on both pitch and heave was determined by recalculating the zero-speed pitch and heave in head seas. This recalculation was made by increasing the original bare hull damping coefficients by the same percent (percentage based on bare hull values) obtained from the measured damping increase due to large bilge keels. The damping experiments are briefly outlined in the section on calculation of roll.

The results of the recalculation are indicated in Table 7 which presents results for the 15-knot SWATH (Ship D) with and without bilge keels. In comparing the results with and without bilge keels, it must be recalled that these passive damping modifications are expected to influence responses only in the vicinity of resonance, i.e., in the area where the dynamic behavior of the SWATH is potentially unsatisfactory. A comparison of the pitch, heave, and vertical accelerations at the CG and—equally important—the relative bow motion at section L_C indicates quite clearly that substantial motions occur near resonance, i.e., the 10- and 14-second modal periods. More specifically, compared to base hull values, bilge keels provided a 23–33 percent reduction in pitch, a 5–10 percent reduction in heave, a 12-percent reduction in vertical accelerations at the CG, and a 6–22 percent reduction in relative bow motions. Clearly, the addition of large bilge keels can be expected to substantially improve the near-resonance motion (pitch) of SWATH Ship D. In fact, results suggest that the low-frequency, near-resonance motion responses may be satisfactorily controlled by means of passive damping devices.

INFLUENCE OF BILGE KEELS ON SHIP RESPONSES IN BEAM SEAS

Since Ship A, the presently employed workboat, is known to have less than satisfactory roll motion characteristics at low speeds, it was considered appropriate to evaluate the roll responses of the different candidate ships in beam seas. The monohull candidates were therefore evaluated with and without bilge keels. However, responses of the SWATH ships and the column-stabilized catamaran in the surfaced condition (i.e., as Ship F) were

* Automatically controlled such as antiroll fins.

calculated only with bilge keels; it was considered that the accuracy with which the effect of bilge keels could be predicted was too low to be of value for these types. The procedures employed have been briefly discussed in the section on calculation of roll. These calculations were not performed for Ship G because roll may be expected to be very small for this ship; moreover, it seems unlikely that it can be considered as a serious candidate for the PMR workboat.

Results of these zero-speed, beam-sea calculations are presented in Table 4 in terms of RMS responses in waves with a 6-foot significant height. Both RMS acceleration and roll values were calculated; these may be converted to significant values by multiplying them by two.

It is emphasized that significant improvements in ship responses can be expected only in seas whose modal periods approach resonance. It is evident that despite the improvement (16 to 17 percent) in monohull roll achieved near resonance, the SWATH roll is still less by an order of magnitude. Their superior behavior in roll and their lower acceleration levels should make the SWATHs better workboat candidates than are monohulls. This conclusion is premised on the belief that the difference in payload growth potential between the SWATHs and monohulls is not very important. In other words, the SWATHs are likely to be better workboats if they are not forced to carry payloads significantly greater than allowed for in the design.

On the basis of the foregoing seakeeping evaluations, the 20-knot SWATH is considered to be the best of the ship candidates. Economic factors, of course, did not enter into the seakeeping evaluation.

CONCLUSIONS AND RECOMMENDATIONS

The behavior of the candidate ships in waves up to 6 feet high is of primary importance in establishing comparative seaway performance. Consequently, their survival capabilities were not examined to any significant extent. The following conclusions are based on considerations of the environment of the intended worksite area.

1. SWATHs are better workboat candidates than monohulls from the seakeeping point of view.
2. In its present stage of development, the column-stabilized catamaran is the worst workboat candidate even though its survival capability appears to be the best of all.
3. The 20-knot SWATH is substantially better than the 15-knot SWATH primarily because of its superior in-transit performance in various sea conditions and its superior roll performance at low speed.

4. Monohulls have substantially better relative motions at low stationkeeping speeds than do SWATHs and thus are better suited for launch/retrieval of floating objects at minimum roll headings.

The following specific recommendations are made:

1. If a preliminary design of the best two candidate workboats is intended, then either Ships E and C or Ships D and E should be examined as the final two candidates.

2. The final two candidates should be evaluated in competitive model experiments.

3. This experimental evaluation should include (a) comparison of the candidates at zero speed in moderate head, bow, and beam seas (stationkeeping); (b) establishment of SWATH behavior in moderate quartering and following seas (low encounter periods); and (c) the survival characteristics of the candidates should be determined if the workboat must accomplish its mission in the open ocean without an option of returning to harbor in severe seas.

4. The load-carrying capacity of the SWATH should be improved by incorporating some of the pumping/ballasting features inherent in Ship F/G.

5. The use of large damping devices, such as bilge keels, is also recommended as an integral initial part of the preliminary SWATH ship design.

ACKNOWLEDGMENT

The authors would like to acknowledge the contribution made by Mr. Richard M. Curphey to this report for the computations of the transfer functions of the roll motion and the wave-exciting roll moment.

APPENDIX A

DEFINITION OF RELATIVE BOW MOTION

Relative bow motion (RBM) is defined as the difference between the absolute motion V_q and the wave r_q at some point (L_C or X_4) on the ship; see Figure A.1 and Figure 2.

RBM_q is calculated on the centerline of the ship with no allowances for trim and sinkage. Their neglect is not considered significant because both are small (trim less than 1 foot and sinkage less than 1 degree) for the monohulls at the low, stationkeeping speeds considered. Trim and sinkage increase with increasing ship speed and are most severe for the monohulls, particularly Ship A, the smallest. Even though trim and sinkage may exceed their stationkeeping values at design speeds, the values are still considered small enough so that the relative ranking of these ships is not affected. It may be assumed that at 0 and 5 knots, the SWATHs would operate at zero trim and sinkage and that at the higher speeds, the active or semiactive fins would maintain zero trim and only a slight sinkage or rise.

Figure A.1 presents a graphical definition of the relative bow motion and Figure A.2 summarizes the various motion components used to calculate the RBM. It may be seen that RBM is constructed from the wave at the origin r_0 . This value and those for heave and pitch motion of the ship at the origin were obtained by summing 100 component sine waves of amplitude r_{0k} and with phase γ_k , that is,

$$r_0(t) = \sum_{k=1}^{100} r_{0k} e^{i(\omega_E t + \gamma_k)} \quad (1)$$

where $\omega_E = \omega \frac{\omega^2}{g} V \cos \mu$

ω = circular frequency of the wave

V = ship speed

g = gravity

μ = ship heading relative to wave

The amplitudes of the component waves are modeled in accordance with the Bretschneider wave spectrum $S_\gamma(\omega)$ defined at 100 discrete frequencies, i.e., ω_k 's. In other words, r_{0k} is the mean square wave amplitude over the frequency interval $\Delta\omega$ with a center frequency ω_k given by

$$r_{0k} = \left[2 \int_{\omega_k - \Delta\omega/2}^{\omega_k + \Delta\omega/2} S_{\zeta}(\omega) d\omega \right]^{1/2} \quad (2)$$

and the wave spectrum $S(\omega)$ is

$$S_{\zeta}(\omega) = A\omega^{-5} e^{-[B/\omega^4]} \quad (3)$$

$$\text{where } A = 483.5 (\tilde{\zeta}_w)_{1/3}^2 / T_0^4$$

$$B = 1944.5 / T_0^4$$

$$(\tilde{\zeta}_w)_{1/3} = \text{significant wave height}$$

$$T_0 = \text{modal period of the Bretschneider wave spectrum } S(\omega)$$

The random phase γ_k associated with each sine wave of frequency ω_k is obtained by means of a random number generator.

In order to calculate r_{ρ} , the wave height at the location L_C or X_4 (see Figures A.1 and 2), the wave height at the origin r_0 is shifted by the product of the distance l from the origin X_4 and wave number ω^2/g , that is,

$$r_{\rho}(t) = \sum_{k=1}^{100} r_{0k} e^{i(\omega_E t + \omega^2/g l + \gamma_k)} \quad (4)$$

The time history of the response η is obtained from

$$\eta_j(t) = \sum_k^{100} \eta_{jk} e^{i(\omega_E t - \epsilon_{jk} + \gamma_k)} \quad (5)$$

Here $j = 3$ represents heave, $j = 5$ represents pitch, and η_{jk} , ϵ_{jk} represent the amplitude of response j and the associated phase at ω_k taken from the RAOs calculated by the first series of computer programs. The absolute motion at position L_C is

$$V_{\rho}(t) = \eta_3(t) + |l| \eta_5(t) \quad (6)$$

Finally at L_c , relative bow motion RBM_g becomes

$$RBM_g(t) = V_g(t) - r_g(t) \quad (7)$$

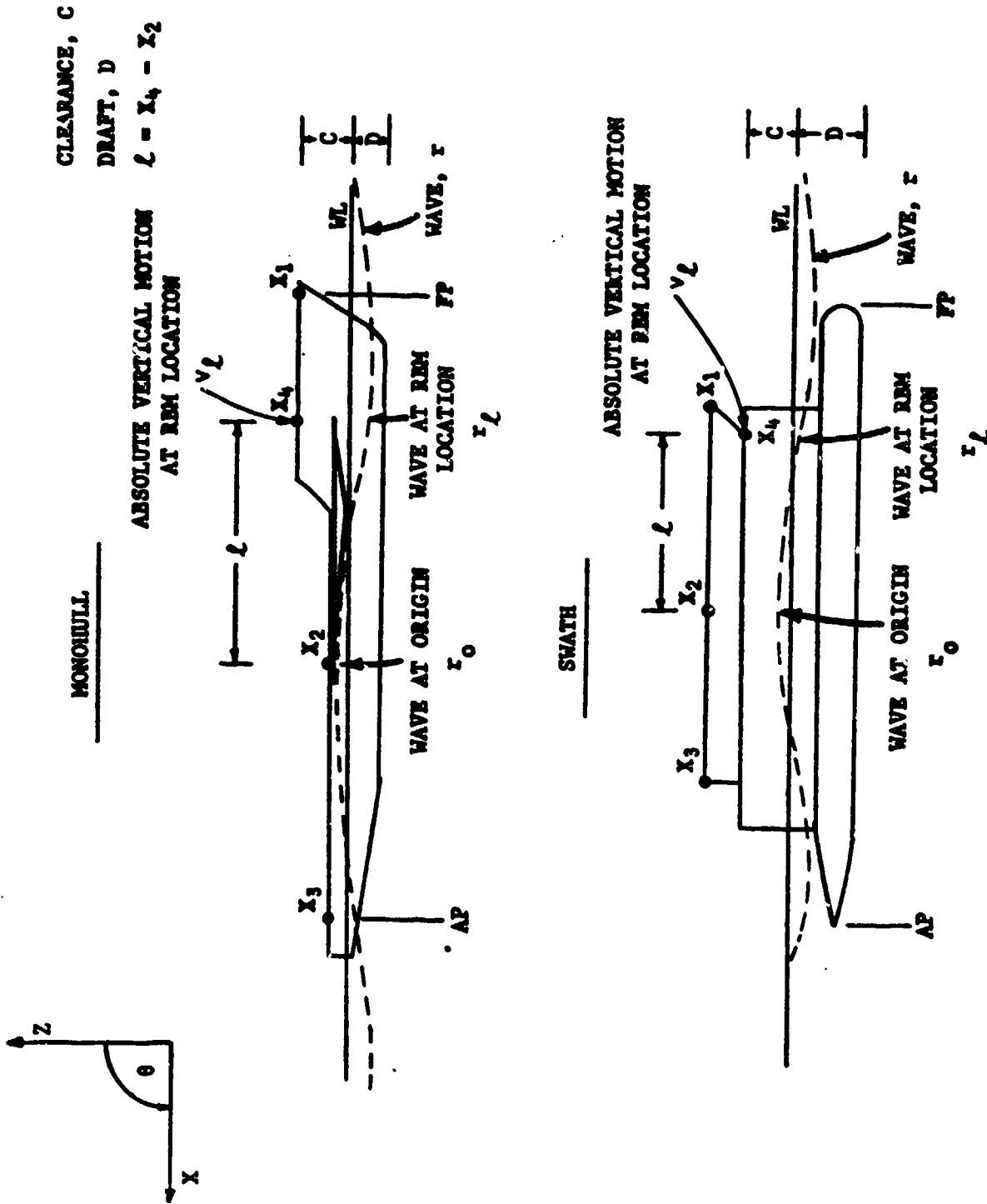


Figure A.1 - Definition of Relative Bow Motion on Snip Centerline

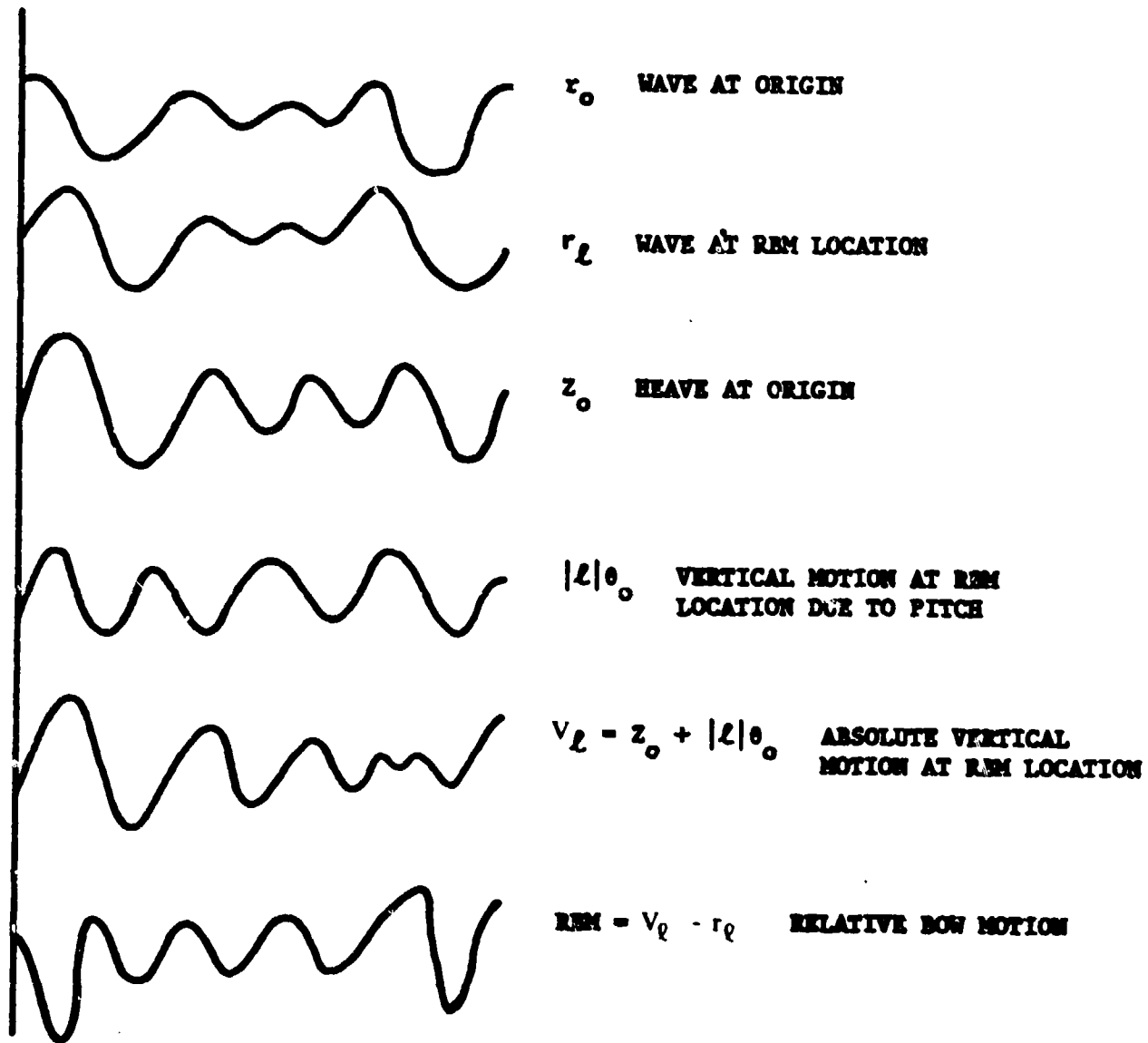


Figure A.2 - Summary of Relative Bow Motion Calculations

APPENDIX B

WAVE-EXCITING FORCES AND MOMENTS FOR WORKBOAT CANDIDATES AND FEASIBILITY OF ACTIVE FIN STABILIZERS

The wave-exciting forces and moments that act on the various workboat candidates are presented in graphical form (Figure B.1) in order (1) to provide data from which the feasibility of motion reduction by means of active fins can be established and (2) to illustrate some of the reasons for the basic differences in the responses of the various ship types.

The results of Figure B.1 are for excitation at zero speed in head (pitch and heave) and beam (roll) seas. Since the effect of forward speed on the magnitude of the wave excitations is small, the zero-speed excitations are considered to represent the excitations at all speeds insofar as fin feasibility and basic response characteristics are concerned.

Pitch and roll moments are given per unit of ship displacement times wave amplitude; heave force is given in the same units and then multiplied by ship length in feet. The waves which correspond to the resonance periods of roll and pitch are denoted by vertical lines labeled by ship type. Note that these resonance periods, or waves, correspond to the waves which produce the maximum ship response per unit of wave height as determined from the RAOs, i.e., roll in beam seas and pitch in head seas.

The basic reason for the differences in the responses of the low waterplane area ship candidates and the monohulls/catamarans is demonstrated by the location (frequency) of the maximum values of the wave excitations and the resonant ship response periods. Maximum values of the monohull and catamaran wave excitation moments tend to occur near the maximum value of the ship roll and pitch responses, i.e., near the resonance values labeled in Figure B.1; in contrast, wave excitations are quite small for the SWATH ship candidates in the vicinity of the resonant roll and pitch motions.

Before discussing the feasibility of active fins for ship motion reduction, it should be mentioned that ship responses depend on the magnitude of the wave excitations and their frequencies. Thus wave excitations at frequencies near the angular ship response resonances tend to produce large responses and those far removed from these motion resonances tend to produce small responses. Essentially, wave excitations are a function only of ship geometry and the waves. On the other hand, the location of motion resonances* (and thus the expected response magnitudes) depend on the load distribution (metacentric height (GM) and mass moment of inertia) of the ship once displacement and LCG have been fixed. Thus substantial reductions in motion may be realized if the load distribution can be altered sufficiently to

*SWATH motion resonance frequencies are also quite sensitive to waterplane area distribution.

move the resonant motion period from the peak of the wave excitation. For example, an increase in the roll period of Ship A from 1 to 1.5 seconds would reduce roll.

It is considered appropriate to develop fins which reduce ship motions that occur near the ship response resonances. Thus fins intended to reduce the heave and pitch of SWATHs should be designed for periods of around 12.5 seconds for Ship D and for about 17.4 seconds for Ship E. The forces generated by the fins must approach the magnitude of the wave excitations in order to reduce motion substantially. For purposes of this fin feasibility examination it may be assumed that the fins should provide a moment which exactly cancels the ship motions. This assumption will, of course, result in relatively large fins at the fin design conditions. Nevertheless, the fin sizes that can be developed on the basis of this assumption will establish the appropriate relative ranking for motion stabilizers for the various workboat candidates. It is evident from Figure B.1 that the wave excitations for monohulls and catamarans are very much larger than for SWATHs.

The feasibility of motion stabilization is now demonstrated by considering the non-dimensional roll and pitch wave excitations at resonance for Ships C, E, and F:

	Ship C	Ship E	Ship F
Pitch Moment	4.2	0.13	2.25
Roll Moment	0.19	0.06	0.55

We convert these pitch moments into forces (tons) by locating the fins, say, $0.4 L_{pp}$ from the LCG. Similarly, we convert the roll moments into forces (tons) by locating the fins rather arbitrarily at a certain distance from the centerline: 1.2 times the draft for Ships C and E and 24 feet for Ship F. The following forces result:

	Ship C	Ship E	Ship F
Pitch, tons	38.9	2.1	34.2
Roll, tons	11.7	3.2	23.6

These are wave excitation forces per foot of wave amplitude that stabilizers must provide in order to completely cancel the ship motions due to waves.

Now assume a fin design speed of 15 knots and select 0.040 lift curve slopes per degree of fin angle, as obtained from some typical full-scale roll fin experiments.²¹ The resulting total sizes for fin travel-limited to ± 28 degrees is given below for seas with a significant wave height of 6 feet. (The limit of ± 28 -degree fin angle was taken from the fin limits employed on the Vosper fins installed on the U. S. Navy PG 100; see Reference 21.)

	Ship C	Ship E	Ship F
Pitch, feet ²	363	20	319
Roll, feet ²	110	30	235

On the basis of these preliminary fin area results as well as the sizes of roll fins installed on monohulls, it is concluded that pitch stabilization is impractical for monohulls and catamarans. In other words, pitch reduction to zero by means of fins in 6-foot significant seas is impractical though not impossible. On the other hand, pitch and roll reduction appears to be quite practical for the SWATH ship. Finally, stabilization of the monohull to zero roll in 6-foot beam seas is also somewhat impractical although much less so than is true for the catamarans. It should be noted that for adequate conventional roll stabilization, fin size for Ship C can be reduced to about 60 square feet.

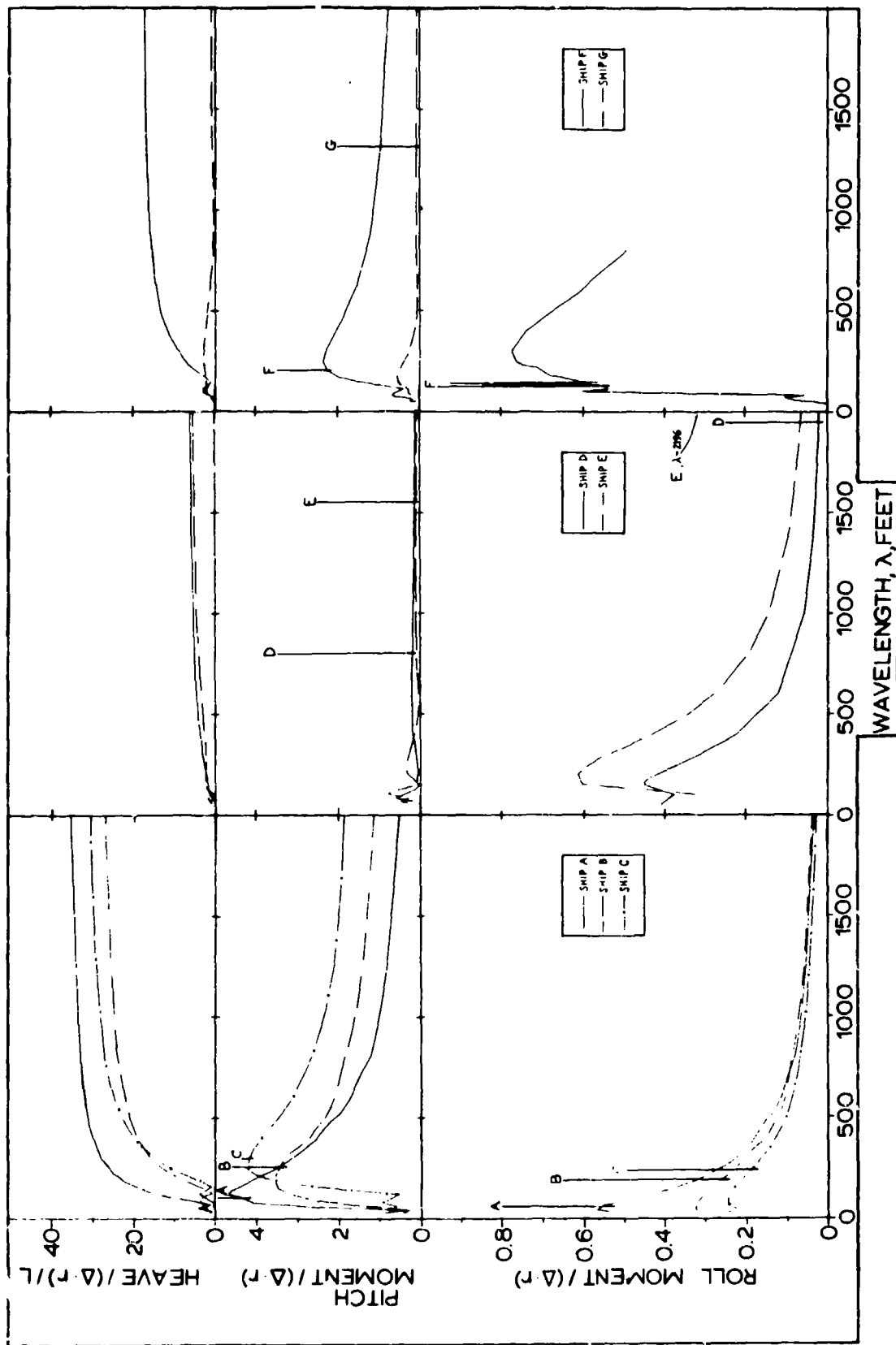


Figure B.1 — Wave-Exciting Forces and Moments for the Ship Candidates

REFERENCES

1. Meyers, W. G. et al., "Manual NSRDC Ship Motion and Sea Load Computer Program," NSRDC Report 3376 (Feb 1975).
2. Salvesen, N. et al., "Ship Motions and Sea Loads," Trans. SNAME, Vol. 78, pp. 250-287 (1970).
3. Frank, W. and N. Salvesen, "The Frank Close-Fit Ship-Motion Computer Program," NSRDC Report 3289 (1970).
4. Jones, H. D., "Catamaran Motion Prediction in Regular Waves," NSRDC Report 3700 (1972).
5. Zarnick, E. E. and J. A. Diskin, "Modeling Techniques for the Evaluation of Anti-Roll Tank Devices," Third Ship Control Symposium, Bath, England (Sep 1972).
6. Withrington, J. K., "Analytical Methods for Verifying the Structural Integrity of LNG Carriers," Third International Conference on Liquefied Natural Gas, Washington, D. C. (Sep 1972).
7. Baitis, A. E. et al., "LNG Cargo Tanks: A Ship Motions Analysis of Internal Dynamic Loadings," GASTECH 74, International LNG and LPG Congress, Amsterdam (Nov 1974).
8. Pierson, J. W. and L. Moskowitz, "A Proposed Spectral Form for Fully Developed Wind Seas Based on the Similarity Theory of S. S. Kitaigorodskii," J. Geophys. Res., Vol. 69, No. 24 (1964).
9. Hadler, J. B. and T. H. Sarchin, "Seakeeping Criteria and Specifications," SNAME Seakeeping Symposium, Webb Inst Nav Arch, Glen Cove, N. Y. (Oct 1973).
10. Baitis, A. E. et al., "Design Acceleration and Ship Motions for LNG Cargo Tanks," Tenth Symposium on Naval Hydrodynamics (Jun 1974).
11. Cummins, W. E., "Prediction of Seakeeping Performance," 17th American Towing Tank Conference State of the Art Report - Seakeeping, Pasadena, California (Jun 1974).
12. Hoffman, D., "Analysis of Measured and Calculated Spectra," International Symposium on the Dynamics of Marine Vehicles and Structures in Waves, University College, London (Apr 1974).
13. Hoffman, D., "Environmental Condition Representation," 17th American Towing Tank Conference State of the Art Report - Seakeeping, Pasadena, California (Jun 1974).
14. Bretschneider, C. L., "Wave Variability and Wave Spectra for Wave Generated Gravity Waves," Department of the Army, Corps of Engineers Technical Memorandum 118 (1959).

15. Pore, N. A. et al., "Wave Climatology for the Great Lakes," Nat. Ocean Atmosp. Admin. Technical Memorandum NWS TDL-40 (Feb 1971).
16. Ploeg, J., "Wave Climate Study Great Lakes and Gulf of St. Lawrence," SNAME T & R Bulletin 2-17 (1971).
17. St. Denis, M., "The Winds, Currents, and Waves at the Site of the Floating City Off Waikiki," Univ. Hawaii Report 7 (Dec 1974).
18. Homer, P. S., "Characteristics of Deep Water Waves in Oahu Area for a Typical Year " Report prepared by Marine Advisers, LaJolla, California, for Board of Commissioners, State of Hawaii under Contract 5772 (1964).
19. Ho, F. P. and L. A. Sherretz, "A Preliminary Study of Ocean Waves in the Hawaiian Area," Univ. Hawaii, Hawaii Inst. Geophys. Report H 16-69-16 (1969).
20. Salvesen, N., "A Note on the Seakeeping Characteristics of Small-Waterplane-Area-Twin-Hull Ships," Paper Presented at Advance Marine Vehicles Meeting, Annapolis, Maryland; J. Hydromech., Vol. 7, No. 1, pp. 3-10 (Jan 1973).
21. Baitis, A. E. et al., "The Evaluation of Active Fin Roll-Stabilizers," Third Ship Control Symposium, Bath, England (Sep 1972).

SHIP DESCRIPTION	MONOHULLS				SMATH			COLUMN STABILIZED		
	SHIP A 85 FOOT HARDCHINE	SHIP B 15 KNOT	SHIP C 20 KNOT	SHIP D 15 KNOT	SHIP E 20 KNOT	SHIP F SURFACED	SHIP G SUBMERGED			
HULL FORM AT SECTION L _C										
LENGTH (FT.)	85	160	200	155	200	170	170	170	170	
BEAM AT L _C (FT.)	9.5	19.1	16.5	49.5	53.5	64.0	64.0	64.0	64.0	
DRAFT (FT.)	3.77	8.0	9.35	16.5	19.4	12.5	12.5	24.0	24.0	
CLEARANCE (FT.)	6.82	18.0	17.65	12.0	12.1	4.2	4.2	12.0	12.0	
L _C (FT.)	17.0	32.0	40.0	30.0	41.44	14.4	14.4	14.4	14.4	
B (FT.) } SEE FIG. 4	7.5	10.0	10.0	25.0	27.0	35.0	35.0	35.0	35.0	
DISPLACEMENT (L.T.)	74	565	741	785	1286	1032	1032	1614	1614	
DESIGN SPEED (KT.)	20	15	20	15	20	15	15	5	5	
TOTAL PROJECTED FIN OR BILGE KEEL AREA (SQ. FT.)	--	192	240	AFT 240 FWD 60	AFT 318 FWD 80	--	--	--	--	
WATERPLANE AREA (SQ. FT.)								1162	3783	690
G _L (FT.)	--	216.0	--	20.0	20.0	150.7	150.7	14.2	14.2	
G _T (FT.)	5.3	3.6	4.0	4.0	4.0	85.4	85.4	2.24	2.24	
I _Z (SEC.)	4.7	4.4	4.8	6.6	8.5	4.3	4.3	14.4	14.4	
I _φ (SEC.)	3.4	6.1	6.8	19.5	20.7	5.0	5.0	--	--	
T _θ (SEC.)	4.5	7.1	7.7	12.5	17.4	6.3	6.3	16.0	16.0	

Figure 1 - Ship Particulars

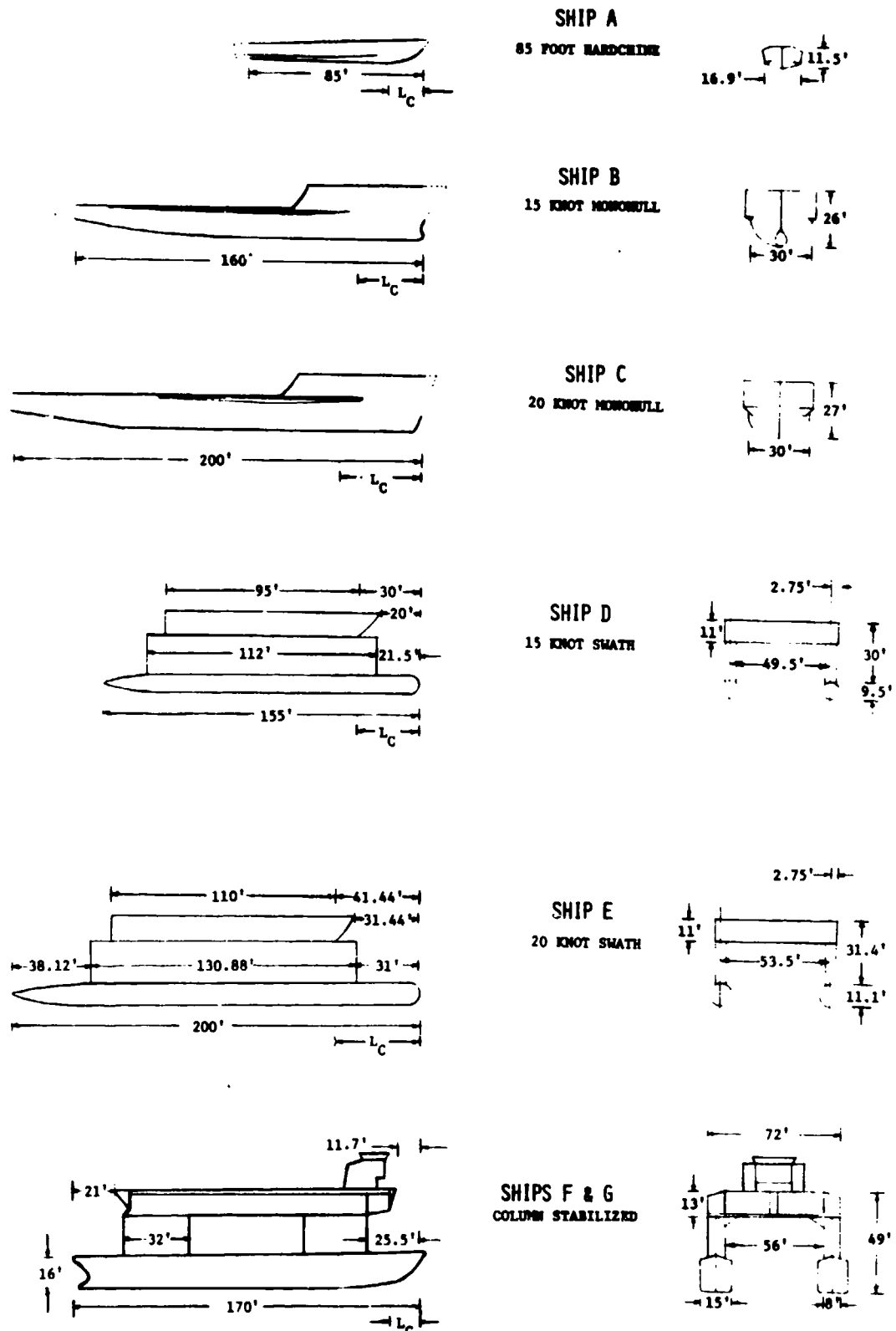


Figure 2 - Comparison of Candidate Ship Types

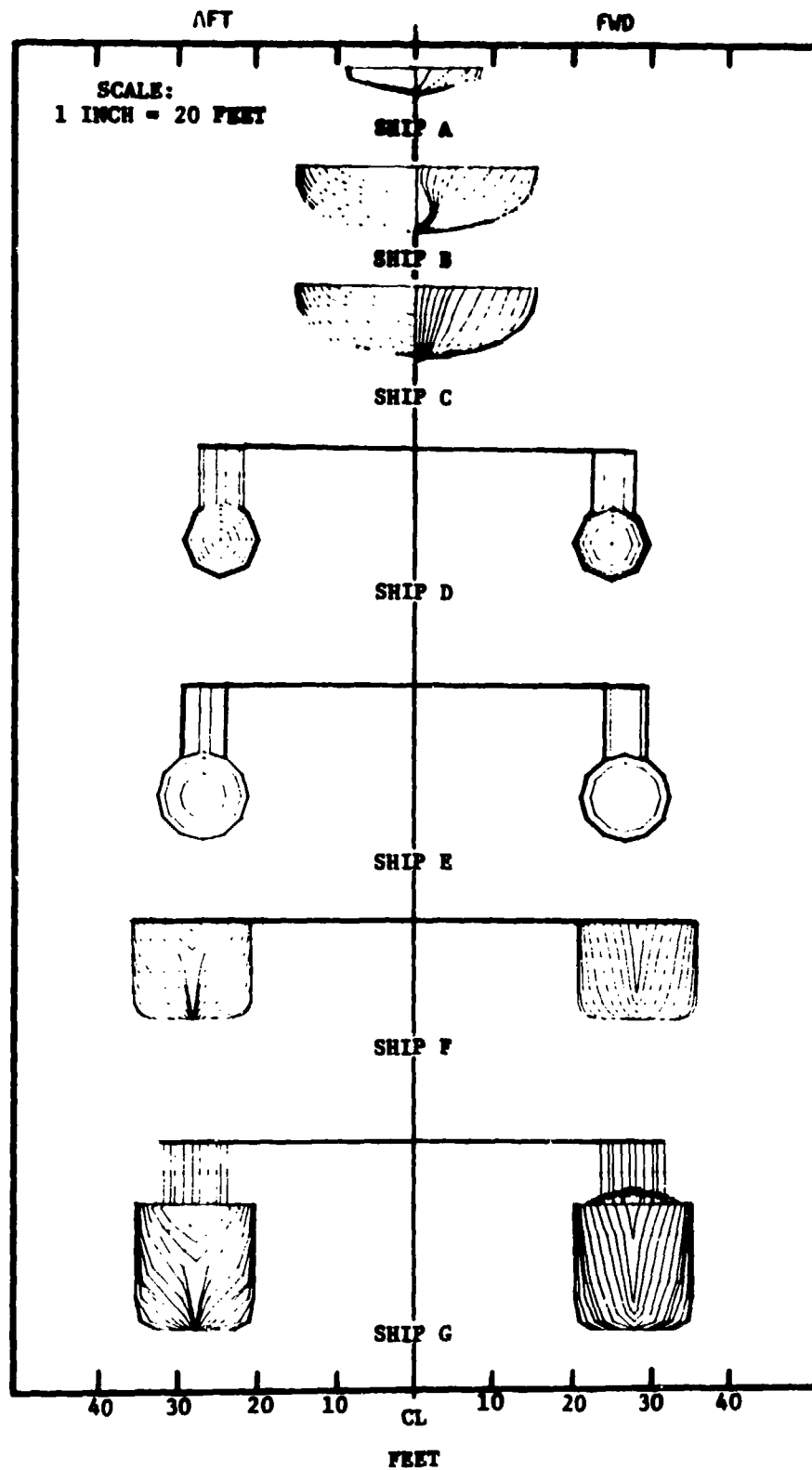


Figure 3 - Computer Fit of Body Plans for Candidate Ship Types

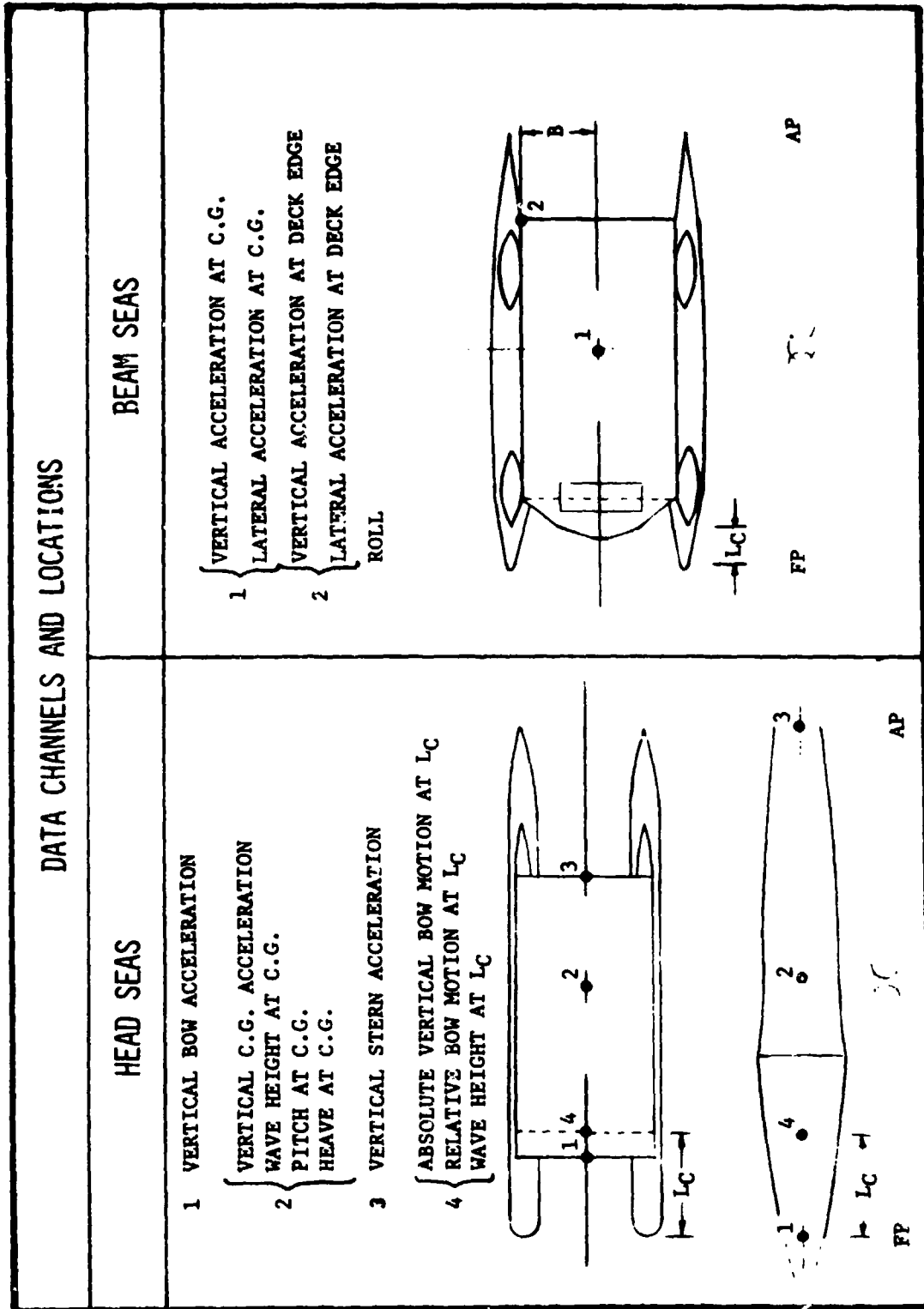


Figure 4 - Data Channels and Ship Locations for Which Responses Calculated

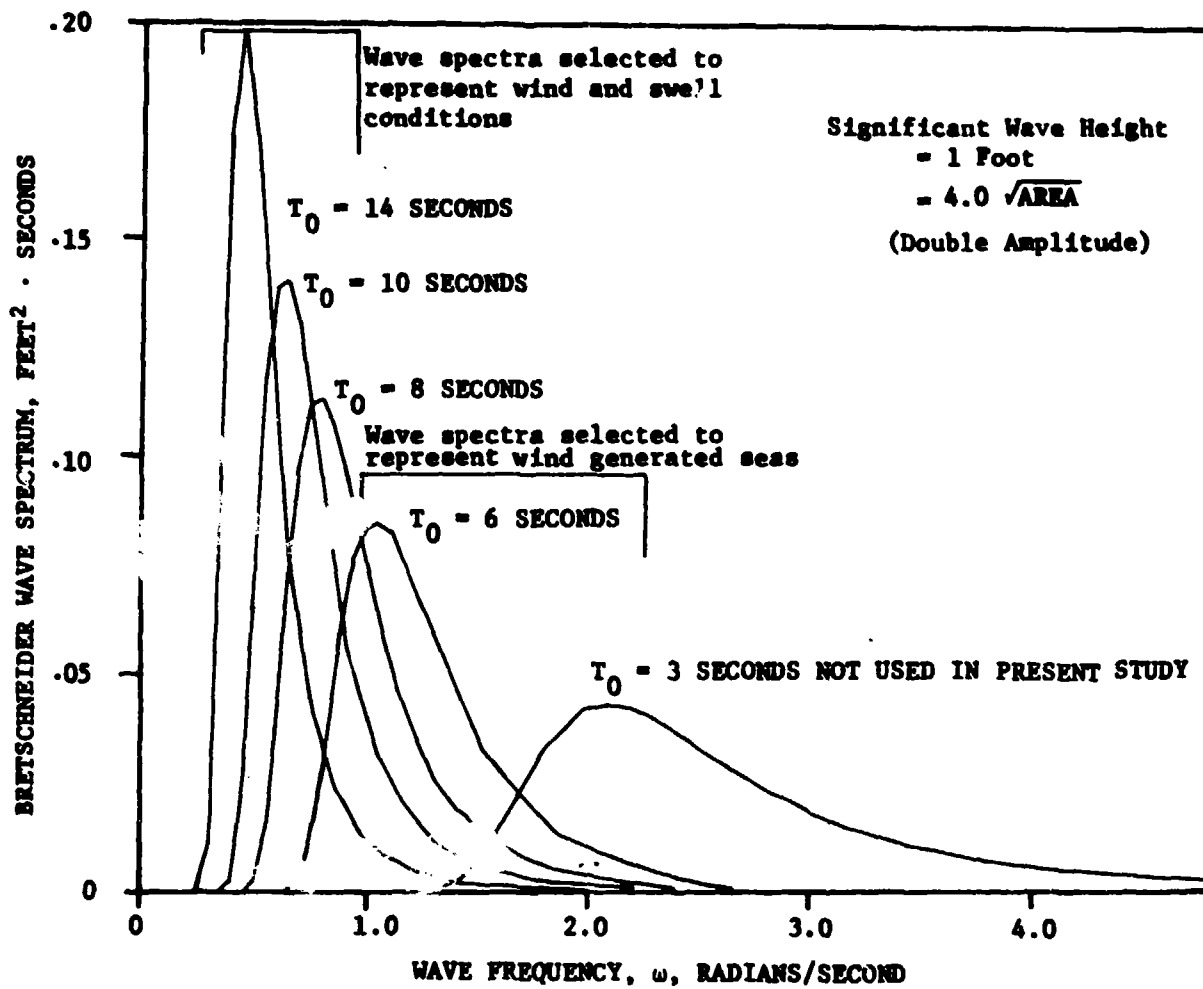


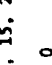






Figure 5 - Theoretical Spectra Used to Represent Sea Conditions

SHIP DESCRIPTION	MONOHULLS				SHATH			COLUMN STABILIZED	
	SHIP A 55 FOOT BUCARINE	SHIP B 15 KNOT	SHIP C 20 KNOT	SHIP D 15 KNOT	SHIP E 20 KNOT	SHIP F SURFACED	SHIP G EMERGED		
HULL FORM AT SECTION L _C									
HULL DAMPING CONDITIONS	WITHOUT BILGE KEELS	WITH AND WITHOUT BILGE KEELS	WITH AND WITHOUT BILGE KEELS	WITH FINS WITH AND WITHOUT BILGE KEELS	WITH FINS	WITHOUT DAMPING PLATES	WITHOUT DAMPING PLATES		
SPEED (KNOTS) (180°) (90°)	0, 5, 15, 20 0	0, 5, 15 0	0, 5, 15, 20 0	0, 5, 15 0	0, 5, 15, 20 0	0, 5, 15, 20 0	0, 5 MA		
HEADINGS (DEGREES)	180, 90	180, 90	180, 90	180, 90	180, 90	180, 90	180		
MODAL PERIODS (SECONDS) SEA STATE SIGNIFICANT WAVE HEIGHTS (FEET)	6, 8, 10, 14 2, 4, 6	6, 8, 10, 14 2, 4, 6	6, 8, 10, 14 2, 4, 6	6, 8, 10, 14 2, 4, 6	6, 8, 10, 14 2, 4, 6	6, 8, 10, 14 2, 4, 6	6, 8, 10, 14 2, 4, 6	6, 8, 10, 14 2, 4, 6	6, 8, 10, 14 2, 4, 6

180° = HEAD SEAS
90° = BEAM SEAS

Figure 6 - Summary of Calculation Conditions

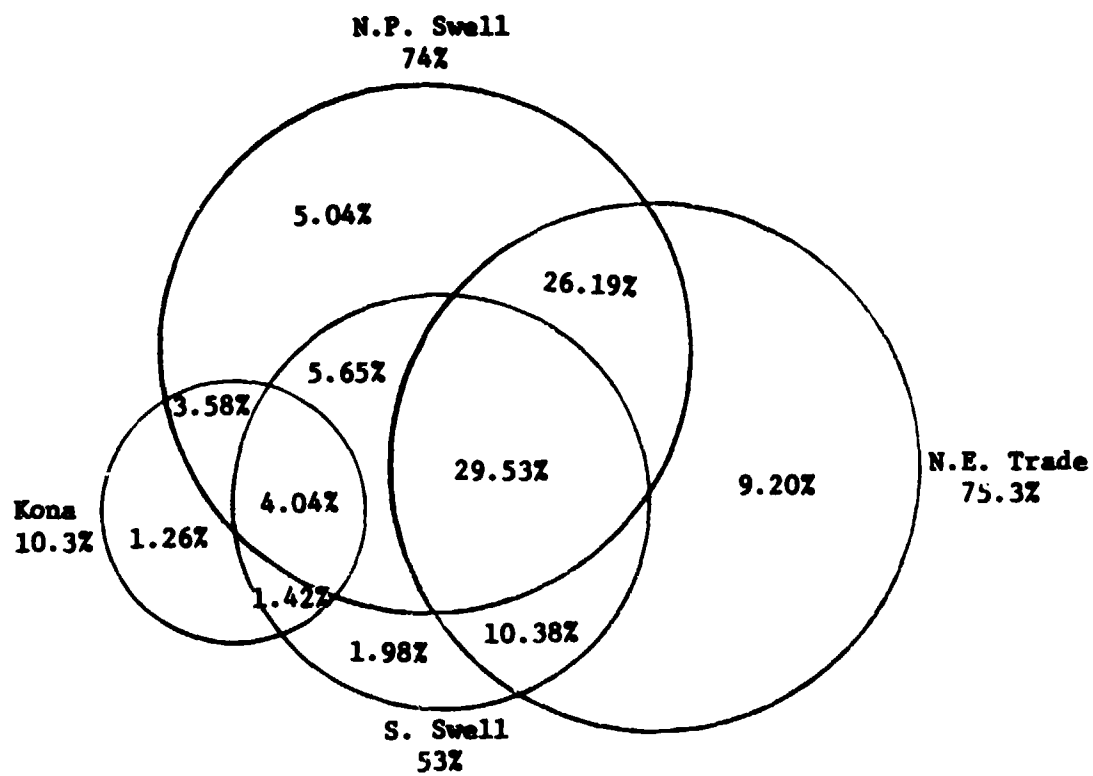


Figure 7 - Relative Frequencies at Which Individual Wave Systems or Combined Systems Occur

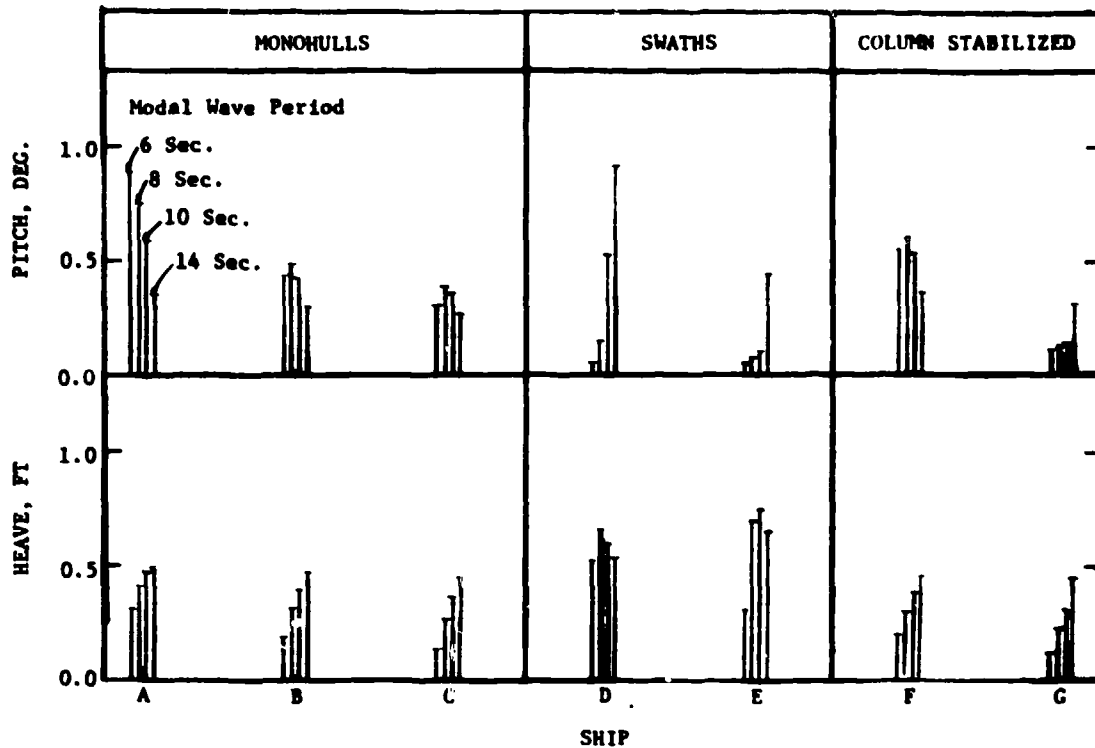


Figure 8a - At 0 Knots

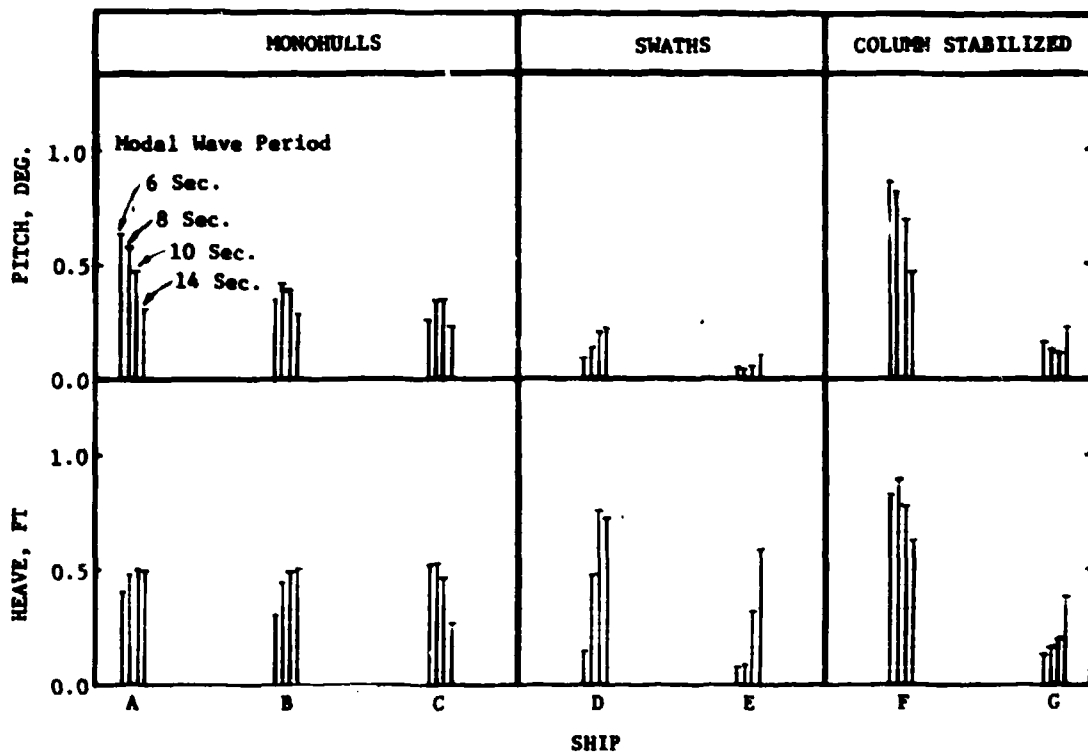


Figure 8b - At Design Speeds

Figure 8 - Influence of Modal Sea Period on the Significant Single Amplitude Pitch and Heave of Ship Candidates

(In seas with 1-foot significant wave height)

Figure 9 - Influence of Modal Sea Period on the Significant Single Amplitude Relative Bow Motion and Vertical Accelerations of the Ship Candidates

(Data for three positions on the centerline in seas with 1-foot significant wave height)

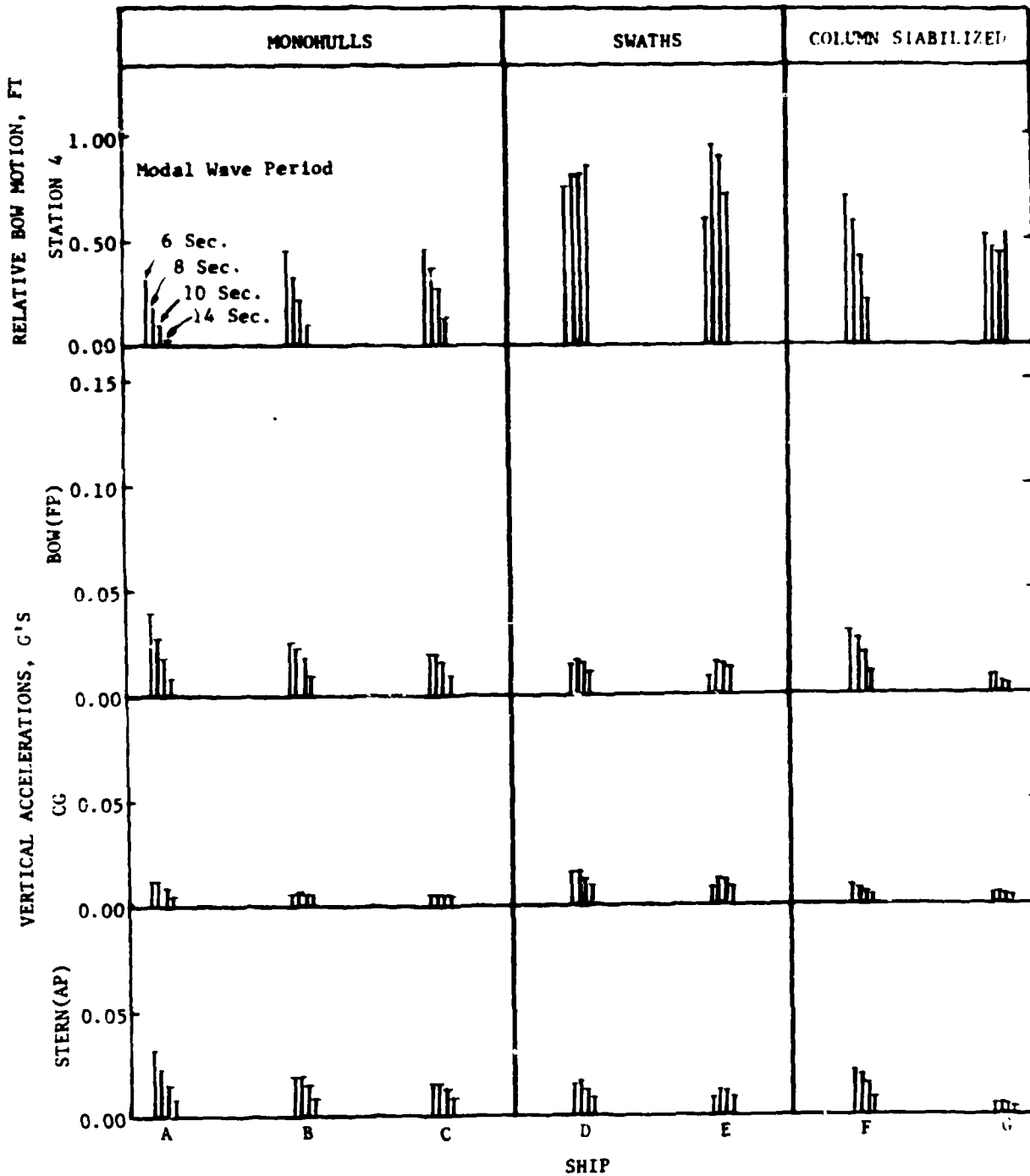


Figure 9a - At 0 Knots

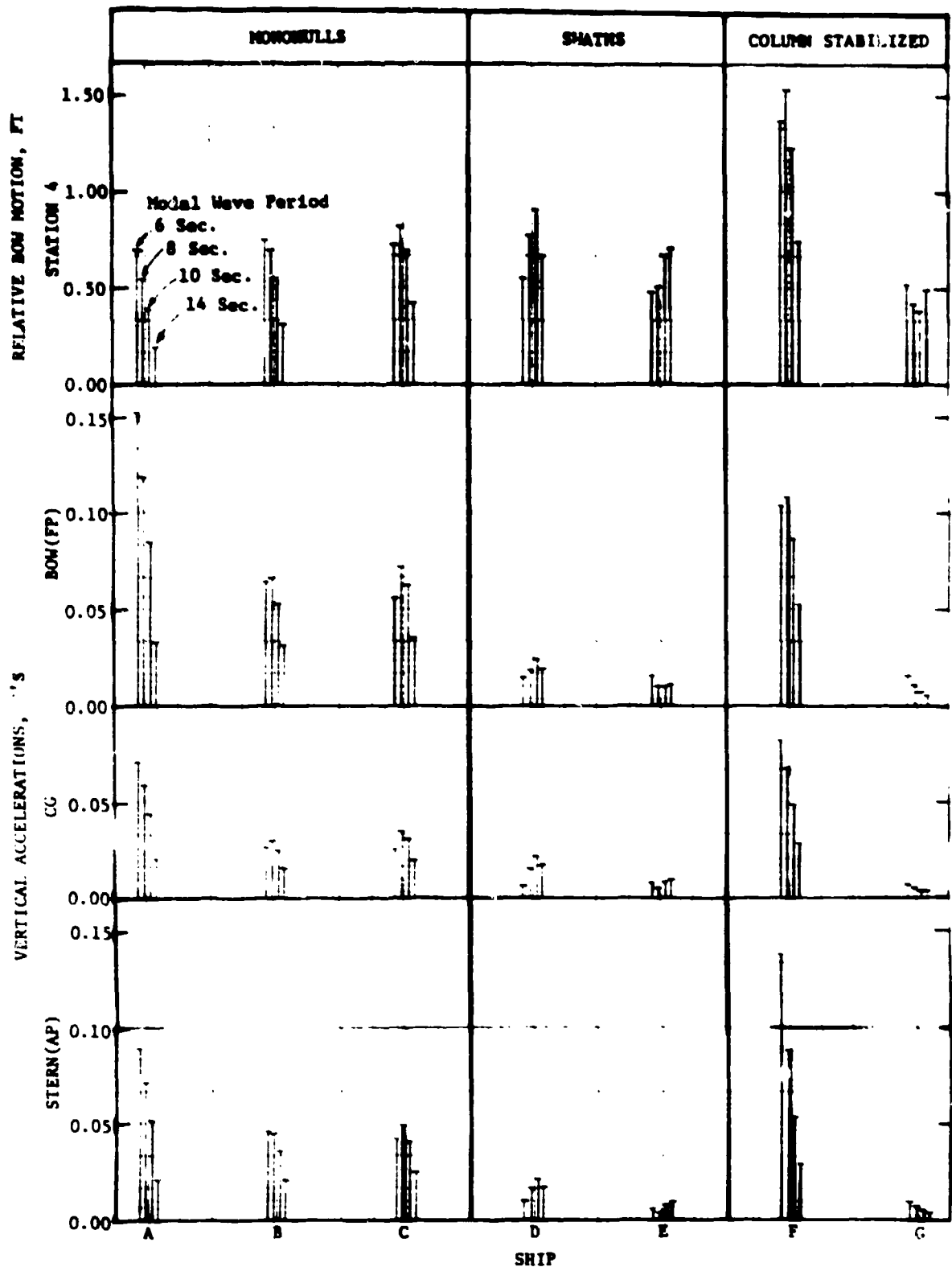


Figure 9b - At Design Speeds

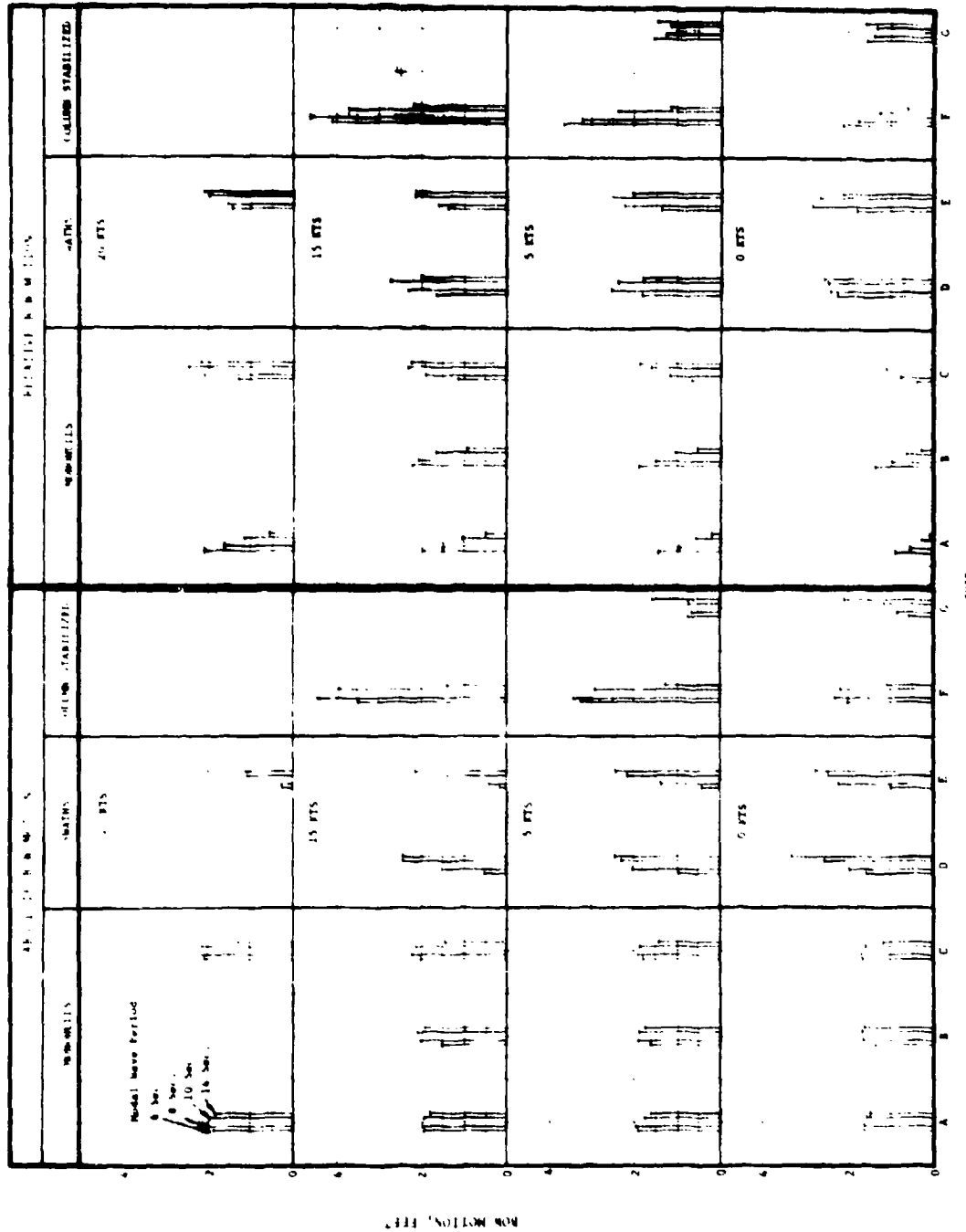


Figure 10 - Influence of Ship Speed and Modal Sea Period on the Significant Single Amplitude Relative Bow Motion and Comparable Absolute Vertical Motion of the Candidate Ships
 (In seas with 6-foot significant wave height)

Figure 11 - Influence of Ship Speed and Modal Sea Period on Significant Wave Height Levels Critical for Various Ship Candidates

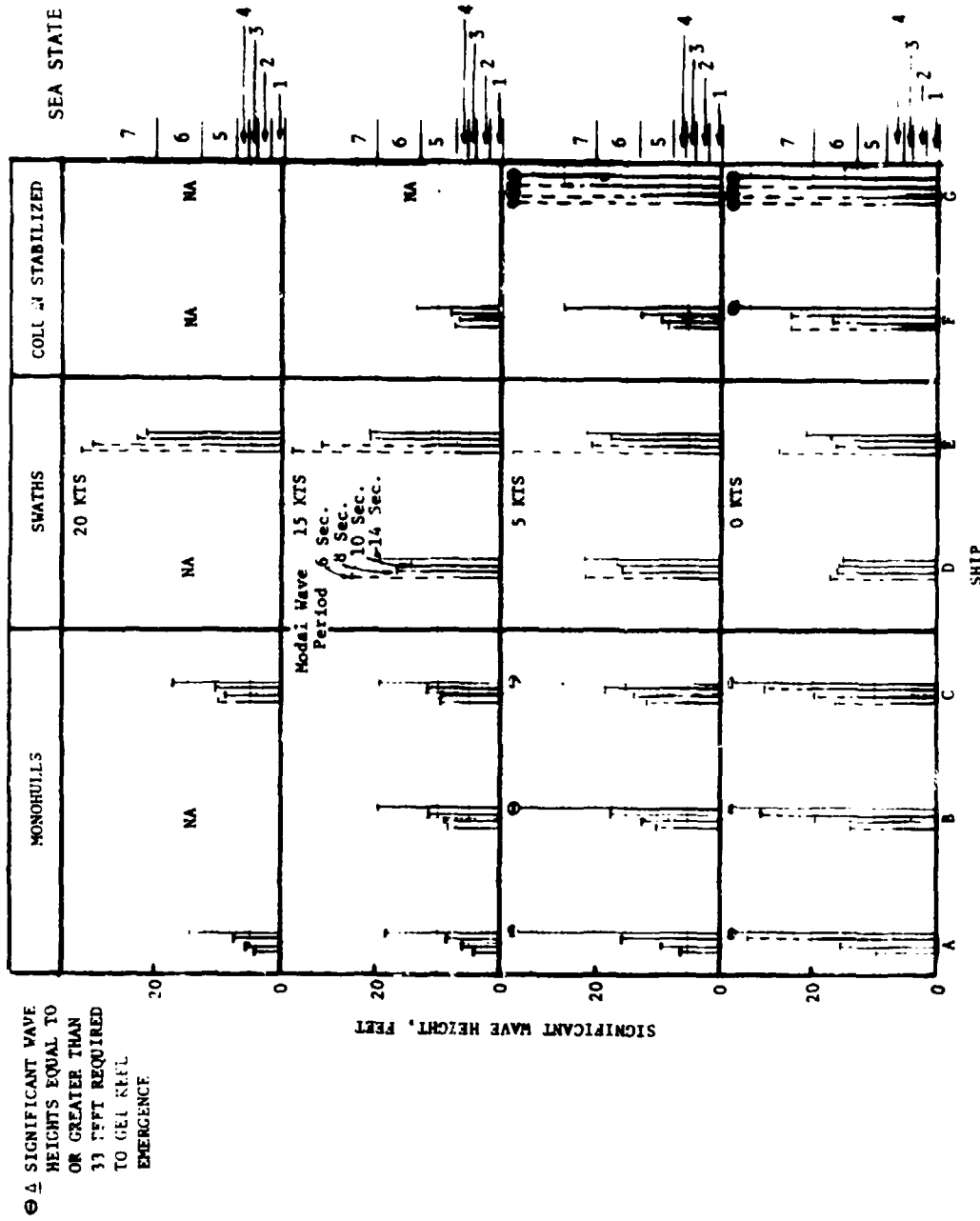
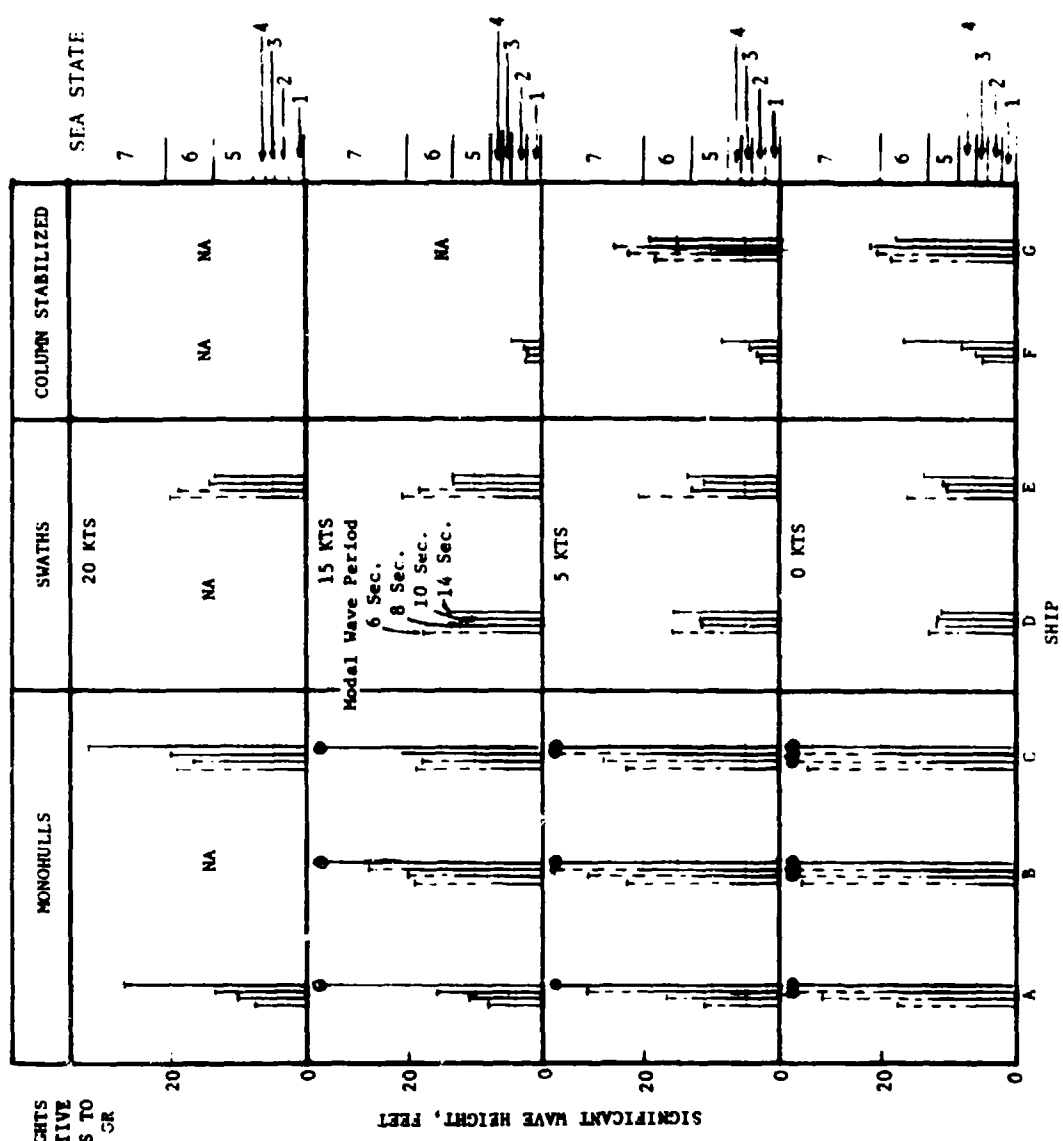


Figure 11a - Level at Which Average 1/10 Highest Relative Bow Amplitudes Exceed Ship Draft



Δ SIGNIFICANT WAVE HEIGHTS
 REQUIRED TO GET RELATIVE
 BOW MOTION AMPLITUDES TO
 EXCEED THE FREEBOARD OR
 THE CROSS STRUCTURE
 CLEARANCE

Figure 11b - Levels at Which Average 1/10 Highest Relative Bow Motion Amplitudes
 Exceed the Freeboard or Above-Water Clearance to the Hull Cross Structure

Figure 12 - Influence of Ship Speed and Modal Sea Period on the Mission-Interrupting Events

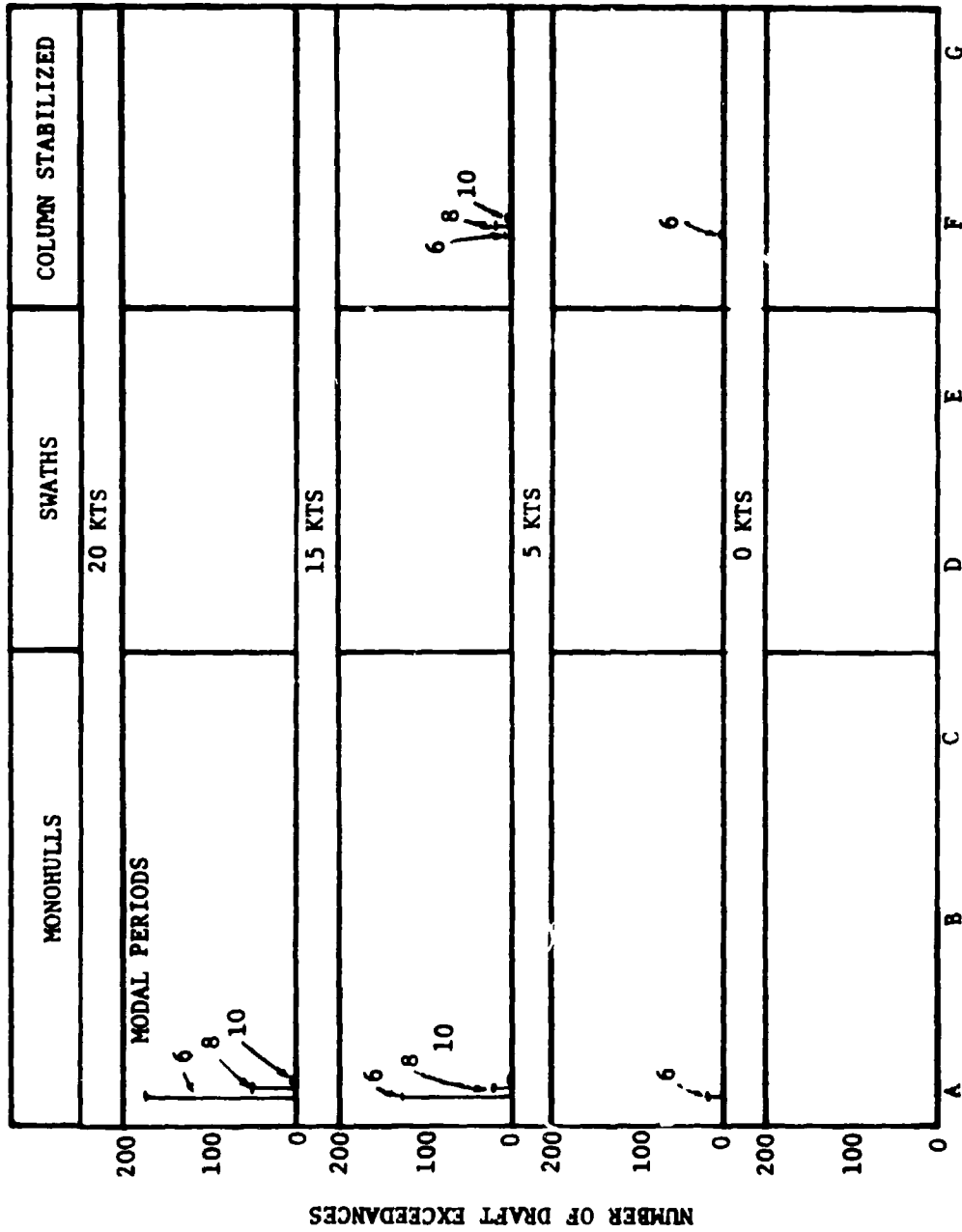


Figure 12a - Number of Slams per 30 Minutes of Operation in 6-Foot Significant Wave Height Seas

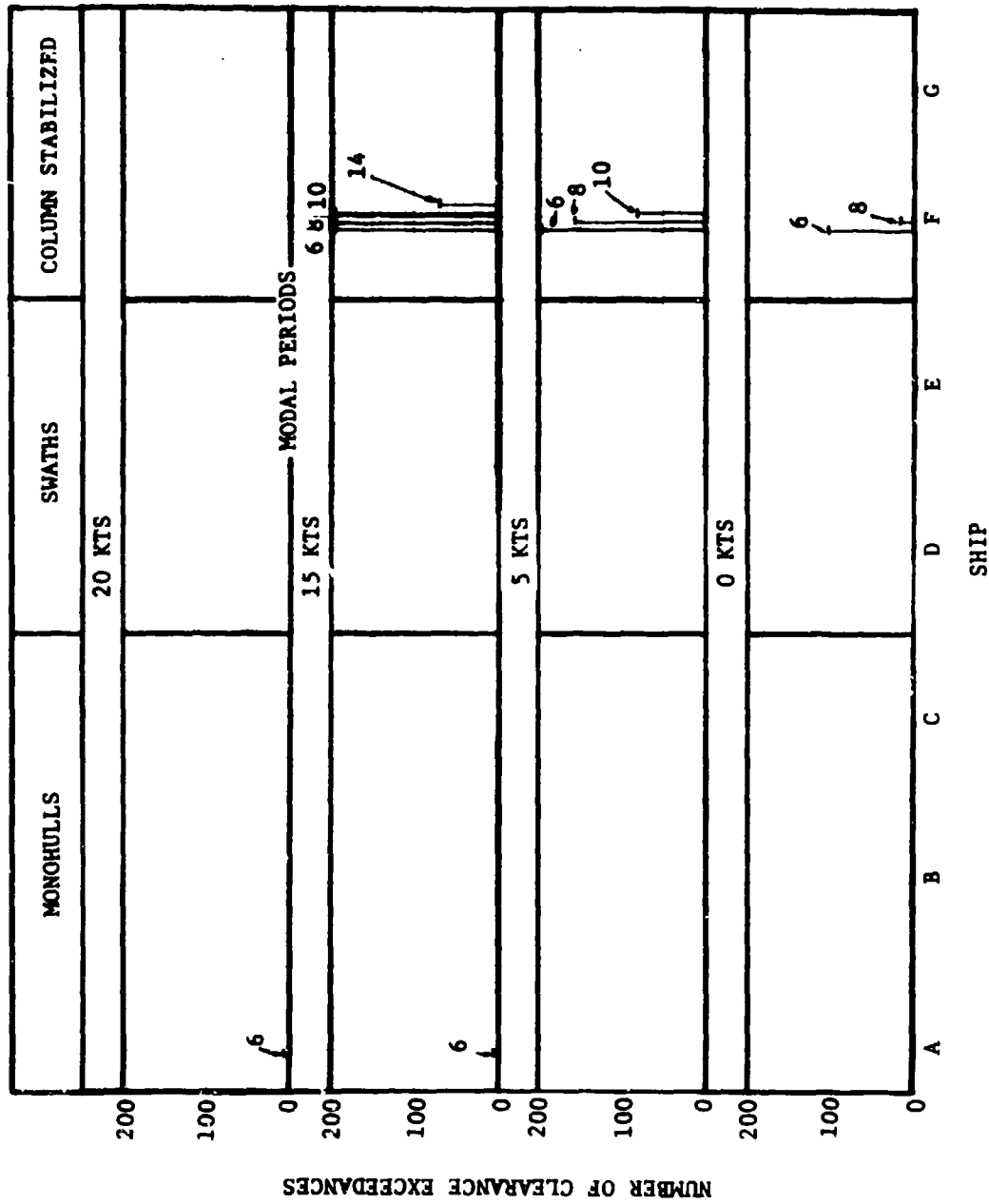


Figure 12b - Number of Deck Wetness Occurrences or Cross-Structure Impacts per 30 Minutes of Operation in 6-Foot Significant Wave Height Seas

TABLE 1 – DEFINITION OF SEA STATES

State	Ranges of Significant Wave Heights $(\tilde{\xi}_w)^{1/3}$ ft	Ranges of Modal Wave Periods T_0 sec
1	0 – 1.92	0 – 3.08
2	1.92 – 4.13	3.08 – 4.52
3	4.13 – 5.66	4.52 – 5.29
4	5.66 – 7.35	5.29 – 6.03
5	7.35 – 13.04	6.03 – 8.03
6	13.04 – 20.80	8.03 – 10.15
7	20.80 – 40.33	10.15 – 14.13
8	40.33 – 61.58	14.13 – 17.45

NOTE: 1. T_0 periods corresponding to the steepest, partially developed wind-generated waves, short fetch, high wind, moving hurricane, Bretschneider Reference 14.
 2. Steeper waves do occur, but they are rare and are generally associated with land locked bays or lakes, References 15 and 16.
 3. $T_0 = [(\tilde{\xi}_w)^{1/3} / 0.202]^{1/2}$ Modal period of partially developed hurricane sea (Bretschneider).
 4. $T_0 = [(\tilde{\xi}_w)^{1/3} / 0.127]^{1/2}$ Modal period of fully developed wind sea (Pierson-Neumann-James).
 5. $\lambda_0 / (\tilde{\xi}_w)^{1/3} = 1/40$ Pierson-Moskowitz wave spectra, i.e., (4)
 6. $\lambda_0 / (\tilde{\xi}_w)^{1/3} = 1/25$ Bretschneider, i.e., (3)
 7. $\lambda_0 / (\tilde{\xi}_w)^{1/3} = 1/10$ Steepest observed, Hogben and Lumb Reference

λ_0 = Wavelength corresponding to period of spectrum peak, T_0

TABLE 2 – CONSTANTS FOR SINGLE-AMPLITUDE STATISTICS AND EQUATION FOR TWO-PARAMETER BRETSCHNEIDER SPECTRUM

<u>SINGLE AMPLITUDE STATISTICS</u>		<u>BRETSCHNEIDER SPECTRUM $S_f(\omega)$</u>	
Root mean square amplitude, rms	1.00 σ	$S_f(\omega) = A\omega^{-5} \exp [-B/\omega^4]$ in ft ² /sec	
Average amplitude	1.25 σ	A = 483.5 $(\tilde{\zeta}_w)_{1/3}^2 / T_0^4$, ft ² sec ⁻⁴	
Average of highest 1/3 amplitudes, significant	2.00 σ	B = 1944.5 / T_0^4 , sec ⁻⁴	
Highest expected amplitude in 10 successive amplitudes	2.15 σ	$(\tilde{\zeta}_w)_{1/3}$ = Average of highest 1/3 wave heights	
Average of highest 1/10 amplitudes	2.55 σ	T_0 = Modal period of spectrum, i.e., period corresponding to peak of spectrum	
Highest expected amplitude in 30 successive amplitudes	2.61 σ		
Highest expected amplitude in 50 successive amplitudes	2.80 σ		
Highest expected amplitude in 100 successive amplitudes	3.03 σ		
Highest expected amplitude in 200 successive amplitudes	3.25 σ		
Highest expected amplitude in 1000 successive amplitudes	3.72 σ		

DEFINITIONS

σ^2 = Statistical variance of time history

N = Number of successive amplitudes

CONSTANT = $\sqrt{2} (\ln N)^{1/2}$, where CONSTANT relates σ to the highest expected amplitude in N successive amplitudes.

NOTES:

1. The highest expected amplitude in N amplitudes is the most probable extreme value in N amplitudes. This value may be exceeded 63 percent of the time.
2. To obtain wave height or double amplitude statistics from rms values, multiply single amplitude constants by 2.0.

**TABLE 3 – YEARLY AVERAGE STATISTICS OF FOUR MAJOR
HAWAIIAN WAVE SYSTEMS**

(From St. Denis¹⁷)

Wave Group	Direction of Origin deg true	Average Significant Height ft	Average Significant Period sec	Frequency of Occurrence percent
NE trade wind- generated waves	78	4.79	8.63	75.3
North Pacific swell	320	4.79	13.89	74.0
Kona Storm waves	187	3.52	6.18	10.3
Southern swell	194	2.60	13.07	53.0

TABLE 4 - RMS RESPONSES OF SHIP A, 85-FOOT HARDCHINE MONOHULL

T ₀ SEC.	HEAD SEAS H1/3 = 6. FEET CHANNEL	LPP = 85.0 FEET CLEARANCE, C = 6.87 FEET DRAFT, D = 3.77 FEET			
		SPEEDS			
		0. KTS	5. KTS	15. KTS	20. KTS
6	WAVE HEIGHT AT ORIGIN	1.43532	1.43685	1.43517	1.43801
	WAVE HEIGHT AT STA. 4	1.43535	1.43753	1.43517	1.43832
	HEAVE	.90941	.92588	1.18784	1.23011
	PITCH	2.64230	2.47992	2.04841	1.84970
	VERT. MOT. AT STA. 4	1.64730	1.69017	1.94914	1.87705
	RRM AT STA. 4	.90777	1.44765	1.94654	2.04672
	VERT. ACC. AT STERN (AP)	.04463	.12838	.22140	.26845
	VERT. ACC. AT CG	.03275	.06093	.16693	.21095
	VERT. ACC. AT HOB (FP)	.11826	.23296	.40437	.45740
	H1/3 AT WHICH RRM/C=1	17.7	11.1	8.0	7.7
H1/3 AT WHICH RRM/D=1 (FEET)	9.8	6.1	4.4	4.2	
8	WAVE HEIGHT AT ORIGIN	1.46770	1.45368	1.44783	1.45394
	WAVE HEIGHT AT STA. 4	1.46781	1.45371	1.44787	1.45390
	HEAVE	1.271393	1.17642	1.37029	1.43821
	PITCH	2.22493	2.14374	1.82673	1.73244
	VERT. MOT. AT STA. 4	1.64826	1.65147	2.00439	2.00400
	RRM AT STA. 4	.56401	.76043	1.47251	1.61223
	VERT. ACC. AT STERN (AP)	.06993	.09424	.16677	.21127
	VERT. ACC. AT CG	.03092	.05153	.13444	.17660
	VERT. ACC. AT HOB (FP)	.06430	.16231	.30047	.35547
	H1/3 AT WHICH RRM/C=1	25.4	16.7	10.4	10.0
H1/3 AT WHICH RRM/D=1 (FEET)	13.7	9.2	6.0	5.7	
10	WAVE HEIGHT AT ORIGIN	1.47176	1.45445	1.46687	1.46320
	WAVE HEIGHT AT STA. 4	1.47201	1.45442	1.46684	1.46370
	HEAVE	1.35274	1.31029	1.45222	1.50500
	PITCH	1.74723	1.70144	1.51116	1.47122
	VERT. MOT. AT STA. 4	1.73504	1.74294	1.96377	1.97095
	RRM AT STA. 4	.24269	.36345	1.04154	1.16666
	VERT. ACC. AT STERN (AP)	.04741	.06471	.11402	.15210
	VERT. ACC. AT CG	.02577	.03946	.07030	.09193
	VERT. ACC. AT HOB (FP)	.05435	.10215	.21204	.25372
	H1/3 AT WHICH RRM/C=1	34.7	24.5	15.4	13.8
H1/3 AT WHICH RRM/D=1 (FEET)	18.3	12.7	8.0	7.6	
14	WAVE HEIGHT AT ORIGIN	1.49330	1.47626	1.46407	1.46176
	WAVE HEIGHT AT STA. 4	1.49360	1.47624	1.46407	1.46180
	HEAVE	1.44309	1.41745	1.46291	1.50294
	PITCH	1.60255	1.65145	.98744	.92046
	VERT. MOT. AT STA. 4	1.63262	1.60510	1.87354	1.85467
	RRM AT STA. 4	.06474	.20004	.48550	.54417
	VERT. ACC. AT STERN (AP)	.02166	.02774	.04563	.06214
	VERT. ACC. AT CG	.01634	.02246	.04652	.06281
	VERT. ACC. AT HOB (FP)	.02228	.03805	.07753	.10061
	H1/3 AT WHICH RRM/C=1	149.4	80.2	33.0	27.0
H1/3 AT WHICH RRM/D=1 (FEET)	104.7	44.3	18.3	14.9	

TABLE 5 - RMS RESPONSES OF SHIP B, 15-KNOT MONOHULL

T ₀ SEC.	CHANNEL	LPM = 100.0 FT/1 CLEARANCE, C = 14.00 FEET UNAFI, U = 4.00 FEET		
		0. KTS	5. KTS	15. KTS
6	WAVE HEIGHT AT ORIGIN	1.43532	1.43645	1.43512
	WAVE HEIGHT AT STA. 4	1.43533	1.43775	1.43530
	HEAVE	.53651	.66436	.42194
	PITCH	1.29037	1.30792	1.05129
	VERT. MOT. AT STA. 4	1.36914	1.61351	1.52204
	RRM AT STA. 4	1.34167	1.88512	2.22445
	VERT. ACC. AT STERN (AP)	.05966	.08538	.13471
	VERT. ACC. AT CG	.01798	.03578	.04047
	VERT. ACC. AT HULL (FP)	.07389	.13439	.14628
	H _{1/3} AT WHICH RMM/0=1	31.0	22.5	19.0
H _{1/3} AT WHICH RMM/0=1 (FEET)	14.0	10.0	8.5	
8	WAVE HEIGHT AT ORIGIN	1.46770	1.45368	1.46743
	WAVE HEIGHT AT STA. 4	1.46889	1.45409	1.46777
	HEAVE	.91511	1.00476	1.36793
	PITCH	1.42479	1.44340	1.29730
	VERT. MOT. AT STA. 4	1.88544	1.90047	2.09749
	RRM AT STA. 4	.98930	1.30771	2.10700
	VERT. ACC. AT STERN (AP)	.05540	.07867	.13854
	VERT. ACC. AT CG	.01945	.03617	.04903
	VERT. ACC. AT HULL (FP)	.08892	.12015	.14957
	H _{1/3} AT WHICH RMM/0=1	46.0	29.1	26.1
H _{1/3} AT WHICH RMM/0=1 (FEET)	19.0	12.5	8.4	
10	WAVE HEIGHT AT ORIGIN	1.47116	1.45845	1.46857
	WAVE HEIGHT AT STA. 4	1.47227	1.45844	1.47000
	HEAVE	1.18358	1.21350	1.49156
	PITCH	1.26239	1.28218	1.17361
	VERT. MOT. AT STA. 4	1.88129	1.88366	2.11903
	RRM AT STA. 4	.66578	1.07597	1.64611
	VERT. ACC. AT STERN (AP)	.04370	.06114	.10774
	VERT. ACC. AT CG	.01733	.03040	.04574
	VERT. ACC. AT HULL (FP)	.07194	.09134	.13414
	H _{1/3} AT WHICH RMM/0=1	53.0	39.4	25.7
H _{1/3} AT WHICH RMM/0=1 (FEET)	25.5	17.5	11.4	
14	WAVE HEIGHT AT ORIGIN	1.44328	1.47627	1.46607
	WAVE HEIGHT AT STA. 4	1.44370	1.47628	1.46708
	HEAVE	1.44352	1.34472	1.52114
	PITCH	.87191	.94224	.84663
	VERT. MOT. AT STA. 4	1.85420	1.74586	1.93555
	RRM AT STA. 4	.85570	.83013	.95411
	VERT. ACC. AT STERN (AP)	.07420	.04371	.06167
	VERT. ACC. AT CG	.01382	.02043	.04452
	VERT. ACC. AT HULL (FP)	.02718	.04774	.04384
	H _{1/3} AT WHICH RMM/0=1	144.2	43.4	44.4
H _{1/3} AT WHICH RMM/0=1 (FEET)	65.4	37.0	19.7	

TABLE 6 - RMS RESPONSES OF SHIP C, 20-KNOT MONOHULL

T ₀ SEC.	CHANNEL	LPP = 200.0 FEET CLEARANCE, C = 17.65 FEET UNAFI, U = 9.35 FEET			
		0. KTS	5. KTS	15. KTS	20. KTS
6	WAVE HEIGHT AT ORIGIN	1.43532	1.43645	1.43512	1.43577
	WAVE HEIGHT AT STA. 4	1.43530	1.43776	1.43576	1.43527
	HEAVE	.39449	.33010	.41512	.37224
	PITCH	.90365	.95424	.81224	.87927
	VERT. MOT. AT STA. 4	1.17002	1.42119	1.49822	1.27833
	RPM AT STA. 4	1.35402	1.06844	2.25245	2.14444
	VERT. ACC. AT STERN (AP)	.04635	.07031	.11072	.12522
	VERT. ACC. AT CG	.01245	.02695	.06584	.07701
	VERT. ACC. AT HULL (FP)	.05946	.10572	.16700	.15601
	H _{1/3} AT WHICH RMS/σ = 1	30.7	26.2	18.4	19.0
H _{1/3} AT WHICH RMS/σ = 1 (FEET)	15.2	11.8	9.8	10.1	
8	WAVE HEIGHT AT ORIGIN	1.46770	1.45368	1.44783	1.45399
	WAVE HEIGHT AT STA. 4	1.46693	1.45431	1.44765	1.45377
	HEAVE	.77839	.87391	1.27602	1.41170
	PITCH	1.14712	1.19610	1.12226	1.03844
	VERT. MOT. AT STA. 4	1.59101	1.84826	2.15682	2.13989
	RPM AT STA. 4	1.10383	1.60524	2.32784	2.47024
	VERT. ACC. AT STERN (AP)	.04992	.07090	.11824	.14784
	VERT. ACC. AT CG	.01359	.02423	.08006	.10514
	VERT. ACC. AT HULL (FP)	.07940	.10597	.19211	.21560
	H _{1/3} AT WHICH RMS/σ = 1	37.6	25.9	17.8	16.4
H _{1/3} AT WHICH RMS/σ = 1 (FEET)	19.4	13.7	9.5	8.9	
10	WAVE HEIGHT AT ORIGIN	1.47176	1.45895	1.44867	1.46495
	WAVE HEIGHT AT STA. 4	1.47254	1.45897	1.47032	1.46955
	HEAVE	1.09835	1.12002	1.44255	1.59455
	PITCH	1.00029	1.12579	1.00814	1.04222
	VERT. MOT. AT STA. 4	1.66697	1.89623	2.24544	2.31395
	RPM AT STA. 4	.87350	1.19448	1.44415	2.04465
	VERT. ACC. AT STERN (AP)	.02903	.05750	.09610	.12324
	VERT. ACC. AT CG	.01754	.02640	.06897	.07481
	VERT. ACC. AT HULL (FP)	.04793	.08438	.15914	.18665
	H _{1/3} AT WHICH RMS/σ = 1	32.2	34.8	22.0	19.4
H _{1/3} AT WHICH RMS/σ = 1 (FEET)	21.7	18.4	11.7	10.5	
14	WAVE HEIGHT AT ORIGIN	1.49328	1.49027	1.49007	1.48175
	WAVE HEIGHT AT STA. 4	1.49388	1.49034	1.48605	1.48215
	HEAVE	1.14667	1.35000	1.49481	1.58082
	PITCH	.87302	.89482	.82045	.75067
	VERT. MOT. AT STA. 4	1.68738	1.79428	2.02145	2.14034
	RPM AT STA. 4	.81121	.86308	1.13630	1.22335
	VERT. ACC. AT STERN (AP)	.02947	.03463	.05834	.07457
	VERT. ACC. AT CG	.01757	.01883	.04494	.04827
	VERT. ACC. AT HULL (FP)	.04663	.04905	.09767	.11565
	H _{1/3} AT WHICH RMS/σ = 1	19.6	20.1	36.5	32.4
H _{1/3} AT WHICH RMS/σ = 1 (FEET)	9.8	10.0	19.4	17.1	

TABLE 7 - RMS RESPONSES OF SHIP D, 15-KNOT SWATH WITH AND WITHOUT BILGE KEELS

TABLE 7A - WITHOUT BILGE KEELS

T ₀ SEC.	CHANNEL	SPEEDS		
		0 KTS	5 KTS	15 KTS
6	MEAN SEAS H1/3 = 6. FEET	LPP = 155.0 FEET CLEARANCE, C = 17.00 FEET UNAFI, D = 16.50 FEET		
	WAVE HEIGHT AT ORIGIN	1.43532	1.43691	1.43519
	WAVE HEIGHT AT STA. 4	1.43534	1.43775	1.43512
	HEAVE	1.57699	.97868	.63480
	PITCH	.14835	.20737	.29127
	VERT. MOT. AT STA. 4	1.56568	.98439	.53615
	RHM AT STA. 4	2.24630	1.80406	1.63606
	VERT. ACC. AT STERN (AP)	.04875	.03620	.03211
	VERT. ACC. AT CG	.04757	.03355	.01944
	VERT. ACC. AT BOW (FP)	.04768	.03556	.04300
	H1/3 AT WHICH RHM/C=1	12.6	15.7	17.3
	H1/3 AT WHICH RHM/D=1 (FEET)	17.3	21.5	23.7
8	WAVE HEIGHT AT ORIGIN	1.46770	1.45370	1.46800
	WAVE HEIGHT AT STA. 4	1.46858	1.45349	1.44793
	HEAVE	1.88792	1.97080	1.45092
	PITCH	.42643	.22781	.40994
	VERT. MOT. AT STA. 4	1.97902	2.02167	1.51799
	RHM AT STA. 4	2.41634	2.52825	2.33429
	VERT. ACC. AT STERN (AP)	.04993	.05651	.05119
	VERT. ACC. AT CG	.04962	.05639	.04827
	VERT. ACC. AT BOW (FP)	.05040	.05744	.05440
	H1/3 AT WHICH RHM/C=1	11.7	11.2	12.1
	H1/3 AT WHICH RHM/D=1 (FEET)	16.1	15.4	16.6
	10	WAVE HEIGHT AT ORIGIN	1.47176	1.45405
WAVE HEIGHT AT STA. 4		1.47217	1.45407	1.46934
HEAVE		1.77663	2.12053	2.27609
PITCH		1.60120	.66452	.62215
VERT. MOT. AT STA. 4		2.52865	2.31182	2.43789
RHM AT STA. 4		2.46368	2.38472	2.73606
VERT. ACC. AT STERN (AP)		.03988	.05238	.06607
VERT. ACC. AT CG		.03954	.05356	.06546
VERT. ACC. AT BOW (FP)		.04436	.05558	.07117
H1/3 AT WHICH RHM/C=1		11.5	11.6	10.3
H1/3 AT WHICH RHM/D=1 (FEET)		15.4	16.3	14.2
14		WAVE HEIGHT AT ORIGIN	1.44326	1.47639
	WAVE HEIGHT AT STA. 4	1.44368	1.47634	1.46421
	HEAVE	1.54790	1.87017	2.20473
	PITCH	2.75560	1.03322	.68665
	VERT. MOT. AT STA. 4	3.34315	2.45697	2.43245
	RHM AT STA. 4	2.56385	1.74303	2.02525
	VERT. ACC. AT STERN (AP)	.02476	.03333	.05111
	VERT. ACC. AT CG	.02358	.03546	.05236
	VERT. ACC. AT BOW (FP)	.03559	.03453	.05711
	H1/3 AT WHICH RHM/C=1	11.0	15.7	13.9
	H1/3 AT WHICH RHM/D=1 (FEET)	15.1	21.7	19.2

TABLE 7B - WITH BILGE KEELS

T ₀ SEC.	HEAD SEAS	LPP= 155.0 FEET
	M _{1/3} = 6. FEET	CLEARANCE, C = 12.00 FEET DRAFT, D = 16.50 FEET
	CHANNEL	SPEEDS R, KTS
6	WAVE HEIGHT AT ORIGIN	1.43532
	WAVE HEIGHT AT STA. 4	1.43534
	HEAVE	1.41789
	PITCH	.16039
	VERT. MOT. AT STA. 4	1.40000
	RPM AT STA. 4	2.19786
	VERT. ACC. AT STEERN (AP)	.04552
	VERT. ACC. AT CG	.04389
	VERT. ACC. AT HOU (FP)	.04452
	M _{1/3} AT WHICH RPM/C=1	12.8
M _{1/3} AT WHICH RPM/D=1 (FEET)	17.7	
8	WAVE HEIGHT AT ORIGIN	1.46750
	WAVE HEIGHT AT STA. 4	1.46858
	HEAVE	1.46797
	PITCH	.40017
	VERT. MOT. AT STA. 4	1.79418
	RPM AT STA. 4	2.41890
	VERT. ACC. AT STEERN (AP)	.04466
	VERT. ACC. AT CG	.04450
	VERT. ACC. AT HOU (FP)	.04503
	M _{1/3} AT WHICH RPM/C=1	11.7
M _{1/3} AT WHICH RPM/D=1 (FEET)	16.1	
10	WAVE HEIGHT AT ORIGIN	1.47176
	WAVE HEIGHT AT STA. 4	1.47217
	HEAVE	1.60833
	PITCH	1.16542
	VERT. MOT. AT STA. 4	2.24615
	RPM AT STA. 4	2.31490
	VERT. ACC. AT STEERN (AP)	.03455
	VERT. ACC. AT CG	.03571
	VERT. ACC. AT HOU (FP)	.03446
	M _{1/3} AT WHICH RPM/C=1	12.2
M _{1/3} AT WHICH RPM/D=1 (FEET)	16.7	
14	WAVE HEIGHT AT ORIGIN	1.49328
	WAVE HEIGHT AT STA. 4	1.49368
	HEAVE	1.51875
	PITCH	1.85952
	VERT. MOT. AT STA. 4	2.75525
	RPM AT STA. 4	2.00309
	VERT. ACC. AT STEERN (AP)	.01928
	VERT. ACC. AT CG	.02128
	VERT. ACC. AT HOU (FP)	.03032
	M _{1/3} AT WHICH RPM/C=1	14.1
M _{1/3} AT WHICH RPM/D=1 (FEET)	19.4	

TABLE 8 - RMS RESPONSES OF SHIP E, 20-KNOT SWATH

T ₀ SEC.	CHANNEL	LMP = 200.0 FEET CLEARANCE, C = 12.10 FEET DRAFT, D = 19.60 FEET			
		0. KTS	5. KTS	15. KTS	20. KTS
6	WAVE HEIGHT AT MIDSHIP	1.43532	1.43691	1.43520	1.43121
	WAVE HEIGHT AT STA. #	1.43532	1.43790	1.43501	1.43423
	HEAVE	.00573	.02356	.17901	.21279
	PITCH	.17104	.23041	.16747	.15361
	VEPT. ACC. AT STA. #	.00697	.00237	.16354	.20004
	DRM AT STA. #	1.76703	1.34054	1.37074	1.43130
	VEPT. ACC. AT STEER (AMP)	.02204	.02517	.02473	.01467
	VEPT. ACC. AT CG	.02146	.02245	.02315	.02114
VEPT. ACC. AT MID (FP)	.02530	.02742	.02837	.04491	
HEIGHT AT WHICH RMS/CR1		17.4	20.6	20.4	19.9
HEIGHT AT WHICH RMS/CR1 (FEET)		25.7	33.1	33.3	31.4
8	WAVE HEIGHT AT MIDSHIP	1.43700	1.43584	1.43744	1.43401
	WAVE HEIGHT AT STA. #	1.43700	1.43214	1.43704	1.43391
	HEAVE	.00573	.02356	.17901	.21279
	PITCH	.17104	.23041	.16747	.15361
	VEPT. ACC. AT STA. #	.00697	.00237	.16354	.20004
	DRM AT STA. #	1.76703	1.34054	1.37074	1.43130
	VEPT. ACC. AT STEER (AMP)	.02204	.02517	.02473	.01467
	VEPT. ACC. AT CG	.02146	.02245	.02315	.02114
VEPT. ACC. AT MID (FP)	.02530	.02742	.02837	.04491	
HEIGHT AT WHICH RMS/CR1		17.4	20.6	20.4	19.9
HEIGHT AT WHICH RMS/CR1 (FEET)		25.7	33.1	33.3	31.4
10	WAVE HEIGHT AT MIDSHIP	1.43700	1.43584	1.43744	1.43401
	WAVE HEIGHT AT STA. #	1.43700	1.43214	1.43704	1.43391
	HEAVE	.00573	.02356	.17901	.21279
	PITCH	.17104	.23041	.16747	.15361
	VEPT. ACC. AT STA. #	.00697	.00237	.16354	.20004
	DRM AT STA. #	1.76703	1.34054	1.37074	1.43130
	VEPT. ACC. AT STEER (AMP)	.02204	.02517	.02473	.01467
	VEPT. ACC. AT CG	.02146	.02245	.02315	.02114
VEPT. ACC. AT MID (FP)	.02530	.02742	.02837	.04491	
HEIGHT AT WHICH RMS/CR1		17.4	20.6	20.4	19.9
HEIGHT AT WHICH RMS/CR1 (FEET)		25.7	33.1	33.3	31.4
14	WAVE HEIGHT AT MIDSHIP	1.43700	1.43584	1.43744	1.43401
	WAVE HEIGHT AT STA. #	1.43700	1.43214	1.43704	1.43391
	HEAVE	.00573	.02356	.17901	.21279
	PITCH	.17104	.23041	.16747	.15361
	VEPT. ACC. AT STA. #	.00697	.00237	.16354	.20004
	DRM AT STA. #	1.76703	1.34054	1.37074	1.43130
	VEPT. ACC. AT STEER (AMP)	.02204	.02517	.02473	.01467
	VEPT. ACC. AT CG	.02146	.02245	.02315	.02114
VEPT. ACC. AT MID (FP)	.02530	.02742	.02837	.04491	
HEIGHT AT WHICH RMS/CR1		17.4	20.6	20.4	19.9
HEIGHT AT WHICH RMS/CR1 (FEET)		25.7	33.1	33.3	31.4

TABLE 9 - RMS RESPONSES OF SHIP F, COLUMN STABILIZED UP

T ₀ SEC.	CHANNEL	HEAD SEAS H _{1/3} = 0. FEET		
		0. KTS	5. KTS	15. KTS
6	WAVE HEIGHT AT ORIGIN	1.43532	1.43716	1.43496
	WAVE HEIGHT AT STA. 4	1.43530	1.43750	1.43544
	HEAVE	.59705	1.01266	2.49281
	PITCH	1.03628	2.33550	2.58193
	VERT. MOT. AT STA. 4	2.02455	3.26283	3.48908
	HEAVE AT STA. 4	2.11507	3.63107	4.11246
	VERT. ACC. AT STERN (AP)	.06310	.13283	.41356
	VERT. ACC. AT CG	.07023	.08091	.24485
	VERT. ACC. AT HULL (HP)	.09025	.21630	.31096
	H _{1/3} AT WHICH WAVE/CEL	5.7	2.7	2.4
H _{1/3} AT WHICH WAVE/CEL (FEET)	15.9	7.1	7.2	
8	WAVE HEIGHT AT ORIGIN	1.46770	1.45347	1.44763
	WAVE HEIGHT AT STA. 4	1.46495	1.45435	1.44737
	HEAVE	.70138	1.20568	2.69180
	PITCH	1.80712	2.42490	2.46615
	VERT. MOT. AT STA. 4	2.31300	3.41189	4.41654
	HEAVE AT STA. 4	1.74080	3.20760	4.60245
	VERT. ACC. AT STERN (AP)	.05593	.10538	.26589
	VERT. ACC. AT CG	.02348	.05285	.20230
	VERT. ACC. AT HULL (HP)	.07950	.19266	.32556
	H _{1/3} AT WHICH WAVE/CEL	5.7	3.1	2.1
H _{1/3} AT WHICH WAVE/CEL (FEET)	15.9	9.2	6.4	
10	WAVE HEIGHT AT ORIGIN	1.47176	1.45877	1.45909
	WAVE HEIGHT AT STA. 4	1.47257	1.45888	1.45795
	HEAVE	1.01702	1.31444	2.36005
	PITCH	1.88235	2.02088	2.08904
	VERT. MOT. AT STA. 4	2.18114	2.93103	3.96132
	HEAVE AT STA. 4	1.65042	2.36076	3.70335
	VERT. ACC. AT STERN (AP)	.04771	.07717	.16046
	VERT. ACC. AT CG	.01555	.04119	.10046
	VERT. ACC. AT HULL (HP)	.05978	.14270	.25995
	H _{1/3} AT WHICH WAVE/CEL	7.2	4.2	2.7
H _{1/3} AT WHICH WAVE/CEL (FEET)	20.4	12.5	7.9	
14	WAVE HEIGHT AT ORIGIN	1.47324	1.47611	1.46386
	WAVE HEIGHT AT STA. 4	1.47391	1.47645	1.46386
	HEAVE	1.47350	1.42302	1.48805
	PITCH	1.29911	1.29104	1.40426
	VERT. MOT. AT STA. 4	1.47641	2.16572	2.81414
	HEAVE AT STA. 4	.80644	1.18260	2.21804
	VERT. ACC. AT STERN (AP)	.02304	.04046	.08901
	VERT. ACC. AT CG	.01342	.02347	.06649
	VERT. ACC. AT HULL (HP)	.03165	.07245	.15719
	H _{1/3} AT WHICH WAVE/CEL	10.3	5.4	4.5
H _{1/3} AT WHICH WAVE/CEL (FEET)	34.5	24.4	13.3	

TABLE 10 - RMS RESPONSES OF SHIP G, COLUMN STABILIZED DOWN

T ₀ SEC.	HEAD SEAS H _{1/3} = 6. FEET	LPP = 170.0 FEET CLEARANCE, C = 12.00 FEET DRAFT, D = 24.00 FEET	
	CHANNEL	U, KTS	SPEEDS S, KTS
6	WAVE HEIGHT AT ORIGIN	1.43532	1.43654
	WAVE HEIGHT AT STA. 4	1.43530	1.43804
	HEAVE	.36235	.39104
	PITCH	.35048	.48698
	VERT. MOT. AT STA. 4	.58666	.72563
	RPM AT STA. 4	1.52347	1.56123
	VERT. ACC. AT STERN (AP)	.01434	.03061
	VERT. ACC. AT CG	.01115	.02113
	VERT. ACC. AT H _{0W} (FP)	.02202	.04664
	H _{1/3} AT WHICH RRM/C=1 H _{1/3} AT WHICH RRM/D=1 (FEET)	17.5 37.1	15.1 36.2
8	WAVE HEIGHT AT ORIGIN	1.46770	1.45325
	WAVE HEIGHT AT STA. 4	1.46695	1.45413
	HEAVE	.56500	.47424
	PITCH	.40477	.39756
	VERT. MOT. AT STA. 4	.86029	.60474
	RPM AT STA. 4	1.36545	1.27502
	VERT. ACC. AT STERN (AP)	.01617	.02341
	VERT. ACC. AT CG	.01307	.01643
	VERT. ACC. AT H _{0W} (FP)	.02202	.03169
	H _{1/3} AT WHICH RRM/C=1 H _{1/3} AT WHICH RRM/D=1 (FEET)	20.7 41.3	22.1 44.3
10	WAVE HEIGHT AT ORIGIN	1.47176	1.45905
	WAVE HEIGHT AT STA. 4	1.47254	1.45925
	HEAVE	.51575	.61042
	PITCH	.40940	.34605
	VERT. MOT. AT STA. 4	1.15473	.73267
	RPM AT STA. 4	1.31276	1.16487
	VERT. ACC. AT STERN (AP)	.01454	.01804
	VERT. ACC. AT CG	.01344	.01347
	VERT. ACC. AT H _{0W} (FP)	.01374	.02164
	H _{1/3} AT WHICH RRM/C=1 H _{1/3} AT WHICH RRM/D=1 (FEET)	21.5 43.0	24.2 48.5
14	WAVE HEIGHT AT ORIGIN	1.44324	1.47654
	WAVE HEIGHT AT STA. 4	1.44342	1.47644
	HEAVE	1.34250	1.14511
	PITCH	.75044	.54200
	VERT. MOT. AT STA. 4	2.10132	1.54913
	RPM AT STA. 4	1.57345	1.48320
	VERT. ACC. AT STERN (AP)	.01958	.01252
	VERT. ACC. AT CG	.01145	.01134
	VERT. ACC. AT H _{0W} (FP)	.01714	.01650
	H _{1/3} AT WHICH RRM/C=1 H _{1/3} AT WHICH RRM/D=1 (FEET)	17.4 35.7	19.0 36.1

TABLE 11 - BEAM SEA RMS ACCELERATIONS AND ROLL OF CANDIDATE SHIPS

(ξ_w) _{1/3} = 6 feet Speed = 0 knots	Monohulls														
	Ship A			Ship B without Bilge Keels			Ship B with Bilge Keels			Ship C without Bilge Keels			Ship C with Bilge Keels		
	6	8	10	6	8	10	6	8	10	6	8	10	6	8	10
Modal Wave Periods (seconds)	6	8	10	6	8	10	6	8	10	6	8	10	6	8	10
Point 1	8.1	5.7	4.1	2.4	5.4	4.4	3.4	2.1	5.4	4.4	3.4	2.1	7.4	5.4	4.0
Point 2	4.9	3.7	2.9	1.8	3.6	3.1	2.5	1.7	3.6	3.1	2.5	1.6	4.7	3.7	2.8
Roll (degrees)	11.2	7.5	5.3	3.0	4.7	3.9	3.1	2.0	4.5	3.6	2.9	1.8	6.7	4.8	3.4
	4.7	3.7	2.9	1.8	2.9	2.7	2.3	1.6	2.9	2.7	2.3	1.6	3.0	2.4	1.6
	10.1	6.4	4.3	2.3	5.5	6.7	5.4	3.2	4.6	5.6	4.6	2.8	4.0	6.4	5.7

(ξ_w) _{1/3} = 6 feet Speed = 0 knots	SWATHs											
	Ship D with Bilge Keels			Ship E with Bilge Keels			Ship F without Bilge Keels			Ship G		
	6	8	10	6	8	10	6	8	10	6	8	10
Modal Wave Periods (seconds)	6	8	10	6	8	10	6	8	10	6	8	10
Point 1	5.0	2.1	4.0	2.5	2.8	4.2	3.8	2.5	3.8	3.1	2.5	1.6
Point 2	2.1	2.1	1.9	1.4	1.7	1.9	1.8	1.3	2.6	2.2	1.9	1.2
Roll (degrees)	5.0	5.0	4.0	2.5	2.8	4.2	3.8	2.5	8.8	6.7	4.9	2.8
	1.9	2.1	2.1	1.6	1.4	1.7	1.7	1.4	9.0	6.4	4.4	2.4
	0.3	0.6	1.3	0.2	0.2	0.3	0.9	0.3	3.3	2.5	1.8	1.0

Column Stabilized SWATH

N.A.

DEFINITIONS

Point 1 is CG location on main deck
 Point 2 is furthest outboard location aft on main deck
 LV is vertical acceleration
 LA is lateral acceleration